

Provided for non-commercial research and education use.
Not for reproduction, distribution or commercial use.



The Canadian Journal of Veterinary Research is published by the Canadian Veterinary Medical Association. The attached copy is furnished to readers for personal, non-commercial research and education use. Other uses, including reproduction and distribution, or selling or licensing copies, or posting to personal, institutional or third party Web sites are prohibited. Those who require further information regarding reprints or archiving and manuscript policies are encouraged to contact hbroughton@cvma-acmv.org.



Canadian Journal of Veterinary Research

Revue Canadienne de Recherche Vétérinaire

Articles

Immuno-modulation and anti-inflammatory benefits of antibiotics: The example of tilmicosin
André G. Buret 1

Characterization of *Salmonella* Typhimurium isolates associated with septicemia in swine
Nadia Bergeron, Jonathan Corriveau, Ann Letellier, France Daigle, Sylvain Quesy . . . 11

Identification and differentiation of *Taylorella equigenitalis* and *Taylorella asinigenitalis* by lipopolysaccharide O-antigen serology using monoclonal antibodies
Brian W. Brooks, Cheryl L. Lutze-Wallace, Leann L. MacLean, Evgeny Vinogradov, Malcolm B. Perry 18

Protective potential of an attenuated *Pasteurella multocida*, which expresses only the N-terminal truncated fragment of *P. multocida* toxin
Jayoung Seo, Semi Lee, Hyoju Pyo, Jaeil Lee, Taejung Kim 25

Activation of the ovine hypothalamic-pituitary-adrenal axis and febrile response by interleukin-6: A comparative study with bacterial lipopolysaccharide endotoxin
Niel A. Karrow, Qiumei You, Carl McNicoll, Jack Hay 30

The effect of body position, sedation, and thoracic bandaging on functional residual capacity in healthy deep-chested dogs
Elizabeth A. Rozanski, Daniela Bedenice, Jennifer Lofgren, Julie Abrams, Jonathan Bach, Andrew M. Hoffman 34

Degradation of foot-and-mouth disease virus during composting of infected pig carcasses
J. Guan, M. Chan, C. Grenier, B.W. Brooks, J.L. Spencer, C. Kranendonk, J. Copps, A. Clavijo 40

January/janvier 2010, Vol. 74 No. 1

table of contents continued on back cover/
la table des matières se poursuit sur la
couverture arrière

Canadian Journal of Veterinary Research

Formerly **CANADIAN JOURNAL OF COMPARATIVE MEDICINE**

The research journal of the Canadian Veterinary Medical Association

The journal publishes the results of original research in veterinary and comparative medicine. Manuscripts must be as concise as possible, and the research described must represent a significant contribution to knowledge in veterinary medicine. Full-length papers, short communications, and review papers are welcome. All manuscripts will be reviewed for scientific content and editorial accuracy.

Manuscripts must conform to the Instructions for Authors found on the CVMA Web site. Consultation of a recent issue of the journal to ensure that the manuscript conforms to current style is also recommended. Please use the Web site (www.canadianveterinarians.net) to submit articles. **A publication charge of \$80 per published page, plus a cost of \$10 per table and \$15 per illustration, is payable by contributors.** Instructions for ordering reprints are sent with the galley proofs. Color illustrations will only be published if the author(s) agree to pay the extra cost.

Revue canadienne de recherche vétérinaire

Remplace la **REVUE CANADIENNE DE MÉDECINE COMPARÉE**

La revue de recherche de l'Association canadienne des médecins vétérinaires

La revue publie les résultats de recherches originales en médecine vétérinaire et comparative. Les manuscrits doivent être aussi brefs que possible et la recherche décrite doit apporter une contribution importante à la médecine vétérinaire. Les exposés complets, les communications brèves et les comptes rendus sont bienvenus. Nous vérifierons le fonds scientifique et la forme de tous les manuscrits.

Les manuscrits doivent être conformes aux directives aux auteurs qui se trouvent sur le site Web de l'ACMV. La consultation d'un récent numéro de la revue est aussi profitable, afin de s'assurer qu'un manuscrit se conforme au style courant. Veuillez utiliser le site Web (www.veterinairesauCanada.net) pour soumettre les articles. **Les auteurs doivent acquitter des frais de 80 \$ par page publiée, 10 \$ pour chaque tableau et 15 \$ pour chaque illustration.** Un formulaire de commande de tirés à part accompagne l'envoi des épreuves d'un manuscrit. Les illustrations en couleurs ne seront publiées que si les auteurs en assument les frais supplémentaires.

Canadian Journal of Veterinary Research Revue canadienne de recherche vétérinaire

Editor — Rédacteur

Éva Nagy, Guelph, Ontario

Associate Editor — Rédacteur adjoint

Deborah M. Haines, Saskatoon, Saskatchewan

Assistant Editors — Assistants à la rédaction

Serge Messier, Saint-Hyacinthe (Québec)

Jeffrey J. Wichtel, Charlottetown, Prince Edward Island

Paul Kitching, Abbotsford, British Columbia

Managing Editor — Directrice de la rédaction

Heather Broughton, Ottawa, Ontario

Assistant Managing Editor — Directrice adjointe à la rédaction

Stella Wheatley, Ottawa, Ontario

Advertising Manager — Gérante de la publicité

Laima Laffitte, Wendover, Ontario

Editorial Assistant/Adjointe à la rédaction

Beverly Prieur, Ottawa, Ontario

Canadian Veterinary Medical Association L'Association canadienne des médecins vétérinaires

President — Présidente

Julie E. de Moissac, Outlook, Saskatchewan

President-elect — Président élu

Doug Roberts, Kentville, Nova Scotia

Vice-president — Vice-président

Lloyd Keddie, Fairview, Alberta

Executive Director — Directeur général

Jost am Rhyn, Ottawa, Ontario

Chairman, Editorial Committee — Président du Comité de rédaction

Ronald Lewis, Abbotsford, British Columbia

Abstracted and/or indexed in/Résumé et/ou catalogué dans :

Biological Abstracts	Index Veterinarius
Chemical Abstracts	Nutrition Abstracts
Current Contents (Agric. Section)	Science Citation Index
EMBASE/Excerpta Medica	Veterinary Bulletin
Index Medicus	Derwent Veterinary Drug File

Address all correspondence to/Adresser toute correspondance à :

Canadian Journal of Veterinary Research

Revue canadienne de recherche vétérinaire

339, rue Booth Street, Ottawa, Ontario K1R 7K1

Tel./Tél. : (613) 236-1162 — Fax/Télécopieur : (613) 236-9681

e-mail/Courriel : hbroughton@cvma-acmv.org

Typesetting/Typographie

AN Design Communications

www.an-design.ca

Subscriptions/Abonnements —	2010
Canada	\$135 \$ (+ \$6.75 \$ GST/TPS)
Foreign/Étranger	\$150 \$ US/É.-U.
Back issues/Anciens numéros	\$25 \$ (+ \$1.25 \$ GST/TPS) each/chacun

Published quarterly by the Canadian Veterinary Medical Association
Publication trimestrielle de l'Association canadienne des médecins vétérinaires

Return undeliverable Canadian addresses to: 339 rue Booth Street, Ottawa, Ontario K1R 7K1, e-mail: hbroughton@cvma-acmv.org

© Canadian Veterinary Medical Association 2010

© L'Association canadienne des médecins vétérinaires 2010

Immuno-modulation and anti-inflammatory benefits of antibiotics: The example of tilmicosin

André G. Buret

Abstract

Exaggerated immune responses, such as those implicated in severe inflammatory reactions, are costly to the metabolism. Inflammation and pro-inflammatory mediators negatively affect production in the food animal industry by reducing growth, feed intake, reproduction, milk production, and metabolic health. An ever-increasing number of findings have established that antibiotics, macrolides in particular, may generate anti-inflammatory effects, including the modulation of pro-inflammatory cytokines and the alteration of neutrophil function. The effects are time- and dose-dependent, and the mechanisms responsible for these phenomena remain incompletely understood. Recent studies, mostly using the veterinary macrolide tilmicosin, may have shed new light on the mode of action of some macrolides and their anti-inflammatory properties. Indeed, research findings demonstrate that this compound, amongst others, induces neutrophil apoptosis, which in turn provides anti-inflammatory benefits. Studies using tilmicosin model systems *in vitro* and *in vivo* demonstrate that this antibiotic has potent immuno-modulatory effects that may explain why at least parts of its clinical benefits are independent of anti-microbial effects. More research is needed, using this antibiotic and others that may have similar properties, to clarify the biological mechanisms responsible for antibiotic-induced neutrophil apoptosis, and how this, in turn, may provide enhanced clinical benefits. Such studies may help establish a rational basis for the development of novel, efficacious, anti-microbial compounds that generate anti-inflammatory properties in addition to their antibacterial effects.

Résumé

*Les réponses immunes excessives, telles que celles impliquées lors de réactions inflammatoires sévères, sont coûteuses pour le métabolisme. Les médiateurs inflammatoires et pro-inflammatoires affectent négativement la production dans l'industrie animale en réduisant la croissance, la prise de nourriture, la reproduction, la production laitière et la santé métabolique. De plus en plus de découvertes ont établi que les antibiotiques, en particulier les macrolides, peuvent avoir des effets anti-inflammatoires, incluant la modulation de cytokine pro-inflammatoires et une altération de la fonction des neutrophiles. Les effets sont temps- et dose-dépendant, et le mécanisme responsable de ces phénomènes demeurent non-complètement élucidés. Des études récentes, utilisant principalement le macrolide vétérinaire tilmicosin, pourrait avoir fourni de nouvelles informations sur le mode d'action des macrolides et leurs propriétés anti-inflammatoires. En effet, des trouvailles récentes ont démontré que ce produit avait, entre autres, induit l'apoptose chez les neutrophiles, ce qui avait des effets anti-inflammatoires bénéfiques. Des études utilisant des modèles *in vitro* et *in vivo* ont démontré que cet antibiotique à des effets immuno-modulateurs marqués qui pourraient expliquer pourquoi une partie de ses effets cliniques bénéfiques sont indépendants des effets antimicrobiens. En utilisant cet antibiotique et d'autres qui ont des propriétés similaires, plus de recherche sont nécessaires afin de clarifier les mécanismes biologiques responsables de l'apoptose des neutrophiles induite par l'antibiotique, et comment ce fait augmente les effets cliniques bénéfiques. De telles études pourraient aider à fournir une base rationnelle pour le développement de composés anti-microbiens nouveaux et efficaces qui ont des propriétés anti-inflammatoires en plus de leurs effets antibactériens.*

(Traduit par Docteur Serge Messier)

Introduction

Infection-induced inflammatory reactions directly and indirectly affect growth, feed intake, milk production, reproduction, and metabolic health. Therapeutic compounds that generate both anti-bacterial as well as anti-inflammatory effects are therefore likely to be most effective at treating bacteria-induced inflammatory diseases.

Over the past 2 decades, there has been increasing interest in the potential anti-inflammatory effects of macrolides, as well as those of azalides, in which a methyl-substituted nitrogen atom is added into the lactone ring. During infection, both bacterial virulence factors as well as the host inflammatory response, which implicates local infiltration by polymorphonuclear leukocytes (neutrophils), are responsible for pathophysiology, tissue destruction and, in some

Inflammation Research Network, Department of Biological Sciences, 2500 University Drive, University of Calgary, Calgary, Alberta T2N 1N4.

Address all correspondence to Dr. André G. Buret; telephone: (403) 220-2817; fax: (403) 289-9311; e-mail: aburet@ucalgary.ca

Received July 16, 2008. Accepted September 18, 2008.

Table I. Examples of metabolic costs due to inflammation. Inflammatory mediators may inhibit growth directly and indirectly

Physiological parameter affected	Mediator implicated	References
Growth	TNF α , IL-1 β , IGF-1, IL-6, cortisol	16–22,90,94
Feed intake	TNF α , IL-1 β , IGF-1, cortisol	16–18,21,22
Reproduction	cortisol, PGF-2alpha	21,91,92
Milk production	unclear	21,93,94
Periparturient metabolic health	decreased plasma Ca $^{++}$	21

cases, death. Neutrophils are bacterial killers that migrate to the site of infection and therefore constitute a critical line of host defense. Uncontrolled infiltration and necrosis of neutrophils at the site of inflammation, however, leads to the release, by these cells, of large amounts of toxic compounds that target the invading bacteria, but concurrently contribute to the self-perpetuating inflammatory injury. In contrast, neutrophil death by apoptosis helps resolve inflammation and avoid immunopathology. Recent findings indicate that some antibiotics, such as the 16-membered macrolide tilmicosin, may generate anti-inflammatory benefits by modulating the production of pro-inflammatory mediators, and by inducing neutrophil apoptosis. The aim of this review is to discuss how antibiotics with such immuno-modulatory and anti-inflammatory effects may improve animal health and production. Using tilmicosin and the treatment of respiratory disease as an example, this article also critically reviews how induction of neutrophil apoptosis at the site of inflammation may confer anti-inflammatory properties to an antibiotic.

Immunity and metabolic costs

The interplay between the immune, endocrine, and nervous systems is at the core of the homeostatic network (1). Immune output influences overall physiological balance and metabolism. Conversely, neural pathways mediate immune reactivity in health and disease. For example, stress may be responsible for immunosuppression in some instances, or promote immune hyper-reactivity such as in intestinal anaphylaxis in others (2–4). It is also well known that the immune system is compromised in stressed cattle, which contributes to the high incidence of respiratory disease in feedlot cattle during their first 45 days on feed (5). The reality of these tight interactive processes at least in part explains why fighting infection may be associated with significant costs to metabolic rates, protein synthesis, and growth. Animals rely on energy and proteins to mount and maintain immune functions, whether cellular or humoral (6–8). These resources are limited, particularly in the young and growing animal, forcing trade-offs to occur between immune, metabolic, and physiological processes. While some findings indicate that basal immune responsiveness is not necessarily detrimental to nutrient-dependent body demands (9,10), excess immune reactions implicated in the immunopathology of various inflammatory disorders impair metabolic performance. For example, excessive immune responses occur at the expense of antioxidant nutrients, trace minerals, and vitamins, similarly to what occurs in stress (11). In other words, an exaggerated investment in immune reactions negatively affects growth and development.

A wide variety of molecules regulate the critical communications between cellular and humoral immune responses. As these may

be proteins or lipids (cytokines or eicosanoids for example), these mediators also require an adequate balance between dietary input and immunological synthesis. Dietary fats for example may alter the composition of membrane phospholipids, which are the precursors of eicosanoid synthesis. Indeed, bioactive eicosanoids are released upon cleavage of membrane phospholipids by the enzyme phospholipase A₂, an important factor in diseases that involve infection and inflammation (12). The inflammatory response may be altered by dietary fats, which can cause Th1–Th2 T helper lymphocyte switching (13). These changes are mediated by effects on the various cytokines, prostaglandins, leukotrienes, and other eicosanoids, that are released to coordinate inflammatory reactions (13). Indeed, fish oil supplementation has been found to attenuate the production of IL-1 β , prostaglandin E₂, and cortisol, in pigs challenged with *Escherichia coli* lipopolysaccharide (14). Conversely, the collateral damage due to exaggerated inflammation primarily driven by IL-1, and TNF α cytokines, and by the eicosanoid leukotriene B₄, may cause decreased food intake, nutrient loss, and reduced weight gain (15). The reduction in growth caused by excessive immune reactions is often greater than can be explained by decreases in feed intake alone (16). Indeed, there is evidence to suggest that cytokines like IGF-1 or IL-1 β , may directly alter growth hormone receptor signaling (17). The current hypothesis for the decreased muscle mass gain during intense immune reactions proposes that because of reduced amino acids from decreased feed intake, amino acids shunt the skeletal muscle to go to the liver and other sites, to support the synthesis of pro-inflammatory mediators (18–20). Moreover, some inflammatory mediators, such as IL-1 and TNF α , have direct anorectic properties (18). As illustrated in Table I, severe inflammatory reactions may therefore negatively affect growth, reproduction, milk production, and general metabolic health (21). These observations stem from scientific evidence mostly related to mastitis and bovine respiratory disease (BRD). During BRD caused by *Mannheimia (Pasteurella) haemolytica*, production of acute phase proteins, antibodies, and inflammatory cells was found to decrease dry matter intake, which in turn reduces nitrogen balance and causes metabolic stress (22). These events, at least in part, contribute to the decreased performance and carcass quality of animals that had a BRD event (22). Thus, the complexities associated with animal production, where feed conversion and carcass quality are paramount, also depend on optimally managing immune processes. This becomes particularly crucial in cases of inflammatory diseases, and in conditions of high intensity housing, where disease transmission and stress are common. The most logical approach to minimize the detrimental effects of immune hyperactivity on metabolism and production is to minimize the incidence and severity of infection and inflammation.

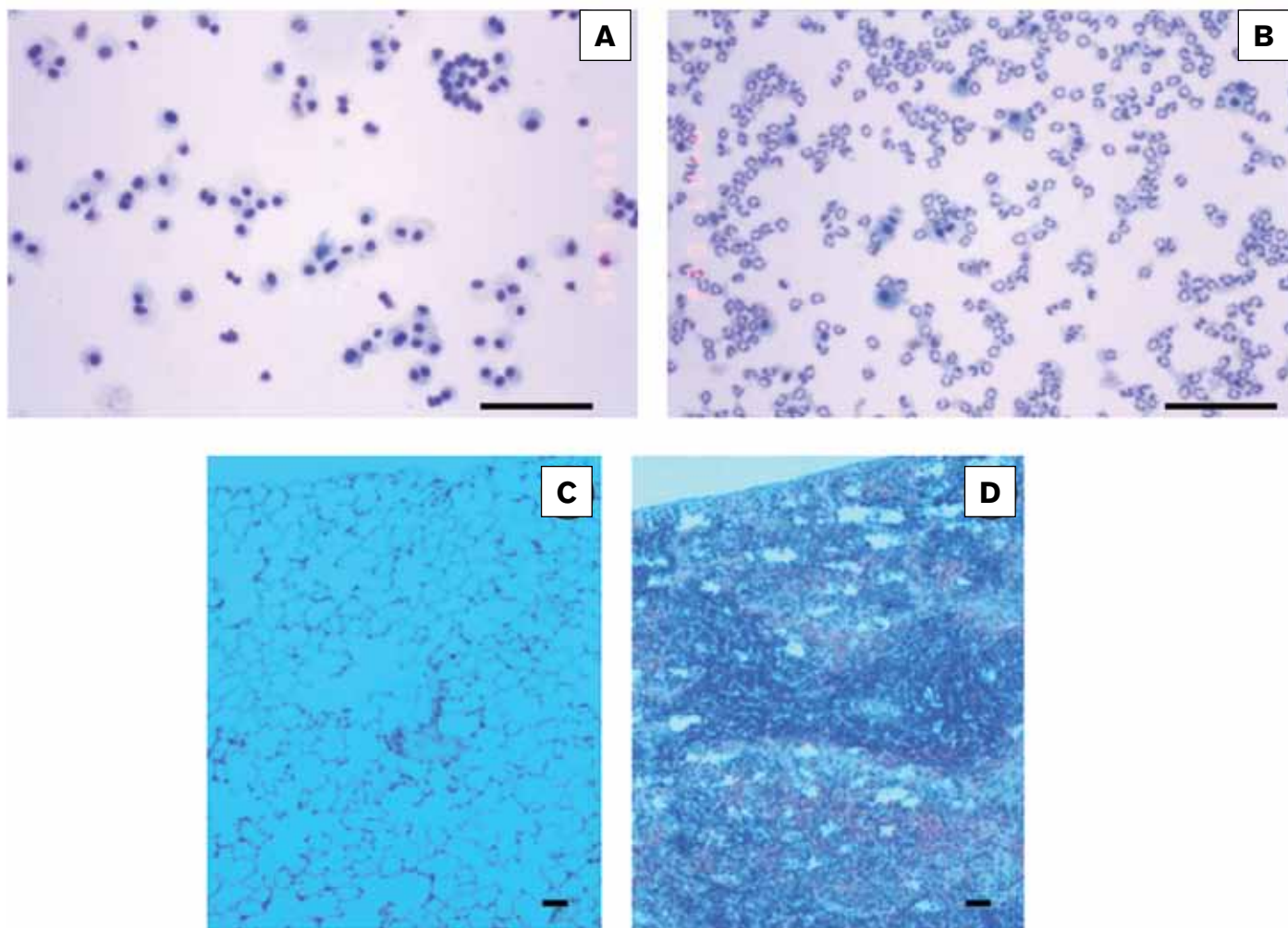


Figure 1. Light micrographs from cytospin slides of broncho-alveolar lavages (A, B) or from histological preparations (eosin and hematoxylin; C,D) from calves 24 h after intratracheal inoculation with sterile endotoxin-free saline (controls, A, C), or with 2×10^8 live *M. haemolytica* in saline (infected, B, D). Infection induces a rapid migration of neutrophils to the broncho-alveolar space (B). In homeostatic conditions, neutrophils serve to protect the lung against the invading bacteria; however, when unchecked, this accumulation of neutrophils is responsible for severe inflammatory injury. In lesional areas (D), inflammation during this infection produces classical pathological signs of bovine respiratory disease (BRD), including alveolar obstruction by inflammatory infiltrates and fibrin deposition. Bars = 100 μ m.

Therefore, it is likely that antibiotics with potent anti-inflammatory properties will optimize our ability to support maximal growth and efficiency in meat- and milk-producing animals.

Infection, neutrophil death, and inflammation

Alveolar macrophages represent the first line of innate immune defense in the lung. Upon inhalation of foreign particles, including infectious bacteria, macrophages initiate phagocytic elimination of these materials, and, in the process, release chemoattractants for neutrophils to migrate to the site. This migration is fast and extensive, as illustrated in the *M. haemolytica*-infected lung, where neutrophils may represent over 90% of the alveolar cell population very early post-infection (23). While bacterial leukotoxin evidently affects these cells, at least part of these pro-inflammatory effects is mediated by *M. haemolytica* lipopolysaccharide, a potent inducer of IL-1 β and TNF α in bovine pasteurellosis (24). This characteristic, severe,

inflammatory reaction can be readily observed in bronchoalveolar lavages collected from infected cattle (Figure 1). In homeostatic conditions, migration of neutrophils to the inflamed site serves to protect the host from disease-causing microbes or other foreign materials. However, excessive and sustained recruitment of these cells to the lung leads to extensive inflammatory damage (Figure 1), pulmonary failure, and death during BRD. Similar pathophysiological processes can be observed in all mucosal surfaces, including in the mammary gland during mastitis (25,26). Indeed, infiltration by neutrophils is at the core of tissue inflammation. The mode of clearance and death of these cells from the site dictates how inflammation will be resolved. Neutrophil death may occur in two ways: via apoptosis or necrosis. When neutrophils at an inflammatory site die via necrosis, the cells swell and burst, spilling pathogenic compounds such as oxygen radicals, proteolytic enzymes, and cationic proteins into the surrounding tissues (27,28). In turn, this amplifies local inflammatory

injury. In contrast to necrosis, neutrophil apoptosis is a key mechanism for the nonphlogistic removal of extravasated neutrophils, and contributes to the resolution of inflammation (29,30). In the *M. haemolytica*- or *Actinobacillus pleuropneumoniae* — infected lung, the self-regulatory control of neutrophil infiltration and apoptosis is overwhelmed and pathogenic accumulation of viable and necrotic neutrophils in pulmonary tissue ensues (23,31). This results in persistent inflammation and severe tissue injury, thereby causing the often fatal fibrinous pneumonia seen in cattle or swine infected with *M. haemolytica* or *A. pleuropneumoniae*. As discussed above, inflammation is also responsible for the detrimental effects on growth and metabolism in animals with BRD. Therefore, a better understanding of this immunopathological cascade will help establish a rational basis for developing more effective pharmaceutical interventions that control both the microbial invasion as well as the host inflammatory reaction.

Resolution of inflammation: The role of neutrophil apoptosis

Apoptosis in neutrophils, as well as in other cell types, is associated with characteristic morphological changes (29,32). These include cell shrinking and membrane blebbing, vacuolation of the cytoplasm, nuclear membrane delamination, and chromatin condensation. In contrast to necrosis, the cell retains the integrity of its membrane and organelles. Eventually, nuclear DNA breaks down to form mono/oligo-nucleosomes, and the cell tears itself apart in membrane-bound apoptotic bodies, which remain sealed from the environment. Throughout this process, again in contrast to necrosis, the cell does not spill its contents into the extracellular milieu. These morphological characteristics are recognized as classical markers of apoptosis. In addition, a number of biochemical events accompany apoptotic death. Perhaps one of the best known early biochemical change during apoptosis is the loss of membrane phospholipid asymmetry, whereby phosphatidylserine translocates onto the outer portion of the membrane bi-layer (33). Other biochemical changes include the loss of sialic acid residues on cell membrane components, and the decreased expression of the glycosylphosphatidylinositol-linked protein CD16 (FcγRIII) (34,35). Ultimately, apoptotic cells and fragments are removed by cells such as macrophages (Figure 2) and, in some instances, other “nonprofessional” phagocytes, including neighboring epithelial cells (29,36). This phagocytic elimination is facilitated by receptors on the macrophages which recognize targets that are newly expressed on apoptotic target cells (37–43). For example, macrophages have phosphatidylserine receptors that allow the selective elimination of apoptotic cells (29,36); hence, apoptotic neutrophils are cleared before they are given the opportunity to undergo secondary necrosis.

Most significantly, the phagocytic elimination of apoptotic cells does not induce the release of pro-inflammatory compounds otherwise associated with macrophage phagocytosis, and instead triggers the production of anti-inflammatory mediators. For example, this phagocytic clearance process is not associated with the release of pro-inflammatory IL-1 β , TNF α , IL-8, Thromboxane B $_2$, or Monocyte Chemoattractant Protein-1 (44–47). Moreover, uptake of apoptotic cells triggers the production of anti-inflammatory mediators such as TGF β , PAF and PGE $_2$ by the macrophages (44,46). Results from recent

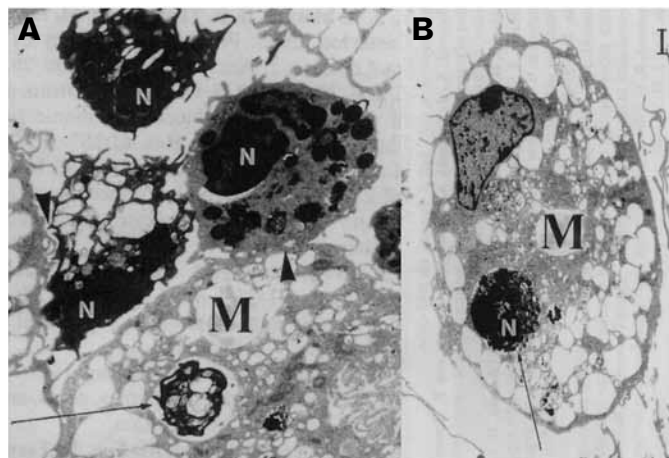


Figure 2. Transmission electron micrographs (A and B) of bovine neutrophils (N) exposed for 2 h to tilmicosin (0.5 $\mu\text{g}/\text{mL}$), and co-incubated for 2 h with bovine monocyte-derived esterase-positive macrophages (M). Neutrophils exposed to the antibiotic exhibit characteristic signs of apoptosis, including nuclear membrane delamination, chromatin condensation, and cytoplasmic vacuolation, while keeping their plasma membrane and cytoplasmic organelles intact. Exposure to tilmicosin significantly enhanced phagocytic uptake of apoptotic neutrophils by macrophages, as illustrated by tight membrane contacts (arrowhead) and full phagocytic inclusion of neutrophils in advanced stages of apoptosis within the macrophages (arrows). Bar = 1 μm . (Modified from reference 83).

studies indicate that these signals could be overcome by proteases, including neutrophil elastase, which are released during lysis of necrotic cells (48). Together, these findings have established that the clearance mechanism of apoptotic neutrophils by phagocytes represents a central feature of the resolution of inflammation, and that the final outcome of an inflammatory reaction will be dictated by which cell elimination predominates (apoptosis or necrosis). Of course, other mechanisms actively regulate the resolution of inflammation, including the production of various mediators, such as the newly discovered Resolvin E1 (49–52). Regardless, anti-inflammatory mechanisms and microenvironmental signals that promote apoptosis in neutrophils and their clearance by phagocytes offer promising research grounds from which to develop new therapeutics (49,52–54). For example, it was recently suggested that cyclin-dependent kinase inhibitors could be used to enhance the resolution of inflammation by inducing neutrophil apoptosis, which was proposed as a novel therapeutic strategy for inflammatory diseases (55).

Immuno-modulatory effects of macrolides

Traditional knowledge had based the efficacy of a given antibiotic on its direct anti-microbial effects. However, an ever-increasing body of research evidence suggests that there may be another central component to the mode of action of some antibiotics, that is, their capability to generate anti-inflammatory effects. The anti-inflammatory potential of macrolides has been the topic of a number of recent reviews (56–61). Macrolides exhibit a broad spectrum of antibacterial activity against gram-negative and gram-positive (*Streptococcus pneumoniae*) pathogens. This combines with their good tissue penetration, including significant uptake into neutrophils, giving macrolides excellent pharmacodynamic properties. Macrolides also have a broad spectrum of non-antibiotic properties, including motilin receptor

Table II. Examples illustrating the anti-inflammatory effects of macrolides

Antibiotic	Cellular parameters	References
Effects on pro-inflammatory mediators		
• erythromycin, clarithromycin, roxithromycin	Reduced gene expression and production of ICAM-1	60,100,101
• erythromycin, roxithromycin, clarithromycin, azithromycin	Reduced production of IL-6, IL-8, IL-1 β , TNF α	60,68,93,102,103,104
• erythromycin	Reduction of epithelial-cell derived neutrophil attractant 78 (ENA-78)	104
• erythromycin, clarithromycin	Suppression of endothelin-1 mRNA and production	40,94
• erythromycin, roxithromycin	Suppression of GMCSF production	102
Effects on neutrophil function		
• erythromycin, roxithromycin, azithromycin	Inhibition of neutrophil chemotaxis	60,105
• erythromycin	Inhibition of neutrophil elastolytic activity	105
• erythromycin, roxithromycin, azithromycin, dirithromycin	Inhibition of neutrophil oxidative burst (at high concentrations) ^a	93,94,105
• erythromycin	Inhibition of β_2 -integrin expression (CD11b/CD18)	93
• roxithromycin	Inhibition of neutrophil adhesion	60
Induction of neutrophil apoptosis		
tilmicosin, erythromycin, clarithromycin, azithromycin, tulathromycin		69,70,71,74,82,83,84

^a At low concentrations, studies suggest that macrolides have pro-oxidant effects or no effect (91,92).

stimulation (62), anticancer activity (63,64), and anti-angiogenesis effects (64). Moreover, it is now well-established that macrolides modulate host immune cell function, and tissue inflammation. The numerous immunomodulatory effects that have been described include the reduced accumulation of pro-inflammatory mediators and the modulation of neutrophil function and apoptosis (Table II). Macrolides such as erythromycin and clarithromycin have also been shown to modify mucosal function, for example by directly reducing mucus secretion and/or decreasing lipopolysaccharide-stimulated goblet cell secretion (65,66). Finally, some macrolides have been found to modulate vaccine-induced humoral immune responses (67).

Clarithromycin induces apoptosis in cancer cells (62,63,68). Other findings suggest that erythromycin and roxithromycin activate neutrophil apoptosis in vitro (69,70). A number of studies, in vitro and in vivo, have established that tilmicosin promotes neutrophil apoptotic clearance (see the following text). Recent observations indicate that tulathromycin also may induce apoptosis in bovine neutrophils in vitro (71). The possibility that these phenomena may at least in part account for the anti-inflammatory effects of these macrolides is intriguing. As is the case for tilmicosin (72), the human 15-ring azalide azithromycin has a high affinity for uptake in neutrophils (73). Azithromycin also induces apoptosis in human circulating neutrophils, in experimental settings where penicillin, erythromycin, or dexamethasone had no pro-apoptotic effects (74). Intriguingly, *Streptococcus pneumoniae* seems to abolish the pro-apoptotic effects of azithromycin (74). Future research will determine whether this effect may contribute to the difficulties in treating such infections, which would offer further support to the hypothesis that antibiotic-induced neutrophil apoptosis offers significant clinical benefits. Indeed, other findings have suggested that macrolides known to

induce neutrophil apoptosis may significantly reduce the inflammatory injury associated with *Haemophilus influenzae* infections of the lower respiratory tract via unexplained mechanisms (75). However, the physiological significance of antibiotic-induced neutrophil apoptosis remains incompletely understood, and little published clinical evidence is available to support that this effect occurs during treatment in vivo. Much remains to be learned about the mechanisms responsible for this property. Also, the dose-dependent expression of some of these anti-inflammatory effects may at times confuse their clinical significance. To date, the most compelling body of evidence suggesting that antibiotic-induced neutrophil apoptosis confers anti-inflammatory benefits to an antibiotic comes from research carried out on tilmicosin.

Neutrophil apoptosis and anti-inflammatory benefits: Effects of tilmicosin

The veterinary drug tilmicosin is a 16-ring macrolide antibiotic with antimicrobial activity against gram-positive and gram-negative bacteria [including *Pasteurella* sp. (*Mannheimia* sp.), *Actinobacillus* sp., and *Mycoplasma* sp.]. Tilmicosin is used as a subcutaneous formulation to treat respiratory infections in cattle, or as a feed formulation to control bacterial pneumonia in swine (76,77). The treatment success of tilmicosin was initially attributed to its pharmacodynamic concentration in appropriate tissues and low inhibitory concentrations (78–81). Tilmicosin has a very high affinity for uptake within neutrophils, in which intracellular concentrations 40 \times greater than those achievable in the serum have been reported (72). In addition, there is now increasing evidence to suggest that tilmicosin also generates anti-inflammatory effects, via mechanisms that have yet to be fully characterized (79,82–84).

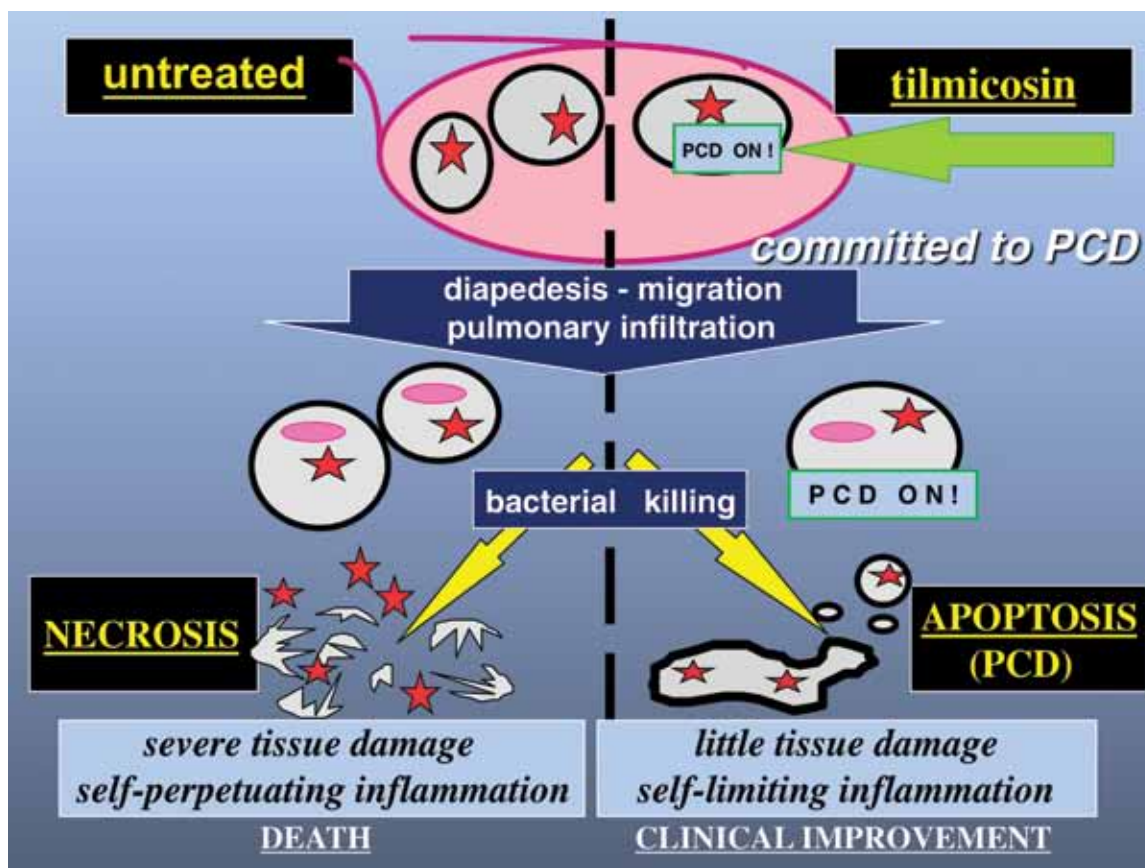


Figure 3. Schematic illustration demonstrating how tilmicosin, by promoting neutrophil apoptosis, also called programmed cell death (PCD), may generate clinical benefits. By inducing neutrophil apoptosis, antibiotics such as tilmicosin prevent severe tissue damage secondary to leukocyte necrosis. Induction of neutrophil apoptosis confers anti-inflammatory properties to the antibiotic, without interfering with cell diapedesis, migration, and pulmonary infiltration.

Studies *in vivo* demonstrate that tilmicosin induces apoptosis in pulmonary neutrophils of calves experimentally infected with *M. haemolytica*, and that this effect is associated with a reduction of pro-inflammatory Leukotriene B₄ (LTB₄) in broncho-alveolar lavages (82). Indeed, significantly higher levels of apoptosis are detected in pure bronchoalveolar neutrophil populations of tilmicosin-treated calves versus untreated infected animals 3 h after the inoculation of live bacteria. In the untreated infected lungs, pro-inflammatory LTB₄ accumulated as the inflammatory reaction worsened, while tilmicosin treatment was associated with an inhibition of LTB₄ synthesis (82). Subsequent studies using circulating bovine neutrophils *in vitro* showed that this effect could be observed regardless of the presence or absence of live bacteria, clearly demonstrating that tilmicosin had direct pro-apoptotic properties, independently of variable bacterial numbers in the lungs (83,84). This effect is also associated with direct inhibition of LTB₄ in bovine neutrophils *in vitro* (84). Consistent with this immuno-modulating effect, recent data indicate that tilmicosin reduces the synthesis, by activated bovine alveolar macrophages *in vitro*, of another potent lipid mediator, prostaglandin E₂ (85). In these experimental settings, other antibiotics, including penicillin, ceftiofur, and oxytetracycline, or the corticosteroid dexamethasone, did not induce neutrophil apoptosis at similar concentrations (83). Moreover, exposure of bovine neutrophils to tilmicosin enhances

their subsequent phagocytic uptake by monocyte-derived macrophages (Figure 2), which bind to translocated phosphatidylserine on apoptotic neutrophils (83), further supporting the view that this effect may generate anti-inflammatory benefits (44–47,55). A recent field study demonstrated that treatment with tilmicosin, but not with ceftiofur, significantly increases the level of apoptosis in bronchoalveolar neutrophils of calves with subacute or chronic airway diseases (86). In contrast, another study was unable to detect significant levels of apoptosis in circulating neutrophils of tilmicosin-treated calves experimentally infected with *M. haemolytica* (87). However, the significance of these results remains difficult to interpret as apoptosis was only measured in circulating cells rather than in bronchoalveolar cells in that study (87). Indeed, the authors also failed to detect apoptosis in circulating neutrophils of animals given camptothecin, a known pro-apoptotic agent (87). Additional findings further confirmed the pro-apoptotic and anti-inflammatory properties of tilmicosin in pigs infected with *Actinobacillus pleuropneumoniae* (88). In summary, the induction of neutrophil apoptosis by tilmicosin has been observed in purified bovine cells as well as in live infected calves and in infected pigs, in the presence or absence of live bacteria, and the effect is at least in part drug-specific. Importantly, these effects occur without altering the antimicrobial properties of neutrophils, including cell chemotaxis, chemokinesis,

oxidative burst, and phagocytic activity (82,88). Taken together, these observations indicate that tilmicosin directly induces apoptosis in bovine neutrophils, and that this effect is associated with anti-inflammatory benefits in the infected lung via mechanisms that have not yet been fully elucidated (Figure 3). Moreover, tilmicosin directly reduces gene expression of cyclooxygenase-2 (COX-2) and inducible nitric oxide synthase (iNOS) in macrophages activated by bacterial lipopolysaccharide (89). Cyclooxygenase-2 activation is a powerful mediator of inflammation (12). Adding to these direct anti-inflammatory effects, findings from the same study also found that tilmicosin significantly decreased the production by these macrophages of pro-inflammatory eicosanoids and cytokines, 6-keto-PGF_{1 α} , PGE₂, TNF α , IL-1 β , and IL-6, respectively (89). Conversely, tilmicosin increased the synthesis of macrophage IL-10, a cytokine with well-established anti-inflammatory properties (89). Clearly, additional evidence is needed to unequivocally distinguish what components of the antibiotic's anti-inflammatory effects are directly due to the induction of neutrophil apoptosis, and which components reflect the anti-microbial properties of the drug. Studies using models of inflammation devoid of a microbial stimulus will help answer this question. Finally, recent research found that tilmicosin's immunomodulatory capacity may positively interact with dietary energy intake in cattle (90). Therefore, studies using macrolides such as tilmicosin may offer powerful model systems to investigate the mechanisms whereby promotion of neutrophil apoptosis and other processes may confer anti-inflammatory benefits to an antibiotic.

Conclusion

Ample evidence demonstrates that infection-induced inflammatory reactions directly and indirectly affect growth, feed intake, milk production, reproduction and metabolic health. Therefore, compounds that generate both antibacterial as well as anti-inflammatory effects are likely to be most effective at treating bacteria-induced inflammatory diseases. The role of neutrophil apoptosis in the final outcome of an inflammatory reaction is the topic of ardent research. It has been well established that neutrophil apoptosis is an injury-limiting disposal mechanism which, during severe inflammation, protects tissues against the potentially harmful contents of necrotic neutrophils. These effects are time and dose-dependent. For example, studies have found that macrolides may induce apoptosis in neutrophils without affecting their antimicrobial properties, including oxidative burst, pulmonary infiltration rates, and phagocytic activity (74,82,91,92). Other studies, mostly carried out *in vitro* and which used higher concentrations and/or longer experimental exposure times to the macrolides, indicate that these same parameters of neutrophil function may be altered upon treatment (75,93,94). Regardless, macrolides are well known for their immuno-modulating properties in addition to their antimicrobial effects. A number of reports suggest that these drugs inhibit pro-inflammatory cytokine production. Recent observations indicate that clinical concentrations of tilmicosin and other macrolides may induce neutrophil apoptosis, and that this effect exhibits at least some degree of drug specificity. Extensive studies *in vitro* and *in vivo*, using tilmicosin as a model, have demonstrated that antibiotic-induced neutrophil apoptosis provides anti-inflammatory benefits.

We postulate that macrolide/azalide-induced neutrophil apoptosis is responsible, at least in part, for their anti-inflammatory benefits, and that this phenomenon contributes to their clinical efficacy. It is too early to speculate on the molecular events responsible for the pro-apoptotic effects of macrolides, but one area of interest may be the characterization of how the antibiotics may modulate NF KappaB, a central transcription factor during inflammation, and one that was previously found to modulate programmed cell death. Elucidation of specific mechanisms whereby these phenomena occur may help design novel anti-infective compounds. Recent observations indicate that tilmicosin may offer a powerful model system to study these mechanisms at the cellular level as well as in their true clinical setting.

Acknowledgments

Parts of the experimental findings discussed in this chapter have been generated with the financial support of the Natural Sciences and Engineering Research Council of Canada, the Alberta Agricultural Research Institute, the Margaret Gunn Endowment for Animal Health Research, and Provel Division Eli Lilly Canada Inc.

References

- Husband AJ. The immune system and integrated homeostasis. *Immunol Cell Biol* 1995;73:377–382.
- Kenison DC, Elsasser TH, Fayer R. Tumor necrosis factor as a potential mediator of acute metabolic and hormonal responses to endotoxemia in calves. *Am J Vet Res* 1991;52:1320–1326.
- Axelrod J, Reisine TD. Stress hormones: Their interactions and regulation. *Science* 1984;224:452–459.
- Buret AG. How stress induces intestinal hypersensitivity. *Am J Pathol* 2006;168:3–5.
- Roth JA, Perino LJ. Immunology and prevention of infection in feedlot cattle. *Vet Clin N Am Food Anim Pract* 1998;14:233–256.
- Fair JM, Hansen ES, Ricklefs RE. Growth development stability and immune response in juvenile Japanese quails. *Proc R Soc Lond B* 1999;266:1735–1742.
- Hansen SA, Hasselquist D, Folstad I, Eridstad KE. Costs of immunity: Immune responsiveness reduces survival of a vertebrate. *Proc R Soc Lond B Biol Sci* 2004;271:925–930.
- Norris K, Evans MR. Ecological immunology: Life history trade-offs and immune defense in birds. *Behav Ecol* 2000;11:19–26.
- Pilorz V, Jaeckel M, Knudsen K, Trillich F. The cost of specific immune response in young guinea pigs. *Physiol Behav* 2005;85:205–211.
- Horak P, Ots I, Tegelman L, Moller AP. Health impact of phytoagglutinin-induced immune challenge on great tit nestlings. *Can J Zool* 2000;78:905–910.
- Nockels CF. Mineral alterations associated with stress, trauma, and infection, and the effects on immunity. *The Compendium* 1990;12:1133–1139.
- Hurley BP, McCormick BA. Multiple roles of phospholipase A₂ during lung infection and inflammation. *Infect Immun* 2008;76(6):2259–2272.

13. Korver DR, Klasing KC. Dietary fish oil alters specific and inflammatory immune responses in chicks. *J Nutr* 1997;127:2039–2046.
14. Liu YL, Li DF, Gong LM, Yi GF, Gaines AM, Carroll JA. Effects of fish oil supplementation on the performance and the immunological, adrenal, and somatotropic responses of weaned pigs after and *Escherichia coli* lipopolysaccharide challenge. *J Anim Sci* 2003;81:2758–2765.
15. Klasing KC. Protecting animal health and well-being: Nutrition and immune function. In: Recent advances in animal nutrition, Garnsworthy RC, Wiseman J, eds., Nottingham Univer Pr, 2005, pp 13–20.
16. Tracey KL, Wei H, Manogue K, et al. Cachetin/tumor necrosis factor induces cachexia, anemia, and inflammation. *J Exp Med* 1988;167:1211–1227.
17. Boisclair YR, Wang J, Shi J, Hurst KR, Oi GT. Role of the suppressor of cytokine signaling-3 in mediating the inhibitory effects of interleukin-1 beta on the growth hormone-dependent transcription of the acid-labile subunit gene in liver cells. *J Biol Chem* 2000;275:3841–3847.
18. Johnson RW. Inhibition of growth by pro-inflammatory cytokines: An integrated view. *J Anim Sci* 1997;75:1244–1255.
19. Gabler NK, Spurlock E. Intergrating the immune system with the regulation of growth and efficiency. *J Anim Sci* 2008; 86(E. Suppl.):E64–E74.
20. Klasing KC, Johnstone BJ. Monokines in growth and development. *Poult Sci* 1991;70:1781–1789.
21. Waldhorn MR, Overton TR. Effects of inflammation on nutrition: Is sickness causing weakness in your diet? In: 21st Ann SW Nutr and Manag Conf, Tempe, Arizona, USA. 2006: 164–173.
22. Burciaga-Robles LO, Step DL, Holland BP, et al. Effects of an intratracheal *Mannheimia haemolytica* challenge on intake and nitrogen balance in fed and fasted steers. 2006. [page on Internet]. Available from <http://www.ansi.okstate.edu/research/> Last accessed 23 July, 2009.
23. Walker RD, Hopkins FM, Schultz TW, McCracken MD, Moore RN. Changes in leukocyte populations in pulmonary lavage fluids of calves after inhalation of *Pasteurella haemolytica*. *Am J Vet Res* 1985;46:2429–2433.
24. Yoo HS, Maheswaran SK, Lin G, Townsend EL, Ames TR. Induction of inflammatory cytokines in bovine alveolar macrophages following stimulation with *Pasteurella haemolytica* lipopolysaccharide. *Infect Immun* 1995;63:381–388.
25. Tsai KS, Grayson MH. Pulmonary defense mechanisms against pneumonia and sepsis. *Curr Op Pulm Med* 2008;14:260–265.
26. Paape MJ, Bannerman DD, Zhao X, Lee JW. The bovine neutrophil: Structure and function in blood and milk. *Vet Res* 2003;34:597–627.
27. Squier MKT, Shenert AJ, Cohen JJ. Apoptosis in leukocytes. *J Leukoc Biol* 1995;57:2–10.
28. Henson PM, Johnston RB. Tissue injury in inflammation: Oxidants, proteinases, and cationic proteins. *J Clin Invest* 1987; 79:669–678.
29. Savill JS, Wyllie AH, Henson JE, Walport MJ, Henson PM, Haslett C. Macrophage phagocytosis of aging neutrophils in inflammation. Programmed cell death in the neutrophil leads to its recognition by macrophages. *J Clin Invest* 1989;83: 865–875.
30. Cox GJ, Crossely J, Xing Z. Macrophage engulfment of apoptotic neutrophils contributes to the resolution of acute pulmonary inflammation in vivo. *Am J Respir Cell Mol Biol* 1995;12: 232–237.
31. Lechtenberg KR, Shryock TR, Moore GM. Characterization of an *Actinobacillus pleuropneumoniae* seeder pig challenge-exposure model. *Am J Vet Res* 1994;55:1703–1709.
32. Kerr JFR, Wyllie AH, Currie AR. Apoptosis: A basic biological phenomenon with wide-ranging implications in tissue kinetics. *Br J Cancer* 1972;26:239–257.
33. Fadok VA, Voelker DR, Campbell PA, Cohen JJ, Bratton DL, Henson PM. Exposure of phosphatidylserine on the surface of apoptotic lymphocytes triggers specific recognition and removal by macrophages. *J Immunol* 1992;148:2207–2216.
34. Morris RG, Hargreaves AD, Duvall E, Wyllie AH. Hormone-induced cell death. II Surface changes in thymocytes undergoing apoptosis. *Am J Pathol* 1984;115:426–430.
35. Dransfield I, Buckle AM, Savill JS, McDowall A, Haslett C, Hogg N. Neutrophil apoptosis is associated with a reduction in CD16 expression. *J Immunol* 1994;153:1254–1260.
36. Haslett C. Granulocyte apoptosis and its role in the resolution and control of lung inflammation. *Am J Respir Crit Care Med* 1999;160:S5–S11.
37. Hughes J, Liu Y, VanDamme J, Savill J. Human glomerular mesangial cell phagocytosis of apoptotic neutrophils: Mediation by a novel CD36-independent vitronectin receptor/thrombospondin recognition mechanism that is uncoupled from chemokine secretion. *J Immunol* 1997;158:4389.
38. Hart SP, Ross JA, Ross K, Haslett C, Dransfield I. Molecular characterization of the surface of apoptotic neutrophils: Implications for functional deregulation and recognition by phagocytes. *Cell Death Differ* 2000;7:493–499.
39. Takizawa F, Tsuji S, Nagasawa S. Enhancement of macrophage phagocytosis upon iC3b deposition on apoptotic cells. *FEBS Lett* 1996;397:269–275.
40. Mevorach D, Mascarenhas JO, Gershow D, Elkon KB. Complement-dependent clearance of apoptotic cells by human macrophages. *J Exp Med* 1998;188:2313.
41. Ren Y, Stuart L, Lindberg FP, et al. Nonphlogistic clearance of late apoptotic neutrophils by macrophages: Efficient phagocytosis independent of $\beta 2$ integrins. *J Immunol* 2001;166: 4743–4750.
42. Schagat TL, Wofford JA, Wright JR. Surfactant Protein A enhances alveolar macrophage phagocytosis of apoptotic neutrophils. *J Immunol* 2001;166:2727–2733.
43. Savill J. Apoptosis in resolution of inflammation. *J Leukocyte Biol* 2000;61:375.
44. Savill J, Fadok VA. Corpse clearance defines the meaning of cell death. *Nature* 2000;407:784–788.
45. Meagher LC, Savill JS, Baker A, Fuller RW, Haslett C. Phagocytosis of apoptotic neutrophils does not induce macrophage release of thromboxane B2. *J Leukocyte Biol* 1992;52: 269–276.

46. Fadok VA, Bratton DL, Konowal A, Freed PW, Westcott JY, Henson PM. Macrophages that have ingested apoptotic cells in vitro inhibit proinflammatory cytokine production through autocrine/paracrine mechanisms involving TGF-beta, PGE2, and PAF. *J Clin Invest* 1998;101:890-899.
47. Godson C, Mitchell S, Harvey K, Petasis NA, Hogg N, Brady HR. Cutting edge: Lipoxins rapidly stimulate nonphlogistic phagocytosis of apoptotic neutrophils by monocyte-derived macrophages. *J Immunol* 2000;164:1663-1667.
48. Fadok VA, Bratton DL, Guthrie L, Henson PM. Differential effects of apoptotic versus lysed cells on macrophage production of cytokines: Role of proteases. *J Immunol* 2001;166:6847-6854.
49. Gilroy DW. Inflammatory resolution: New opportunities for drug discovery. *Nature Rev Drug Discov* 2004;3:401-416.
50. Haworth O, Cernadas M, Yang R, Serhan CN, Levy BD. Resolvin E1 regulates interleukin 23, interferon-gamma, and lipoxin A4 to promote the resolution of allergic airway inflammation. *Nature Immunol* 2008;9:873-879.
51. Schwab JM, Chiang N, Arita M, Serhan CN. Resolvin E1 and protectin D1 activate inflammation-resolution programmes. *Nature* 2007;447:869-874.
52. Serhan CN, Brain SD, Buckley CD, et al. Resolution of inflammation: State of the art, definitions and terms. *FASEB Journal* 2007;21:325-332.
53. Rossi AG, Hallett JM, Sawatzky DA, Teixeira MM, Haslett C. Modulation of granulocyte apoptosis can influence the resolution of inflammation. *Biochem Soc Trans* 2007;35:288-291.
54. Hallett JM, Leitch AE, Riley NA, Duffin R, Haslett C, Rossi AG. Novel pharmacological strategies for driving inflammatory cell apoptosis and enhancing the resolution of inflammation. *Trends Pharmacol Sci* 2008;29:250-257.
55. Rossi AG, Sawatzky DA, Walker A, et al. Cyclin-dependent kinases inhibitors enhance the resolution of inflammation by promoting inflammatory cell apoptosis. *Nature Med* 2006;12:1056-1064.
56. Labro MT. Anti-inflammatory activity of macrolides: A new therapeutic potential? *J Antimicrob Chemother* 1998;41(Suppl.B):37-46.
57. Wales D, Woodhead M. The anti-inflammatory effects of macrolides: Erythromycin and clarithromycin attenuate cytokine-induced endothelin-1 expression in human bronchial epithelial cells. *Thorax* 1999;54(Suppl.2):S58-S62.
58. Ianaro A, Ialenti A, Maffia P, et al. Anti-inflammatory activity of macrolide antibiotics. *J Pharmacol Exp Therapeut* 2000;292:156-163.
59. Rubin BK, Tamaoki J. Macrolide antibiotics as biological response modifiers. *Curr Opin Invest Drugs* 2000;1:169-172.
60. Cervin A. The anti-inflammatory effects of erythromycin and its derivatives, with special reference to nasal polyposis and chronic sinusitis. *Acta Otolaryngol* 2001;121:83-92.
61. Azuma A. Roles of macrolides in treatment of lung injury. In: Parnham MJ, Rubin BK, Tamaoki J, eds. *Antibiotics as Anti-inflammatory and Immunomodulatory Agents*. Basel: Birkhaeuser (Basel, Springer), 2005:219-226.
62. Peeters TL. Erythromycin and other macrolides as prokinetic agents. *Gastroenterology* 1993;105:1886-1899.
63. Mikasa K, Sawaki M, Kita E, et al. Significant survival benefits to patients with advanced non-small-cell lung cancer from treatment with clarithromycin. *Chemotherapy* 1997;43:288-296.
64. Yatsunami J, Fukuno Y, Nagat M, et al. Antiangiogenic and antitumor effects of 14-membered macrolides on mouse B16 melanoma cells. *Clin Exp Metastasis* 1999;17:361-367.
65. Rubin BK, Druce H, Ramirez OE, Palmer R. Effect of clarithromycin on nasal mucus properties in healthy subjects and in patients with purulent rhinitis. *Am J Respir Crit Care Med* 1997;155:2018-2023.
66. Tamaoki J, Takemyama K, Yamawaki I, Kondo M, Konno K. Lipopolysaccharide-induced goblet cell hypersecretion in the guinea pig trachea: Inhibition by macrolides. *Am J Physiol* 1997;272:L15-L19.
67. Woo PC, Tsoi HW, Wong LP, Leung HC, Yuen KY. Antibiotics modulate vaccine-induced humoral immune response. *Clin Diagn Lab Immunol* 1999;6:832-837.
68. Sassa K, Mizushima Y, Kobayashi M. Differential modulatory effects of clarithromycin on the production of cytokines by a tumor. *Antimicrob Agents Chemother* 1999;43:2787-2789.
69. Aoshiba K, Nagai A, Konno K. Erythromycin shortens neutrophil survival by accelerating apoptosis. *Antimicrob Ag Chemother* 1995;39:872-877.
70. Inamura K, Ohta N, Fukaze S, Kasajima N, Aoyagi M. The effects of erythromycin on human peripheral neutrophil apoptosis. *Rhinology* 2000;38:124-129.
71. Fisher CD, Zvaigzne C, Morck DW, Lucas MJ, Robb EJ, Buret AG. Tulathromycin inhibits NF-kB signaling and induces apoptosis in bovine neutrophils in caspase-3-dependent fashion. *FASEB J* 2008;22:1b591.
72. Scorneaux B, Shryock TR. Intracellular accumulation, subcellular distribution, and efflux of tilmicosin in bovine mammary, blood, and lung cells. *J Dairy Sc* 1999;82:1202-1212.
73. Bonnet M, van der Auwera P. In vitro and in vivo intraleukocytic accumulation of azithromycin (CP-62,993). *Antimicrob Ag Chemother* 1992;36:1302-1309.
74. Koch CC, Esteban DJ, Chin AC, et al. Apoptosis, oxidative metabolism and interleukin-8 production in human neutrophils exposed to azithromycin: Effects of *Streptococcus pneumoniae*. *J Antimicrob Chemother* 2000;46:19-26.
75. Khair OA, Devalia JL, Abdelaziz MM. Effects of erythromycin on *H. influenzae* endotoxin-induced release of IL-6, IL-8, and sICAM-1 by cultured human bronchial epithelial cells. *Eur Respir J* 1995;8:1451-1457.
76. Gorham PE, Carroll LH, McAskill JW. Tilmicosin as a single injection treatment for respiratory disease of feedlot cattle. *Can J Vet Res* 1990;31:826-829.
77. Moore GM, Mowrey DH, Tonkinson LV, Lechtenberg KF, Schneider JH. Efficacy dose determination study of tilmicosin phosphate in feed for control of pneumonia caused by *Actinobacillus pleuropneumoniae* in swine. *Am J Vet Res* 1996;57:220-223.
78. Jordan WH, Byrd RA, Cochrane RL. A review of the toxicology of the antibiotic Micotil 300. *Vet Hum Toxicol* 1993;35:151-158.

79. Morck DW, Merrill JK, Gard MS. Treatment of experimentally induced pneumonic pasteurellosis of young calves with tilmicosin. *Can J Vet Res* 1997;61:187–192.
80. Moore GM, Basson RP, Tonkinson LV. Clinical field trials with tilmicosin phosphate in feed for the control of naturally acquired pneumonia caused by *Actinobacillus pleuropneumoniae* and *Pasteurella multocida* in swine. *Am J Vet Res* 1996;57:224–227.
81. Diarra MS, Malouin F, Jacques M. Postantibiotic and physiological effects of tilmicosin, tylosin, and apramycin at sub-minimal and suprainhibitory concentrations on some swine and bovine respiratory tract pathogens. *Int J Antimicrob Ag* 1999;12:229–237.
82. Chin A, Morck DW, Merrill JK, et al. Anti-inflammatory benefits of tilmicosin in calves with *P. haemolytica*-infected lungs. *Am J Vet Res* 1998;59:765–771.
83. Chin A, Lee WD, Murrin KA, et al. Tilmicosin induces apoptosis in bovine neutrophils in the presence or in the absence of *P. haemolytica* and promotes neutrophil phagocytosis by macrophages. *Antimicrob Ag Chemother* 2000;44:2465–2470.
84. Lee WD, Flynn AN, LeBlanc JM, et al. Tilmicosin-induced bovine neutrophil apoptosis is cell-specific and downregulates spontaneous LTB₄ synthesis without increasing Fas expression. *Vet Res* 2004;35:213–224.
85. Lakritz J, Tyler JW, Marsh AE, Romesburg-Cockrell M, Smith K, Holle JM. Tilmicosin reduces lipopolysaccharide-stimulated bovine alveolar macrophage prostaglandin E₂ production via a mechanism involving phospholipases. *Vet Ther* 2002;3:7–21.
86. Weinhold U, Hofmann W, Mulling C, Budras KD. Untersuchungen von Bronchialzellsedimenten lungenkranker Kaelber waehrend der Behandlung mit den Antibiotika Tilmicosin und Ceftiofur auf das Vorkommen der Apoptosis der neutrophilen Granulozyten, *Tieraerztl. Umschau* 2003;58:191–199.
87. Fajt VR, Apley MD, Roth JA, et al. The effects of danofloxacin and tilmicosin on neutrophil function and lung consolidation in beef heifer calves with induced *Pasteurella (Mannheimia) haemolytica* pneumonia, *J Vet Pharmacol Therap* 2003;26:173–179.
88. Nerland EM, Leblanc JM, Fedwick JP, et al. Oral Tilmicosin induces leukocyte apoptosis, reduces Leukotriene B₄, and attenuates inflammation in the *Actinobacillus pleuropneumoniae*-Infected Porcine Lung. *Am J Vet Res* 2005;66:100–107.
89. Cao XY, Dong M, Shen JZ, et al. Tilmicosin and tylosin have anti-inflammatory properties via modulation of COX-2 and iNOS gene expression and production of cytokines in LPS-induced macrophages and monocytes. *Int J Antimicrob Ag* 2006;27:431–438.
90. Reuter RR, Carroll JA, Dailey JW, Cook BJ, Galyean ML. Effects of dietary energy source and level and injection of tilmicosin phosphate on immune function in lipopolysaccharide-challenged beef steers. *J Anim Sci* 2008 (April 11; epub ahead of print).
91. Levert H, Gressier B, Brunte C, et al. Time and concentration dependent influence of dirithromycin on neutrophils oxidative burst. *J Antibiot* 1999;52:127–133.
92. Kanota JI, Iwashita T, Matsubara Y, et al. Inhibitory effect of erythromycin on superoxide anion production by human neutrophils primed with granulocyte-colony stimulating factor. *Antimicrob Ag Chemother* 1998;42(7):1866–1867.
93. Lin HC, Wang CH, Liu CY, Yu CT, Kuo HP. Erythromycin inhibits β 2-integrins (CD11b/CD18) expression, interleukin-8 release and intracellular oxidative metabolism in neutrophils. *Respir Med* 2000;94:654–660.
94. Takisawa H, Desaki M, Ohtoshi T. Erythromycin and clarithromycin attenuate cytokine-induced endothelin-1 expression in human bronchial epithelial cells. *Eur Respir J* 1998;12:57–63.
95. Frost RA, Nystrom GJ, Lang CH. Lipopolysaccharide regulates pro-inflammatory cytokine expression in mouse myofibroblasts and skeletal muscle. *Am J Physiol Integr Comp Physiol* 2002;283:R698–R709.
96. Schrick FN, Hockett ME, Saxton AM, Lewis MJ, Dowlen HH, Oliver SP. Influence of subclinical mastitis during early lactation on reproductive parameters. *J Dairy Sci* 2001;84:1407–1412.
97. Hockett ME, Hopkins FM, Lewis MJ, et al. Endocrine profiles of dairy cows following experimentally induced clinical mastitis during early lactation. *Anim Reprod Sci* 2000;58:241–251.
98. Rajala-Schultz PJ, Grohn YT, McCulloch CE, Guard CL. Effects of clinical mastitis on milk yield in dairy cows. *J Dairy Sci* 1999;82:1213–1220.
99. Shuster DE, Kehrli ME, Baumrucker CR. Relationship of inflammatory cytokines, growth hormone, and insulin-like growth factor-1 to reduced performance during infectious disease. *Proc Soc Exp Biol Med* 1995;210:140–149.
100. Miyanochara T, Ushikai M, Matsune S, Ueno K, Katahira S, Kurono Y. Effects of clarithromycin on cultured human nasal epithelial cells and fibroblasts. *Laryngoscope* 2000;110:126–131.
101. Kawasaki S, Takisawa H, Ohtoshi T. Roxithromycin inhibits cytokine production by and neutrophil attachment to human bronchial epithelial cells in vitro. *Antimicrob Ag Chemother* 1998;42:1499–1502.
102. Fujita K, Shimizu T, Majima Y, Sakakura Y. Effects of macrolides on interleukin-8 secretion from human nasal epithelial cells. *Eur Arch Otorhinolaryngol* 2000;257:199–204.
103. Schultz M, Speelman P, Zaat S. Erythromycin inhibits TNF-alpha and IL-6 production induced by heat-killed *S. pneumoniae* in whole blood. *Antimicrob Ag Chemother* 1998;42:1605–1609.
104. Schultz MJ, Speelman P, Hack CE, Buurman WA, van Deventer SJH, van der Poll T. Intravenous infusion of erythromycin inhibits CXC chemokine production, but augments neutrophil degranulation in whole blood stimulated with *S. pneumoniae*. *J Antimicrob Ag Chemother* 2000;46:235–240.
105. Ichikawa Y, Ninomiya H, Koga H. Erythromycin reduces neutrophil-derived elastolytic-like activity in the lower respiratory tract of bronchiolitis patients. *Am Rev Resp Dis* 1992;146:196–203.

Characterization of *Salmonella* Typhimurium isolates associated with septicemia in swine

Nadia Bergeron, Jonathan Corriveau, Ann Letellier, France Daigle, Sylvain Quessy

Abstract

Salmonella Typhimurium is frequently isolated from pigs and may also cause enteric disease in humans. In this study, 33 isolates of *S. Typhimurium* associated with septicemia in swine (CS) were compared to 33 isolates recovered from healthy animals at slaughter (WCS). The isolates were characterized using phenotyping and genotyping methods. For each isolate, the phage type, antimicrobial resistance, and pulsed-field gel electrophoresis (PFGE) DNA profiles were determined. In addition, the protein profiles of each isolate grown in different conditions were studied by Coomassie Blue-stained sodium dodecyl sulfate polyacrylamide gel electrophoresis (SDS-PAGE) and immunoblot. Various phage types were identified. The phage type PT 104 represented 36.4% of all isolates from septicemic pigs. Resistance to as many as 12 antimicrobial agents, including some natural resistances, was found in isolates from CS and WCS. Many genetic profiles were identified among the PT 104 phage types. Although it was not possible to associate one particular protein with septicemic isolates, several highly immunogenic proteins, present in all virulent isolates and in most isolates from clinically healthy animals, were identified. These results indicated that strains associated with septicemia belong to various genetic lineages that can also be recovered from asymptomatic animals at the time of slaughter.

Résumé

Salmonella Typhimurium est souvent isolée de porcs et peut causer une gastro-entérite chez l'humain. Dans cette étude, des isolats provenant de porcs septicémiques (ASC) (n = 33) ont été comparés à des isolats provenant de porcs sains à l'abattoir (SSC) (n = 33). Ces isolats ont été caractérisés par des méthodes phénotypiques et génotypiques. Le type phagique, le profil d'antibiorésistance et l'analyse des profils d'ADN en gel d'électrophorèse en champ pulsé (PFGE) ont été déterminés pour chacun des isolats. Le profil des protéines pour chacun des isolats, cultivés dans différentes conditions de croissance, a aussi été déterminé par la méthode Coomassie Blue-stained sodium dodecyl sulfate polyacrylamide gel electrophoresis (SDS-PAGE) et l'immunogénicité des protéines a été évaluée par immunobuvardage. Différents types phagiques ont été identifiés parmi les isolats. Chez les souches provenant de porcs septicémiques, le type phagique PT 104 représentait 36,4 % des isolats. Les isolats pouvaient être résistants à 12 antimicrobiens, si l'on considère aussi les résistances naturelles, autant chez les souches ASC que celles appartenant au groupe SSC. Parmi les souches PT 104, plusieurs groupes génétiques ont été identifiés. Il n'a toutefois pas été possible d'identifier une protéine en particulier chez le groupe d'isolats provenant de porcs septicémiques. Il a été possible d'identifier des protéines immunogènes chez tous les isolats virulents et chez la majorité des isolats provenant de porcs sains. Ces résultats indiquent que les souches associées aux porcs septicémiques proviennent de lignées génétiques variées dont certaines peuvent être aussi retrouvées chez les porcs asymptomatiques au moment de l'abattage.

(Traduit par les auteurs)

Introduction

Salmonella is an important problem in both humans and animals worldwide. More than 2500 serotypes have been isolated in the *Salmonella* genus: most are potential human pathogens, but only a few serotypes have been regularly associated with human infections. *Salmonella* cause diseases in humans ranging from a mild gastro-enteritis to a systemic disease that can result in death. *Salmonella* Enteritidis and Typhimurium are quantitatively the most important

causative agents in human foodborne illnesses. For the serovar Typhimurium alone, more than 200 definitive phage types have been identified. The phage type PT 104 causes particular concerns because of its increasing prevalence and the presence of resistance genes to many antibiotics (1).

Although most animals may carry the bacterium without exhibiting clinical signs, in pigs, *Salmonella* are associated with diseases and economic losses. Swine may represent a reservoir for human infection (2). The infection of pigs with the serovar

Chaire de recherche en salubrité des viandes (CRSV), Groupe de recherche sur les maladies infectieuses du porc (GREMIP), Département de pathologie et microbiologie, Faculté de médecine vétérinaire, Université de Montréal, Saint-Hyacinthe, Québec (Bergeron, Corriveau, Letellier, Quessy); Département de microbiologie et immunologie, Faculté de médecine, Université de Montréal, Montréal, Québec (Daigle).

Address all correspondence to Dr. Sylvain Quessy; telephone: (450) 773-8521 ext. 8398; fax: (450) 778-8157; e-mail: sylvain.quessy@umontreal.ca
Dr. Quessy's current address is Faculté de médecine vétérinaire, Université de Montréal, CP 5000, Saint-Hyacinthe, Québec J2S 7C6.

This paper is part of a PhD thesis by Nadia Bergeron.

Received April 4, 2008. Accepted January 5, 2009.

Choleraesuis is usually associated with systemic disease, whereas infection with the serovar Typhimurium is associated with enteric disease. However, septicemic episodes of *S. Typhimurium*, associated with severe clinical signs and sudden death, have been observed (3,4). In these animals, the serovar Typhimurium can be isolated from multiple organs; however, at slaughter, *S. Typhimurium* is one of the most frequently isolated serovar in apparently healthy pigs (5).

Infections caused by septicemic strains of *S. Typhimurium* can be associated with significant mortality in finishing pigs. Since previous studies showed persistence of strains in various tissues for many days following infection, the presence of these strains in finishing animals also represents a food safety concern (6). Thus, it is important to better characterize these isolates in order to understand the pathogenesis of infection and develop appropriate control measures. Asymptomatic animals may, following a stress period, begin to shed the bacteria and contaminate other animals during transportation and in the lairing pen at the slaughterhouse. During evisceration procedures, direct or cross-contamination of meat may result in human foodborne infections.

Studies on the diversity of salmonellae indicate that generally *Salmonella* species have low genetic diversity. To date, various phenotypic methods have been used to characterize this bacterium, including phage typing, biotyping, and antimicrobial resistance profiling (7,8). Genotyping methods such as pulsed-field gel electrophoresis (PFGE) (8,9), amplified-fragment length polymorphism (AFLP) (10), plasmid profiling (7–9), IS200 restriction fragment length polymorphism (RFLP) (11), and ribotyping (9) were also used. The current “gold standard” method of choice for molecular typing of *Salmonella* is PFGE (12).

Some phage types such as PT 104 of *S. Typhimurium* are known to harbor genes encoding resistance to many antibiotics. Multidrug-resistant PT 104 is an important human and animal pathogen that is widespread in western and eastern Europe, North America, and the Middle East (13). For instance, PT 104 are very often found to be resistant to ampicillin, chloramphenicol, streptomycin, sulfonamides, and tetracycline (R-Type AmpChlStrSulTet) (1,8,13,14). Multiple resistance to antimicrobial agents is an important concern for human health.

The aim of this study was to compare, using phenotypic and genotypic methods, isolates of *S. Typhimurium* associated with septicemia in swine and isolates recovered from clinically healthy pigs at slaughter.

Materials and methods

Bacterial isolates

Salmonella isolates ($n = 33$) recovered from extra-intestinal organs and/or feces of dead pigs (CS; clinical signs) (with diagnosis of salmonellosis) and submitted for necropsy were obtained from Dr. S. Messier (Faculté de médecine vétérinaire, Université de Montréal, Saint-Hyacinthe, Québec). Isolates ($n = 33$) from healthy pigs (WCS; without clinical signs) were collected at slaughter from animals with no macroscopic lesions (5). Unless otherwise noted, bacterial cultures were carried out at 37°C in Luria-Bertani (LB)

Muller Broth (Difco Laboratories, Detroit, Michigan, USA) or on LB containing 1.5% (w/v) agar. Isolates were stored at –70°C in LB supplemented with 35% (v/v) glycerol.

Serotyping and phage typing

Isolates were serotyped and phage typed at the Laboratoire d'Épidémiologie Animale du Québec (LEAQ) in Saint-Hyacinthe, Québec or at the Laboratory for Foodborne Zoonoses, Public Health Agency of Canada, Guelph, Ontario.

Antimicrobial resistance

Resistance of all isolates to various antimicrobial agents was determined by the Kirby-Bauer disk diffusion method following criteria established by the Clinical and Laboratory Standards Institute's (CLSI) guidelines (15). The range of antimicrobial agents tested covers many classes of antibiotics: amikacin (30 µg/disk) (Amk), amoxicillin-clavulanic acid (20/10 µg/disk) (Amc), ampicillin (10 µg/disk) (Amp), bacitracin (10 IU/disk) (Bac), cefoxitin (30 µg/disk) (Fox), ceftiofur (30 µg/disk) (Ctf), ceftriaxone (30 µg/disk) (Cro), cephalothin (30 µg/disk) (Cef), chloramphenicol (30 µg/disk) (Chl), ciprofloxacin (5 µg/disk) (Cip), clindamycin (2 µg/disk) (Cli), enrofloxacin (5 µg/disk) (Enr), erythromycin (15 µg/disk) (Ery), gentamicin (10 µg/disk) (Gen), kanamycin (30 µg/disk) (Kan), nalidixic acid (30 µg/disk) (Nal), neomycin (30 µg/disk) (Neo), quinupristin/dalfopristin (4.5/10.5 µg/disk) (Q/D), streptomycin (10 µg/disk) (Str), sulfisoxazole (250 µg/disk) (Sul), tetracycline (30 µg/disk) (Tet), trimethoprim-sulfamethoxazole (1.25/23.75 µg/disk) (Sxt), and vancomycin (30 µg/disk) (Van). Results were interpreted according to the CLSI guidelines (15,16) or in accordance with the manufacturer's instructions. The diameter zone of apramycin (15 µg/disk) (Apr) was interpreted in accordance with Mathew et al (17). All the antimicrobial agents were purchased from Oxoid (Nepean, Ontario) except ceftriaxone and sulfoxazole which were purchased from Becton Dickinson (BD-Canada, Oakville, Ontario). *Escherichia coli* ATCC 25922 was used as the standard reference strain. In this study, isolates with intermediate phenotype were grouped with susceptible isolates to prevent over-estimation of occurrence of resistance.

Growth conditions for protein production

The growth conditions known to encourage the *Salmonella* invasion process include anaerobiosis, high osmolarity, late-log-phase growth, and neutral pH (18,19). Aerobic growth conditions for bacterial cultures were induced by vigorous agitation (200 rpm) of tubes. Anaerobic conditions were induced by static incubation in an anaerobe jar equipped with a pressure gauge (Oxoid) and supplied with a gas generator envelope and a resazurin strip (Oxoid); the gauge and strip served to confirm the establishment of an anaerobic environment. The effect of high osmolarity (0.3 M NaCl) was assessed by the use of LB or nutrient broth (NB) (Difco Laboratories) supplemented with NaCl. The effect of iron was tested by supplementing NB with 40 µM FeSO₄ (Sigma-Aldrich Canada, Oakville, Ontario) and depleting iron with 100 µM 2,2'-dipyridyl (Sigma). To analyze the effect of pH, strains were grown in NB buffered with 0.1 M MES [2-(*N*-morpholino)ethanesulfonic acid] (Sigma) at pH of 5.0 or 6.5.

SDS-PAGE

LB agar plates were first inoculated with bacteria stored in frozen glycerol and incubated at 37°C overnight. A 50-mL sample of one of the media described herein was inoculated with single colonies and incubated for 20 h at 37°C. Optical density (OD) of ~0.6 at 600 nm was obtained. The bacterial suspensions were centrifuged and resuspended in PBS and sonicated twice, for 2 min each time, on ice (Sonics Material, Danbury, Connecticut, USA). The suspension was centrifuged again for 20 min at 4°C. Proteins present in the supernatant were harvested, mixed with an equal volume of buffer to insure solubility, boiled 5 min and separated by SDS-PAGE standard technique in 12.5% polyacrylamide vertical slab gel with 4.5% stacking gel. Gels were stained with Coomassie brilliant blue stain (Bio-Rad Laboratories, Mississauga, Ontario).

Production of antisera

Pigs ($n = 5$) were injected intramuscularly once a week for 6 wk with 1 mL of a formalin-killed (0.5% v/v, 18 h) suspension of 10^9 CFU/mL of a field isolate serovar Typhimurium PT 104 (obtained from a septicemic pig) and grown overnight in NB. Pigs were euthanized 1 wk later and blood was collected. All procedures using animals were done in accordance with guidelines of the Guide to the Care and Use of Experimental Animals of the Canadian Council on Animal Care.

Western blotting

Following SDS-PAGE, proteins were transferred to the nitrocellulose membrane (Bio-Rad) by electroblotting in a transblot apparatus (Bio-Rad) with methanol-Tris-glycine buffer according to the standard technique. Casein (2%, w/v) in Tris-buffered saline was used to block unreacted sites and the nitrocellulose membrane was incubated overnight with 1:400 (v/v) dilutions of the pig antisera raised against whole cell antigen (see above). After washing in Tris-NaCl, the membrane was incubated with a peroxidase-conjugated goat anti-swine IgG (heavy + light chains) (Jackson ImmunoResearch Laboratories, West Grove, Pennsylvania, USA) for 60 min at a dilution of 1:2000 in 2% (w/v) casein in Tris-NaCl. After repeated washings, the presence of bound antigens was visualized by reacting the nitrocellulose membrane with 0.06% 4-chloro-1-naphthol (Sigma) in cold (-20°C) methanol mixed to 0.02% H₂O₂ in Tris-NaCl. Apparent molecular weights were calculated by comparison with standards of known molecular weight (Bio-Rad).

Pulsed-field gel electrophoresis (PFGE)

Genomic DNA was prepared in agarose gel plugs from an overnight bacterial culture on LB agar using a modified protocol (20). Briefly, bacterial cultures were resuspended to obtain an OD of 1.4 at 610 nm. Bacterial culture and Seakem Gold agarose 1.5% (Cambrex Corporate, East Rutherford, New Jersey, USA) were mixed in a mold to form plugs. The agarose plugs were incubated 2 h at 54°C in lysis solution and proteinase K (Quiagen, Mississauga, Ontario). Cell debris and any excess proteinase K were removed by washing twice with millipore water and 4 times with Tris-EDTA buffer. Genomic DNA was digested with restriction endonucleases,

SpeI (recognition sequence ACTAGT) and *XbaI* (recognition sequence TCTAGA) (Invitrogen Canada, Burlington, Ontario).

The PFGE was performed using a CHEF DR II system (Bio-Rad) on a horizontal agarose gel electrophoresis in a 1% (w/v) SeaKem Gold agarose gel at 6 V/cm with 0.5× Tris-Borate electrophoresis buffer. Gels were stained with SYBR Safe DNA Gel Stain (Invitrogen) and photographed on a UV transilluminator. *Salmonella* Braenderup "Universal Marker" was used as the reference marker (21). The PFGE patterns obtained were analyzed by the Bionumerics Software (Applied Maths, Kortrijk, Belgium) using algorithm for clustering and the unweighted pair group method with arithmetic mean (UPGMA) tree-building approach with optimization of 2.0% and 4.0% and 3.5% for position tolerance for *XbaI* and *SpeI*, respectively. Visual inspection of the patterns was performed as a final validation step.

Statistical analysis

Computer software (SAS version 9.1; SAS Institute, Cary, North Carolina, USA) was used to analyze the data. Univariate analysis using the exact chi-squared test examined the relationship between various categorical variables. The comparison was made between the isolates from septicemic pigs and isolates from healthy pigs. Another comparison was made between the isolates from phage type PT 104 and isolates from the group of other phage types. The statistical significance was set at $P < 0.05$.

Results

Typing of isolates

Salmonella Typhimurium was the only serovar identified in this study out of the 33 isolates from CS. When isolates were phage typed, it was found that 36.4% (12/33) belonged to PT 104 while the others belonged to 11 different phage types. For the 33 isolates from WCS, the prevalence of strains belonging to PT 104 was 51.5% (17/33) while the second most prevalent type was PT 193 (8/33). No association was found between the origin of the isolates and the phage type PT 104 ($P = 0.32$). Only 3 isolates could not be phage typed.

Salmonella isolates were found in extra-intestinal organs or feces from pigs. Animals came from a total of 55 farms, 7 farms were sampled more than once. Among these 7 farms, isolates from both CS and WCS were found in 3 farms.

Antimicrobial susceptibility testing

In this study, 24 antimicrobial agents (AMA) were tested. Among those showing resistance, 5 AMA were considered as natural resistance (Bac, Cli, Ery, Q/D, Van). All isolates were resistant to up to 7 AMA among the 19 remaining AMA tested. Six isolates in both groups showed no resistance, but none of these were PT 104. Among all isolates, 19 different antimicrobial resistance profiles were identified. Twelve different profiles were observed in isolates from CS, 13 different profiles were found in isolates from WCS while 6 profiles were common to both CS and WCS isolates. The most prevalent resistance profile (Amp, Chl, Neo, Tet, Kan, Bac, Cli, Ery, Q/D, Van, Str, Sul) was found in both CS and WCS.

Among the *S. Typhimurium* PT 104 isolates from CS, 3 different profiles were observed, whereas among PT 104 isolates from WCS, 4 antimicrobial resistance profiles were found. Two profiles were common in PT 104 isolates from both CS and WCS. Among the 3 non-typable isolates 2 showed the same antimicrobial resistance profiles.

PT 104 isolates from CS were significantly more resistant to some AMA compared with other phage types from CS: Amp ($P = 0.0002$), Chl ($P < 0.0001$), Kan ($P = 0.009$), Neo ($P = 0.009$), Str ($P = 0.0008$), and Sul ($P = 0.01$). PT 104 isolates from WCS were also more resistant to some AMA versus other phage types: Amp ($P = 0.0003$), Chl ($P < 0.0001$), Kan ($P = 0.02$), and Str ($P = 0.002$). Other phage types were more resistant than PT 104 in WCS: Gen ($P = 0.02$).

Protein profiles by SDS-PAGE and Western blotting

In order to reflect the various environmental conditions encountered by *Salmonella* during colonization and invasion of the host, different growth conditions were used to study the protein profiles of the 2 groups of isolates. For a given environmental growth condition, protein profiles of isolates associated with septicemia and those isolated from clinically healthy pigs were similar (data not shown). It was not possible to relate any proteins to septicemic isolates; however, several different patterns were expressed when a given isolate was grown under different environmental conditions (data not shown). For instance, when grown in iron-restricted media, expression of a ~33 kDa protein was observed on Western blots for all isolates in both groups of pigs. In addition, few immunogenic proteins were found to be expressed in all growth conditions.

Pulsed-field gel electrophoresis (PFGE)

A total of 17 different PFGE profiles were found when *Xba*I was used. Twelve different profiles were observed for isolates from CS compared with 11 profiles for isolates from WCS. Six profiles were common among isolates from CS and WCS. Profile 1 was significantly more prevalent in isolates from CS compared with WCS ($P = 0.03$). A total of 19 different profiles were found with *Spe*I. Using *Spe*I, 11 different profiles were identified in isolates from CS, while 13 profiles were identified from isolates from WCS. Five profiles were common to isolates of both CS and WCS. Profile 20 was significantly more prevalent among isolates from WCS compared with CS ($P = 0.02$).

For *Xba*I, among the *S. Typhimurium* PT 104 isolates from CS, 7 different genotypes were observed, profile 2 being significantly more prevalent in PT 104 isolates compared with other phage types ($P < 0.0001$). Profile 1 was significantly more prevalent in isolates from other phage types compared with PT 104 ($P = 0.03$). Profiles 2, 7, 16, and 17 for isolates from CS and profiles 2, 5, and 11 for isolates from WCS were found in PT 104 isolates only. The 3 non-typable isolates harboured different profiles for *Xba*I.

For *Spe*I, among the *S. Typhimurium* PT 104 isolates from CS, 8 different profiles were found; none more frequently than another. It was not possible to identify a major profile with *Spe*I in the group of PT 104 isolates and in the group of other phage types. Profiles 30 and 35 for isolates from CS and profiles 29, 30, and 34 for isolates from WCS were found in PT 104 isolates. Only 2 of the 3 isolates, which could not be typed, had the same *Spe*I profile. Summaries of the results are presented in Tables I and II.

Discussion

In this study, PT 104 isolates were compared with all other phage types because of their antimicrobial resistance, recognition as food-borne pathogens, greater virulence, suggested clonal origin, and zoonotic potential (9,13,22). Phage type PT 104 was found to be the most prevalent phage type in characterized isolates. This agrees with other studies that reported similar results in Ontario, the United States, and France in isolates from apparently healthy animals (23–25). However, previous studies from Quebec and Spain indicated that PT 104 was the second phage in importance after PT 108 and PT 193, respectively (4,26).

Phage type PT 104 was found in 31.4% (11/35) of *S. Typhimurium* isolates from apparently healthy food-producing animals in Japan, as determined by the Japanese Veterinary Antimicrobial Resistance Monitoring Program (1999–2001) (27). It was found that the percentage of PT 104 isolates was lower in animals from WCS, as opposed to what was observed in our study. On the other hand, another similar study completed by the same group between 2002 and 2005 showed a significant decrease ($P < 0.01$) to 4.1% (2/48) of the PT 104 *S. Typhimurium* isolates (28).

In the current study, PT 104 isolates were generally found to be more resistant to antimicrobial agents than other phage types but it was not possible to associate this phage type to pigs with CS. Many authors from various countries reported that most isolates of *S. Typhimurium* PT 104 are resistant to ampicillin, chloramphenicol, streptomycin, sulfonamides, and tetracycline (1,8,13,14,24,29,30) and that some isolates are also kanamycin resistant. In our study, 89.7% (26/29) of PT 104 isolates possess the complete pentaresistance profile; among these isolates, 69.0% (20/29) showed additional resistance to kanamycin and neomycin. It has been described that the pentaresistance genes in PT 104 isolates are situated on the chromosome and located on integrons, and thus rarely horizontally transmissible (13,31–33). The origin of DNA containing the pentaresistance genes is unknown, previous studies proposing a possible clonal dissemination of the *S. Typhimurium* PT 104 in the population (9,22,30,31). Our antimicrobial resistance results suggested that other genetic lineages can be found in PT 104 isolates from swine in Canada, particularly in healthy animals.

Bacteria obtained from infected animals are routinely examined by SDS-PAGE and immunoblotting to search for the presence of putative virulence determinants. In our study, we had the opportunity to compare isolates from diseased animals to isolates from healthy animals. Although we made the assumption that isolates from healthy animals were less likely to express some virulence factors, we cannot rule out the possibility that some of the isolates from healthy animals were in fact isolates from animals that had recovered from disease. However, since the occurrence of outbreaks associated with *S. Typhimurium* is quite low in Quebec, it seemed reasonable to expect that isolates from healthy animals were less likely to be virulent. Nevertheless, although differences in protein profiles were observed when strains were grown in different environmental growth conditions, it was not possible to associate a particular protein to septicemic strains. On the other hand, we observed the expression of a ~33 kDa protein when isolates were grown under iron-limiting conditions. Expression of a protein

Table I. Antimicrobial resistance and pulsed-field gel electrophoresis (PFGE) profiles of *S. Typhimurium* PT 104 isolates from diseased and healthy pigs

Antimicrobial profile	PFGE (<i>Xba</i> I) ^{ab}	PFGE (<i>Spe</i> I) ^{ab}
Amp, Chl, Neo, Tet, Kan, Bac, Cli, Ery, Q/D, Van, Str, Sul	5 ^{aa} 17 ^a 1 ^{ab} 2 ^{aaaabbbb}	23 ^a 24 ^{aa} 25 ^a 35 ^a 18 ^{ab} 19 ^{abb} 30 ^{ab}
	3 ^{bbb} 6 ^{bb} 7 ^b 9 ^b	20 ^{bb} 22 ^b 26 ^b 27 ^b 29 ^{bb} 34 ^b
Amp, Chl, Tet, Bac, Cli, Ery, Q/D, Van, Str, Sul	7 ^a 16 ^a 2 ^{ab} 1 ^b 5 ^b	19 ^a 21 ^a 23 ^a 18 ^b 20 ^b 27 ^b
Amp, Neo, Tet, Sxt, Kan, Bac, Cli, Ery, Q/D, Van, Sul	8 ^a	23 ^a
Tet, Bac, Cli, Ery, Q/D, Van, Sul	1 ^b	18 ^b
Neo, Kan, Bac, Cli, Ery, Q/D, Van, Str	11 ^b	19 ^b

^a Isolates with clinical signs (CS).

^b Isolates without clinical signs (WCS).

Table II. Antimicrobial resistance and pulsed-field gel electrophoresis (PFGE) profiles of *S. Typhimurium* isolates belonging to phage types other than PT 104 from diseased and healthy pigs

Antimicrobial profile	PFGE (<i>Xba</i> I) ^{ab}	PFGE (<i>Spe</i> I) ^{ab}
Amp, Chl, Neo, Tet, Kan, Bac, Cli, Ery, Q/D, Van, Str, Sul	1 ^a 5 ^a 8 ^a 14 ^a 3 ^b 13 ^b	18 ^a 25 ^a 28 ^a 24 ^{ab} 27 ^b
Bac, Cli, Ery, Q/D, Van	1 ^{aaaa} 4 ^b 6 ^b	18 ^a 21 ^{aa} 31 ^a 20 ^b 26 ^b
Apr, Gen, Tet, Sxt, Bac, Cli, Ery, Q/D, Van, Sul	3 ^a 10 ^a 1 ^{aab}	21 ^{aa} 28 ^a 32 ^a 36 ^b
Tet, Bac, Cli, Ery, Q/D, Van	1 ^{aa} 3 ^b 10 ^b	18 ^{aab} 19 ^b
Neo, Tet, Kan, Bac, Cli, Ery, Q/D, Van, Sul	15 ^a 4 ^b	19 ^a 20 ^b
Amp, Tet, Bac, Cli, Ery, Q/D, Van	1 ^a 12 ^a	18 ^{aa}
Apr, Gen, Tet, Sxt, Bac, Cli, Ery, Q/D, Van, Str, Sul	1 ^a	23 ^a
Amp, Tet, Sxt, Bac, Cli, Ery, Q/D, Van, Sul	1 ^a	18 ^a
Tet, Bac, Cli, Ery, Q/D, Van, Str	1 ^a	18 ^a
Bac, Cli, Ery, Q/D, Van, Sul	1 ^a	18 ^a
Gen, Tet, Bac, Cli, Ery, Q/D, Van, Str, Sul	3 ^b 4 ^{bb}	20 ^b 22 ^b 33 ^b
Apr, Gen, Neo, Tet, Sxt, Bac, Cli, Ery, Q/D, Van, Sul	1 ^{bb}	18 ^b 25 ^b
Amp, Neo, Tet, Kan, Bac, Cli, Ery, Q/D, Van, Str, Sul	4 ^b	22 ^b
Tet, Bac, Cli, Ery, Q/D, Van, Str, Sul	9 ^b	26 ^b
Amp, Neo, Tet, Kan, Bac, Cli, Ery, Q/D, Van	7 ^b	22 ^b

^a Isolates with clinical signs (CS).

^b Isolates without clinical signs (WCS).

of a similar molecular weight, named SitA, under iron-limiting conditions was also reported by Zhou et al (34). These authors identified an iron transport system, encoded within the *Salmonella* pathogenicity island 1 (SPI1) of *S. Typhimurium*. As observed in this study, the induction of *sit* gene expression was prevented by the addition of Fe²⁺ to the growth medium. Furthermore, Janakiraman and Schlauch (35) demonstrated that the putative iron transport system SitABCD encoded on SPI1 is required for full virulence of *S. Typhimurium*. The fact that this protein was found in both types of isolates suggests that it may also be needed for colonization of pigs in sub-clinical infections.

Although no protein was associated with septicemic isolates, many proteins that are strongly recognized by swine antisera were found in both type of isolates in all growth conditions. In particular, a ~37 kDa protein was found to be present in all septicemic isolates and in most isolates from clinically healthy animals and might be considered for vaccine production given its high immunogenicity.

Among genotyping methods, PFGE is considered the reference method for DNA fingerprinting in *Salmonella* and other foodborne pathogens (12), and has been proposed as a system for differentiating epidemic strains from endemic ones (36). The use of PFGE (*Xba*I) is considered a good tool for the epidemiological typing of

S. Typhimurium (37). If genetic variation does not significantly impact the size or electrophoretic mobility of a restriction fragment, then the change may not be identified as a separate pulsotype (8). By the use of 2 or more enzymes for PFGE analysis, the discriminatory power of the method may be enhanced for differentiating *Salmonella* isolates (38). Some authors, however, have emphasized that *S. Typhimurium* has often been considered very clonal and PFGE may not have sufficient discriminatory power to differentiate the various phage types (39). In this study, PFGE was able to demonstrate genetic variability among *S. Typhimurium* isolates in general, while it was also instrumental in demonstrating that some genetic clusters were associated with isolates from diseased animals.

In this study, different procedures were used in order to differentiate *S. Typhimurium* isolates recovered from septicemic animals from those of healthy pigs. Overall, a poor correlation was observed between the various typing methods, as previously observed in other studies (8,9). Usually a multiple typing approach is used to increase the ability to differentiate strains, especially when trying to separate isolates that appear to have clonal distribution (8,9).

However, we demonstrated, using genetic typing methods, a very high genetic diversity in isolates from sick animals, suggesting that multiple genetic lineages might be responsible for clinical outbreaks

in swine herds. Some genetic profiles, however, were found almost exclusively in diseased animals. In a recent study that compared genetic variability of both groups of isolates within the herds (40), a significantly higher difference of genetic diversity in strains from asymptomatic animals was also observed, suggesting that once a virulent strain is established within a herd, this genetic lineage may persist for a prolonged period. In addition, the fact that some genetic clusters can be found in both types of isolates can be explained by transport up to the slaughter period and septicemic isolates following recovery from the disease.

Acknowledgments

This work was supported by NSERC. We would like to thank Dr. S. Messier and Dr. N. Rheault for contributing strains. We thank Johanne Bisailon, Guillaume Gauthier-Larivière, Valérie Normand, and Stéphanie St-Jean for technical assistance. We thank Dr. Guy Beauchamp of the Université de Montréal for the statistical analysis.

References

- Glynn MK, Bopp C, Dewitt W, Dabney P, Mokhtar M, Angulo FJ. Emergence of multidrug-resistant *Salmonella enterica* serotype Typhimurium DT104 infections in the United States. *N Engl J Med* 1998;338:1333–1338.
- Berends BR, Van Knapen F, Snijders JMA, Mossel DAA. Identification and quantification of risk factors regarding *Salmonella* spp. on pork carcasses. *Int J Food Microbiol* 1997;36:199–206.
- Desrosiers R. Les maladies en émergence chez le porc. *Méd Vét Québec* 1999;29:185–188.
- Letellier A, Messier S, Paré J, Ménard J, Quessy S. Distribution of *Salmonella* in swine herds in Québec. *Vet Microbiol* 1999;67:299–306.
- Letellier A, Messier S, Quessy S. Prevalence of *Salmonella* spp. and *Yersinia enterocolitica* in finishing swine at Canadian abattoirs. *J Food Prot* 1999;62:22–25.
- Côté S, Letellier A, Lessard L, Quessy S. Distribution of *Salmonella* in tissues following natural and experimental infection in pigs. *Can J Vet Res* 2004;68:241–248.
- Threlfall EJ, Frost JA. The identification, typing and fingerprinting of *Salmonella*: Laboratory aspects and epidemiological applications. *J Appl Bacteriol* 1990;68:5–16.
- Foley SL, White DG, McDermott PF, et al. Comparison of subtyping methods for differentiating *Salmonella enterica* serovar Typhimurium isolates obtained from food animal sources. *J Clin Microbiol* 2006;44:3569–3577.
- Liebana E, Garcia-Migura L, Clouting C, et al. Multiple genetic typing of *Salmonella enterica* serotype Typhimurium isolates of different phage types (DT104, U302, DT204b, and DT49) from animals and humans in England, Wales, and Northern Ireland. *J Clin Microbiol* 2002;40:4450–4456.
- Lindstedt BA, Heir E, Vardund T, Kapperud G. A variation of the amplified-fragment length polymorphism (AFLP) technique using three restriction endonucleases, and assessment of the enzyme combination *BglII-MfeI* for AFLP analysis of *Salmonella enterica* subsp. *enterica* isolates. *FEMS Microbiol Lett* 2000;189:19–24.
- Baquar N, Threlfall EJ, Rowe B, Stanley J. Phage type 193 of *Salmonella* Typhimurium contains different chromosomal genotypes and multiple IS200 profiles. *FEMS Microbiol Lett* 1994;115:291–295.
- Swaminathan B, Barrett TJ, Hunter SB, Tauxe RV. PulseNet: The molecular subtyping network for foodborne bacterial disease surveillance, United States. *Emerg Infect Dis* 2001;7:382–389.
- Humphrey T. *Salmonella* Typhimurium definitive type 104. A multi-resistant *Salmonella*. *Int J Food Microbiol* 2001;67:173–186.
- Gebreyes WA, Altier C. Molecular characterization of multidrug-resistant *Salmonella enterica* subsp. *enterica* serovar Typhimurium isolates from swine. *J Clin Microbiol* 2002;40:2813–2822.
- Clinical and Laboratory Standards Institute (CLSI). Performance Standards for Antimicrobial Disk and Dilution Susceptibility Tests for Bacteria Isolated from Animals; Approved Standard. 2nd ed. [CLSI Document M31-A2] Wayne, Pennsylvania: CLSI, 2002.
- Clinical and Laboratory Standards Institute (CLSI). Performance Standards for Antimicrobial Susceptibility Testing; Thirteenth Informational Supplement. [CLSI Document M100-S13] Wayne, Pennsylvania: CLSI, 2003.
- Mathew AG, Saxton AM, Upchurch WG, Chatten SE. Multiple antibiotic resistance patterns of *Escherichia coli* isolates from swine farms. *Appl Environ Microbiol* 1999;65:2770–2772.
- Galan JE, Curtiss R, 3rd. Expression of *Salmonella* Typhimurium genes required for invasion is regulated by changes in DNA supercoiling. *Infect Immun* 1990;58:1879–1885.
- Lee CA, Falkow S. The ability of *Salmonella* to enter mammalian cells is affected by bacterial growth state. *Proc Natl Acad Sci U S A* 1990;87:4304–4308.
- Michaud S, Arbeit RD, Gaudreau C. Molecular strain typing of *Campylobacter jejuni* by pulsed-field gel electrophoresis in a single day. *Can J Microbiol* 2001;47:667–669.
- Hunter SB, Vauterin P, Lambert-Fair MA, et al. Establishment of a universal size standard strain for use with the PulseNet standardized pulsed-field gel electrophoresis protocols: Converting the national databases to the new size standard. *J Clin Microbiol* 2005;43:1045–1050.
- Baggesen DL, Sandvang D, Aarestrup FM. Characterization of *Salmonella enterica* serovar Typhimurium DT104 isolated from Denmark and comparison with isolates from Europe and the United States. *J Clin Microbiol* 2000;38:1581–1586.
- Farzan A, Friendship RM, Dewey CE, Muckle AC, Gray JT, Funk J. Distribution of *Salmonella* serovars and phage types on 80 Ontario swine farms in 2004. *Can J Vet Res* 2008;72:1–6.
- Gebreyes WA, Altier C, Thakur S. Molecular epidemiology and diversity of *Salmonella* serovar Typhimurium in pigs using phenotypic and genotypic approaches. *Epidemiol Infect* 2006;134:187–198.
- Lailler R, Grimont F, Jones Y, Sanders P, Brisabois A. Subtyping of *Salmonella* Typhimurium by pulsed-field gel electrophoresis and comparisons with phage types and resistance types. *Pathol Biol (Paris)* 2002;50:361–368.

26. García-Feliz C, Collazos JA, Carvajal A, et al. *Salmonella enterica* infections in Spanish swine fattening units. *Zoonoses Public Health* 2007;54:294–300.
27. Esaki H, Morioka A, Kojima A, et al. Epidemiological characterization of *Salmonella* Typhimurium DT104 prevalent among food-producing animals in the Japanese Veterinary Antimicrobial Resistance Monitoring Program (1999–2001). *Microbiol Immunol* 2004;48:553–556.
28. Kawagoe K, Mine H, Asai T, et al. Changes of multi-drug resistance pattern in *Salmonella enterica* subspecies *enterica* serovar Typhimurium isolates from food-producing animals in Japan. *J Vet Med Sci* 2007;69:1211–1213.
29. Daly M, Buckley J, Power E, et al. Molecular characterization of Irish *Salmonella enterica* serotype Typhimurium: Detection of class I integrons and assessment of genetic relationships by DNA amplification fingerprinting. *Appl Environ Microbiol* 2000;66:614–619.
30. Ng LK, Mulvey MR, Martin I, Peters GA, Johnson W. Genetic characterization of antimicrobial resistance in Canadian isolates of *Salmonella* serovar Typhimurium DT104. *Antimicrob Agents Chemother* 1999;43:3018–3021.
31. Ridley A, Threlfall EJ. Molecular epidemiology of antibiotic resistance genes in multiresistant epidemic *Salmonella* Typhimurium DT 104. *Microb Drug Resist* 1998;4:113–118.
32. Schmieger H, Schicklmaier P. Transduction of multiple drug resistance of *Salmonella enterica* serovar Typhimurium DT104. *FEMS Microbiol Lett* 1999;170:251–256.
33. Threlfall EJ, Frost JA, Ward LR, Rowe B. Epidemic in cattle and humans of *Salmonella* Typhimurium DT 104 with chromosomally integrated multiple drug resistance. *Vet Rec* 1994;134:577.
34. Zhou D, Hardt WD, Galan JE. *Salmonella* Typhimurium encodes a putative iron transport system within the centisome 63 pathogenicity island. *Infect Immun* 1999;67:1974–1981.
35. Janakiraman A, Slauch JM. The putative iron transport system SitABCD encoded on SPI1 is required for full virulence of *Salmonella* Typhimurium. *Mol Microbiol* 2000;35:1146–1155.
36. Tenover FC, Arbeit RD, Goering RV, et al. Interpreting chromosomal DNA restriction patterns produced by pulsed-field gel electrophoresis: Criteria for bacterial strain typing. *J Clin Microbiol* 1995;33:2233–2239.
37. Doran G, Morris D, O'Hare C, et al. Cost-effective application of pulsed-field gel electrophoresis to typing of *Salmonella enterica* serovar Typhimurium. *Appl Environ Microbiol* 2005;71:8236–8240.
38. Ridley AM, Threlfall EJ, Rowe B. Genotypic characterization of *Salmonella* Enteritidis phage types by plasmid analysis, ribotyping, and pulsed-field gel electrophoresis. *J Clin Microbiol* 1998;36:2314–2321.
39. Weill FX, Guesnier F, Guibert V, et al. Multidrug resistance in *Salmonella enterica* serotype Typhimurium from humans in France (1993 to 2003). *J Clin Microbiol* 2006;44:700–708.
40. Perron GG, Quessy S, Letellier A, Bell G. Genotypic diversity and antimicrobial resistance in asymptomatic *Salmonella enterica* serotype Typhimurium DT104. *Infect Genet Evol* 2007;7:223–228.

Identification and differentiation of *Taylorella equigenitalis* and *Taylorella asinigenitalis* by lipopolysaccharide O-antigen serology using monoclonal antibodies

Brian W. Brooks, Cheryl L. Lutze-Wallace, Leann L. MacLean,
Evgeny Vinogradov, Malcolm B. Perry

Abstract

Lipopolysaccharides (LPSs) from *Taylorella equigenitalis*, the causative agent of contagious equine metritis, and *T. asinigenitalis* were compared by sodium dodecyl sulphate-polyacrylamide gel electrophoresis (SDS-PAGE). Lipopolysaccharide profiles of 11 *T. equigenitalis* strains were similar, but different from the profiles of 3 *T. asinigenitalis* strains, and the profiles of 2 *T. asinigenitalis* strains were similar to each other. The serological specificities of the LPSs from these 14 strains were examined by immunoblotting and enzyme-linked immunosorbent assay with monoclonal antibodies (MAbs) to the LPSs of the *T. equigenitalis* and *T. asinigenitalis* type strains and *T. asinigenitalis* strain 2329-98. A MAb to *T. equigenitalis* LPS O-polysaccharide (O-PS) (M2560) reacted with LPSs from all *T. equigenitalis* strains but did not react with LPSs from the 3 *T. asinigenitalis* strains or with 43 non-*Taylorella* bacteria. Three MAbs to the *T. asinigenitalis* type strain LPS O-PS or core epitopes (M2974, M2982, M3000) reacted with the homologous strain and *T. asinigenitalis* strain Bd 3751/05, but not with any of the other bacteria. Five MAbs to *T. asinigenitalis* 2329-98 LPS O-PS or core epitopes (M2904, M2907, M2910, M2923, M2929) reacted only with this strain. Proton nuclear magnetic resonance spectra of the O-PSs of the type strains of *T. equigenitalis* and *T. asinigenitalis* provided fingerprint identification and differentiation of these 2 organisms. The serological results were consistent with our previous finding that the O-antigen of the type strain of *T. equigenitalis*, being a linear polymer of disaccharide repeating [\rightarrow 4)- α -L-GulpNAc3NAcA-(1 \rightarrow 4)- β -D-ManpNAc3NAcA-(1 \rightarrow)] units, differs from that of the *T. asinigenitalis* O-antigen polymer that is composed of repeating [\rightarrow 3)- β -D-QuipNAc4NAc-(1 \rightarrow 3)- β -D-GlcpNAmA-(1 \rightarrow)] units. Lipopolysaccharide O-PS could be a specific marker for identification and differentiation of *T. equigenitalis* and *T. asinigenitalis*, and provide the basis for the development of specific detection assays for *T. equigenitalis*.

Résumé

Les lipopolysaccharides (LPSs) provenant de *Taylorella equigenitalis*, l'agent étiologique de la métrite contagieuse équine, et *T. asinigenitalis* ont été comparés par électrophorèse sur gel de polyacrylamide avec du sulfate de dodécyl sodique (SDS-PAGE). Les profils de LPSs de 11 souches de *T. equigenitalis* étaient similaires, mais différaient des profils de 3 souches de *T. asinigenitalis*, et les profils de 2 souches de *T. asinigenitalis* étaient similaires entre eux. Les spécificités sérologiques des LPSs de ces 14 souches ont été examinées par immunobuvardage et immuno-essais avec des anticorps monoclonaux (Mabs) contre les LPSs des souches types de *T. equigenitalis* et *T. asinigenitalis* et la souche 2329-98 de *T. asinigenitalis*. Un MAb contre le polysaccharide O (O-PS) du LPS de *T. equigenitalis* (M2560) a réagit avec les LPSs de toutes les souches de *T. equigenitalis* mais n'a pas réagit avec les LPSs des 3 souches de *T. asinigenitalis* ou des 43 bactéries différentes de *Taylorella*. Trois MAbs dirigés contre le O-PS LPS ou les épitopes du core de la souche type de *T. asinigenitalis* (M2974, M2982, M3000) ont réagit avec la souche homologue et avec la souche Bd 3751/05 de *T. asinigenitalis*, mais avec aucune autre bactérie. Cinq MAbs dirigés contre le O-PS du LPS ou les épitopes du core de *T. asinigenitalis* 2329-98 (M2904, M2907, M2910, M2923, M2929) n'ont réagit qu'avec cette souche. Le spectre des O-PSs des souches types de *T. equigenitalis* et *T. asinigenitalis* obtenu par résonance magnétique nucléaire protonique a fourni des empreintes pour l'identification et la différenciation de ces 2 organismes. Les résultats sérologiques étaient compatibles avec nos résultats précédents qui indiquaient que l'antigène O de la souche type de *T. equigenitalis*, qui est un polymère linéaire d'unités répétées du disaccharide [\rightarrow 4)- α -L-GulpNAc3NAcA-(1 \rightarrow 4)- β -D-ManpNAc3NAcA-(1 \rightarrow)], diffère du polymère de l'antigène O de *T. asinigenitalis* qui est composé d'unités répétées de [\rightarrow 3)- β -D-QuipNAc4NAc-(1 \rightarrow 3)- β -D-GlcpNAmA-(1 \rightarrow)]. Le O-PS du LPS pourrait être un marqueur spécifique pour l'identification et la différenciation de *T. equigenitalis* et *T. asinigenitalis*, et il fournit les éléments de base pour le développement d'épreuves spécifiques de détection de *T. equigenitalis*.

(Traduit par Docteur Serge Messier)

Canadian Food Inspection Agency, Ottawa Laboratory (Fallowfield), Ottawa, Ontario K2H 8P9 (Brooks, Lutze-Wallace); National Research Council of Canada, Institute of Biological Sciences, Ottawa, Ontario K1A 0R6 (MacLean, Vinogradov, Perry).

Address all correspondence to Dr. Brian W. Brooks; telephone: (613) 228-6698; fax: (613) 228-6670; e-mail: brian.brooks@inspection.gc.ca

Dr. Brooks' current address is Canadian Food Inspection Agency Ottawa Laboratory (Fallowfield), 3851 Fallowfield Road, P.O. Box 11300, Station H, Ottawa, Ontario K2H 8P9.

Received August 27, 2008. Accepted December 8, 2008.

Introduction

The gram-negative bacterium *Taylorella equigenitalis* is the causative agent of contagious equine metritis (CEM), a highly contagious venereal disease of members of the horse family (1). This disease was first described in Thoroughbred horses in England (2) and Ireland (3) in 1977 and has since been diagnosed in many countries worldwide (4). Contagious equine metritis is the focus of considerable international concern to the horse industry because of its potential to cause short-term infertility in broodmares, and the ease with which the carrier state can be established in both mares and stallions. Although endemic in various parts of the world, Canada and several other countries are recognized as being free of CEM. In countries free of this disease, stringent CEM regulatory diagnostic testing programs have been implemented for imported horses.

Isolation and identification of *T. equigenitalis* is the confirmatory test for diagnosis of CEM (5). However, the fastidious nature and relatively slow growth of this organism makes isolation difficult. Furthermore, this organism is non-reactive in many traditional metabolic and physiological tests, and identification of an isolate as *T. equigenitalis* is made on a limited number of positive characteristics. In addition to culture, an agglutination test that is based on polyclonal antibodies is commonly used for *T. equigenitalis* antigenic identification in routine testing laboratories. A complement fixation test has been used successfully as an adjunct to culture for *T. equigenitalis* in screening mares after being bred with a carrier stallion (6). Polymerase chain reaction (PCR) assays have also been developed for detection of this organism (7–9). Phylogenetically *T. equigenitalis* is closely related to *Bordetella bronchiseptica*, *Alcaligenes xylosoxidans*, and *Oligella urethralis* (10,11).

Diagnosis of CEM can be complicated by infection with *T. asinigenitalis*. *T. asinigenitalis* was first isolated from the genital tract of 3 male donkeys in the USA in 1997 (12,13), and has since been isolated in Sweden (14) and France (9). *T. asinigenitalis* is phenotypically very similar to *T. equigenitalis*, and *T. asinigenitalis* cells cross react with polyclonal anti-*T. equigenitalis* serum (5). *T. asinigenitalis* differs from *T. equigenitalis* in 16S ribosomal DNA sequence, growth rate, and disease production. *T. asinigenitalis* does not cause apparent disease in susceptible mares, whereas *T. equigenitalis* causes endometritis, cervicitis, and vaginitis.

Lipopolysaccharide (LPS), a characteristic component of gram-negative bacteria, is structurally and antigenically diverse, and may provide a basis for improved identification of *T. equigenitalis* and *T. asinigenitalis* and for differentiation of these 2 organisms. The LPS molecule generally comprises 3 regions: lipid A, core oligosaccharide, and O-polysaccharide (O-PS) (15). The O-PS has been found to be highly pleomorphic in the majority of bacterial species studied, and in general even related species have few or no O-PS types in common (16). Diversity has also been demonstrated in the LPS core region of various bacteria such as *Escherichia coli* and *Salmonella* (17).

Chemical analyses of O-PS reveal that assigned serological antigenic factors can be related to oligosaccharide structural epitopes contained within the O-PS linear structures and, in particular, to epitopes located in the non-reducing terminal oligosaccharide regions of the O-PS (18–20) thus providing a molecular level understanding of antibody binding specificities. Recent work on the structural analysis

Table I. *Taylorella equigenitalis* and *Taylorella asinigenitalis* strains used to study the serological specificities of their lipopolysaccharides

Organism	Strain	Host source
<i>Taylorella equigenitalis</i>	ATCC 35865 [†]	Horse
<i>Taylorella equigenitalis</i>	NCTC 11225	Horse
<i>Taylorella equigenitalis</i>	ADRI 1890	Horse
<i>Taylorella equigenitalis</i>	ADRI 1891	Horse
<i>Taylorella equigenitalis</i>	ADRI 1892	Horse
<i>Taylorella equigenitalis</i>	ADRI 1893	Horse
<i>Taylorella equigenitalis</i>	03IM117-1AM	Horse
<i>Taylorella equigenitalis</i>	01IM463 4CM	Horse
<i>Taylorella equigenitalis</i>	01IM282-5C ^a	Horse
<i>Taylorella equigenitalis</i>	96IMPNG655-2A ^a	Horse
<i>Taylorella equigenitalis</i>	99IMPNG99 ^a	Horse
<i>Taylorella asinigenitalis</i>	ATCC 700933 ^{Tb}	Donkey
<i>Taylorella asinigenitalis</i>	2329-98 ^c	Donkey
<i>Taylorella asinigenitalis</i>	Bd 3751/05 ^d	Horse

ATCC — American Type Culture Collection; NCTC — National Collection of Type Cultures; ADRI — Animal Diseases Research Institute.

[†] Type strain.

^a Streptomycin sensitive.

^b Isolated from a donkey jack in California.

^c Isolated from a donkey jack in Kentucky.

^d Isolated from a stallion in Sweden.

of the lipopolysaccharide O-PSs produced by the type strains of *T. equigenitalis* (21) and *T. asinigenitalis* (22) showed that they had virtually identical core oligosaccharide regions. They did, however, have respective O-PS components of linear unbranched chains of repeating disaccharide units composed of chemically and structurally unrelated glucose residues. Thus, the respective LPSs provide target macromolecules for the development of both chemical and serological methods for the differentiation of the 2 *Taylorella* species.

In the present study, monoclonal antibodies (MAbs) were produced to the LPSs from 3 *T. equigenitalis* and *T. asinigenitalis* strains. The serological specificities of *T. equigenitalis* and *T. asinigenitalis* LPS were evaluated by examining the reactivity of the MAbs with various *T. equigenitalis* and *T. asinigenitalis* strains and with non-*Taylorella* bacteria. Monoclonal antibodies specific for *T. equigenitalis* were identified and these reagents may be potentially useful for the development of improved diagnostic tests for CEM.

Materials and methods

Bacterial strains and growth conditions

The *T. equigenitalis* and *T. asinigenitalis* strains used in this study are listed in Table I. All strains were grown on modified Eugon chocolate agar containing 5 mg/L amphotericin B (MECA + A) at 35°C in 7.5% CO₂ for 48 h. Cells were harvested, suspended in 0.01 M phosphate buffered saline, pH 7.2 (PBS) to a concentration of approximately 1 × 10¹⁰ colony forming units (CFUs)/mL and stored at –20°C.

Forty-three non-*Taylorella* bacteria were used in this study. Thirty-three of these organisms were described previously (23), and the other 10 were *Achromobacter xylosoxidans* Animal Diseases Research Institute Culture Collection (ADRI) 1916, *Bordetella bronchiseptica* American Type Culture Collection (ATCC) 10580, *Mannheimia haemolytica* ADRI 1909, *Moraxella bovis* ADRI 1917, *M. bovis* ADRI 1918, *Oligella urethralis* ATCC 17960, *Salmonella* Pullorum National Veterinary Services Laboratory (NVSL) 11, *S. Pullorum* NVSL 77, *Str. zooepidemicus* ADRI 1919, and *S. zooepidemicus* ADRI 1920. *O. urethralis* was grown on MECA + A at 37°C for 48 h. *B. bronchiseptica* and *Alcaligenes faecalis* were grown on MECA + A at 37°C in 5.0% CO₂ for 24 h. *Arcobacter* spp., *Campylobacter* spp., and *Helicobacter* spp. were grown on Mueller Hinton (MH) agar containing 10% sheep blood at 37°C under microaerophilic conditions (*A. butzleri* aerobically) for 48 to 72 h. The other bacteria were grown on trypticase or MH agar containing 10% sheep blood at 37°C aerobically for 16–18 h. Cells were harvested, suspended in 0.01M Tris buffer pH 7.5 to a concentration of approximately 1 × 10¹⁰ CFUs/mL and stored at –20°C.

SDS-PAGE and silver staining

Sodium dodecyl sulfate-polyacrylamide gel electrophoresis (SDS-PAGE) and silver staining were used to examine the LPSs of the *T. equigenitalis* and *T. asinigenitalis* strains and other selected bacteria. SDS-PAGE was conducted as described previously (24). Briefly, proteinase K (pK) cell digests were prepared by the procedure of Hitchcock and Brown (25). Components in the pK digests were separated by electrophoresis using a discontinuous buffer system with a 6% stacking gel and 12% separating gel. Electrophoresis was conducted with 20 mA constant current per gel at 15°C for approximately 3.5 h. Bands were detected by periodate oxidation-silver staining (26).

Monoclonal antibodies

Monoclonal antibodies to the LPSs of selected *T. equigenitalis* and *T. asinigenitalis* strains were produced using methods previously described (23). Briefly, BALB/c and ND4 mice were immunized on days 0, 14, 28, and 44 with formalin-killed cells of *T. equigenitalis* ATCC 35865, *T. asinigenitalis* 2329-98 or *T. asinigenitalis* ATCC 700933. Spleens were harvested on day 48. Hybridomas were produced by fusion of spleen cells with Sp 2/0-Ag-14 myeloma cells. Hybridoma tissue culture fluids were screened for specific antibody using an indirect enzyme-linked immunosorbent assay (ELISA) and immunoblotting. Approximately 30 hybridomas were selected for each of the 3 *Taylorella* strains and cloned twice, and the isotype of the antibody produced by these hybridomas was determined. All experiments involving animals were approved by the local Animal Care Committee under the guidelines of the Canadian Council on Animal Care.

Indirect ELISA

An indirect ELISA with a pK digest of *T. equigenitalis* ATCC 35865, *T. asinigenitalis* 2329-98 or *T. asinigenitalis* ATCC 700933 cells as antigen was used for initial screening of hybridoma tissue culture fluids. Proteinase K digests were prepared by adding 1 volume of pK (Sigma P4914, 2.5 mg/mL in PBS) to 5 volumes of cells,

heating at 60°C for 60 min and then heating at 100°C for 30 min. Microplate (Nunc 475094) wells were passively coated overnight with pK digests diluted approximately 1 in 100 in 0.06 M carbonate buffer pH 9.6. The antigen-coated plates were washed with 0.01 M phosphate buffer pH 7.2 containing 0.15 M NaCl and 0.05% Tween 20 (PBST), hybridoma tissue culture fluid was added, and the plates incubated for 2 h. The plates were washed with PBST, horseradish peroxidase-conjugated goat anti-mouse IgG (Jackson ImmunoResearch Laboratories, West Grove, Pennsylvania, USA) diluted 1 in 10 000 with PBST added, and the plates incubated for 1 h. The plates were washed again, 3,3',5,5'-tetra-methylbenzidine/hydrogen peroxide substrate (Kirkegaard and Perry Laboratories, Gaithersburg, Maryland, USA) was added, and the plates shaken for 10 min. The optical density (OD) was determined at 620 nm using a microplate reader (Titertek Multiskan MCC/340, Labsystems, Needham Heights, Massachusetts, USA).

A similar indirect ELISA procedure with pK digests of *Taylorella* and non-*Taylorella* bacteria as antigen and the anti-LPS MABs in tissue culture fluid from 2X cloned hybridomas was used to determine the specificity of *T. equigenitalis* and *T. asinigenitalis* LPSs. An ELISA OD 620 ≥ 0.10 was interpreted as a positive result.

Immunoblotting

Immunoblotting with MABs was used to analyze the LPSs of selected *T. equigenitalis* and *T. asinigenitalis* strains. The procedure used was essentially as described by Brooks et al (24). *T. equigenitalis* ATCC 35865, *T. asinigenitalis* 2329-98, and *T. asinigenitalis* ATCC 700933 cells were digested with pK. Lipopolysaccharides in the pK digests were separated by SDS-PAGE, and the separated components transferred electrophoretically from gels to nitrocellulose membranes. The membranes were washed for 1 min with 0.02 M Tris buffered saline pH 7.4 (TBS). The unbound sites on the membranes were blocked by incubation for 1 h at 35°C with TBS containing 0.05% Tween 20 (TBST). After blocking, the membranes were incubated for 16 h at 20°C with hybridoma tissue culture fluid diluted 1 in 2 with TBST. The membranes were washed with TBST and incubated for 2 h with alkaline phosphatase-conjugated goat anti-mouse IgG (Zymed Laboratories, supplied by Mandel, Guelph, Ontario) diluted 1 in 1000 with TBST. The membranes were washed again and incubated for 10 min with 5-bromo-4-chloro-3-indolyl phosphate/p-nitroblue tetrazolium chloride substrate (Kirkegaard and Perry Laboratories).

Extraction of LPS, preparation of O-polysaccharides, and nuclear magnetic resonance (NMR) spectroscopy

Fermenter grown cells of the type strains of *T. equigenitalis* (ATCC 35865) and *T. asinigenitalis* (ATCC 700933) were extracted by a modified aqueous phenol procedure (27) and the LPSs were obtained (ca 6% yield) by a 3-fold ultracentrifugation (105 000 × g, 4°C, 8 h) of the concentrated dialyzed extract and the final precipitated gels were lyophilized from their water solution.

The LPS preparations (100 mg) were subjected to hydrolysis with 1.5% (v/v) acetic acid (50 mL, 100°C, 2 h) and following removal of precipitated lipid A by low speed centrifugation, the concentrated aqueous solution was subjected to Sephadex G-50 column

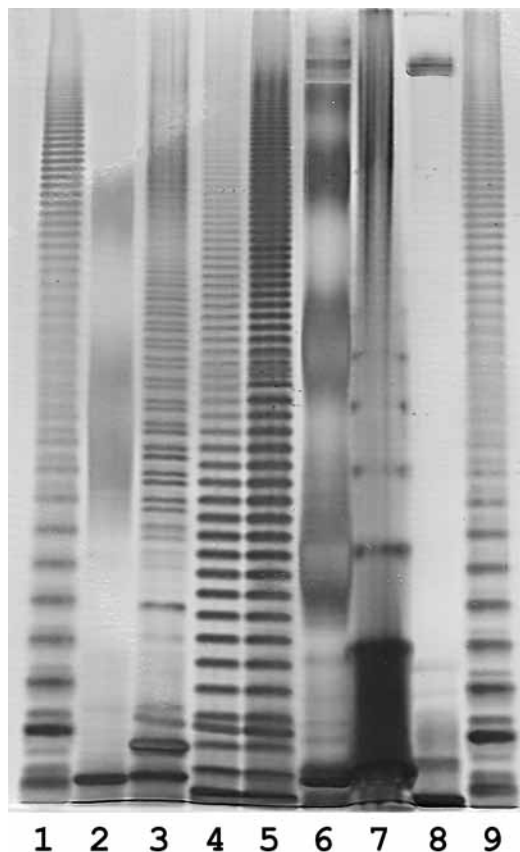


Figure 1. Periodate oxidized and silver stained SDS-PAGE profiles of purified lipopolysaccharides from *Salmonella* Typhimurium (lanes 1 and 9), and pK digests of *T. equigenitalis* ATCC 35865 (lane 2), *T. asinigenitalis* 2329-98 (lane 3), *T. asinigenitalis* ATCC 700933 (lane 4), *T. asinigenitalis* Bd 3751/05 (lane 5), *B. bronchiseptica* ATCC 10580 (lane 6), *O. urethralis* ATCC 17960 (lane 7), and *A. faecalis* ATCC 8750 (lane 8).

chromatography (2 × 50 cm) in 0.05 M pyridinium acetate buffer (pH 5.2) and the high molecular mass eluting O-PS fraction (K_{av} 0.01–0.12) was collected and lyophilized.

¹H-NMR spectra of O-PS exchanged and dissolved in 99% D₂O at 25°C were recorded using a Varian Inova 500 MHz under standard conditions as previously described (28).

Results

SDS-PAGE analysis of LPS from *T. equigenitalis* and *T. asinigenitalis*

A silver-stained gel of pK-treated cell lysates of *T. equigenitalis*, *T. asinigenitalis* and other selected bacteria is shown in Figure 1. SDS-PAGE of *S. Typhimurium* LPS, included as a control and for comparison (Figure 1, lanes 1 and 9), produced a ladder-like pattern of bands typical of smooth-type LPS. The fastest migrating band was core oligosaccharide (no O-PS) and each successive band was core oligosaccharide plus increasing numbers of repeating O-PS units. A ladder-like pattern of bands was also seen with LPS from *T. asinigenitalis* strains 2329-98, ATCC 700933 and Bd 3751/05 (lanes 3, 4, 5, respectively). The profiles of *T. asinigenitalis* strains ATCC 700933 and Bd 3751/05 were virtually identical but differed

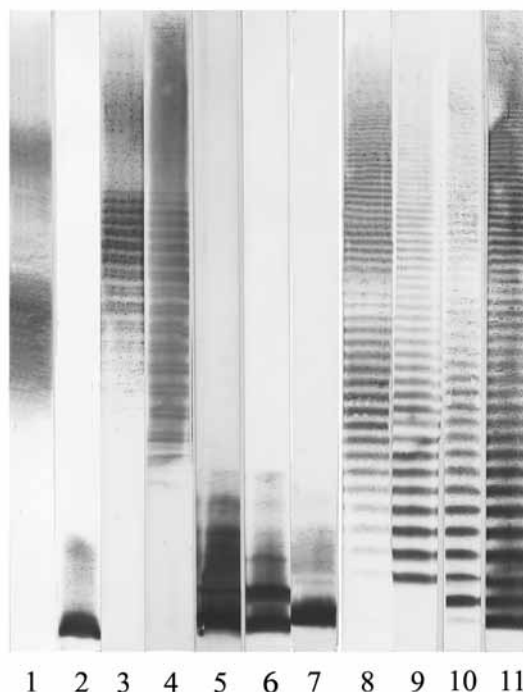


Figure 2. Immunoblots of pK digests of *T. equigenitalis* ATCC 35865 (lanes 1 and 2), *T. asinigenitalis* 2329-98 (lanes 3–7) and *T. asinigenitalis* ATCC 700933 (lanes 8–11) with monoclonal antibodies M2560 (lane 1), M2565 (lane 2), M2907 (lane 3), M2929 (lane 4), M2904 (lane 5), M2910 (lane 6), M2923 (lane 7), M2974 (lane 8), M3000 (lane 9), M2975 (lane 10), and M2982 (lane 11).

from that of *T. asinigenitalis* strain 2329-98. High molecular mass LPS was detected in 2 areas of the gel but no ladder-like pattern of bands was observed with *T. equigenitalis* ATCC 35865 (lane 2), and a similar profile was observed with the other 10 *T. equigenitalis* strains (results not shown). High molecular mass LPS but no ladder-like pattern of bands was also observed with *Bordetella bronchiseptica* ATCC 10580 (lane 6). Low molecular mass (LMM) core oligosaccharide was observed in the LPS profiles of all 4 *Taylorella* strains (lanes 2–5), *B. bronchiseptica* (lane 6), *O. urethralis* (lane 7), and *A. faecalis* (lane 8).

Analysis of *T. equigenitalis* and *T. asinigenitalis* LPS by immunoblotting with MAbs

Monoclonal antibodies were produced to the LPS from 3 *Taylorella* strains. The reactivity of the LPS from these 3 strains was examined by immunoblotting with MAbs to the homologous LPS.

Thirty-two MAbs were produced to *T. equigenitalis* ATCC 35865 LPS. Two different patterns of reactivity were seen on immunoblots with these MAbs. The patterns observed with MAbs M2560 and M2565 were selected as representative (Figure 2, lanes 1 and 2, respectively). MAb M2560 reacted with O-PS whereas MAb M2565 reacted with core oligosaccharide. The isotype of MAb M2560 is IgG1 and the isotype of MAb M2565 is IgG3.

Twenty-nine MAbs were produced to *T. asinigenitalis* strain 2329-98 LPS. Five immunoblotting patterns were observed and are represented by the reactions with MAbs M2907, M2929, M2904, M2910, and M2923 (Figure 2, lanes 3, 4, 5, 6, and 7, respectively). Monoclonal antibodies M2907 and M2929 both reacted with O-PS and both

Table II. Reactivity of proteinase K digested cell lysates of *Taylorella equigenitalis* and *T. asinigenitalis* strains and non-*Taylorella* bacteria with selected monoclonal antibodies by ELISA

Monoclonal antibody	ELISA OD620 with proteinase K digested cell lysates of				
	<i>Taylorella equigenitalis</i> (11) ^a	<i>Taylorella asinigenitalis</i> 2329-98	<i>Taylorella asinigenitalis</i> ATCC 700933	<i>Taylorella asinigenitalis</i> Bd 3751/05	Other bacteria ^b (43)
M2560	0.85 ± 0.10 ^c	0.05	0.05	0.05	0.05 ± 0.01
M2565	1.34 ± 0.45	1.35	1.39	1.84	0.36 ± 0.35
M2907	0.08 ± 0.02	1.18	0.06	0.05	0.05 ± 0.01
M2929	0.06 ± 0.01	2.07	0.05	0.05	0.05 ± 0.01
M2904	0.06 ± 0.02	1.90	0.05	0.05	0.05 ± 0.01
M2910	0.05 ± 0.01	1.82	0.05	0.05	0.05 ± 0.01
M2923	0.05 ± 0.01	1.11	0.05	0.05	0.05 ± 0.01
M2974	0.05 ± 0.01	0.05	1.39	2.03	0.06 ± 0.01
M3000	0.05 ± 0.01	0.05	0.49	0.76	0.05 ± 0.01
M2975	0.05 ± 0.01	0.05	0.86	1.08	0.06 ± 0.04
M2982	0.05 ± 0.01	0.05	2.09	2.27	0.06 ± 0.02

^a Number of strains — see Table I.

^b See Material and methods, Bacterial strains and growth conditions.

^c Mean ± standard deviation (s).

reacted with LPS components with relatively high numbers of O-PS units. Monoclonal antibody M2929, but not M2907, also reacted with components with lower numbers of O-PS units. Monoclonal antibodies M2904, M2910, and M2923 reacted with core oligosaccharide. The isotype of MAb 2907 is IgG3, the isotype of MAbs M2929, M2904, and M2910 is IgG1, and the isotype of MAb M2923 is IgG2a.

Thirty-four MAbs were produced to *T. asinigenitalis* ATCC 700933 LPS. Four immunoblot patterns were obtained, as represented by the reaction with M2974, M3000, M2975, and M2982 (Figure 2, lanes 8, 9, 10, and 11, respectively). Monoclonal antibodies M2974, M3000, and M2975 reacted with O-PS. Monoclonal antibody M2975 reacted with LPS with the lower numbers of O-PS units, compared to MAbs M2974 and M3000. Monoclonal antibody M2982 reacted with both HMM and LMM LPS components. The isotype of MAb M2974 is IgG3 and the isotype of MAb M2982 is IgG1. Monoclonal antibodies M3000 and M2975 are IgA.

Specificity of *T. equigenitalis* and *T. asinigenitalis* LPS determined by ELISA with MAbs

The ELISA reactivity of LPS from *T. equigenitalis*, *T. asinigenitalis*, and 43 non-*Taylorella* bacteria with selected MAbs is shown in Table II. Monoclonal antibody M2560 reacted with all 11 strains of *T. equigenitalis*, but did not react with the 3 *T. asinigenitalis* strains or with the 43 non-*Taylorella* bacteria tested. Thus at least one epitope of *T. equigenitalis* O-PS appears to be highly specific for this organism. In contrast, MAb M2565 reacted with all 14 *Taylorella* strains and with 29 of the 43 non-*Taylorella* bacteria, indicating that an epitope of *T. equigenitalis* LPS core oligosaccharide is shared by various bacteria.

Monoclonal antibodies M2907, M2929, M2904, M2910, and M2923 reacted only with *T. asinigenitalis* strain 2329-98 and not with the other bacteria tested. Thus, several O-PS and core oligosaccharide epitopes of *T. asinigenitalis* 2329-98 LPS appear to be essentially unique to this organism.

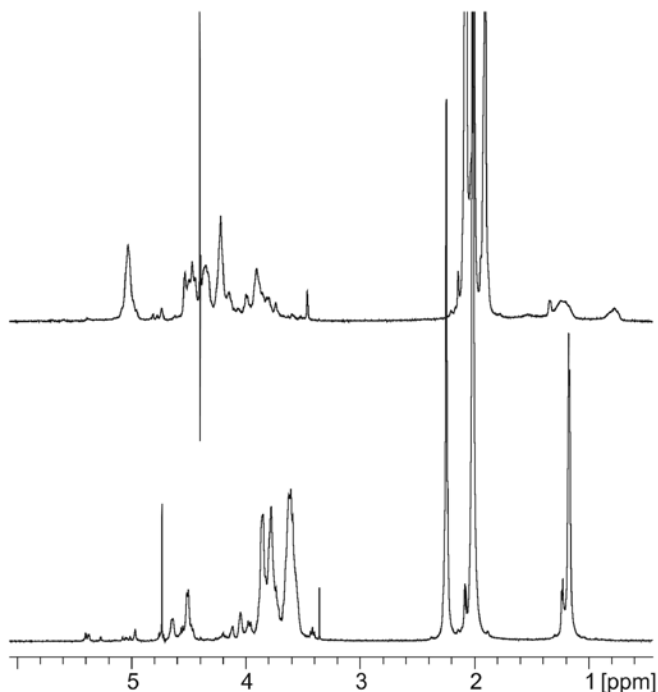
Monoclonal antibodies M2974, M3000, and M2982 reacted only with *T. asinigenitalis* strains ATCC 700933 and Bd 3751/05, and therefore the LPS of these 2 strains appears to be very similar and highly specific to these 2 organisms. Monoclonal antibody M2975 reacted with *T. asinigenitalis* ATCC 700933 and Bd 3751/05, but also cross reacted with *Mannheimia haemolytica* ADRI 1909 (OD 0.26). It is of note that the conserved oligosaccharide (29) of the LPSs produced by O-serotypes of *M. haemolytica* in common with *Taylorella* cores express epitopes involving D-glycero-D-manno-heptose residues that may account for observed serological cross-reactions.

NMR spectroscopy

The proton NMR spectra of the O-PS preparations made in this study (Figure 3) were consistent with the resonance assignments previously determined from the use of 2D heteronuclear NMR experiments (21,22). The characteristic chemical shifts of the anomeric proton signals (4.5–6.0 ppm region), the unique methyl resonances of the 6-deoxyhexose residue (~1.17 ppm of D-QuiNAc4NAc in the *T. asinigenitalis* O-PS), and the complex of glycosyl ring region protons provide a simple fingerprint for the identification and differentiation of the respective antigenic O-PSs of *T. equigenitalis* and *T. asinigenitalis* type strains.

Discussion

In the present study, analysis by SDS-PAGE and by ELISA with anti-LPS MAbs demonstrated that the LPSs of all 11 *T. equigenitalis* strains examined were virtually identical, but differed from the LPSs of 3 *T. asinigenitalis* strains. In addition, the LPS of *T. asinigenitalis* strains ATCC 700933 and Bd 3751/05 (California and Swedish isolates, respectively) were indistinguishable from each other, but distinct from the LPS of *T. asinigenitalis* 2329-98 (Kentucky isolate). These results show that selected anti-LPS MAbs can be employed



Top: *T. equigenitalis* O-chain ^1H NMR at 60°C
 Bottom: *T. asinigenitalis* O-chain ^1H NMR at 30°C

Figure 3. ^1H -NMR spectra of the O-PS preparations from the LPS of (A) *T. equigenitalis* (ATCC 35865) and (B) *T. asinigenitalis* (ATCC 700933).

for identification of *T. equigenitalis*, for differentiation of *T. equigenitalis* from *T. asinigenitalis*, and for distinction between strains of *T. asinigenitalis*.

In a previous study, Gradinaru et al (30) characterized LPS and protein components of 9 *T. equigenitalis* strains by SDS-PAGE. The pattern of LPS components detected after silver staining was similar for all strains examined, with a major component of molecular mass of approximately 22 kDa. In contrast, in the present study both HMM and LMM components were detected in the LPS profile of the *T. equigenitalis* type strain and the other 10 *T. equigenitalis* strains examined by SDS-PAGE and silver staining and by immunoblotting with MAb M2560 and other anti-*T. equigenitalis* O-PS MAbs. Gradinaru et al (30) also produced MAbs that were specific to *T. equigenitalis* but these MAbs reacted with epitopes of protein components.

Nuclear magnetic resonance spectral and chemical analysis confirmed that the LPS O-PSs from the type strains of *T. equigenitalis* (ATCC 35865) and *T. asinigenitalis* (ATCC 700933) were substantially structurally different. The *T. equigenitalis* O-PS antigen was found to be a polymer of partially amidated disaccharide units composed of 2,3-diacetamido-2,3-dideoxy-D-mannuronic acid (D-ManNAc3NAcA) and 2,3-diacetamido-2,3-dideoxy-L-guluronic acid (D-GulNAcA3NAcA) having the structure $[\rightarrow 4)\text{-}\alpha\text{-L-GulpNAc3NAcA-(1}\rightarrow 4)\text{-}\beta\text{-D-ManpNAc3NAc-(1}\rightarrow)]_n$ in which the terminal nonreducing $\alpha\text{-L-GulpNAc3NAcA}$ residue was methylated at its O-4 position. The *T. asinigenitalis* O-PS was determined to be a polymer of a disaccharide repeating unit composed

of 2,4-diacetamido-2,4-dideoxy-D-quinovose (D-QuiNAc4NAc, 2,4-diacetamido-2,4,6-trideoxy-D-glucose) and 2-acetidimidoylamino-2-deoxy-D-glucuronic acid (D-GlcNAcA) residues having the structure $[\rightarrow 3)\text{-}\beta\text{-D-QuipNAc4NAc-(1}\rightarrow 3)\text{-}\beta\text{-D-GlcpNAcA-(1}\rightarrow)]_n$ (21,22). The significant structural differences between the LPS O-PS of *T. equigenitalis* and *T. asinigenitalis* provide a basis for serological differentiation of these 2 organisms. *T. equigenitalis* and *T. asinigenitalis* can be identified by reference to their respective analyzed and reported (21,22) 2-D ^1H - ^{13}C HSQC correlation spectra, or more simply, from their 1-D proton NMR spectra (Figure 3) using readily extracted LPS or derived O-PS, or by the possible use of magic angle spinning NMR spectroscopy requiring only a suspended sample of whole bacterial cells collected from a single plate colony (31). The major differences in the two structures are revealed in the glycosyl anomeric proton signals (5.03 and 5.05 ppm) and (4.64 and 4.51 ppm) in the respective *T. equigenitalis* and *T. asinigenitalis* spectra and the unique C-6 methyl signal (1.17 ppm) of the D-QuipNAc4NAc residue in the *T. asinigenitalis* O-antigen.

Since *T. equigenitalis* and *T. asinigenitalis* LPSs are structurally distinct from each other, it may also be possible to identify *T. equigenitalis* and *T. asinigenitalis* using PCR assays targeting regions within the genes involved in LPS biosynthesis. In various gram-negative bacteria, many of the enzymes involved in O-PS biosynthesis are encoded in an *rfb* gene cluster, and PCR assays targeting regions within *rfb* gene clusters have been used for identification of O serogroups of *Salmonella* (32), *Escherichia coli* (33), *Shigella* (34) and other bacteria. Similarly, sequences in the genes involved in the biosynthesis of the LPS O-PS and the core oligosaccharide may provide useful probes for identification and differentiation of *T. equigenitalis* and *T. asinigenitalis*.

In summary, based on serological and structural evidence, the LPS O-PS can be used as a specific marker for identification and differentiation of *T. equigenitalis* and *T. asinigenitalis*, and thus provides the basis for the development of specific detection assays for *T. equigenitalis*.

Acknowledgments

The authors gratefully acknowledge the expert contributions of the CFIA Ottawa Laboratory (Fallowfield) Monoclonal Antibody Unit and animal care staff in production of the monoclonal antibodies, and Perry Flemming at the NRC for the large-scale production of bacterial cell mass required for chemical structural analysis of LPS. We also thank V. Båverud for providing *T. asinigenitalis* strain Bd 3751/05 and J. Devenish for providing the other *Taylorella* strains.

References

1. Timoney PJ. Contagious equine metritis. *Comp Immunol Microbiol Infect Dis* 1996;19:199-204.
2. Crowhurst RC. Genital infection in mares. *Vet Rec* 1977;100:476.
3. Timoney PJ, Ward J, Kelly P. A contagious genital infection of mares. *Vet Rec* 1977;101:103.
4. Timoney PJ, Powell DG. Contagious equine metritis—epidemiology and control. *J Equine Vet Sci* 1988;8:42-46.

5. Anonymous. Contagious equine metritis. In: OIE Manual of Diagnostic Tests and Vaccines for Terrestrial Animals. Paris: Office international des épizooties, 2005.
6. Croxton-Smith P, Benson JA, Dawson FLM, Powell DG. A complement fixation test for antibody to the contagious equine metritis organism. *Vet Rec* 1978;103:275–278.
7. Bleumink-Pluym NM, Werdler ME, Houwers DJ, Parlevliet JM, Colenbrander B, van der Zeijst BA. Development and evaluation of PCR test for detection of *Taylorella equigenitalis*. *J Clin Microbiol* 1994;32:893–896.
8. Anzai T, Eguchi M, Sekizaki T, Kamada M, Yamamoto K, Okuda T. Development of a PCR test for rapid diagnosis of contagious equine metritis. *J Vet Med Sci* 1999;61:1287–1292.
9. Duquesne F, Pronost S, Laugier C, Petry S. Identification of *Taylorella equigenitalis* responsible for contagious equine metritis in equine genital swabs by direct polymerase chain reaction. *Res Vet Sci* 2007;82:47–49.
10. Rossau R, Kersters K, Falsen E, et al. *Oligella*, a new genus including *Oligella urethralis* comb. nov. (formerly *Moraxella urethralis*) and *Oligella ureolytica* sp. nov. (formerly CDC Group IVe): Relationship to *Taylorella equigenitalis* and related taxa. *Int J Syst Bacteriol* 1987;37:198–210.
11. Bleumink-Pluym NM, van Dijk L, van Vliet AH, van der Giessen JW, van der Zeijst BA. Phylogenetic position of *Taylorella equigenitalis* determined by analysis of amplified 16S ribosomal DNA sequences. *Int J Syst Bacteriol* 1993;43:618–621.
12. Katz JB, Evans LE, Hutto DL, et al. Clinical, bacteriologic, serologic, and pathologic features of infections with atypical *Taylorella equigenitalis* in mares. *J Am Vet Med Assoc* 2000;216:1945–1948.
13. Jang SJ, Donahue JM, Arata AB, et al. *Taylorella asinigenitalis* sp. nov., a bacterium isolated from the genital tract of male donkeys (*Equus asinus*). *Int J Syst Evol Microbiol* 2001;51:971–976.
14. Båverud V, Nyström C, Johansson KE. Isolation and identification of *Taylorella asinigenitalis* from the genital tract of a stallion, first case of a natural infection. *Vet Microbiol* 2006;116:294–300.
15. Raetz CRH. Biochemistry of bacterial endotoxins. *Annu Rev Biochem* 1990;59:129–170.
16. Reeves PR, Hobbs M, Valvano MA, et al. Bacterial polysaccharide synthesis and gene nomenclature. *Trends Microbiol* 1996;4:495–503.
17. Whitfield C, Kaniuk N, Fridrich E. Molecular insights into the assembly and diversity of the outer core oligosaccharide in lipopolysaccharides from *Escherichia coli* and *Salmonella*. *J Endotoxin Res* 2003;9:244–249.
18. Perry MB, MacLean LL. Structural characterization of the O-polysaccharide of the lipopolysaccharide produced by *Salmonella milwaukee* O:43 (group U) which possesses human blood group B activity. *Biochem Cell Biol* 1992;70:49–55.
19. Perry MB, MacLean LL. Structure of the polysaccharide O-antigen of *Salmonella riogrande* O:40 (group R) related to blood group A activity. *Carbohydr Res* 1992;232:143–150.
20. Vinogradov E, Pepler MS, Perry MB. The structure of the nonreducing terminal groups in the O-specific polysaccharides from two strains of *Bordetella bronchiseptica*. *Eur J Biochem* 2000;267:7230–7237.
21. Vinogradov E, MacLean LL, Brooks BW, Lutze-Wallace C, Perry MB. The structure of the polysaccharide antigen of the lipopolysaccharide produced by *Taylorella* (formerly *Haemophilus*) *equigenitalis* type strain (ATCC 35865). *Carbohydrate Res* 2008;343:3079–3084.
22. Vinogradov E, MacLean LL, Brooks BW, Lutze-Wallace C, Perry MB. Structure of the O-polysaccharide of the lipopolysaccharide produced by *Taylorella asinigenitalis* type strain (ATCC 700933). *Biochem Cell Biol* 2008;86:278–284.
23. Brooks BW, Robertson RH, Lutze-Wallace CL, Pfahler W. Monoclonal antibodies specific for *Campylobacter fetus* lipopolysaccharides. *Vet Microbiol* 2002;87:37–49.
24. Brooks BW, Garcia MM, Robertson RH, Lior H. Electrophoretic and immunoblot analysis of *Campylobacter fetus* lipopolysaccharides. *Vet Microbiol* 1996;51:105–114.
25. Hitchcock PJ, Brown TM. Morphological heterogeneity among *Salmonella* lipopolysaccharide chemotypes in silver-stained polyacrylamide gels. *J Bacteriol* 1983;154:269–277.
26. Tsai CM, Frasch CE. A sensitive silver stain for detecting lipopolysaccharides in polyacrylamide gels. *Anal Biochem* 1982;119:115–119.
27. Johnson KG, Perry MB. Improved techniques for the preparation of bacterial lipopolysaccharides. *Can J Microbiol* 1976;22:29–34.
28. MacLean LL, Perry MB. Structural studies on the O-polysaccharide of the lipopolysaccharide produced by *Citrobacter rodentium* (ATCC 51459). *Eur J Biochem* 2001;268:5740–5746.
29. Brisson JR, Crawford E, Uhrin D, et al. The core oligosaccharide component from *Mannheimia* (*Pasteurella*) *haemolytica* serotype A1 lipopolysaccharide contains L-glycero-D-manno- and D-glycero-D-manno-heptoses: Analysis of the structure and conformation by high-resolution NMR spectroscopy. *Can J Chem* 2002;80:949–963.
30. Gradinaru DA, Helmer JM, Klein F. Production and characterization of monoclonal antibodies against *Taylorella equigenitalis*. *Vet Res* 1997;28:65–76.
31. Szymanski CM, Michael FS, Jarrell HC, et al. Detection of conserved N-linked glycans and phase variable lipooligosaccharides and capsules from campylobacter cells by mass spectrometry and high resolution magic angle spinning spectroscopy. *J Biol Chem* 2003;278:24509–24520.
32. Luk JMC, Kongmuang U, Reeves PR, Lindberg AA. Selective amplification of abequose and paratose synthase genes (*rfb*) by polymerase chain reaction for identification of *Salmonella* major serogroups (A, B, C2, and D). *J Clin Microbiol* 1993;31:2118–2123.
33. Feng L, Senchenkova SN, Tao J, et al. Structural and genetic characterization of enterohemorrhagic *Escherichia coli* O145 O antigen and development of an O145 serogroup-specific PCR assay. *J Bacteriol* 2005;187:758–764.
34. Feng L, Tao J, Guo H, et al. Structure of the *Shigella dysenteriae* 7 O antigen gene cluster and identification of its antigen specific genes. *Microb Pathog* 2004;36:109–115.

Protective potential of an attenuated *Pasteurella multocida*, which expresses only the N-terminal truncated fragment of *P. multocida* toxin

Jayoung Seo, Semi Lee, Hyoju Pyo, Jaeil Lee, Taejung Kim

Abstract

Pasteurella multocida serogroup D causes progressive atrophic rhinitis in pigs and produces a potent, intracellular, mitogenic toxin known as *P. multocida* toxin (PMT), which is encoded by the *toxA* gene. Highly toxic to cells, PMT is a poor antigen and becomes more immunogenic after its native structure has been destroyed. Previously, we found that the N-terminal fragment of PMT (N-PMT) can induce a strong immune response that is protective against wild-type challenge. Here, an attenuated *P. multocida* mutant expressing only N-PMT was developed and its protective effect was evaluated. The mutant provides protective immune responses against bacterial and toxin challenges, and so is a good live vaccine candidate.

Résumé

Pasteurella multocida séro-groupe D est responsable de la rhinite atrophique progressive du porc et produit une toxine intracellulaire puissante et mitogène dénommée toxine de *P. multocida* (PMT) qui est codée par le gène *toxA*. PMT est fortement toxique pour les cellules mais est un pauvre antigène et devient immunogène après que sa structure primaire ait été détruite. Précédemment, nous avons trouvé que le fragment N-terminal de PMT (N-PMT) peut induire une forte réponse immune qui est protectrice contre une infection défi avec une souche sauvage. Ici, un mutant atténué de *P. multocida* exprimant uniquement N-PMT a été développé et son effet protecteur évalué. Le mutant induit des réponses immunes contre une infection défi avec la bactérie et l'administration de toxine, et serait ainsi un bon candidat comme vaccin vivant.

(Traduit par Docteur Serge Messier)

Introduction

Pasteurella multocida-induced pneumonia and progressive atrophic rhinitis (PAR) are widespread diseases that cause growth retardation and a reduction in the efficiency of feed utilization among grower-finisher pigs (1–3). *Pasteurella multocida* toxin (PMT), a monomeric 146 kDa protein encoded by the *toxA* gene, is produced by some *P. multocida* serotype A and D strains (4). A poor antigen, PMT becomes more immunogenic after its native structure has been destroyed (5). Partially truncated proteins have been predicted to be good antigens (6). In a previous study, vaccination with a mixture of 3 recombinant fragments of PMT with/without inclusion of intact *P. multocida* resulted in high levels of neutralizing antibody (Ab) and protection against PMT challenge (6).

Attenuation of *P. multocida* can be achieved by the abrogation of the appropriate metabolic gene. In a previous study, an *aroA* mutant of *P. multocida* successfully protected calves against challenge with the pathogenic wild type (7). However, PMT was not involved since the toxin is expressed only in serotypes A and D in pigs (4). Previously, we demonstrated that none of the mice vaccinated with a *toxA* knock-out mutant that does not produce PMT were capable of surviving challenge with the wild type (8) indicating that mouse

Abs against outer structural and/or inner cytosolic proteins of *P. multocida* are not protective. So, it is clear that the targeting of the protection against *P. multocida* serotypes A and/or D should be focused on PMT.

We have previously shown that the N-terminal fragment of PMT (N-PMT, amino acids 1–390) is the most immunogenic portion of the protein, and that N-PMT is partially protective for mice against wild type challenge (9). To clarify whether N-PMT expressed in vivo can induce protective immunity against bacterial and toxin challenge, a *P. multocida* mutant capable of expressing only N-PMT instead of the intact toxin was developed and its protective effect was evaluated.

Materials and methods

Escherichia coli and plasmids

Escherichia coli JM109 (Invitrogen, Carlsbad, California, USA) was used to propagate the plasmid construct. The pGEM®-T easy vector (Promega, Madison, Wisconsin, USA) was used for cloning procedures. *Escherichia coli* manipulations were performed according to the manufacturer's instructions. Standard DNA and protein manipulations were carried out as previously described (10,11). Red

Biotherapy Human Resources Center, College of Veterinary Medicine, Chonnam National University, Gwangju 500-757, Republic of Korea.

Address all correspondence to Dr. Taejung Kim; telephone: 82-62-530-2858; fax: 82-62-530-2857; e-mail: tjkim@chonnam.ac.kr

Dr. Kim's current address is 300 Yongbong-dong, Buk-gu, College of Veterinary Medicine, Chonnam National University, Gwangju 500-757, Republic of Korea.

Received July 13, 2008. Accepted December 10, 2008.

Table I. Nucleotide sequences of the primers used in this study (GenBank reference numbers: AF240778 for *toxA* gene in *P. multocida* and AY048744 for *kanR* gene in pKD13)

Primers		Nucleotide sequence (5'–3')
P1	<i>toxA</i> -N-F	GCGC <u>CTCGAG</u> * ATGAAAACAAAACATTTTT
P2	<i>toxA</i> -N-R	GCGC <u>AGATCT</u> * GAGTAATGAAGAGCATAGT
P3	<i>toxA</i> -C-F	GCGC <u>GGTACC</u> * ATTGACTTTTTCCTAAATAA
P4	<i>toxA</i> -C-R	AATT <u>GGATCC</u> * TTATAGTGCTCTTGTAAAGC
P5	<i>kan^R</i> -F	GGCC <u>AGATCT</u> * ATGATTGAACAAGATGGAT
P6	<i>kan^R</i> -R	AATT <u>GGTACC</u> * TCAGAAGAACTCGTCAAGA

*Underlined: enzyme sites.

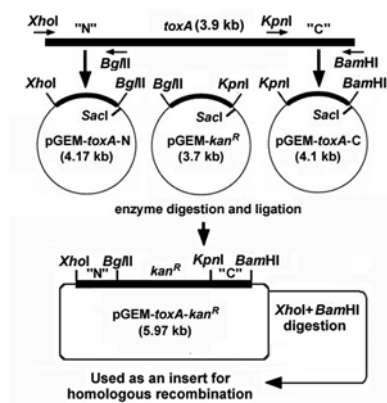


Figure 1. Diagram of cloning strategy. After cloning, an insert was prepared by digesting pGEM-toxA-kan^R with XhoI and BamHI restriction enzymes.

helper plasmid pKD46 (12), which expresses λ Red recombinase, was used to allow the homologous recombination of linear DNA in strain JM109. pKD13 (12) was used as a template for the generation of kanamycin resistance gene (*kan^R*). pKD46 is a temperature sensitive replicon, thus allowing its easy elimination at 43°C.

Cloning of *toxA* and *kan^R* fragments

Pasteurella multocida type D was originally obtained from the National Veterinary Research & Quarantine Service, Korea. The N-terminal (amino acids 1–390) and C-terminal (amino acids 921–1285) regions of *toxA* were amplified using *P. multocida* genomic DNA as a template. For the selection of knock-out colonies, *kan^R* was used for transformant selection, which was amplified by polymerase chain reaction (PCR) using pKD13 as a template. Six PCR primers (P1–P6) were designed using the Gene Runner software program (Hastings Software, Hastings, New York, USA) from the nucleotide sequences in the GenBank database (Table I). The amplified DNA products were electrophoresed on a 1.2% (w/v) agarose gel, purified using a PCR purification kit (Qiagen, Valencia, California, USA) according to the manufacturer's instructions, and cloned into a pGEM[®]-T easy vector (Qiagen) to generate pGEM-toxA-N, pGEM-toxA-C, and pGEM-kan^R (Figure 1). The construct was transformed into chemically competent *E. coli* JM109. The transformants were selected and the mini-scale isolation of the plasmid DNA was used to prepare the recombinant plasmid for sequencing on the plasmid DNA QIAprepSpin Mini Kit (Qiagen). EcoRI restriction analysis and DNA sequencing confirmed the presence and

orientation of each gene or gene segment. DNA sequencing reactions were performed using an automated DNA sequencer (ABI PRISM 3100 Genetic Analyzer; Applied Biosystems, Foster City, California, USA).

Cloning strategy

Two constructs (pGEM-toxA-N and pGEM-kan^R) were digested with BglII and SacI, and the *kan^R* gene was inserted into the BglII+SacI site of pGEM-toxA-N, generating pGEM-toxA-N-kan^R. pGEM-toxA-C was digested with KpnI and SacI and inserted into KpnI+SacI site of pGEM-toxA-N-kan^R, generating pGEM-toxA-kan^R. A linear 2.97 kb DNA fragment (*toxA*-N-kan^R-*toxA*-C) produced by digestion with XhoI and BamHI was used as an insert (100 ng/ μ L) for homologous recombination. The cloning strategy is depicted in Figure 1.

Gene disruption by homologous recombination

A 5-mL volume of a fresh overnight *P. multocida* culture was inoculated into 500 mL Brain-Heart Infusion (BHI). Cells were grown to an optical density at 600 nm (OD₆₀₀) of approximately 0.5, chilled on ice for 20 min, and centrifuged at 4000 \times g for 15 min at 4°C. The supernatant was removed and the pellet was concentrated 100-fold and washed 3 times with ice-cold 10% glycerol. The final preparation represented the competent cells.

For the induction of λ Red recombinase, competent cells were transformed with pKD46 using a Gene Pulser Xcell electroporation system (Bio-Rad, Hercules, California, USA) according to the manufacturer's instructions. Transformants carrying pKD46 were grown in 5 mL SOB containing 10 mM each of ampicillin and L-arabinose (final) at 30°C to an OD₆₀₀ of approximately 0.5, and then made electro-competent by concentrating 100-fold and washing 3 times with ice-cold 10% glycerol. Electro-competent cells (40 μ L) were transformed with 1 μ L (100 ng) of insert DNA (*toxA*-N-kan^R-*toxA*-C) by electroporation according to the manufacturer's instructions. Knock-out mutants were selected on LB plates containing 50 μ g/mL kanamycin.

PCR verification

Three PCR procedures were used to show that mutants had the correct genomic structure. Genomic DNA from a mutant colony was prepared (50 ng/ μ L) and used as a template. The expected sizes and targets of the 3 PCR approaches are represented in Figure 2.

Table II. Experimental design for toxigenicity test and protection study. Mice in groups 1 and 2 were vaccinated with live PMT mutant *P. multocida* bacterial culture, while controls (groups 3 and 4) with PBS. For challenge study, group 2 and 4 were challenged with W/T *P. multocida*, while group 1 and 3 with W/T bacterial lysate

Group	Route	Dosage per mouse	Trial number	Challenge with
1	Intraperitoneal	PMT mutant (1×10^7 cells)	12	Bacterial lysate 500 μ L
2	Intraperitoneal	PMT mutant (1×10^7 cells)	12	Bacterial culture (1×10^7 cells)
3	Intraperitoneal	PBS 100 μ L	12	Bacterial lysate 500 μ L
4	Intraperitoneal	PBS 100 μ L	12	Bacterial culture (1×10^7 cells)

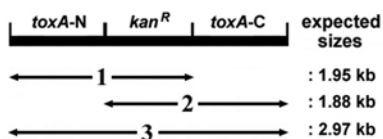


Figure 2. Diagram of PCR verification for genomic structure. The expected sizes and targets of three PCR approaches (1–3) were obtained.

P1 and P6 were used for PCR 1, P5 and P4 for PCR 2, and P1 and P4 for PCR 3.

In vitro expression of N-PMT

The expression of N-PMT in vitro was confirmed by a Western blot assay. Briefly, freshly prepared lysate of the PMT mutant was subjected to 10% sodium dodecyl sulfate-polyacrylamide gel electrophoresis (SDS-PAGE) and transferred to a 0.45- μ m nitrocellulose membrane (Bio-Rad). For immunodetection, the membrane was blocked in phosphate buffered saline (PBS) + 0.05% Tween-20 (pH 7.4) (PBST) containing 1% skim milk for 1 h. The membrane was washed 3 times with PBST before being incubated with the primary and secondary Abs for 1 h at 37°C. Anti-N-PMT mouse polyclonal Ab was produced by immunization of mice with recombinant N-PMT produced in *E. coli* (9), and used as a primary Ab. Goat anti-mouse IgG horseradish peroxidase (HRP)-conjugated Ab (Serotec, Oxford, United Kingdom) was used as the secondary Ab. The membrane was developed in a diaminobenzidine (DAB) substrate buffer containing a DAB concentrate (Serotec) until brownish bands were observed. Color development was quenched by thorough washing in PBS.

Vaccination with PMT mutant

Pasteurella multocida toxin mutant bacterial cultures were prepared in BHI broth at a concentration of 1×10^8 cells/mL. Forty-eight 6-week-old ICR mice of both sexes (Charles River, Yokohama, Japan) were divided into 4 groups (Table II). Experimental groups were inoculated with 100 μ L of freshly prepared culture (1×10^7 bacteria/mouse) and controls received 100 μ L PBS. This was followed by 3 more booster injections with bacteria or PBS at 2-week intervals.

Ab induction in vivo

To check if partial truncated N-PMT expressed by PMT mutant in vivo could induce Abs, mouse blood samples were collected from the tail vein 7 d after the final booster injection and were used for

an enzyme-linked immunosorbent (ELISA) assay. Briefly, 96-well plates (Maxisorp; Nunc, Roskilde, Denmark) were coated with recombinant N-PMT (1 μ g/well/90 μ L) as previously described (9). The plates were blocked with PBS containing 1% skim milk and washed with PBST. The sera for IgG analysis were prepared at a 1:100 dilution (shown in preliminary experiments to be the optimal dilution). Ab in 90 μ L PBST were incubated for 1 h at 37°C, emptied, and washed with PBST 3 times. The bound IgG was detected using goat anti-mouse HRP-conjugated IgG (Pierce, Rockford, Illinois, USA) diluted 1:500. The secondary Ab was incubated for 1 h at 37°C, emptied, and washed 3 times with PBST. A substrate solution consisting of 10 mL of 0.1 M citric acid buffer (pH 4.0), 250 μ L of 3-ethylbenzthiazoline-6-sulfonic acid (ABTS) stock solution (ABTS 100 mg ABTS in 4.5 mL distilled water), and 50 μ L hydrogen peroxide (H_2O_2) was used to detect the presence of any bound secondary Ab. The plate was developed in the dark at room temperature for 15 min. The absorbance at 405 nm was read using a Multiskan EX ELISA reader (Thermo LabSystems, Beverly, Massachusetts, USA). The results were expressed as the average \pm standard deviation (*s*) of the end-point titers. A *t*-test was used to examine the differences in the mean Ab values using GraphPad InStat Software 3.05 (GraphPad software, La Jolla, California, USA).

Bacterial and toxin challenges

For the preparation of bacterial toxin as previously described (8), 50 mL of wild type *P. multocida* overnight cultures (1×10^8 cells/mL) were washed twice with 10 mL PBS, sonicated, and the supernatants filtered through a 0.2- μ m membrane filter. Fifteen days after vaccination, groups 1 and 3 were challenged with 500 μ L of freshly prepared bacterial lysate (bacterial toxin, which corresponds to LD100), while groups 2 and 4 were challenged with 100 μ L of freshly prepared wild type *P. multocida* culture (corresponds to LD100). The mortality rate was recorded for 10 d after the inoculation. A *t*-test was used to examine the differences in the protection rates.

Results

Disruption of *toxA* by homologous recombination

Figure 3 shows the results of the PCR verification. As expected, the 1.95 kb PCR1, 1.88 kb PCR2, and 2.97 kb PCR3 fragments were

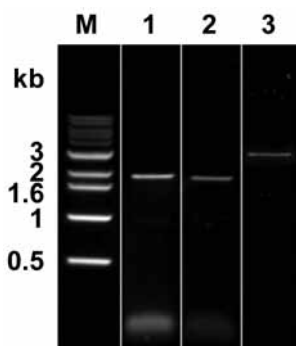


Figure 3. Results of PCR verification. PCR products with expected sizes (1.95 kb for PCR1, 1.88 kb for PCR2, and 2.97 kb for PCR3) were produced. Lane 1: PCR1, lane 2: PCR2, lane 3: PCR3.

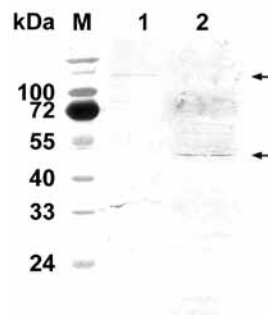


Figure 4. Antigenic recognition of N-PMT. Mouse polyclonal Ab raised against the recombinant N-PMT reacted with intact PMT (lane 1 upper arrow, approximately 146 kDa) and a bacterial protein of approximately 47 kDa (lane 2 lower arrow). M: molecular size marker.

Table III. Result of challenge studies using live bacterial culture or lysate

Group	Days after challenge					Total
	1	3	5	7	10	
1	—	—	—	—	2	2/12*
2	—	—	—	—	1	1/12*
3	2	10	—	—	—	12/12
4	—	6	—	—	6	12/12

* Two-sided *P*-value is lower than 0.0001, which is extremely significant on Fisher's exact test.

produced. The sequences of the PCR verification products were analyzed and confirmed by DNA sequencing (data not shown).

Expression of N-PMT in vitro

Anti-N-PMT mouse polyclonal Ab raised against recombinant N-PMT reacted with intact PMT from wild type *P. multocida* lysate and against a PMT mutant protein of approximately 47 kDa (Figure 4), confirming the in vitro production of a truncated N-PMT.

Ab induction in vivo

Mouse Abs against N-PMT expressed in vivo were successfully induced, as shown by an ELISA. Analysis of the mouse IgG level against N-PMT demonstrated that the mice, intraperitoneally immunized with the mutant *P. multocida*, successfully produced IgG (mean OD value = 1.472, *s* = 0.195, *P* < 0.001). However, no significant increase in IgG level was shown in the control group (mean OD value = 0.267, *s* = 0.025).

Bacterial and toxin challenge

Most of the mice immunized with mutant *P. multocida* were protected upon challenge (Table III). In total, 21 of the mice (87.5%) survived in the PMT mutant-immunized group, while none survived in the PBS control group (*P* < 0.0001).

Discussion

Recently, a genetically modified PMT toxin produced by replacing the serine at position 1164 with alanine, and the cysteine at position 1165 with serine led to a complete loss of the toxic effects of PMT

without impairing the ability to induce protective immunity in pigs (13). Also, vaccination of sows with a mixture of 3 recombinant fragments of the PMT fragments (N-terminal, middle, and C-terminal) with/without intact *P. multocida* produced high levels of neutralizing Ab and protection of offspring against a PMT challenge (13). These suggest that the induction of IgG and/or IgA protective immunity against pasteurellosis can be achieved when the appropriate immunogens and administration routes are used.

Currently, clinical PAR is usually controlled by combined vaccination with *Bordetella bronchiseptica* and *P. multocida*, which consists mainly of toxoid and/or somatic antigens of both bacteria. Using these vaccines, pathogenic lesions, excretion of bacteria, and the time to market under experimental and field conditions are decreased. Some vaccines also have been shown to protect pigs against the development of lung lesions when administered properly. Although vaccination has unquestionable beneficial effects, current vaccines are not able to eliminate the bacteria (14). Also, in our previous study (8), none of the mice vaccinated with a PMT-eliminated mutant (*toxA* knock-out) survived after wild type challenge, indicating that mouse Abs against outer structural and/or inner cytosolic proteins of *P. multocida* are not protective. So, the toxigenicity of this bacterium seemed to be derived mainly from PMT and the protective immunity against wild type *P. multocida* can be acquired only when protection against PMT has been established (13). Also, animals vaccinated with recombinant N-PMT are successfully protected after wild type challenge (9), which prompted us to develop a mutant expressing only N-PMT.

Expression of N-PMT in vitro and in vivo was confirmed by western blot and ELISA indicating that the elimination of the middle

and C-terminal fragments of PMT has no influence on protein expression. Mice immunized with mutant successfully produced anti-N-PMT Abs without any pathogenic effects of PMT, indicating this mutant has been well attenuated and N-terminal itself has little damage to animals. In the challenge experiments, only 3 out of 24 mice in groups 1 and 2 (12.5%) were killed, while all control mice succumbed. This indicates that protective Ab against PMT can be induced by purified (9) and/or bacterial (this study) recombinant N-PMT.

In this study, we constructed an attenuated *P. multocida* expressing only N-PMT to demonstrate the potential of this mutant to elicit a protective immune response in mice. Although further experiments with pigs will be performed, we conclude that this mutant represents a good candidate for the development of live bacterial vaccine.

Acknowledgment

The authors thank Ms. Myeonghwa Kim (College of Veterinary Medicine, Chonnam National University) for her excellent technical assistance.

References

- de Jong MF. Progressive and nonprogressive atrophic rhinitis. In: Straw BE, D'Allaire S, Mengeling WL, Taylor DJ, eds. Diseases of Swine. Ames, Iowa: Iowa State Univer Pr, 1999:355–384.
- Pijoan C. 1999. Pneumonic pasteurellosis. In: Straw BE, D'Allaire S, Mengeling WL, Taylor DJ, eds. Diseases of Swine. Ames, Iowa: Iowa State Univer Pr, 1999:511–520.
- Hunt ML, Adler B, Townsend KM. The molecular biology of *Pasteurella multocida*. Vet Microbiol 2000;72:3–25.
- Pullinger GD, Bevir T, Lax AJ. The *Pasteurella multocida* toxin is encoded within a lysogenic bacteriophage. Mol Microbiol 2004;51:255–269.
- van Diemen PM, de Vries Reilingh G, Parmentier HK. Immune response of piglets to *Pasteurella multocida* toxin and toxoid. Vet Immunol Immunopathol 1994;41:307–321.
- Liao CM, Huang C, Hsuan SL, et al. Immunogenicity and efficacy of three recombinant subunit *Pasteurella multocida* toxin vaccines against progressive atrophic rhinitis in pigs. Vaccine 2006;24:27–35.
- Hodgson JC, Finucane A, Dagleish MP, et al. Efficacy of vaccination of calves against hemorrhagic septicemia with a live *aroA* derivative of *Pasteurella multocida* B:2 by two different routes of administration. Infect Immun 2005;73:1475–1481.
- Kim TJ, Lee JI, Lee BJ. Development of a *toxA* gene knock-out mutant of *Pasteurella multocida* and assessment of its protective effects. J Microbiol 2006;44:320–326.
- Seo JY, Pyo HJ, Lee SM, et al. Expression of 4 truncated fragments of *Pasteurella multocida* toxin and their immunogenicity. Can J Vet Res 2009;73:184–189.
- Ausubel FM, Brent R, Kingston RE, et al. Short Protocols in Molecular Biology. New York, New York: John Wiley & Sons, 2002.
- Sambrook J, Fritsch EF, Maniatis T. 2001. Molecular Cloning: A Laboratory Manual. Cold Spring Harbor, New York: Cold Spring Harbor Lab Pr, 2001.
- Datsenko KA, Wanner BL. One-step inactivation of chromosomal genes in *Escherichia coli* K-12 using PCR products. Proc Natl Acad Sci USA 2000;97:6640–6645.
- To H, Someno S, Nagai S. Development of a genetically modified nontoxic *Pasteurella multocida* toxin as a candidate for use in vaccines against progressive atrophic rhinitis in pigs. Am J Vet Res 2005;66:113–118.
- Haesebrouck F, Pasmans F, Chiers K, Maes D, Ducatelle R, Decostere A. Efficacy of vaccines against bacterial diseases in swine: What can we expect? Vet Microbiol 2004;100:255–268.

Activation of the ovine hypothalamic-pituitary-adrenal axis and febrile response by interleukin-6: A comparative study with bacterial lipopolysaccharide endotoxin

Niel A. Karrow, Qiumei You, Carl McNicoll, Jack Hay

Abstract

Sheep were subjected to immune challenge with either recombinant human interleukin-6 (rhIL-6; 2.0 µg/kg; $n = 5$), *Escherichia coli* lipopolysaccharide (LPS) endotoxin (400 ng/kg; $n = 7$), or saline ($n = 6$) to determine if IL-6 activates the febrile and hypothalamic-pituitary-adrenal axis (HPAA) responses in sheep, and to compare these responses with those associated with endotoxemia. Blood was collected over time to measure plasma adrenocorticotrophic hormone (ACTH) and serum cortisol concentrations as indicators of HPAA activity. Unlike LPS, rhIL-6 was not pyrogenic in sheep at this challenge dose. In contrast, rhIL-6 elicited ACTH and cortisol responses that peaked earlier than those induced by LPS. These results suggest that this dose of IL-6, alone, is not sufficient to elicit the febrile response in sheep, however, it is a potent activator of the ovine HPAA response.

Résumé

Des moutons ont été immunisés avec un des produits suivants, de l'interleukine-6 humaine recombinante (rhIL-6; 2,0 µg/kg; n = 5), de l'endotoxine du lipopolysaccharide (LPS) de Escherichia coli (400 ng/kg; n = 7), ou de la saline (n = 6) afin de déterminer si IL-6 active la réponse fébrile et la réponse de l'axe hypothalamo-hypophyso-surrénalien (HPAA) chez les moutons, et de comparer ces réponses avec celles associées à une endotoxémie. Du sang a été prélevé dans le temps afin de mesurer les concentrations plasmatiques d'hormone adrénocorticotrope (ACTH) et les concentrations sériques de cortisol comme indicateurs de l'activité HPAA. Contrairement au LPS, la rhIL-6 n'était pas pyrogène chez le mouton à la concentration testée. Par contre, rhIL-6 a induit des augmentations d'ACTH et de cortisol qui ont atteint des maximums plus tôt que celles induites par le LPS. Ces résultats suggèrent que l'IL-6 seule n'est pas suffisante pour induire la réponse fébrile chez le mouton, toutefois, c'est un puissant activateur de la réponse HPAA chez le mouton.

(Traduit par Docteur Serge Messier)

Introduction

Bi-directional communication occurs between the neuroendocrine and immune systems during gram-negative bacterial infections as a means to maintain or restore physiological homeostasis (1). Toll-like receptor 4 (TLR-4) complexes expressed on the surface of host sentinel cells initially mediate pathogen recognition by ligating to lipopolysaccharide (LPS) endotoxin derived from the bacterial membrane. This ligation initiates the induction of numerous gene products, including the cytokines TNF- α , IL-1, and IL-6. These pro-inflammatory cytokines contribute to the activation of thermoregulatory neurons within the hypothalamus (2), and to the activation of the hypothalamic-pituitary-adrenal axis (HPAA), which leads to secretion of corticotrophin-releasing factor (CRF) and arginine vasopressin (AVP) from the hypothalamus. Both CRF and AVP subsequently initiate the synthesis and release of adrenocorticotrophic hormone (ACTH) from the anterior pituitary into the circulatory system, which stimulates the adrenal cortex to secrete glucocorticoids such as cortisol into the circulatory system (1). Glucocorticoids

have a wide range of immunomodulatory properties, one of which includes controlling the potentially damaging host inflammatory response that was mounted against the pathogen (3).

Interleukin-6 is a pleiotropic cytokine with reported bioactivities that include activation of the febrile response in rats during endotoxemia (4), and activation of the HPAA response in mice (5), and primates (6). A number of studies, several of which were carried out in our laboratory, have reported increased circulating IL-6 concentrations in sheep experiencing endotoxemia (7–11). However, we have been unable to correlate increased IL-6 concentration with the febrile and HPAA response in sheep, raising question about its involvement in eliciting these responses in this species (9–11).

Therefore, the purpose of this study was to determine if IL-6 activates the febrile and HPAA responses in sheep, and to compare these responses with those associated with endotoxemia. Sheep were systemically challenged with either recombinant human IL-6 (rhIL-6), *Escherichia coli* LPS, or saline, and the febrile and HPAA responsiveness were assessed over time; previous studies have demonstrated that rhIL6 is bioactive in guinea pigs (12), rabbits (13), and ruminants (14).

Centre for the Genetic Improvement of Livestock, Department of Animal and Poultry Science, University of Guelph, Guelph, Ontario N1G 2W1 (Karrow, You, McNicoll); Department of Immunology, University of Toronto, Toronto, Ontario M5S 1A8 (Hay).

Address all correspondence to Dr. Niel Karrow; telephone: (519) 824-4120 x53646; fax: (519) 767-0573; e-mail: nkarrow@uoguelph.ca

Received August 27, 2008. Accepted January 5, 2009.

Materials and methods

Experimental animals

Six-month-old, Rideau-Arcott ewe lambs were subjected to bolus IV challenge with either LPS from *E. coli* (serotype 0111:B4, $n = 7$, 400 ng/kg; Sigma Chemical, St. Louis, Missouri, USA), rhIL-6 ($n = 5$, 2.0 µg/kg, R&D Systems, Minneapolis, Minnesota, USA), or saline as a control ($n = 6$). The LPS dose was determined from a previous dose-response study (10), whereas the dose of rhIL-6 was estimated from the literature (12). The challenge studies were carried out over a period of 6 d to facilitate sample collection. Body temperatures were monitored during the challenges by measuring rectal temperature with a standard digital thermometer. All animals were held at the Ontario Ministry of Agriculture and Food and Rural Affairs Ponsonby Sheep Research Station, Ontario, and housed in individual pens with access to food and water ad libitum during the challenge. The University of Guelph Animal Care Committee approved all procedures involving these animals.

Blood collection

Jugular blood was collected into either heparinized, or silicon gel and clot activator Vacutainer tubes (Becton Dickinson and Company, Oakville, Ontario) 0, 0.25, 0.5, 1, 2, and 3 h post immune challenge to obtain plasma and serum, respectively. Blood was centrifuged at $1000 \times g$ for 15 min at room temperature to obtain plasma and serum. For serum collection, the blood was allowed to clot for approximately 45 min at room temperature prior to centrifugation. Plasma and serum were aliquoted into microcentrifuge tubes and stored at -80°C .

ACTH and cortisol response to immune challenge

Plasma ACTH concentrations were determined using a commercially available chemiluminescence enzyme-linked immunosorbent assay (ELISA) kit (Calbiotech, Spring Valley, California, USA) and a Victor 3 plate reader (Perkin-Elmer, Wellesley, Massachusetts, USA). The ACTH response in plasma samples from all subject animals was assessed for the time periods 0, 0.25, 0.5, 1, 2, and 3 h post-immune challenge. Samples were analyzed in triplicate with an average intra-assay CV of 3.8% for all plates.

Serum cortisol concentrations were measured using a commercially available luminescence immunoassay kit (IBL Hamburg, Minneapolis, Minnesota, USA) and a Victor 3 plate reader. The cortisol response was measured 0, 1, 2, and 3 h post-immune challenge. Samples were analyzed in triplicate with an average intra-assay coefficient of variation (CV) of 8.5% for all plates.

Statistical analysis

Data were analyzed as a complete block design using SAS (SAS 2002; SAS Institute, Cary, North Carolina, USA), and considered significant when $P < 0.05$. Residual plots were examined to assess variance homogeneity, and natural log transformations were utilized when required. Statistical analysis was carried out using the PROC MIXED procedure with repeated measurements over time, and the mixed procedure, incorporating the best fitting covariance structure, included in the model (15). Time trends across the 3 h study were

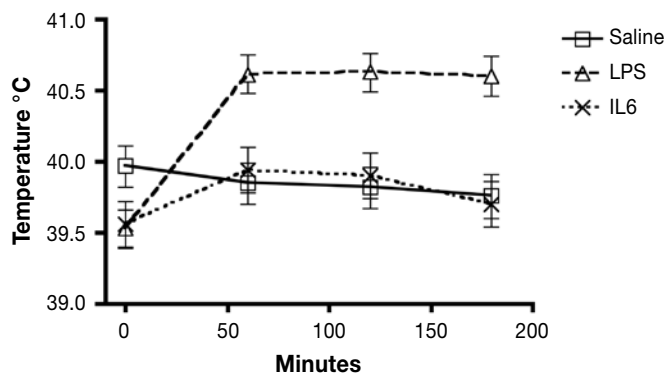


Figure 1. Ovine febrile response to systemic challenge with recombinant human IL-6 (rhIL-6; 2.0 µg/kg; $n = 5$), *Escherichia coli* lipopolysaccharide (LPS) endotoxin (400 ng/kg; $n = 7$), or saline ($n = 6$). Results are presented as the mean concentration \pm standard deviation (s).

compared among treatment groups (LPS, rhIL-6, saline) from differences of linear and quadratic orthogonal polynomial contrasts across time among treatment groups (16).

Results

Sheep responded significantly to the LPS challenge with an increase in body temperature (Figure 1). Significant LPS*saline ($P < 0.01$) and LPS*rhIL-6 ($P < 0.01$) linear contrasts were observed between treatments. Significant rhIL-6*saline quadratic contrasts ($P = 0.02$) were also observed; however, they are not deemed to be biologically significant given that the difference between these treatments was largely determined by different 0 h temperature measurements.

Both LPS and IL-6 challenges induced serum cortisol in sheep (Figure 2). Significant linear contrasts between LPS*saline ($P < 0.01$) and LPS*rhIL-6 ($P < 0.01$), and quadratic contrasts between LPS*saline ($P < 0.01$) and rhIL-6*saline ($P < 0.01$) were measured (Figure 2A). The cortisol response to LPS peaked within 2 h and remained elevated for the 3-h duration of the study. In contrast, the peak cortisol response to rhIL-6 challenge occurred around 1 h and returned to basal levels within 2 h post-challenge.

Plasma ACTH was induced during LPS and rhIL-6 challenge (Figure 2B). Significant LPS*saline ($P > 0.01$) and LPS*rhIL-6 ($P < 0.02$) linear contrasts, and rhIL-6*saline ($P < 0.01$) quadratic contrasts were observed between the treatments. The ACTH response to LPS peaked within 2 h and remained elevated for the duration of the study, whereas the peak ACTH response to rhIL-6 challenge occurred around 30 min and returned to basal levels within 2 h post-challenge.

Discussion

Circulating concentrations of the pro-inflammatory cytokine IL-6 increase as part of the host response to bacterial infection. This cytokine is critical for regulating the innate and acquired immune systems (17) and is, in part, responsible for inducing the febrile and HPA axis response associated with endotoxemia (4,5).

Circulating concentrations of ovine IL-6 have also been reported to increase during endotoxemia (7–11). A study by Kabaroff et al

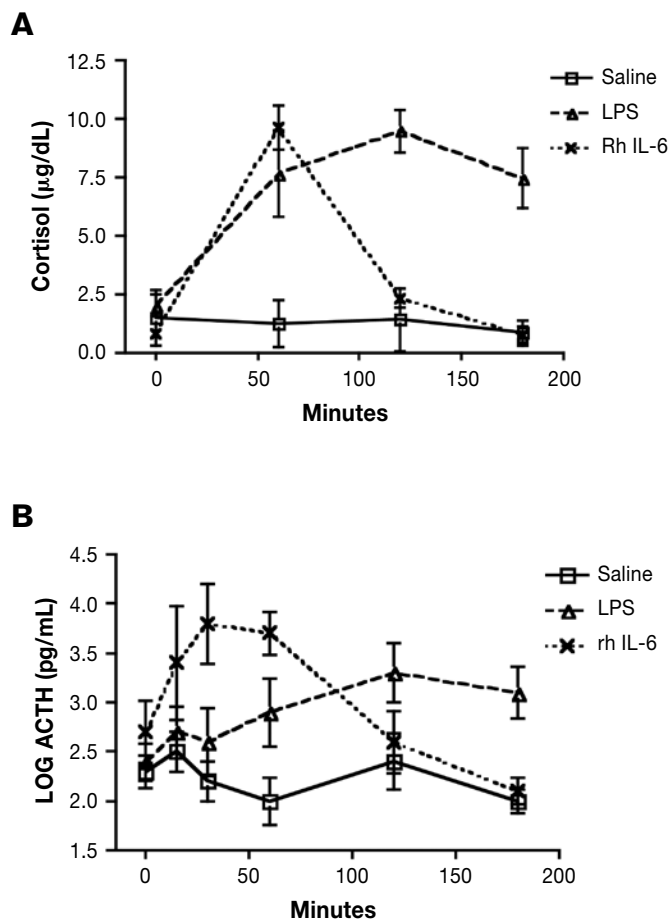


Figure 2. Ovine cortisol response (A) and ACTH response (B) to systemic challenge with recombinant human IL-6 (rhIL-6; 2.0 µg/kg; n = 5), *Escherichia coli* lipopolysaccharide (LPS) endotoxin (400 ng/kg; n = 7), or saline (n = 6). Results are presented as the mean concentration ± standard deviation (s).

(10), for example, showed that systemic challenge with LPS (400 or 600 ng/kg) caused a significant and sustained increase in serum IL-6 concentration 3–7 h post-challenge; however, serum IL-6 concentrations did not correlate with either serum cortisol concentration, or the febrile response. Another study, conducted by You et al (11), also demonstrated that LPS-induced serum IL-6 concentrations did not correlate with cortisol concentrations in sheep that had been selected based on their phenotypic extreme cortisol response to LPS (400 ng/kg) (11). Kabaroff et al later carried out a LPS challenge study (400 ng/kg) using pregnant and lactating sheep and showed that ovine IL-6 was non-responsive to LPS during early-to-mid-pregnancy, yet febrile and cortisol responses were observed. This was in contrast to late pregnancy, where the IL-6 response to LPS occurred, and correlated with the cortisol but not febrile response to LPS (9). Lastly, a study carried out by McClure et al (8) demonstrated that during late pregnancy, LPS (300 ng/kg) elicited a febrile and IL-6 response that is attenuated in comparison to non-pregnant ewes. Given the variable results of these studies, some of which were likely attributed to hormonal changes associated with pregnancy, it is difficult to assess the significant contribution of IL-6 in the induction of the ovine febrile and HPAA responses during endotoxemia.

The purpose of this study, therefore, was to determine whether or not IL-6, alone, induces the febrile and HPAA response in sheep. The results presented herein suggest that IL-6 is not pyrogenic but elicits transient activation of the HPAA, as determined by increased blood ACTH and cortisol concentrations. The dose of rhIL-6 used in this study was equivalent to 33 ng/mL of plasma [estimated on the basis of 60 mL/kg body weight (BW) for a 35 kg sheep], which is physiologically relevant but higher than peak IL-6 concentrations of 5 ng/mL reported for sheep challenged with 300 ng/kg LPS (8). Since rhIL-6 binding affinity to the IL-6 receptor was not assessed in this study, it is likely that the bioactive concentration was lower than this, and that higher doses of rhIL-6 may be required to induce a febrile response in sheep.

A number of studies have demonstrated that IL-6 is weakly pyrogenic in various species, depending on the route of administration and dose. One study reported that rhIL-6, but not heat-treated rhIL-6, was pyrogenic when administered to rabbits by intracerebroventricular (ICV) injection; the heat treatment demonstrated that rhIL-6 was bioactive as opposed to antigenic (13). An earlier rat study also demonstrated that rhIL-6 was pyrogenic when administered by ICV injection, but not when it was administered by either IV, or IP injection (19). In Guinea pigs, rhIL-6 was not pyrogenic when administered IV at a dose of 1 µg/kg, but caused a dose-independent febrile response between 5–20 µg/kg, and a dose-dependent febrile response at 50 and 100 µg/kg (12). Lastly, low dose infusion of rhIL-6 (140 pg/mL) administered to humans did not elicit significant changes in body temperature despite increases in plasma cortisol concentration (19). We are unaware of any ruminant studies aside from the present study that have evaluated the pyrogenic activity of rhIL-6.

A number of studies have demonstrated that IL-6 is critical signal for HPAA activation. Studies using IL-6 and IL-1 deficient mice, and neutralizing IL-6 antiserum in normal C57BL/6 mice for example, demonstrated that IL-6 is a circulating afferent signal to the HPAA during inflammation (5). Earlier studies by Perlstein et al (20) demonstrated that rhIL-6 alone, and synergistically with rhIL-1 induced circulating ACTH in mice. Lastly, a human study demonstrated that infusion with rhIL-6 induces HPAA activation (19). These studies combined with the present study suggest that IL-6 plays a significant role in the activation of the HPAA response across various species during systemic inflammation.

Temporal differences in HPAA response were observed between the rhIL-6 and LPS challenges in the present study, and this may, in part, explain why IL-6 concentrations were not previously associated with the ovine febrile and HPAA response to LPS in other ovine studies (9–11). These differences may be attributed to potential interaction with other cytokines, such as IL-1, IL-1ra, and IL-10, and the timing of their secretion. Turnbull et al (5) for example, demonstrated that activation of the HPAA by IL-6 was dependent on prior activation of an IL-1 type I receptor. Additionally, Perlstein et al (20) demonstrated that HPAA activation was dependent on synergistic IL-1 and IL-6 signaling. Lastly, Steensberg et al (19) showed that rhIL-6 induced the secretion of circulating IL-1ra and IL-10; both of these anti-inflammatory cytokines are likely to decrease circulating concentrations of IL-1, which may shorten the duration of HPAA activation.

In summary, we have shown that 2 µg/kg of rhIL-6 is not pyrogenic in sheep, but transiently activated the HPAA when compared with LPS. This suggests that IL-6, alone, is not sufficient to activate the febrile response in sheep at the dose used in this study; however, it is an important afferent signal to the HPAA in sheep during systemic inflammation.

Acknowledgments

The authors thank James Godsmark, Yune Kim, Dr. Bhawani Sharma, and Sameer Pant of the Department of Animal and Poultry Science, University of Guelph for their assistance with this study. The authors also thank Dr. Margaret Quinton for her assistance with the statistical analysis of the data. This research was funded, in part, by the Natural Sciences and Engineering Council of Canada, and the Ontario Ministry of Agriculture of Food and Rural Affairs.

References

- Karrow NA. Activation of the hypothalamic-pituitary-adrenal axis and autonomic nervous system during inflammation and altered programming of the neuroendocrine-immune axis during fetal and neonatal development: Lessons learned from the model inflammagen, lipopolysaccharide. *Brain Behav Immunity* 2006;20:144–158.
- Nilsberth C, Elander L, Hamzic N, et al. The role of IL-6 in LPS-induced fever by mechanisms independent of prostaglandin-E2. *Endocrinol* 2009;150:1850–1860.
- Webster JL, Sternberg EM. Role of the hypothalamic-pituitary-adrenal axis, glucocorticoids and glucocorticoid receptors in toxic sequelae of exposure to bacterial and viral products. *J Endocrinol* 2004;181:207–221.
- Harden LM, du Plessis I, Poole S, Laburn HP. Interleukin-6 and leptin mediate lipopolysaccharide-induced fever and sickness behavior. *Physiol Behav* 2006;89:146–155.
- Turnbull A, Prehar S, Kennedy A, Little R, Hopkins S. Interleukin-6 is an afferent signal to the hypothalamo-pituitary-adrenal axis during local inflammation in mice. *Endocrinol* 2003;144:1894–1906.
- Willette AA, Lubach GR, Coe CL. Environmental context differentially affects behavioral, leukocyte, cortisol, and interleukin-6 responses to low doses of endotoxin in the rhesus monkey. *Brain Behav Immun* 2007;21:807–815.
- Grigsby PL, Hirst JJ, Scheerlinck JP, Phillips DJ, Jenkin G. Fetal responses to maternal and intra-amniotic lipopolysaccharide administration in sheep. *Biol Reprod* 2003;68:1695–1702.
- McClure L, O'Connor AE, Hayward S, Jenkin G, Walker DW, Phillips DJ. Effects of age and pregnancy on the circulatory activin response of sheep to acute inflammatory challenge by lipopolysaccharide. *J Endocrinol* 2005;185:139–149.
- Kabaroff L, Boermans H, Karrow NA. Changes in ovine maternal temperature, and serum cortisol and interleukin-6 concentrations after challenge with *Escherichia coli* lipopolysaccharide during pregnancy and early lactation. *J Anim Sci* 2006;84:2083–2088.
- Kabaroff LC, Rodriguez A, Quinton M, Boermans H, Karrow NA. Assessment of the ovine acute phase response and hepatic gene expression in response to *Escherichia coli* endotoxin. *Vet Immunol Immunopathol* 2006;113:113–124.
- You Q, Karrow NA, Quinton M, Mallard BA, Boermans HJ. Enhanced cutaneous hypersensitivity reactions are associated with ovine high and low cortisol responsiveness to acute endotoxin challenge. *Vet Dermatol* 2008;19:174–183.
- Blatteis CM, Quan N, Xin L, Ungar AL. Neuromodulation of acute-phase responses to interleukin-6 in guinea pigs. *Brain Res Bull* 1990;25:895–901.
- Opp M, Obal F Jr, Cady AB, Johannsen L, Krueger JM. Interleukin-6 is pyrogenic but not somnogenic. *Physiol Behav* 1989;45:1069–1072.
- Alsemgeest SP, van't Klooster GA, van Miert AS, Hulskamp-Koch CK, Gruys E. Primary bovine hepatocytes in the study of cytokine induced acute-phase protein secretion in vitro. *Vet Immunol Immunopathol* 1996;53:179–184.
- Wang Z, Goonewardene LA. The use of mixed models in the analysis of animal experiments with repeated measures over time. *Can J Anim Sci* 2004;84:1–11.
- Kuehl RO. *Design of Experiments: Statistical Principles of Research Design and Analysis*, 2nd ed. Pacific Grove, California: Duxbury Press at Books/Cole Publ, 2000.
- Naugler WE, Karin M. The wolf in sheep's clothing: The role of interleukin-6 in immunity, inflammation and cancer. *Trends in Mol Med* 2008;14:109–119.
- LeMay LG, Vander AJ, Kluger MJ. Role of interleukin 6 in fever in rats. *Am J Physiol* 1990;258:R798–803.
- Steensberg A, Fischer CP, Keller C, Møller K, Pedersen BK. IL-6 enhances plasma IL-1ra, IL-10, and cortisol in humans. *Am J Physiol Endocrinol Metab* 2003;285:E433–437.
- Perlstein RS, Mougey EH, Jackson WE, Neta R. Interleukin-1 and interleukin-6 act synergistically to stimulate the release of adrenocorticotrophic hormone in vivo. *Lymphokine Cytokine Res* 1991;10:141–146.

The effect of body position, sedation, and thoracic bandaging on functional residual capacity in healthy deep-chested dogs

Elizabeth A. Rozanski, Daniela Bedenice, Jennifer Lofgren, Julie Abrams,
Jonathan Bach, Andrew M. Hoffman

Abstract

The objective of this study was to determine the effect of body position, chest wrap, and sedation on functional residual capacity (FRC) in 6 healthy dogs. Functional residual capacity was determined by helium dilution (re-breathing) whilst in different clinically relevant conditions. These conditions included the standing (sternal) and lateral positions in unsedated dogs and then again both standing and lateral following chest bandaging, and sedation with acepromazine, IV and butorphanol, IV. The mean FRC at each measurement point was determined, as was the change in FRC (delta FRC) from one measurement point to another. Analysis of variance (ANOVA) with repeated measures with Fisher's LSD post hoc test was used to evaluate the effect of interventions. The differences in delta FRC were evaluated using a *t*-test or Wilcoxon rank-sum test. $P < 0.05$ was considered significant. The mean FRC at baseline, defined as standing, unsedated and unwrapped, was 75.3 ± 23.8 mL/kg. Body position or sedation had the most profound effect on FRC with right lateral recumbency lowering FRC by a median of 20.4 mL/kg and sedation lowering FRC by a median of 19.8 mL/kg. Common clinical procedures and positioning result in lowered FRC in healthy deep-chested dogs. In critically ill or injured dogs, the iatrogenic loss of FRC through chest bandaging, sedation, or body position may be clinically relevant.

Résumé

L'objectif de la présente étude était de déterminer l'effet de la position corporelle, d'un bandage thoracique et de la sédation sur la capacité résiduelle fonctionnelle (FRC) chez 6 chiens en santé. La capacité fonctionnelle résiduelle a été déterminée par dilution de l'hélium (ré-inhalation) lors de différentes conditions cliniques pertinentes. Ces conditions incluaient les positions debout (sternale) et latérale chez des chiens non sous-sédation et par la suite dans les mêmes positions mais suivant un bandage thoracique et sédation avec acépromazine, IV et butorphanol, IV. La FRC moyenne à chaque point de mesure était déterminée, tout comme le changement de FRC (delta FRC) entre un point de mesure à un autre. Une analyse de variance (ANOVA) avec mesures répétées à l'aide d'un test de Fisher post hoc des moindres carrés a été utilisée afin d'évaluer l'effet des interventions. Les différences dans les delta FRC ont été évaluées à l'aide d'un test de *t* ou le test de la somme des rangs de Wilcoxon. Une valeur $P < 0,05$ était considérée comme le seuil significatif. La FRC moyenne de base, définie chez l'animal en position debout, non sous-sédation et sans bandage était de $75,3 \pm 23,8$ mL/kg. La position corporelle ou la sédation avait l'effet le plus marquée sur la FRC avec le décubitus latéral droit réduisant la FRC par une valeur médiane de 20,4 mL/kg et la sédation réduisant la FRC par une valeur médiane de 19,8 mL/kg. Les procédures cliniques courantes et la position résultent en une FRC réduite chez les chiens à thorax profond en santé. Chez les chiens blessés ou atteint d'une maladie critique, la perte iatrogénique de FRC suite à un bandage thoracique, une sédation ou la position corporelle pourrait être cliniquement significative.

(Traduit par Docteur Serge Messier)

Introduction

Normal lung function is vital to adequate oxygenation and ventilation. Lung function may be affected through disease or trauma, or may be disturbed by medical or surgical procedures, in particular, by open thoracotomy. Thoracotomy is commonly performed in dogs for a variety of indications, including trauma, infection, and neoplasia. Both general anesthesia and thoracic surgery are widely known to reduce pulmonary function in dogs as well as people

intra-operatively as well as post-operatively (1–4). Post-operative complications involving the respiratory system may be significant and may include hypoxemia and hypoventilation (5,6). Separate from primary pulmonary pathology, these complications may result from atelectasis due to collapse of a lobe or lobes, loss of normal thoracic cavity recoil pressures, residual pleural space disease, pulmonary edema associated with sudden re-expansion of lung after collapse, and hypoventilation associated with pain or excessive sedation. Barotrauma from over-zealous mechanical ventilation

Lung Function Testing Laboratory, Cummings School of Veterinary Medicine, Tufts University, 200 Westboro Road, North Grafton, Massachusetts 01536, USA.

Address all correspondence to Dr. Elizabeth Rozanski; telephone: (508) 839-5395; fax: (508) 839-7922; e-mail: Elizabeth.rozanski@tufts.edu
Dr. Bach's current address is Department of Medical Sciences, University of Wisconsin School of Veterinary Medicine, 2015 Linden Drive, Madison, Wisconsin 53706, USA.

Received May 29, 2008. Accepted November 19, 2008.

may contribute to lung injury and potentially oxygen toxicity might lead to the development of airway reactivity. Additionally, changes in chest wall mechanics resulting from the incision at the surgical site may develop. However, atelectasis is perhaps the most common clinical problem and may develop from compression of the dependent lung, or absorption atelectasis may occur in oxygen supplemented patients. Atelectasis may lead to hypoxemia by altering ventilation-perfusion (V-Q) relationships.

During anesthetic recovery following a thoracotomy, dogs are often positioned in lateral recumbency and administered analgesics to prevent post-operative pain. Additionally, thoracic bandages are frequently placed to either protect the incision or to protect an indwelling thoracostomy tube. All these iatrogenic factors are hypothesized to combine to worsen lung function by reducing lung volume and therefore effective ventilation.

In dogs, more than in other species, there is a variation in the chest wall conformation. Dogs are considered “deep-chested,” if their chest height is much greater than their chest width, “normal-chested” if their chest height and width are approximately equal, and “barrel-chested” if their chest is wider than it is tall. Ventilation and perfusion are affected to some extent by gravity and body position, with dependent lung lobes being better ventilated.

Functional residual capacity is the volume of gas remaining in the lung at the end of a normal (not forced) expiration. Decreases in FRC will often parallel losses in pulmonary compliance, and represent loss of active lung volume. Peripheral airway collapse often occurs with decreases in FRC, and there may be resultant hypoxemia. A lower FRC in a given patient could be expected to accompany hypoxemia, as healthy lung has undergone atelectasis. Similarly, if routine procedures affect FRC in healthy dogs, simple inexpensive management strategies could improve outcome, such as shifting a dog's body position or removing an excessively tight chest wrap. Although FRC is considered a static lung volume determined by lung versus chest wall compliance, it is in fact alterable by endogenous or exogenous factors. We hypothesized that procedures routinely employed during and after general anesthesia and thoracotomy in dogs would be sufficient to reduce FRC in the absence of surgery in healthy dogs; the magnitude of this decrease may be critical in some patients. The goal of this study was to determine the impact of routine management practices, including body position, sedation, and chest wrapping on functional residual capacity (FRC) in healthy non-operated deep-chested dogs.

Materials and methods

Dogs

Healthy, deep-chested dogs were recruited from the students and staff of the Tufts Cummings School of Veterinary Medicine. Three German shepherds, 2 Irish setters and 1 redbone coonhound were recruited. The mean weight [\pm standard deviation (*s*)] of the dogs was 31.5 ± 6.9 kg and the mean age was 5.5 ± 3.3 y. There were 3 spayed females, 2 castrated males, and 1 intact male. All dogs were assessed as healthy based upon a complete physical examination with no evidence of any cardiopulmonary disorder. Additionally,

all dogs had a hematocrit, total protein, venous blood gas, and electrolyte panel evaluated, which were found to be within normal limits. All dogs were receiving heartworm prophylaxis. Dogs with a poor temperament or those that were over or underweight (Purina body condition score ≤ 3 or ≥ 6 on a scale of 1 to 9) were excluded. The study was approved by the Cummings School of Veterinary Medicine at Tufts University's Institutional Animal Care and Use Committee.

Measurement of functional residual capacity

Functional residual capacity (FRC) was determined using helium dilution as previously described (7,8). Briefly, a known volume ($4 \times$ estimated tidal volume) and concentration of test gas [10% helium (He), 21% oxygen (O₂), balance nitrogen (N)] was used to fill a reservoir bag connected to a 3-way stopcock and a tightly fitting low dead space face mask. Following expiration, the 3-way stopcock was turned to permit ventilation only between the dog and reservoir bag. Re-breathing occurred for 60 s and then following expiration, the 3-way stopcock was turned off to the reservoir bag and the patient returned to breathing room air. The final helium concentration was then determined. Additionally, the final carbon dioxide (CO₂) content of the reservoir bag was determined. The ambient temperature, humidity and barometric pressure of the room were recorded. The initial and final concentrations of He and the final concentration of CO₂ were determined using specified analyzers (Helium analyzer — PK Morgan, Chatham, Kent, United Kingdom; CO₂ analyzer CD-3A — Amtek, Pittsburgh, Pennsylvania, USA). The dilution of He (assumed to be a non-exchangeable gas) gave a measure of FRC according to the following equation:

$$FRC = \left\{ \left[\frac{He_i \times 0.625}{He_f} \times (1 - CO_2) \right] - [0.625 + DS_{ins}] \right\} \times 1.11L(BTPS)$$

where: He_i represents the initial concentration and He_f the final concentration of He, and DS_{ins} the instrument dead space (7).

Measurements of FRC were made in duplicate; if greater than a 5% difference existed or if the dog did not complete the test due to sudden movement, a 3rd measurement was obtained. In addition, FRC was corrected for body weight (FRC/kg).

Experimental design

In order to mimic routine post-operative management, dogs were measured both in the standing body position [Time point 1], in right lateral recumbency (restrained for 10 min and then measured while still in right lateral recumbency), [Time Point 2] following application of a thoracic bandage by a single investigator (ER) to a standard intra-bandage pressure of 5 cm H₂O in standing [Time Point 3] and in right lateral recumbency [Time Point 4]. The intra-bandage pressure was measured by placing an esophageal balloon connected to a water manometer within the bandage and then loosening or tightening the bandage as needed to reach 5 cm H₂O. Next, the dogs were sedated with acepromazine [0.03 mg/kg (4×10^{-7} oz/lb)] IV and butorphanol [0.1 mg/kg (1.6×10^{-6} oz/lb)] IV and with the bandage still in place, measured in sternal recumbency [Time Point 5] and in right lateral recumbency [Time Point 6], and finally, the bandage was removed and the dogs were again measured in right lateral recumbency [Time Point 7] and finally in sternal recumbency [Time Point 8].

Statistical analysis

Data from each time point is shown as mean \pm s or median \pm range. The data from each time point was examined for normalcy with a one-sample Kolmogorov-Smirnov Test. Data were compared using analysis of variance (ANOVA) with repeated measures with a Fisher's LSD post-hoc test to evaluate for differences between time points. As sternal and standing are not considered interchangeable, statistical analysis was not used to attempt to compare the time points, but rather data simply presented. A *P*-value of < 0.05 was considered significant. The average change in FRC (mL/kg) termed delta FRC, was calculated for each individual dog at each time point by determining the difference in FRC in mL/kg at the individual time points. The delta FRC/kg for each time point was determined for the entire group of dogs and compared using a Wilcoxon rank-sum test or *t*-test. Commercially available software was used for analysis (SPSS Version 13; SPSS, Chicago, Illinois, USA).

Results

All dogs tolerated the procedure well. The testing of each dog took approximately 2 h, to permit ample time for washout between measurements. All intra-time point measurements were at least 10 min apart. Dogs were measured standing for the unsedated time points and in sternal recumbency for the sedated time points. While sternal and standing are not interchangeable, the dogs were unwilling to stand while sedated, thus were measured in sternal recumbency. In one case, a triplicate measurement was made, as one of the setters (Dog 4), at the first measurement, struggled at the end of the recording, due to the dog's unfamiliarity with the test equipment. The other samples from this dog, and the other dogs were obtained uneventfully.

The results confirmed a significant difference between time points, with a repeated measures ANOVA *P*-value of 0.02. The mean FRC/kg for each time point is shown in Table I, while the mean FRC results from each individual dog at each time point is shown in Figure 1. The time points 4, 5, 6, and 7, corresponding respectively to lateral bandage no sedation, sternal bandage sedation, lateral bandage sedation and lateral no bandage sedation, were all significantly decreased from baseline (standing, no bandage, no sedation).

Body position

Lateral recumbency lowered FRC in awake, unwrapped dogs by a median of 20.4 mL/kg (range: 13 to 47.0 mL/kg) although this was not significant. In awake dogs with chest wraps, lateral recumbency significantly lowered ($P < 0.001$) the FRC by a median of 19.9 mL/kg (range: -7.4 to 38 mL/kg), while in sedated dogs with chest wraps, the FRC/kg also decreased significantly ($P = 0.003$) with a median decrease in FRC in moving from sternal to lateral recumbency of 6.8 mL/kg (range: 1.7 to 20.8 mL/kg). Finally, in sedated unwrapped dogs, sternal recumbency resulted in a significant increase ($P = 0.004$) in FRC of 15.5 mL/kg (range 0.8 to 60.7 mL/kg).

Sedation

Sedation resulted in a lower FRC in dogs with and without chest wraps. For dogs with chest wraps, sedation results in an apparent

Table I. The mean \pm standard deviation (s) FRC/kg of 6 dogs. *P*-values are for differences in comparison with time point 1. The time points are in brackets in the left hand column and the *P*-values in brackets in the right hand column

Position (time point)	FRC (mL/kg) [<i>P</i> =]
Standing, no bandage, no sedation [1]	75.3 \pm 23.8
Lateral, no bandage, no sedation [2]	50.8 \pm 13.2 [0.10]
Standing, bandage, no sedation [3]	55.2 \pm 19.3 [0.21]
Lateral, bandage, no sedation [4]	38.2 \pm 9.1 [0.009]*
Sternal, bandage, sedation [5]	38.2 \pm 15.2 [0.009]*
Lateral, bandage, sedation [6]	29.1 \pm 8.6 [0.001]*
Lateral, no bandage, sedation [7]	30.4 \pm 10 [0.002]*
Sternal, no bandage, sedation [8]	52 \pm 29.5 [0.10]

* $P < 0.05$.

decline in FRC when measured in the standing or sternal positions. In this case, the dogs were initially measured in a standing position and then became sternal after the sedation. Thus in the standing (unsedated/chest wrap) to sternal (sedated/chest wrap) dogs, there was median delta FRC of 19.8 mL/kg (range: 0.2 to 26.4 mL/kg). As inherent differences exist between sternal and standing, statistical analysis was not used to compare these results. For dogs in lateral recumbency with chest wraps, the addition of sedation resulted in a nonsignificant decrease in FRC ($P = 0.06$) with a median delta FRC of 9.6 mL/kg (range: 3.5 to 14 mL/kg).

In dogs without chest wraps, sedation alone resulted in a significant decrease in both sternal ($P = 0.003$) and lateral recumbency ($P < 0.001$). In sternal recumbency, the median delta FRC was 16.8 mL/kg (range: 2.0 to 52.6 mL/kg), while in lateral recumbency the median delta FRC was 19.2 mL/kg (range: 6.8 to 37.3 mL/kg).

Chest wrap

The addition of a chest wrap to a standing unsedated dog did not significantly lower FRC ($P = 0.07$). In right lateral recumbency, the application of a bandage to an unsedated dog resulted in a significant decrease in FRC ($P < 0.001$). The median decrease in FRC in standing dogs following the addition of a chest wrap was 18.6 mL/kg (range: 3.8 to 45.9 mL/kg) while in lateral dogs, the median decrease was 10.3 mL/kg (range: 2.5 to 24.3 mL/kg). In a sedated dog, the addition of a chest wrap did not significantly lower FRC in sternal ($P = 0.079$) or lateral recumbency ($P = 0.382$).

Discussion

The results of this study demonstrate the substantial impact of body position, chest wrapping, and sedation on FRC as measured by helium dilution in healthy deep-chested dogs. Functional residual capacity is a lung volume that reflects an "equilibrium volume," meaning that the chest wall muscles are relaxed and the elastic recoil forces from both the lung parenchyma and chest wall are equal. The FRC (mL/kg) in the dogs in this study was substantially higher than the values that have been previously reported in beagles, and likely reflects breed-related conformational differences, as beagles are normal-chested (9).

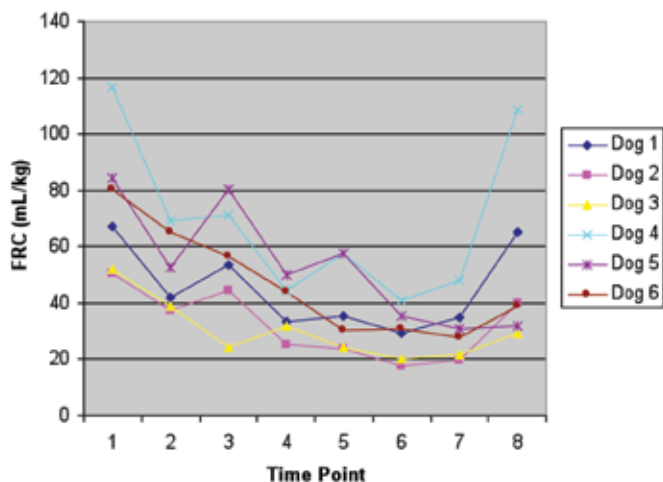


Figure 1. The individual values for FRC (mL/kg) for each dog. The time points are 1 — standing, no bandage, no sedation; 2 — lateral, no bandage, no sedation; 3 — standing, bandage, no sedation; 4 — lateral, bandage, no sedation; 5 — sternal, bandage, sedation; 6 — lateral, bandage, sedation; 7 — lateral, no bandage, sedation; and 8 — sternal, no bandage, sedation.

Functional residual capacity was chosen as a sensitive marker of atelectasis and the loss of exchangeable lung volume. More clinically applicable tests, such as pulse oximetry could also have been used to evaluate lung function; however, pulse oximetry is relatively insensitive to slight changes in oxygenation. Functional residual capacity is dynamic, there is not a “normal value” for all patients, and the value that becomes important is the relationship of the FRC to that while the patient is normal (eupnic, in a normal body position). The consequences of a low FRC include a decrease in the static compliance of the lung, gas trapping, increased intrapulmonary shunt, and hypoxemia (10). A correlation has been identified in decreases in the FRC and increases in the Alveolar-arterial (A-a) gradient (11). Lower airway flow rates will also increase airway resistance (12). Conversely, in diseases accompanied by airway obstruction (such as, human asthmatics) there is an increase in FRC brought about by air-trapping and a lower FRC accompanies clinical improvement (13).

A critique of our methods reveals 2 assumptions. First, we assumed that FRC is determined by physical factors (lung versus chest wall compliance) and is not dynamically altered; it is equivalent to relaxation volume. In fact, FRC is a dynamic value and changes may occur over seconds to minutes, which usually reverse quickly. Thus variation in the measurement of FRC, whatever technique is used, is a biological feature of breathing. Hence, the variation in FRC measurements within and between patients and between treatments may reflect subtle changes in FRC controlled involuntarily by the dogs. The use of duplicate measures was an attempt to minimize the impact of such natural variations, but these may be important in conscious measures of FRC. Second, the technique of helium dilution is precise in subjects for whom inspired helium rapidly equilibrates between the conducting airways and alveoli. In the absence of airway obstruction or emphysema, therefore, helium dilution is an accurate measurement of FRC. We assumed for the purpose of this study, that chest wrapping would induce changes in lung volume due to restriction of the chest wall rather than airway closure, and past studies

support this assumption (14–16). Alternative methods to measure FRC include computed tomography (17) and body plethysmography (18) but these are not practical in un-anesthetized dogs.

In this study, interventions used commonly following thoracotomy to support the surgical chest wound, resulted in reductions in FRC. Body position in particular had a significant effect on FRC. The dogs in this study were deep-chested (greater height versus width), and it is possible that the effect would be lessened in normal (for example, Labrador retriever) or barrel-chested (for example, Pug) dogs. In fact, one study of mixed breed dogs anesthetized with thiopental sodium showed no effect of body position (19). However in horses, lateral recumbency was associated with a significant decline in FRC (20). Body position studies in awake large animals are uncommon due to the inherent challenges in subject positioning. This study was compromised by the inability to measure sedated dogs in a standing position. Biomechanics of standing and sternal body position are not equivalent, and as such, results obtained in one position may not be directed compared with the other.

Body position has previously been evaluated in healthy people, with the highest FRC identified in a sitting (standing) position and the lowest in a supine (face up) position (21). Body position has been examined with increased enthusiasm in critically ill people with acute lung injury in recent years. In patients with acute lung injury, the rotation of the patient from the supine to the prone (face down) positions, has resulted in significant improvement in ventilatory variables (22,23). The mechanism for the improvement in ventilatory variable in acute lung injury patient reflects the recruitment of de-recruited lung and as well as decreased intra-pulmonary shunt; increased FRC will accompany this increase.

The profound effect on FRC of lateral recumbency is multifactorial, and includes a decrease in chest wall recoil, smaller lung volumes, atelectasis, and increased pulmonary recoil. Conformation and body weight are also important. Large animal species, particularly ruminants, develop hypoxemia when placed in lateral recumbency, even unsedated (24,25). The dogs in this study were evaluated in right lateral recumbency. This was chosen as the lung mass on the right side is slightly larger than on the left side in dogs; however, it is possible that a similar effect would have been seen had left lateral recumbency been chosen. Additionally, these pet dogs were not positioned in dorsal recumbency, so the effect of that body position remains unknown in this group of dogs.

Sedation also had a significant impact on the dogs in this study. General anesthesia is widely known to affect FRC (26). In humans, the FRC is reduced by approximately 0.5 L by general anesthesia (3). One previous study in experimental dogs, found no change in FRC associated with anesthesia induced by thiopental sodium while another study found a decrease in FRC of approximately 15% in sheep anesthetized with halothane and nitrous oxide (19,27). One study evaluating the effects of general anesthesia in dogs identified a significant decrease in static compliance. This decrease was prevented with periodic full lung inflations (sighs) and the compliance decrease was hypothesized to be secondary to atelectasis and decrease in FRC (28). In contrast, with conscious sedation, the effect on FRC appears dependent upon the agent used. A decrease of approximately 13% was found in ponies sedated with 0.04 mg/kg of acepromazine IM (26). In women given 10 mg of morphine, a

significant decrease in FRC occurred, while in contrast, in children sedated with ketamine, no significant change in FRC was identified (10,29). Children, as well as other baby mammals such as puppies, have relatively compliant chest walls; this would have been expected to help maintain FRC. Additionally, ketamine is a dissociative anesthetic as well as bronchodilator, these factors may have also supported the maintenance of FRC. The mechanism of the impact on FRC by sedation and anesthesia is likely multifactorial. The largest contributor appears to be lower tidal volume and shallower breathing that accompanies anesthesia. Muscle relaxation within the thoracic wall will further reduce chest wall recoil. This effect is observed in ventilated patients as well as spontaneously breathing patients; thus, independent effects of the anesthetic agent or loss of recruitment maneuvers (sighs) may also be factors. Clearly, in dogs following a thoracotomy, analgesics are warranted. However, the type of agent(s) used should be considered carefully. One drawback of our study design was that the sedation was administered only once, and dogs may have had relatively less sedation by the end of the study than shortly after receiving the agent.

Finally, chest wrapping results in significant decreases in FRC in laterally recumbent unsedated dogs, although not in dogs in sternal or standing or with sedation. In humans, the application of thoracic wraps has been associated with lower FRC while in horses the application of a tight girth has been documented to affect pulmonary function (14–16). The mechanism of loss of FRC in a thoracic wrap is likely through decreased elastic recoil of the thoracic cavity, which then would permit increased static recoil within the lung parenchyma and increased collapse.

Importantly, FRC is normally a dynamic value, and decreases in FRC do not necessarily indicate abnormal lung function. However, excessive decrease in FRC may be associated with pulmonary dysfunction. For example, normal sleep is associated with a loss of FRC in both normal and asthmatic people, but the FRC loss in asthmatics is greater and may contribute to nocturnal dyspnea in some individuals (30).

A potential limitation in this study includes the lack of simultaneous spirometric measurements to exclude inadequate equilibration of helium as a source of measurement error. Helium dilution relies upon adequate ventilation in order for equilibration to occur. Dogs in this study appeared to be ventilating adequately and the values obtained showed a similar level of reproducibility. However, future studies could attempt to measure the minute ventilation or to evaluate the differing equilibration times. In this study, 60 seconds was used for equilibration, which is longer than reported in previous canine studies and longer than that recommended for humans (7).

Not all dogs in the study responded with equivalent alterations in the measured FRC at different time points. Dog 4, the relatively non-compliant Irish setter, in particular, had more variable responses to different interventions, than dogs 2 and 3, which were calmer dogs. Relative “voluntary” contributions to FRC based on chest wall tone and recruitment maneuvers (voluntary sighs) will also impact volumes, and may account for individual patient differences.

This study demonstrates that body position, sedation, and chest wrapping resulted in a significant decrease in FRC as measured by helium dilution in healthy dogs. The impact of these interventions in dogs with pulmonary disease or following a thoracotomy is

unknown, but may be important and warrants further investigation. Future studies that define the alterations in gas exchange, spirometry, and regional effects on lung mechanics associated with these perturbations are also warranted.

References

1. Stobie D, Caywood DD, Rozanski EA, et al. Evaluation of pulmonary function and analgesia after intercostal thoracotomy and use of morphine administered intramuscularly or intrapleurally and bupivacaine administered intrapleurally. *Am J Vet Res* 1995;56:1098–1109.
2. Berg RJ, Orton EC. Pulmonary function in dogs after intercostal thoracotomy: Comparison of morphine, oxymorphone, and selective intercostal nerve block. *Am J Vet Res* 1986;47:471–474.
3. Hedenstierna G, Edmark L. The effects of anesthesia and muscle paralysis on the respiratory system. *Intensive Care Med* 2005;31:1327–1335.
4. Richardson J, Sabanathan S, Shah R. Post thoracotomy spirometric lung function: The effect of analgesia. A review. *J Cardiovasc Surg (Torino)* 1999;40:445–456.
5. Brainard BM, Alwood AJ, Kushner LI, et al. Postoperative pulmonary complications in dogs undergoing laparotomy: Anesthetic and perioperative factors. *J Vet Emerg Crit Care* 2006;16:184–191.
6. Furrer M, Rechsteiner R, Eigenmann V, et al. Thoracotomy and thoracoscopy: Postoperative pulmonary function, pain and chest wall complaints. *Eur J Cardiothorac Surg* 1997;12:82–87.
7. Amis TC, Jones HA. Measurement of functional residual capacity and pulmonary carbon monoxide uptake in conscious greyhounds. *Am J Vet Res* 1984;45:1447–1450.
8. Bedenice D, Rozanski E, Bach J, et al. Canine awake head-out plethysmography (HOP): Characterization of external resistive loading and spontaneous laryngeal paralysis. *Respir Physiol Neurobiol* 2006;151:61–73.
9. Dubin S, Westcott RJ. Functional residual capacity of normal unanesthetized beagle dogs. *Am J Vet Res* 1969;30:2027–2030.
10. Shulman D, Beardsmore CS, Aronson HB, et al. The effect of ketamine on the functional residual capacity in young children. *Anesthesiology* 1985;62:551–556.
11. Hickey RF, Visick D, Fairley HB, et al. Effects of halothane anesthesia on functional residual capacity and alveolar-arterial oxygen difference. *Anesthesiology* 1974;38:20–24.
12. Briscoe WA, Dubois AB. The relationship between airway resistance, airway conductance, and lung volumes in subjects of different ages and body size. *J Clin Invest* 1958;37:1279–1285.
13. Newton MF, O'Donnell DE, Forkert L. Response of lung volumes to inhaled salbutamol in a large population of patients with severe hyperinflation. *Chest* 2002;121:1042–1050.
14. De Troyer A. Mechanics of the chest wall during restrictive thoracic strapping. *Respiration* 1980;39:241–250.
15. van Noord JA, Demedts M, Clement J, et al. Effect of rib cage and abdominal restriction on total respiratory resistance and reactance. *J Appl Physiol* 1986;61:1736–1740.

16. Hoffman AM, Swanson LG, Bruns SJ, et al. Effects of tension of the girth strap on respiratory system mechanics in horses at rest and during hyperpnea induced by administration of lobeline hydrochloride. *Am J Vet Res* 2005;66:1167–1174.
17. Kraye S, Rehder K, Beck KC, et al. Quantification of thoracic volumes by three-dimensional imaging. *J Appl Physiol* 1987;62:591–598.
18. Kendrick AH. Comparison of methods of measuring static lung volumes. *Mondali Arch Chest Dis* 1996;51:431–439.
19. Lai YL, Rodarte JR, Hyatt RE. Respiratory mechanics in recumbent dogs anesthetized with thiopental sodium. *J Appl Physiol: Respirat, Environ Exercise Physiol* 1979;46:716–720.
20. Sorenson PR, Robinson NE. Postural effects on lung volumes and asynchronous ventilation in anesthetized horses. *J Appl Physiol* 1980;48:97–103.
21. Lumb AB, Nunn JF. Respiratory function and ribcage contribution to ventilation in body positions commonly used during anesthesia. *Anesth Analg* 1991;73:422–426.
22. Voggenreiter G, Aufmkolk M, Stiletto RJ, et al. Prone positioning improves oxygenation in post-traumatic lung injury — A prospective randomized trial. *J Trauma* 2005;59:333–343.
23. Mancebo J, Fernandez R, Blanch L, et al. A multicenter trial of prolonged prone ventilation in severe acute respiratory distress syndrome. *Am J Respir Crit Care Med* 2006;173:1233–1239.
24. Wagner AE, Muir WM, Grospitch BJ. Cardiopulmonary effects of position in conscious cattle. *Am J Vet Res* 1990;51:7–10.
25. Hall LW. Cardiovascular and pulmonary effects of recumbency in two conscious ponies. *Equine Vet J* 1984;16:89–92.
26. McDonnell WN, Hall LW. Functional residual capacity in conscious and anesthetized horses. *Br J Anaesth* 1974;46:802–803.
27. Dueck R, Rathbun M, Greenburg AG. Lung volume and VA/Q distribution response to intravenous versus inhalation anesthesia in sheep. *Anesthesiology* 1984;61:55–65.
28. Corcoran BM, Abercromby RH. Effects of general anesthesia on static respiratory compliance in dogs. *Vet Rec* 1989;125:450–453.
29. Tantucci C, Paoletti F, Bruni B, et al. Acute respiratory effects of sublingual buprenorphine: Comparison with intramuscular morphine. *Int J Clin Pharmacol Ther Toxicol* 1992;30:202–207.
30. Ballard RD, Irvin CG, Martin RJ, et al. Influence of sleep on lung volume in asthmatic patients and normal subjects. *J Appl Physiol* 1990;68:2034–2041.

Degradation of foot-and-mouth disease virus during composting of infected pig carcasses

J. Guan, M. Chan, C. Grenier, B.W. Brooks, J.L. Spencer, C. Kranendonk, J. Copps, A. Clavijo

Abstract

The objective of this study was to investigate the inactivation and degradation of foot-and-mouth disease (FMD) virus during composting of infected pig carcasses as measured by virus isolation in tissue culture and by real-time reverse transcriptase polymerase chain reaction (RRT-PCR). Three FMD-infected pig carcasses were composted in a mixture of chicken manure and wood shavings in a biocontainment level 3 facility. Compost temperatures had reached 50°C and 70°C by days 10 and 19, respectively. Under these conditions, FMD virus was inactivated in specimens in compost by day 10 and the viral RNA was degraded in skin and internal organ tissues by day 21. In comparison, at ambient temperatures close to 20°C, FMD virus survived to day 10 in the skin tissue specimen from the pig that had the highest initial level of viral RNA in its tissues and the viral RNA persisted to day 21. Similarly, beta-actin mRNA, tested as a PCR control, persisted to day 21 in specimens held at ambient temperatures, but it was degraded in the remnants of tissues recovered from compost on day 21. Results from this study provide evidence that composting could be used for safe disposal of pig carcasses infected with FMD virus.

Résumé

L'objectif du présent projet était d'étudier l'inactivation et la dégradation du virus de la fièvre aphteuse (FMD) durant le compostage de carcasses de porc infectées tel que mesuré par isolement viral en culture tissulaire et par réaction d'amplification en chaîne réverse par la polymérase en temps réel (RRT-PCR). Trois carcasses de porc infectées par le FMD ont été compostées dans un mélange de fumier de poulet et de copeaux de bois dans des installations de niveau de confinement biologique 3. La température du compost a atteint 50°C et 70°C après respectivement 10 et 19 jours. Dans ces conditions, le virus FMD a été inactivé dans les spécimens dans le compost après 10 jours et l'ARN viral a été dégradé dans la peau et les organes internes au jour 21. En comparaison, à température ambiante près de 20°C, le virus FMD a survécu jusqu'au jour 10 dans l'échantillon de peau du porc qui avait le plus haut niveau initial d'ARN viral dans ses tissus et l'ARN viral a persisté jusqu'au jour 21. De manière similaire, l'ARN de la bêta-actine, utilisé comme témoin du PCR, a persisté jusqu'au jour 21 dans les échantillons gardés à température ambiante, mais il était dégradé dans les restes de tissus récupérés du compost au jour 21. Les résultats de la présente étude fournissent des évidences que le compostage pourrait être utilisé pour l'élimination sécuritaire de carcasses de porc infectées avec le virus FMD.

(Traduit par Docteur Serge Messier)

Introduction

Foot-and-mouth disease (FMD) virus is a member of the *Aphthovirus* genus within the *Picornaviridae* family. Foot-and-mouth disease virus particles lack a lipid envelop, and their infectivity is insensitive to organic solvents, but labile at pH values of < 6.0 (1). The virus causes a highly contagious vesicular disease of domesticated and wild ruminants and pigs. Other susceptible wild species include hedgehogs, armadillos, nutrias, elephants, capybaras, rats, and mice. Ruminants are usually infected via inhalation of infectious droplets exhaled by infected animals (2–4), and pigs are often infected by consumption of unprocessed contaminated animal products (5). In addition, infection may be spread by direct contact with virus on fomites that are contaminated by animal secretions

and excretions, such as saliva, milk, urine, and feces (6). Clinical signs of FMD consist of a febrile response, excessive salivation, and development of vesicular lesions at predilection sites in the oral cavity and on tongue, muzzle, nares, teats, coronary bands, and interdigital spaces (5). Most infected animals eventually recover but often develop sequelae including sterility, abortion, excessive weight loss, significant loss in milk production, heart damage, lameness, and general poor condition.

As FMD can lead to significant economic consequences, many countries implement a “stamping out” policy established by the Office international des épizooties (OIE), where entire herds that contain infected animals are depopulated (7). In the 2001 FMD outbreak in the United Kingdom, more than 6 500 000 animals were slaughtered, and the various methods for disposal of carcasses

Ottawa Laboratory (Fallowfield), Canadian Food Inspection Agency, 3851 Fallowfield Road, Ottawa, Ontario K2H 8P9 (Guan, Chan, Grenier, Brooks, Spencer); National Centre for Foreign Animal Disease, Canadian Food Inspection Agency, 1015 Arlington Street, Winnipeg, Manitoba R3E 3M4 (Kranendonk, Copps, Clavijo).

Address all correspondence to Dr. Jiewen Guan; telephone: (613) 228-6698; fax: (613) 228-6670; e-mail: Jiewen.Guan@inspection.gc.ca

Dr. Clavijo's current address is Texas Veterinary Medical Diagnostic Laboratory, 1 Sippel Road, College Station, Texas 77843, USA.

Received December 8, 2008. Accepted February 17, 2009.

included on-farm burial, on-farm burning, commercial incineration, rendering, licensed landfill, and mass burial in engineered sites (8). However, difficulties were encountered in implementing disposal procedures. On-farm burial was restricted by legislation to protect groundwater supplies. Pyre burning was limited by public concerns related to smoke and other emissions, and both rendering facilities and licensed landfill sites were insufficient to meet the demand. There is a need for environmentally sound alternatives for the safe disposal of animal carcasses in the event of disease outbreaks or major natural disasters. Biosecurity agencies in Canada, the USA, Australia, and New Zealand have recognized the potential benefits of using composting for routine and emergency management of mortalities (9). On-site composting was successfully used for the safe disposal of more than 500 000 chicken carcasses during the 2004 avian influenza outbreak in British Columbia (10). The success of this operation suggested that composting strategies could be developed for the safe disposal of animal carcasses infected with other viruses, including FMD virus. Thus, the objective of the present study was to provide information on the fate of FMD virus in pig carcasses during composting using both real-time reverse transcriptase polymerase chain reaction (RRT-PCR) and tissue culture methods to measure viral presence and survival.

Materials and methods

Compost construction

Chicken manure for the compost was obtained from a cage layer operation at the University of Manitoba, Winnipeg, Manitoba and was mixed with wood shavings on a 1:1 dry weight basis. Sufficient water was added to adjust the moisture content of the mixture to approximately 65%, as measured with an IR-35 moisture analyzer (Denver Instrument, Denver, Colorado, USA). Mixing was done on the university premises using a feed mixer.

The composting experiment was conducted in a biosecure cubicle within a level 3 biocontainment facility at the National Centre for Foreign Animal Disease (NCFAD), Winnipeg, Manitoba. The compost bin, as illustrated in Figure 1, was constructed with Styrofoam panels and aluminium frames for the walls and floor. The interior of the bin was lined with a heavy plastic sheet, as previously described (11). To provide passive aeration, 2 pieces of perforated and flexible Big 'O' plastic drainage tubing (10 cm interior diameter, 3.5-m long; Armtec Limited, Orangeville, Ontario) were installed near the bottom of the bin with the ends projecting out above the top of the compost. The carcasses of 3 pigs that had been infected with FMD virus were buried in the compost mixture. The top of the compost was covered with a vapor barrier fabric. This was then covered with a 20-cm layer of wood shavings that served as insulation.

Infection of pigs by FMD virus

Three 5- to 6-week-old Landrace cross pigs, each weighing 7 to 9 kg, were used for this study. Each pig received a total of $10^{6.7}$ tissue culture infectious doses (TCID₅₀) of a highly virulent FMD virus (serotype O UKG 11/2001) via the oral and intranasal routes and also intradermally by inoculating it onto abraded coronary bands. All pigs were maintained in a biosecure cubicle

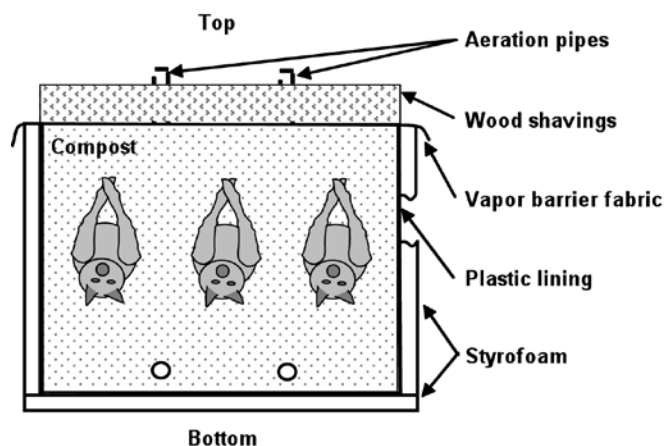


Figure 1. Cross section of the compost bin which had internal dimensions of 120 cm (L) × 110 cm (W) × 100 cm (H). Three pig carcasses were buried horizontally about 50 cm from the bottom of the bin and were spaced about 15 to 20 cm apart. Two pieces of aeration tubing were installed in the bin in a U shape such that the bottom of the U was about 10 cm from the bottom of the bin. The two Us were about 40 cm apart and their ends extended out of the compost.

within a level 3 biocontainment facility at NCFAD. The animal care procedures for this study conformed to guidelines established by the NCFAD Animal Care Committee, and were observed by an NCFAD veterinarian. The 3 pigs were euthanized at 2 or 3 d post-inoculation (dpi) and all 3 carcasses were composted within 24 h of storage at 20°C.

Specimen preparation

Carcasses of the 3 pigs were designated as C1, C2, and C3. Postmortem examinations were performed on C1 and C2 and 2 pools of specimens were collected from each carcass. One pool included skin tissues from coronary bands, interdigital cleft, hock, and snout. The other consisted of tissues from tonsils, thyroids, prescapular lymph nodes, adrenal glands, and kidneys. Each specimen pool was divided into 5 equal-sized portions. One portion was immediately stored at -80°C to serve as a time 0 control. Two others were placed in plastic bags that were held outside of the compost bin as ambient temperature controls. Another 2 specimens were contained in nylon mesh bags that were permeable to air, moisture, and microbes. Tissues in mesh bags were buried in compost where they were surrounded by plastic netting attached to metal chains to facilitate specimen recovery (12). The skin tissues were kept beside the corresponding carcass and organ tissues were placed inside the abdominal cavity that was later closed with sutures. On days 10 and 21, one specimen of both skin and organ tissues from C1 and C2 were removed from compost and from the ambient temperature environment. The C3 carcass was not opened but following removal of small pieces of skin tissues and of the epithelial layer of the tongue to serve as time 0 controls, the carcass was buried in compost. Temperatures within and outside the compost bin were recorded with stainless steel Hobo Temp Data loggers U12-015 (Onset Computer Corporation, Bourne, Massachusetts, USA). One logger was placed inside each of the plastic nettings that surrounded specimens from C1 and C2. In C3, one logger was inserted into the mouth and another into the rectum, and both the mouth and anal openings were then closed with sutures.

Virus extraction

To extract virus from composted and control tissues, the specimens were first homogenized using a mortar and pestle with the aid of Alumdum particles (60 mesh, Fisher Scientific, Ottawa, Ontario) in 50 mL of 10% beef extract (pH 8.0; Becton, Dickinson and Company, Oakville, Ontario). The homogenate was centrifuged at $5000 \times g$ for 60 min at 4°C for separation of compost or tissue debris. The supernatant was collected and 45 mL was mixed with an equal volume of 16% polyethylene glycol 6000 (pH 7.2; Sigma, St. Louis, Missouri, USA) in 0.01 M phosphate buffered saline (PBS, pH 7.2). The mixture was incubated at 4°C overnight, followed by centrifugation at $10\,000 \times g$ for 90 min at 4°C to precipitate the virus. The supernatant was discarded and the pellet was suspended in 12 mL of Dulbecco's PBS (Invitrogen, Burlington, Ontario) for both the RNA extraction and virus isolation.

Virus isolation

The above pellet suspension was treated with a cocktail of streptomycin, vancomycin, nystatin, and gentamycin as described previously (13). The treated suspension was passed through an ultra-low protein binding membrane filter with a pore size of 0.45 µm (Millipore, Nepean, Ontario). The filtrates were serially diluted in Dulbecco's PBS and then inoculated into primary lamb kidney (LK) cell cultures (14). The cell cultures were examined for cytopathic effect (CPE) after 48 h of incubation and were subjected to a freeze and thaw cycle to release virus into the culture fluids. To confirm the presence of the FMD virus in cell cultures with CPE, culture fluids were tested by RRT-PCR as described below and by double antibody sandwich ELISA (15). Rabbit anti-FMD O1 BFS 1860 sera and guinea pig anti-FMD O1 BFS 1860 sera produced at NCFAD were used as the capture antibody and the detector antibody, respectively. The culture fluids from the cell cultures without CPE were inoculated into fresh LK cell cultures for a second passage in an attempt to detect virus.

Quantification of viral RNA

Extraction of RNA was performed using the RNeasy mini kit (Qiagen, Mississauga, Ontario) with 375 µL of culture fluid or pellet suspension that resulted from virus extraction from composted and control specimens. In separate RRT-PCR assays, FMDV-3D primers and probe were used for absolute quantification of FMD viral RNA, and beta-actin primers and probe were used to amplify endogenous beta-actin mRNA from pig tissues as a control against false-negative results (14). Both assays were performed using reagents supplied from the QuantiTect Probe RT-PCR kit (Qiagen). A 25 µL reaction volume was used, including 2 µL of RNA template for the FMD virus assay or 5 µL of RNA template for the beta-actin assay. A final concentration of 0.5 µM of each forward and reverse primer and 0.2 µM of the probe were used in the FMD virus assay, and 1.0 µM of each primer and 0.2 µM of the probe were used for the beta-actin assay. Identical cycling conditions were used for both assays with an SDS 7900HT thermocycler (Applied Biosystems, Foster City, California, USA): reverse transcription at 50°C for 30 min; activation at 95°C for 15 min; followed by 45 cycles of 95°C for 10 s and 60°C for 1 min.

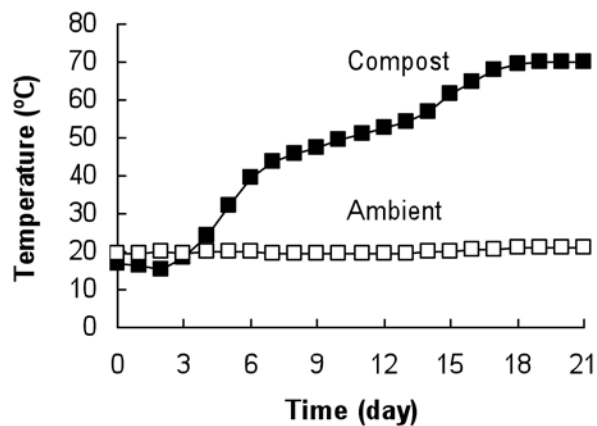


Figure 2. Temperature and time profiles. Data are average temperatures recorded by 8 loggers in compost (dark square) and 2 loggers outside of compost (white square). Standard deviation(s) were < 2°C.

Results

FMD virus infection

Within 2 or 3 d post-inoculation (dpi) with the FMD virus, all 3 pigs developed typical symptoms of disease that included severe depression, vesicles on feet, rupture and bleeding of vesicles, blanching on coronary bands, and some sloughing of the hoof shells. The pigs were euthanized within 3 dpi and their carcasses were composted.

Compost operation

The compost experiment was conducted for 21 d to study the survival of the FMD virus in the pig carcasses. Compost temperatures reached 50°C by day 10 and 70°C by day 19 (Figure 2). When the contents of the compost were examined on day 21, the remains of the carcasses consisted of scattered remnants of skin and muscle and some bones that could be readily crushed by hand.

The fate of FMD virus and viral RNA

Quantitative information on levels of virus in tissues was based on RRT-PCR results. Prior to composting, the concentration of FMD viral RNA was at least $2 \log_{10}$ higher in tissues from C2 than that in tissues from C1 (Figure 3 A & B). In specimens removed from compost on day 10, the viral RNA was not detected in specimens from C1 but there were still more than $4 \log_{10}/g$ of the viral RNA in specimens from C2. No viral RNA was detected in any of the specimens removed from the compost on day 21. In comparison, for specimens held at ambient temperatures (20°C), the viral RNA was detected in the skin tissue specimen from C1 collected on day 10 and in both the skin and the organ tissue specimens from C2 collected on days 10 and 21 (Figure 3 A & B). Beta-actin mRNA was not detected in any specimen removed from the compost on day 21 but it was detected in specimens removed on day 10 and all specimens held at ambient temperatures (data not shown). To more fully study virus survival in carcasses, C3 was kept intact

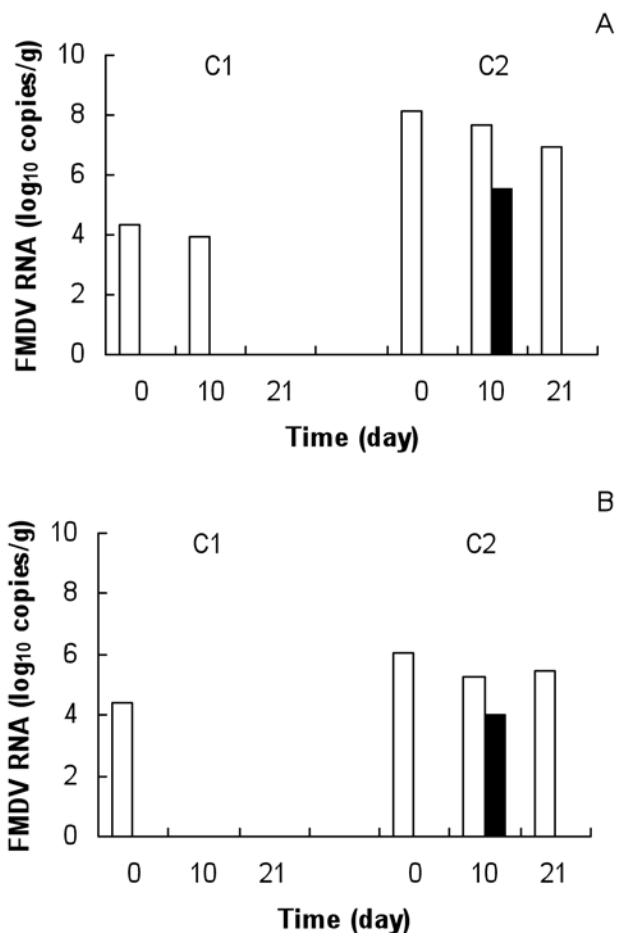


Figure 3. The fate of FMD viral RNA in skin (A) or organ (B) tissues in 2 infected pigs (C1 and C2). White bars represent levels of viral RNA in specimens at time 0 or at ambient temperatures whereas black bars represent the levels in compost.

except for removal of small pieces of external tissues. At time 0, the concentration of the FMD viral RNA in skin tissues from C3 was 8.2 log₁₀ copies/g (data not shown). When the compost study was terminated on day 21, neither viral nor beta-actin mRNA were detected in compost material that contained remnants of skin and other tissues of C3.

Foot-and-mouth disease virus was isolated from all time 0 skin tissue and organ tissue specimens from the 3 carcasses and the findings on skin tissue specimens are reported in Table I. All specimens that were removed from compost on days 10 and 21 were negative for the virus. Among specimens held at ambient temperatures, virus was isolated on day 10 from the skin tissues of C2 but was not isolated from any of the other specimens on days 10 or 21.

Discussion

The present study demonstrated that FMD virus in carcasses of infected pigs could be readily destroyed during composting in a plastic-lined insulated bin that was passively aerated. The temperatures in the compost reached 50°C within 10 d and approached 70°C for a short period by day 19. The feasibility of using the same

Table I. Survival of foot-and-mouth disease virus in skin tissues that were composted or held at ambient temperatures

Origin of skin tissues ^a	FMD virus				
	Time 0	Compost (20°C to 70°C)		Ambient temperatures (20°C)	
		Day 10	Day 21	Day 10	Day 21
C1	+ ^b	–	–	–	–
C2	+	–	–	+	–
C3	+	NA	–	NA	NA

^a Skin tissues were removed from all 3 carcasses (C1, C2, and C3) prior to composting. Tissues from C1 and C2 were contained in mesh bags or plastic bags that were placed in compost or held at ambient temperatures, respectively. Composted materials collected from C3 on day 21 contained remnants of skin.

^b Specimens were tested by the virus isolation method using primary lamb kidney cells. Cell culture fluids were tested by both ELISA and real-time RT-PCR to confirm the presence of FMD virus. NA — specimen not available.

composting methods for disposal of cattle carcasses in the event of an FMD-outbreak was evident from earlier studies where 32 animals, which were free of the virus, were composted. The temperatures in the compost reached 55°C to 65°C and during a 147-day period, all but large bones were converted to compost suitable for disposal on land (16). The heavy plastic liner in the compost bin for the present study contained the leachate, and thereby the virus, to the bin. In fact, as in earlier studies (11,12,16) very little leachate accumulated within the plastic-lined structures. Thus, this type of containment would allow composting to be conducted on farms without causing contamination of groundwater with viruses or other pollutants (17). This is important for disease control purposes since FMD virus has been shown to survive for more than 6 mo on the soil surface under snow (6). In this study, the compost mix surrounding the pig carcasses facilitated good carcass degradation and provided filtration to minimize the release of odor.

In addition to inactivating the FMD virus, the study demonstrated that the viral RNA could be degraded in tissues of infected carcasses within 21 d in compost, provided the temperatures were similar to those achieved herein. As expected, the initial virus loads varied in the tissues derived from different infected animals, and the time required for virus inactivation and viral RNA degradation appeared to be positively correlated with the initial concentrations of the virus in the infected tissues. This observation was consistent with a report on the duration of the virus in wool and in animal excretions (6). It is noteworthy that by 21 d of composting, the FMD virus was inactivated and its viral RNA degraded in the intact carcass as well as in the opened carcasses. The negative tests for FMD viral RNA in tissue specimens recovered from compost on day 10 were not due to inhibition of the assay since beta-actin mRNA was detected in all specimens on that day. As beta-actin mRNA is a component of tissues and would be much more abundant in carcasses than the viral RNA, degradation of beta-actin mRNA may serve as a good indicator for inactivation of the virus. In this study, the degradation of beta-actin mRNA by day 21 was consistent with the observation

that only remnants of tissues could be detected in the compost on that day. The findings support our earlier observations that the RNA of transgenes in bacteria and in plant tissue could be degraded during composting (11,18).

At ambient temperatures close to 20°C, the FMD virus survived for 10 d in the skin tissue that contained the highest initial concentration of viral RNA. Inactivation of the virus at such temperatures may be attributed to the decrease of pH during postmortem biochemical changes in tissues (19) and/or microbial activity during tissue decomposition (20). Degradation of the FMD viral RNA occurred more slowly at ambient temperatures than in compost, and the findings are consistent with observations on degradation of avian influenza and Newcastle disease viral RNA at ambient temperatures and in compost (12).

In conclusion, the present study provided evidence that composting strategies designed to provide a high level of biosecurity could serve as an environmentally desirable alternative for disposal of animal carcasses infected by FMD virus.

Acknowledgments

This study was a part of the CRTI04-0052RD project entitled "On site composting for bio-containment and safe disposal of infectious animal carcasses and manure in the event of a bio-terrorism attack," which was funded by the Canadian Chemical, Biological, Radiological, and Nuclear Research and Technology Initiative. Sincere appreciation is expressed to Dr. J. House and Mr. H. Muc at the University of Manitoba, Winnipeg, Manitoba for their assistance in preparing the compost mix. Appreciation is also extended to the NCFAD Animal Care staff and to Dr. M. Sabara and Ms. K. Hole for their technical support.

References

- Racaniello VR. Picornaviridae: The viruses and their replication. In: Knipe DM, Griffin DE, Lamb RA, et al. eds. *Fields' Virology*. 5th ed. Philadelphia, Pennsylvania: Lippincott Williams & Wilkins, 2007:795–838.
- Sellers RF. Quantitative aspects of the spread of foot and mouth disease. *Vet Bull* 1971;41:431–439.
- Sellers RF, Herniman KA, Donaldson AI. The effects of killing or removal of animals affected with foot-and-mouth disease on the amounts of airborne virus present in looseboxes. *Br Vet J* 1971;127:358–365.
- Donaldson AI, Alexandersen S, Sørensen JH, Mikkelsen T. The relative risks of the uncontrollable (airborne) spread of foot-and-mouth disease by different species. *Vet Rec* 2001;148:602–604.
- Blackwell JH. Internationalism and survival of foot-and-mouth disease virus in cattle and food products. *J Dairy Sci* 1980;63:1019–1030.
- Bartley LM, Donnelly CA, Anderson RM. Review of foot-and-mouth disease virus survival in animal excretions and on fomites. *Vet Rec* 2002;151:667–669.
- Office international des épizooties. *International Animal Health Code*, OIE, Paris, France. 2006.
- Scudamore JM, Trevelyan GM, Tas MV, Varley EM, Hickman G. Carcass disposal: Lessons from Great Britain following the foot-and-mouth disease outbreaks of 2001. *Rev Sci Tech* 2002;21:775–787.
- Wilkinson KG. The biosecurity of on-farm mortality composting. *J Appl Microbiol* 2007;102:609–618.
- Spencer JL, Guan J, Rennie B. Management related diseases—Manure management and environmental contamination. *Proc World Vet Poult Cong, Istanbul, Turkey, 2005*:159–162.
- Guan J, Spencer JL, Ma BL. The fate of the recombinant DNA in corn during composting. *J Environ Sci Health* 2005;40:463–473.
- Guan J, Chan M, Grenier C, Wilkie DC, Brooks BW, Spencer JL. Survival of avian influenza and Newcastle disease viruses in compost and at ambient temperatures based on virus isolation and real-time reverse transcriptase PCR. *Avian Dis* 2009;53:26–33.
- Guan J, Chan M, Ma B, et al. Development of methods for detection and quantification of avian influenza and Newcastle disease viruses in compost by real-time reverse transcription polymerase chain reaction and virus isolation. *Poult Sci* 2008;87:833–843.
- Moniwa M, Clavijo A, Li M, Collignon B, Kitching RP. Performance of a foot-and-mouth disease virus reverse transcription-polymerase chain reaction with amplification controls between three real-time instruments. *J Vet Diagn Invest* 2007;19:9–20.
- Alonso A, Martins MA, da Penha M, Gomes D, Allende R, Söndahl MS. Foot-and-mouth disease virus typing by complement fixation and enzyme-linked immunosorbent assay using monovalent and polyvalent antisera. *J Vet Diagn Invest* 1992;4:249–253.
- Xu W, Reuter T, Inglis D, et al. Development of a composting system for emergency disposal of cattle carcasses and manure during an infectious disease outbreak. *J Environ Qual* 2009;38:437–450.
- Harper AF, DeRouchey JM, Glanville TD, Meeker DL, Straw BF. Swine carcass disposal options for routine and catastrophic mortality. *Council Agr Sci Tech* 2008;39:1–16.
- Guan J, Spencer JL, Sampath M, Devenish J. The fate of a genetically modified *Pseudomonas* strain and its transgene during the composting of poultry manure. *Can J Microbiol* 2004;50:415–421.
- Panina GF, Civard A, Massirio I, Scatozza F, Baldini P, Palmia F. Survival of foot-and-mouth disease virus in sausage meat products (Italian salami). *Int J Food Microbiol* 1989;8:141–148.
- Vass AA. Beyond the grave — understanding human decomposition. *Microbiol Today* 2001;28:190–192.

Pulmonary intravascular macrophages and endotoxin-induced pulmonary pathophysiology in horses

Karin Aharonson-Raz, Baljit Singh

Abstract

Endotoxemia causes significant mortality and morbidity in horses. The mechanisms underlying this complex pathophysiology remain unclear. Therefore, effective tools to treat endotoxemia in horses are lacking. Furthermore, the multifactorial and multiorgan pathophysiology of equine endotoxemia has not been fully addressed, especially the lung injury associated with endotoxemia. Within the context of the broader picture of endotoxemia and lung injury, we offer a perspective on the roles of pulmonary intravascular macrophages in endotoxin-induced lung inflammation in horses.

Résumé

L'endotoxémie est une cause de mortalité et de morbidité important chez les chevaux. Le mécanisme qui sous-tend cette pathophysiologie complexe demeure nébuleux. Ainsi, des outils efficaces pour traiter une endotoxémie chez des chevaux sont manquants. De plus, la pathophysiologie multifactorielle et multi-organes de l'endotoxémie équine n'a pas été complètement étudiée, plus spécifiquement les lésions pulmonaires associées avec l'endotoxémie. Dans le contexte plus global de l'endotoxémie et des lésions pulmonaires, nous offrons une perspective sur les rôles des macrophages pulmonaires intra-vasculaires lors d'inflammation pulmonaire chez les chevaux.

(Traduit par Docteur Serge Messier)

Bacteria and their products, such as endotoxins, cause many inflammatory diseases, such as endotoxemia. Endotoxemia is one of the leading causes of mortality and morbidity in adult horses and foals (1). Endotoxemia is referred to as "inflammation gone awry" (2). A major factor contributing to the inappropriate inflammatory response is the shedding of lipopolysaccharides (LPS) from gram-negative bacteria into the circulation. This pro-inflammatory molecule activates macrophages, neutrophils, and the endothelium of various vascular beds (3). Endotoxins have a critical role in equine diseases, such as acute abdominal disease, adynamic post-operative ileus, laminitis, and neonatal septicemia (4). Earlier data showed that approximately 80% of horses experience colic during their lifetime and a mortality rate of 40% was reported among 2500 horses that had colic and were referred to 12 university hospitals in the United States from 1981 to 1984. Furthermore, the severity of the intestinal lesion as well as the prognosis is directly correlated with the degree of endotoxemia (2). Recently, more data showed that the incidence of colic in different horse populations varied from 3.5 to 10.6 episodes of colic per 100 horses per year and the case fatality rates as a result of colic vary from 6.7% to 15.6%, depending on the population studied and the type of lesion; in some equine populations this is the single most common cause of death (5). These data support the notion that endotoxemia is a significant cause of economic damage to the equine industry.

Horses are unique in their extreme sensitivity to endotoxin-induced cardio-pulmonary shock and mortality. The intraperitoneal lethal dose of LPS for ponies is 200 to 400 µg/kg of bodyweight

(BW), whereas the lethal dose for rabbits and guinea pigs is 3 and 10 mg/kg BW, respectively (6,7). The mechanism of these phenomena remains largely unknown (8). Thus, we describe how the pulmonary intravascular macrophages (PIMs) contribute to the endotoxin-induced lung pathophysiology in horses.

Recent data on the biology of Toll-like receptors (TLR) have enhanced our understanding of innate host responses to pathogens. It is now known that in addition to CD14, TLR4 is essential to ligate and phagocytose LPS (9). The ligation, phagocytosis, or both of LPS leads to activation of cell signalling, resulting in NF-κB activation and elaboration of proinflammatory cytokines (10). Because TLR4 is expressed on macrophages, monocytes, endothelial cells, and neutrophils (3), the consequences of endotoxemia are systemic vascular inflammation, as well as disseminated intravascular coagulation (11). Thus, the cascade ensued may lead to a dysregulated inflammatory response, such as that seen in endotoxemia or sepsis, leading to multiple organ failure, including cardiopulmonary shock.

The progression of endotoxemia to lung injury and respiratory distress is complex and follows multiple interrelated pathways. One proposed pathway is the uptake of endotoxin by the endothelial cells through molecules such as TLR and CD14 in the pulmonary vasculature, which causes direct toxicity to the cells (12). The other proposed pathway is the activation of the complement cascade by endotoxins, particularly C5a and C3a, which are anaphylatoxins and cause an increase in vascular permeability via mast cell degranulation. The endotoxin C5a further activates the lipoxygenase pathway in neutrophils and monocytes, acts as a chemotaxin for leukocytes,

Department of Veterinary Biomedical Sciences, Western College of Veterinary Medicine, University of Saskatchewan, Saskatoon, Saskatchewan S7N 5B4.

Address all correspondence to Dr. Baljit Singh; telephone: (306) 966-7408; fax: (306) 966-7405; e-mail: baljit.singh@usask.ca

Received June 4, 2008. Accepted October 24, 2008.

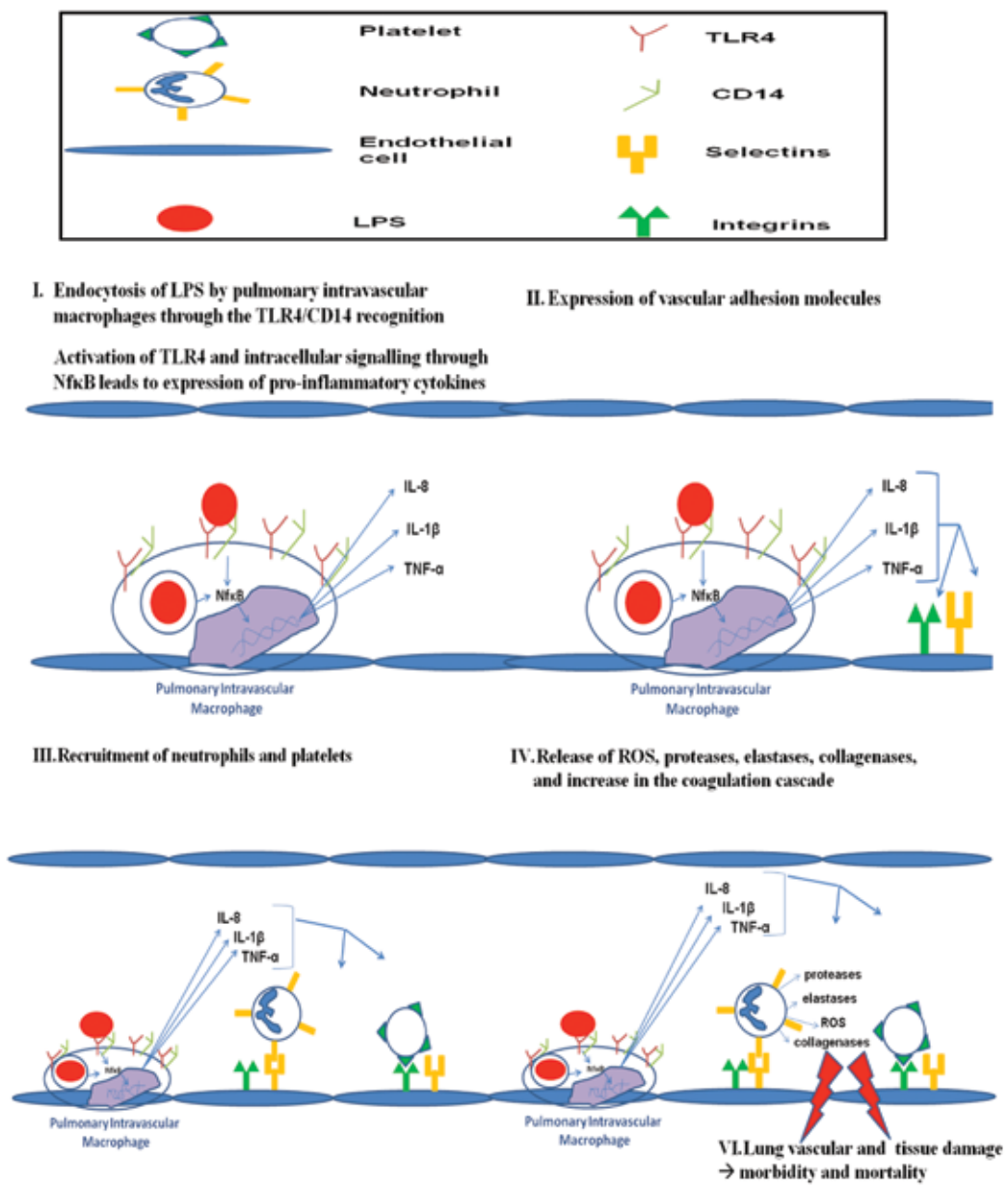


Figure 1. The role of pulmonary intravascular macrophages (PIMs) in the development of lung injury following endotoxemia. Stages I to IV summarize the known data such as the expression of Toll-like receptor-4 (TLR4), the uptake of lipopolysaccharides (LPS), and localization of IL-1β and TNFα in PIMs of LPS-treated horses. The pathways still to be determined include upregulation of vascular adhesion molecules and migration of neutrophils in the lungs of LPS-treated horses.

and promotes neutrophil adhesion to endothelial cells, which subsequently causes activation of neutrophils and their accumulation in the pulmonary microcirculation (12–14). Activated neutrophils live longer and are believed to cause damage to vascular endothelium. The damaged endothelium in pulmonary microcirculation leads to increased permeability and development of lung edema.

Macrophages develop from monocytes and reside in various anatomical compartments in the lung. For example, in addition to well known and characterized alveolar macrophages, lungs also contain interstitial, airway, and intravascular macrophages. One of the earliest reports showing presence of PIMs in calf lungs was published in 1974 (15) followed by the evidence of erythrophagocytosis by PIMs in goats (16) and other species (15–22). The PIMs in the equine lungs

were first described by Atwal et al (17) and subsequently Longworth et al (18). There are reports of smaller populations of PIMs occurring in rabbit and cat lungs as well (19). In postnatal pigs and sheep, the PIMs are sequestered within 4 wk of birth (20,21). However, there are no data on the ontogeny of PIMs in horses. Currently, there are no molecular or evolutionary explanations for the intriguing recruitment of PIMs in the host animal species and their absence in humans and rats.

It has been known for many years that PIM-containing animal species are more prone to lung inflammation (22). For example, an intravenous injection of 0.003 to 1.3 μg of *Escherichia coli* LPS/kg BW induces pulmonary hypertension and cardio-pulmonary shock in horses (22). A conclusive link was established between PIMs

and pulmonary responses in sheep. Neonatal lambs have very few PIMs and show no hemodynamic response to Monastral blue or liposomes (23). However, PIM sequestration in lambs by 2 wk of age is accompanied by enhanced vascular response to the same treatment; this hypertensive response is eliminated by removing the PIMs. Monastral blue is a copper dye that has been used as a phagocytic tracer to study PIMs in cattle, sheep, and horses (17). It is suspected that intravenous infusion of Monastral blue may activate PIMs to cause transient vascular response. Horses show transient pulmonary response following Monastral blue injection and horse PIMs are highly phagocytic for Monastral blue and develop large phago-lysosomes containing the dye following single or multiple intravenous injections (17,24). Multiple injections of Monastral blue results in larger phago-lysosomes compared to the single injection, which indicates that phagocytic capacity of PIMs is not diminished following initial round of phagocytosis of the dye (24). Pulmonary arterial hypertension observed in horses with intravenous injection of *E. coli* is blocked in animals in which PIMs have been depleted or inactivated (8,25). Endotoxin-induced pulmonary vascular responses are generally attributed to production of vasoactive substances, such as thromboxanes by the PIMs. This contention is supported by in vitro data which showed that porcine PIMs produce more arachidonic acid metabolites compared to the alveolar macrophages (26,27). Taken together, the evidence shows a causal relationship between PIMs and endotoxin-induced pulmonary vascular responses.

Macrophages and other cells engage endotoxins and other bacterial products through molecules such as TLR and CD14 (28). Recently, the first data on the expression of TLR4 in PIMs in horses (29), cattle and pigs was reported (29,30). Toll-like receptor-9, which engages bacterial DNA, has been observed in equine PIMs (31). Toll-like receptor-4, expressed in PIMs, is a major component of total TLR4 expression in horse lungs because depletion of PIMs significantly reduced lung expression of TLR4. It is interesting to note that total lung expression of TLR4 protein and mRNA was significantly reduced following depletion of PIMs. These data show that, although lung epithelial and endothelial cells express TLR4 and TLR2, PIMs are the major source of these innate immune receptors. The role of TLR4 is to engage and endocytose endotoxins and initiate cell signalling via NF- κ B pathway, which results in cytokine expression. Previous data showed an association between TLR4 and *E. coli* LPS, as both molecules were co-localized in PIMs of horses treated with the LPS (29). Therefore, a decline in TLR4 in lungs of PIM-depleted horses may result in reduced sensitivity to bacterial products. The strategic vascular location of PIMs, their significant phagocytic ability, and the TLR4-LPS colocalization uniquely enables these cells to sense and respond to circulating endotoxins in conditions such as endotoxemia and subsequently to initiate a pulmonary response (Figure 1).

It is known that the interaction of an endotoxin with a TLR4 or the uptake of LPS by macrophages activates macrophages (32). Once activated, macrophages, including TLR4-expressing PIMs, secrete mediators, such as IL-1 β and TNF- α , to induce expression of adhesion molecules on lung microvascular endothelium (29,33,34). Furthermore, secretion of vasoactive substances, such as thromboxanes and inflammatory cytokines (IL-1 β , TNF- α) by the PIMs into the circulation will affect lung vascular endothelium to initiate lung

inflammation, as reported in horses and other species (35). Horses treated with *E. coli* LPS showed increased expression of TLR2 mRNA (29) and TLR9 (31) in the lungs, which will potentially alter PIM responses to other bacterial ligands, such as lipoteichoic acid and CpG containing motifs. Although it is well recognized that the lung is affected in sepsis (36), lung inflammation is not considered to be a major complicating factor in equine endotoxemia. If this contention is indeed true, it still is possible that cytokines secreted by the activated PIMs into the circulation may affect other organs. Endotoxemia is an important risk factor for development of acute laminitis in horses (37). Local digital cytokine gene expression and infiltration of the lamellar tissue with leukocytes was suggested to be one of the causes of laminitis (38). A remote production of cytokines and vasoactive substances by the PIMs and their secretion into the circulation during endotoxemia would possibly reach the hoof and achieve similar effects.

The involvement of PIMs in equine pulmonary pathophysiology is not limited to endotoxemia. It has been suggested that the changes in pulmonary microvasculature and the subsequent edema seen after infection with African Horse Sickness virus is partially due to the activation of PIMs and the subsequent release of chemical inflammatory mediators (39). Furthermore, exposure to inhaled halothane was shown to induce translocation of the PIMs surface coat into the vacuolar system of the PIMs, followed by enrichment of acid phosphatase in the Golgi apparatus, and a development of extensive lamellipodial extensions. These extensions were suggested to enable the PIMs to interact with platelets within the pulmonary capillaries, forming thrombotic aggregates of platelets (40).

Currently, we know the structure of equine PIMs, their phagocytic abilities and some aspects of their inflammatory phenotype. The data from other species suggest that PIMs depletion may have beneficial effects for the host. However, similar detailed information is still not available on the equine PIMs. Based on the totality of information on the biology of PIMs, we believe that PIMs play a significant role in vascular inflammation in the horse (Figure 1) and merit further investigations in complex conditions such as endotoxemia.

Acknowledgments

The work done in Dr. Singh's laboratory was supported through grants from Natural Sciences and Engineering Research Council of Canada, Alberta Agriculture Research Institute, Saskatchewan Agriculture Development Fund and Equine Health Research Fund Western College of Veterinary Medicine. Dr. Aharonson-Raz is a recipient of a Graduate Student Scholarship from University of Saskatchewan.

References

1. Sykes BW, Furr MO. Equine endotoxaemia — a state-of-the-art review of therapy. *Aust Vet J* 2005;83 (1–2):45–50.
2. Morris DD. Endotoxemia in horses. A review of cellular and humoral mediators involved in its pathogenesis. *J Vet Intern Med/American College of Veterinary Internal Medicine* 1991; 5 (3):167–181.

3. Andonegui G, Bonder CS, Green F, et al. Endothelium-derived Toll-like receptor-4 is the key molecule in LPS-induced neutrophil sequestration into lungs. *J Clin Invest* 2003;111:1011–1020.
4. Werners AH, Bull S, Fink-Gremmels J. Endotoxaemia: A review with implications for the horse. *Equine Vet J* 2005;37:371–383.
5. Archer DC, Proudman CJ. Epidemiological clues to preventing colic. *Vet J* 2006;172:29–39.
6. Burrows GE. Dose-response of ponies to parenteral *Escherichia coli* endotoxin. *Can J Comp Med* 1981;45:207–210.
7. Berczi I, Bertok L, Bereznai T. Comparative studies on the toxicity of *Escherichia coli* lipopolysaccharide endotoxin in various animal species. *Can J Microbiol* 1966;12:1070–1071.
8. Parbhakar OP, Duke T, Townsend HG, Singh B. Depletion of pulmonary intravascular macrophages partially inhibits lipopolysaccharide-induced lung inflammation in horses. *Vet Res* 2005;36:557–569.
9. Elson G, Dunn-Siegrist I, Daubeuf B, Pugin J. Contribution of Toll-like receptors to the innate immune response to Gram-negative and Gram-positive bacteria. *Blood* 2007;109:1574–1583.
10. Palsson-McDermott EM, O'Neill LA. Signal transduction by the lipopolysaccharide receptor, Toll-like receptor-4. *Immunology* 2004;113:153–162.
11. Miyake K. Endotoxin recognition molecules MD-2 and toll-like receptor 4 as potential targets for therapeutic intervention of endotoxin shock. *Curr Drug Targets* 2004;3:291–297.
12. Warner AE, DeCamp MM, Jr., Molina RM, Brain JD. Pulmonary removal of circulating endotoxin results in acute lung injury in sheep. *Laboratory investigation; a journal of technical methods and pathology* 1988;59:219–230.
13. Grisham MB, Everse J, Janssen HF. Endotoxemia and neutrophil activation in vivo. *Am J Physiol* 1988;254 (5 Pt 2):H1017–1022.
14. Ward PA. Role of the complement in experimental sepsis. *J Leukocyte Biol* 2007;83:467–470.
15. Rybicka K, Daly BD, Migliore JJ, Norman JC. Ultrastructure of pulmonary alveoli of the calf. *Am J Vet Res* 1974;35:213–222.
16. Atwal OS, Minhas KJ. In vivo interaction of cationised ferritin with the surface coat and endocytosis by pulmonary intravascular macrophages: A tracer kinetic study. *J Anat* 1992;181:313–325.
17. Atwal OS, Singh B, Staempfli H, Minhas K. Presence of pulmonary intravascular macrophages in the equine lung: Some structural-functional properties. *Anat Rec* 1992;234:530–540.
18. Longworth KE, Jarvis KA, Tyler WS, Steffey EP, Staub NC. Pulmonary intravascular macrophages in horses and ponies. *Am J Vet Res* 1994;55:382–388.
19. Brain JD, Molina RM, DeCamp MM, Warner AE. Pulmonary intravascular macrophages: Their contribution to the mononuclear phagocyte system in 13 species. *Am J Physiol* 1999;276:L146–154.
20. Winkler GC, Cheville NF. Postnatal colonization of porcine lung capillaries by intravascular macrophages: An ultrastructural, morphometric analysis. *Microvasc Res* 1987;33:224–232.
21. Winkler GC, Cheville NF. Monocytic origin and postnatal mitosis of intravascular macrophages in the porcine lung. *Journal of leukocyte biology* 1985;38:471–480.
22. Frevert CW, Warner AE. Respiratory distress resulting from acute lung injury in the veterinary patient. *J Vet Intern Med/American College of Veterinary Internal Medicine*. 1992;6:154–165.
23. Longworth KE, Westgate AM, Grady MK, Westcott JY, Staub NC. Development of pulmonary intravascular macrophage function in newborn lambs. *J Appl Physiol* 1992;73:2608–2615.
24. Singh B, Minhas KJ, Atwal OS. Ultracytochemical study of multiple dose effect of monastral blue uptake by equine pulmonary intravascular macrophages (PIMs). *J Submicrosc Cytol Pathol* 1994;26:235–243.
25. Longworth KE, Smith BL, Staub NC, Steffey EP, Serikov VB. Use of detergent to prevent initial responses to endotoxin in horses. *Am J Vet Res* 1996;57:1063–1066.
26. Chitko-McKown CG, Chapes SK, Brown RE, Phillips RM, McKown RD, Blecha F. Porcine alveolar and pulmonary intravascular macrophages: Comparison of immune functions. *J Leukocyte Biol* 1991;50:364–372.
27. Chitko-McKown CG, Blecha F. Pulmonary intravascular macrophages: A review of immune properties and functions. *Ann Rech Vet* 1992;23:201–214.
28. Aderem A. Role of Toll-like receptors in inflammatory response in macrophages. *Crit Care Med* 2001;29:16–18.
29. Singh Suri S, Janardhan KS, Parbhakar O, Caldwell S, Appleyard G, Singh B. Expression of toll-like receptor 4 and 2 in horse lungs. *Vet Res* 2006;37:541–551.
30. Wassef A, Janardhan K, Pearce JW, Singh B. Toll-like receptor 4 in normal and inflamed lungs and other organs of pig, dog and cattle. *Histol Histopathol* 2004;19:1201–1208.
31. Schneberger D, Caldwell S, Suri SS, Singh B. Expression of toll-like receptor 9 in horse lungs. *Anat Rec (Hoboken)* 2009;292:1068–1077.
32. Fujihara M, Muroi M, Tanamoto K, Suzuki T, Azuma H, Ikeda H. Molecular mechanisms of macrophage activation and deactivation by lipopolysaccharide: Roles of the receptor complex. *Pharmacol Thera* 2003;100:171–194.
33. Springer TA. Traffic signals for lymphocyte recirculation and leukocyte emigration: The multistep paradigm. *Cell* 1994;76:301–314.
34. Antonelli A, Bianchi M, Crinelli R, Gentilini L, Magnani M. Modulation of ICAM-1 expression in ECV304 cells by macrophage-released cytokines. *Blood Cells Mol Dis* 2001;27:978–991.
35. Singh B, Pearce JW, Gamage LN, Janardhan K, Caldwell S. Depletion of pulmonary intravascular macrophages inhibits acute lung inflammation. *Am J Physiol* 2004;286:L363–372.
36. Ware LB, Matthay MA. The acute respiratory distress syndrome. *The New England journal of medicine* 2000;342:1334–1349.
37. Parsons CS, Orsini JA, Krafty R, Capewell L, Boston R. Risk factors for development of acute laminitis in horses during hospitalization: 73 cases (1997–2004). *Journal of the American Veterinary Medical Association* 2007;230:885–889.
38. Loftus JP, Black SJ, Pettigrew A, Abrahamsen EJ, Belknap JK. Early laminar events involving endothelial activation in horses with black walnut-induced laminitis. *American journal of veterinary research* 2007;68:1205–1211.
39. Carrasco L, Sanchez C, Gomez-Villamandos JC, et al. The role of pulmonary intravascular macrophages in the pathogenesis of African horse sickness. *Journal of comparative pathology* 1999;121:25–38.

40. Atwal OS, McDonell W. In vivo interaction of pulmonary intravascular macrophages with activated platelets in microvessels of equine lung after multiple exposures to halothane, isoflurane,

and thiamylal: A comparative ultrastructural and cytochemical study. *Anat Rec A Discov Mol Cell Evol Biol* 2005;284:574-584.

Increased risk of chronic wasting disease in Rocky Mountain elk associated with decreased magnesium and increased manganese in brain tissue

Stephen N. White, Katherine I. O'Rourke, Thomas Gidlewski, Kurt C. VerCauteren, Michelle R. Mousel, Gregory E. Phillips, Terry R. Spraker

Abstract

Chronic wasting disease (CWD) is a transmissible spongiform encephalopathy (TSE) of Rocky Mountain elk in North America. Recent studies suggest that tissue and blood mineral levels may be valuable in assessing TSE infection in sheep and cattle. The objectives of this study were to examine baseline levels of copper, manganese, magnesium, zinc, selenium, and molybdenum in the brains of Rocky Mountain elk with differing prion genotypes and to assess the association of mineral levels with CWD infection. Elk with leucine at prion position 132 had significantly lower magnesium levels than elk with 2 copies of methionine. Chronic wasting disease-positive elk had significantly lower magnesium than control elk. The incorporation of manganese levels in addition to magnesium significantly refined explanatory ability, even though manganese alone was not significantly associated with CWD. This study demonstrated that mineral analysis may provide an additional disease correlate for assessing CWD risk, particularly in conjunction with genotype.

Résumé

La maladie du dépérissement chronique (CWD) est une encéphalopathie spongiforme transmissible (TSE) des wapitis en Amérique du Nord. Des études récentes suggèrent que la mesure des taux de minéraux dans les tissus et le sang seraient utiles pour évaluer une infection par TSE chez les moutons et les bovins. Les objectifs de la présente étude étaient d'examiner les niveaux de base de cuivre, manganèse, magnésium, zinc, sélénium et molybdène dans le cerveau de wapitis avec des génotypes différents de sensibilité envers les maladies à prions et d'évaluer l'association des niveaux de minéraux avec l'infection CWD. Les wapitis avec une leucine à la position 132 du prion présentaient des niveaux significativement plus faibles de magnésium que les wapitis avec deux copies de méthionine. Les wapitis positifs pour CWD avaient des niveaux de magnésium significativement plus faibles que les wapitis témoins. L'ajout des niveaux de manganèse à ceux du magnésium a permis de raffiner significativement la capacité d'explication, même si le manganèse seul n'était pas associé significativement avec le CWD. Cette étude démontre que l'analyse des minéraux peut fournir un corrélat additionnel pour évaluer le risque de CWD, particulièrement en conjonction avec le génotype.

(Traduit par Docteur Serge Messier)

Chronic wasting disease (CWD) is the transmissible spongiform encephalopathy (TSE) of North American deer, elk, and moose (1). The TSEs are fatal neurodegenerative disorders thought to be caused by an infectious prion agent composed of a misfolded variant (PrP^d) of the normally occurring host cellular prion protein (PrP^c) (2). Misfolding of the host PrP^c by exogenous or sporadically misfolded PrP^d initiates the disease process (2). Control of CWD in elk in the United States (US) and Canada includes depopulation or permanent quarantine of infected farmed herds and culling of free-ranging suspects showing clinical signs. Despite these efforts, new outbreaks are reported in both the US and Canada (3,4) and the economic losses to the industry and regulatory bodies are substantial. The management of herds with a small number of animals introduced from infected farms is a concern. Introduction of an animal from an

infected farm is a risk factor for CWD in animals housed together, with substantial increase in risk if the introduced animal developed clinical disease (4). An additional risk factor includes the normal prion protein precursor (PRNP) genotype, with a lower risk of disease in some populations for elk homozygous or heterozygous for the version of the PRNP gene which encodes a leucine residue at position 132 (132L) (5,6).

Levels of tissue minerals known to bind PrP^c are associated with TSEs in several model systems. The association between TSE and copper (Cu) or manganese (Mn) has been reported (7,8); both of these minerals bind PrP^c and may affect the efficiency of protein misfolding (9). Elevated Mn levels in brain and blood have been reported with bovine, ovine, and human TSEs (7,8,10). Additional divalent cations of appropriate size and ionic strength may also have roles in TSEs,

USDA-ARS Animal Disease Unit, Pullman, Washington, USA (White, O'Rourke); Washington State University College of Veterinary Medicine, Pullman, Washington, USA (White, O'Rourke); USDA-APHIS, Veterinary Services (Gidlewski), and USDA-APHIS, Wildlife Services (VerCauteren, Phillips), National Wildlife Research Center, Fort Collins, Colorado, USA; USDA-ARS US Sheep Experiment Station, Dubois, Idaho, USA (Mousel); Colorado State University College of Veterinary Medicine & Biomedical Sciences, Fort Collins, Colorado, USA (Spraker).

Address all correspondence to Dr. Stephen White; telephone: (509) 335-7407; fax: (509) 335-8328; e-mail: swhite@vetmed.wsu.edu

Dr. White's current address is Animal Disease Research Unit, PO Box 646630, Pullman, Washington 99164, USA.

Received April 17, 2008. Accepted December 15, 2008.

although it is not known whether these mineral level changes reflect a predisposing influence on prion protein folding or a downstream effect of the disease processes (11). Baseline data on mineral levels in the brain of Rocky Mountain elk (*Cervus elaphus nelsoni*) are not available, and the confounding effects of varying feed sources and PRNP genotypes are not known. The objectives of this study were to provide baseline data on mineral levels in brain tissue from elk collected during regulatory depopulation of infected herds, to estimate mineral levels in elk of different genotypes without evidence of disease, and to explore potential associations between tissue mineral concentrations and presence of CWD in captive Rocky Mountain elk.

Tissue samples were collected from 223 Rocky Mountain elk that were euthanized as part of a joint federal and state control program. Elk originated from 3 United States farms, each of which had multiple confirmed cases of CWD. Brains, tonsils, retropharyngeal lymph nodes and sometimes liver were collected at necropsy. DNA was extracted from frozen liver or brain and the open reading frame of the gene for PRNP was amplified and sequenced (5). Genotypes at amino acid position 132 were recorded as 132MM (2 copies of methionine) or 132Lx (at least one copy of leucine) (5). Brain, retropharyngeal lymph node, and tonsil were formalin fixed and processed for detection of PrP^d by an automated monoclonal antibody immunohistochemistry assay (12). Animals were considered CWD positive if at least one tissue was positive for PrP^d. Because of the unknown lag between infection and appearance of detectable PrP^d (4), elk exposed to CWD but lacking detectable PrP^d were not defined as CWD negative; these animals were defined as herd-matched controls.

Trace minerals (Cu, Mn, Mg, Zn, Se, and Mo) were analyzed in samples from the cerebrum, parietal lobe, or optic lobe of the brain collected at necropsy. For Cu, Mn, and Zn analyses, the tissues were dried, weighed, ashed overnight in a muffle furnace, and then dissolved in dilute HNO₃. The solutions were then analyzed by flame atomic absorption spectrophotometry (FAAS) (13). Magnesium was measured with a slight modification: a releasing agent (lanthanum oxide in dilute HCl) was added to the HNO₃ solutions prior to FAAS (13). For Se, the tissues were dried, weighed, and then digested with Mg(NO₃)₂ and concentrated HNO₃ overnight on a hot plate under a hood. The digests were ashed in a pre-heated muffle furnace, the cooled ashes were dissolved in dilute HCl, and the solutions were analyzed by Hydride Generation FAAS (14,15). For Mo, the tissues were dried, weighed, ashed overnight in a muffle furnace and then dissolved in dilute HNO₃. Palladium nitrate [Pd(NO₃)₂] and ascorbic acid matrix modifiers were added to the solutions, and the solutions were analyzed by Graphite Furnace Atomic Absorption Spectrophotometry (16). All concentrations were reported in µg/g (dry mass basis), and standard quality control samples spiked with the metal under investigation were included with each analysis.

The relationships between CWD status, PRNP genotype, and mineral levels in the brain were evaluated using a sample of 223 Rocky Mountain elk from 3 US facilities with similar CWD prevalence. These animals were divided into 3 groups based on genotype and CWD status, including 132Lx genotype control elk (*n* = 50), 132MM control elk (*n* = 146), and 132MM CWD elk (*n* = 27). Because no 132Lx animals were positive in this sample, comparisons between 132Lx control elk (*n* = 50) and 132MM control animals (*n* = 146) were

used to compare mineral levels of 132MM and 132Lx elk without detectable PrP^d. Genotypic differences in cation levels in the brain from control elk were examined by using *t*-tests to compare samples from elk with the PRNP 132MM genotype to samples from elk with the 132Lx genotype. Because the samples failed preliminary tests for equal variance, Satterthwaite's method was used to estimate degrees of freedom for *t*-tests.

All CWD positive elk in this study (*n* = 27) had 132MM genotypes; therefore, only 132MM samples (*n* = 146 samples with no detectable PrP^d) were used as controls for CWD investigation. Samples from the CWD positive and the genotype-matched control elk were examined for differing cation levels and the results were evaluated using a *t*-test (SAS Institute, Cary, North Carolina, USA). Logistic regression was used to explore potential relationships between CWD status (response variable) and explanatory variables sex, location, age at death (in years), and mineral concentrations (µg/g) of Cu, Mg, Mn, Mo, Se, and Zn in the brain (logistic procedure in SAS). This analysis used an exploratory approach, and stepwise automated model selection procedures of the SAS logistic procedure were used to evaluate models including up to 9 variables and their interactions. Nagelkerke's adjusted coefficient of determination was used to assess the fraction of variation explained by the resulting model. Incremental change in mineral concentrations associated with doubling of the odds of detecting CWD (odds ratio = 2) were used to interpret the final model, where each mineral concentration was varied while holding others constant at the mean level.

Baseline mineral data for CWD control elk are shown by genotype in Table 1. Brain from control elk with the 132Lx long incubation genotype had significantly lower mean Mg than brain from 132MM control elk (346.1 µg/g versus 412.2 µg/g; *t* = 3.17, 106 df; *P* = 0.002; Table I). None of the other minerals differed by genotype (*P* > 0.05; Table I).

Magnesium levels were lower (314.1 µg/g versus 412.2 µg/g; *t* = 3.12, 36.1 df; *P* = 0.004) in CWD positive elk but other minerals did not differ by CWD status (Table II). Logistic regression models were used to better explain variation in CWD status using multiple explanatory variables. There was little evidence of any relationship between CWD status and sex, location, age, and the cations Cu, Mo, Se, Zn (*P* > 0.05). The final model included levels of Mg (Wald chi-square = 16.3, 1 df; *P* < 0.0001) and Mn (Wald chi-square = 10.7, 1 df; *P* = 0.001) in the brain. Combined use of Mn and Mg explained 21% of variation in CWD status (*R*² = 0.21) compared with 10% using Mg alone (*R*² = 0.10) indicating the value of both metals in supplying complementary information. Table III shows increments of each cation required to double odds of detecting CWD, given the final model and cation levels measured from brain tissue. Each decrease of 85 µg/g Mg doubled the odds of detecting CWD, if Mn levels were held constant. Similarly, each increase of 0.48 µg/g Mn doubled the odds of detecting CWD, if Mg levels were held constant.

The effect of PRNP genotype on baseline Mg was significant in this study; control elk with the 132MM short incubation genotype had higher Mg levels than elk with the 132Lx long incubation genotype from the same facilities. Since Mg plays a critical role in membrane stability, energy balance, oxidative stress, and neurotransmitter release following brain injury (17), the effect of genotype-related differences in baseline Mg may be of interest in understanding the

Table I. Metal concentrations in the brain and their respective standard errors from Rocky Mountain elk with 132MM and 132Lx genotypes in the absence of detectable PrP^d (CWD control elk)

Elk genotype and CWD status	Mg	Mn	Cu	Mo	Zn	Se
132MM-control <i>n</i> = 146	412.2 (12.3)	1.32 (0.05)	12.1 (.40)	0.33 (0.02)	39.4 (1.3)	0.55 (0.01)
132Lx-control <i>n</i> = 50	346.1 ^a (16.8)	1.15 (0.11)	11.6 (0.58)	0.25 (0.02)	36.7 (2.2)	0.51 (0.02)

Mg — magnesium; Mn — manganese; Cu — copper; Mo — molybdenum; Zn — zinc; Se — selenium.

^a Different from the 132MM control elk ($P = 0.002$).

Table II. Metal concentrations in the brain and their respective standard errors from CWD-positive and control Rocky Mountain elk with the 132MM genotype

Elk genotype and CWD status	Mg	Mn	Cu	Mo	Zn	Se
132MM-CWD <i>n</i> = 27	314.1 ^a (29.0)	1.5 (.011)	12.6 (0.86)	0.30 (0.03)	36.7 (3.3)	0.57 (0.03)
132MM-control <i>n</i> = 146	412.2 (12.3)	1.32 (0.05)	12.1 (.40)	0.33 (0.02)	39.4 (1.3)	0.55 (0.01)

Mg — magnesium; Mn — manganese; Cu — copper; Mo — molybdenum; Zn — zinc; Se — selenium.

^a Different from the 132MM control elk ($P = 0.004$).

Table III. Increments of magnesium and manganese associated with doubling the odds of detecting CWD, given the final model and cation levels measured from brain tissue

Brain cation	Odds ratio	95% CI	Change in cation concentration ($\mu\text{g/g}$)
Mg	2.00	- 0.35, - 0.69	- 85.0
Mn	2.00	1.34, 3.12	0.48

Mg — magnesium; Mn — manganese.

CI — confidence interval.

pathogenesis of long incubation TSE phenotypes. Magnesium levels in ruminant livestock are tightly regulated within a range controlled by diet, undefined genetic elements, and reproductive status, particularly in association with lactation (18). Although standards for Mg and other minerals in brain from Rocky Mountain elk are not reported, the levels in this study (Tables I–II) were similar to those reported for liver mineral levels from Tule elk (*Cervus elaphus nannodes*) (19). Consideration of environmental and forage factors in association with PRNP genotype in study populations will be useful in establishing baseline data on mineral levels in captive Rocky Mountain elk.

When only elk with the 132MM short incubation genotype were considered, lower Mg levels were observed in brain from CWD positive elk than in brain from control elk from the same herds. This was true despite the possibility that some of the control animals could have been very early stage positives, which would have made it more difficult to establish significant differences between groups. The finding of reduced Mg in brain from elk with natural CWD is consistent with a similar finding in mice experimentally infected with scrapie (20), which suggests that Mg reduction may be a feature of many TSEs. Reduced magnesium is an almost ubiquitous feature of central nervous system injury (17), however, and the effect is not likely to be specific to the TSEs.

Elevated levels of Mn in the peripheral blood may be useful as an early indicator of TSE infection (7,10). Because disease-causing PrP^d accumulates most heavily in nervous tissue and especially the brain (12), this study examined brain tissue levels of Mn. Although

brain tissue from CWD-positive elk had a trend toward elevated Mn, the relationship was weak. This finding is consistent with a recent report on Mn levels in the central nervous system of sheep, in which Mn levels in infected sheep rose within a month following infection (7). PrP^c binds Mn at 2 sites, both of which are upstream from the residue 132 substitution, so a direct effect of the mutation on Mn binding is not predicted (9).

However, the combined model using Mn while accounting for Mg reveals the potential importance of Mn by quantifying the relationship of Mg and Mn with detection of CWD under the conditions that existed in this study. Nagelkerke's adjusted R^2 suggests that the model with both Mn and Mg explained approximately twice as much variation in CWD status as the use of Mg alone. Changes in concentration well within the range of observed values for either Mg or Mn were associated with a doubling of the odds of CWD. Although this study detected 2 risk-associated minerals for elk of the 132MM genotype, it does not establish a causal link between Mg and Mn concentrations and CWD. However, if absolute levels or changes in tissue Mg and Mn concentrations are symptomatic of CWD, they may have practical application for herd surveillance if additional factors are identified to improve diagnostic precision of models. Because Mg levels differed between genotypes of control elk and because 132MM-CWD elk had similar Mg levels as 132Lx-control elk, it will be important to consider genotype in future studies.

Chronic wasting disease in captive elk is controlled largely by whole herd depopulation. However, the cost of indemnity payments, loss of animal life, and hardship to producers is considerable

and there is no assurance that the disease will not recur following restocking of potentially contaminated facilities (1). Mineral-based approaches to TSE diagnosis and pathogenesis have been proposed but data on baseline levels in captive Rocky Mountain elk is lacking. We report PRNP associated differences in Mg levels in the elk in this study. When PRNP genotype was held constant, Mg and Mn concentrations in brain tissue were related to CWD status in a logistic regression model. If the present results can be replicated with blood or some other easily accessible tissue, understanding of relative risk and disease course for individual animals might be enhanced by studies measuring changes in mineral levels after experimental inoculation with CWD. This study demonstrated potential for using multi-mineral predictors for detecting CWD and the need for additional predictors to enhance diagnostic precision.

Acknowledgments

The authors gratefully acknowledge Codie Hanke for technical assistance, Cathy Bedwell for mineral analysis, veterinarians and technicians with the USDA Animal Plant Health Inspection Service and the state of Colorado for epidemiology and tissue collection, and Jennifer Swenson and Elaine Anderson for meticulous record keeping. Supported by grants from the United States Department of Agriculture, Agricultural Research Service 5348-32000-026-00D, Specific Cooperative Agreement 58-5348-2-678, CSREES 2003-51140-02126, and the College of Veterinary Medicine, Colorado State University.

References

- Williams ES. Chronic wasting disease. *Vet Path* 2005;42:530–549.
- Prusiner SB. Novel proteinaceous infectious particles cause scrapie. *Science* 1982;216:136–144.
- Miller MW, Williams ES, McCarty CW, et al. Epizootiology of chronic wasting disease in free-ranging cervids in Colorado and Wyoming. *J Wildl Dis* 2000;36:676–690.
- Argue CK, Ribble C, Lees VW, McLane J, Balachandran A. Epidemiology of an outbreak of chronic wasting disease on elk farms in Saskatchewan. *Can Vet J* 2008;48:1241–1248.
- O'Rourke KI, Besser TE, Miller MW, et al. PrP genotypes of captive and free-ranging Rocky Mountain elk (*Cervus elaphus nelsoni*) with chronic wasting disease. *J Gen Virol* 1999;80:2765–2769.
- Perucchini M, Griffin K, Miller MW, Goldmann W. PrP genotypes of free-ranging wapiti (*Cervus elaphus nelsoni*) with chronic wasting disease. *J Gen Virol* 2008;89:1324–1328.
- Hesketh S, Sassoon J, Knight R, Hopkins J, Brown DR. Elevated manganese levels in blood and central nervous system occur before onset of clinical signs in scrapie and bovine spongiform encephalopathy. *J Anim Sci* 2007;85:1596–1609.
- Thackray AM, Knight R, Haswell SJ, Bujdoso R, Brown DR. Metal imbalance and compromised antioxidant function are early changes in prion disease. *Biochem J* 2002;362:253–258.
- Brazier MW, Davies P, Player E, Marken F, Viles JH, Brown DR. Manganese binding to the prion protein. *J Biol Chem* 2008;283:12831–12839.
- Hesketh S, Sassoon J, Knight R, Brown DR. Elevated manganese levels in blood and CNS in human prion disease. *Mol Cell Neurosci* 2008;37:590–598.
- Choi CC, Kanthasamy A, Anantharam V, Kanthasamy AG. Interaction of metals with prion protein: Possible role of divalent cations in the pathogenesis of prion diseases. *Neurotoxicology* 2006;27:777–787.
- Spraker TR, Balachandran A, Zhuang D, O'Rourke KI. Variable patterns of PrP-CWD distribution in obex and cranial lymphoid tissues of Rocky Mountain elk with nonclinical chronic wasting disease. *Vet Rec* 2004;155:295–302.
- Helrich HE. Official methods of analysis of the Association of Official Analytical Chemists. Gaithersburg, Maryland: AOAC, 1990:Method 974,27.
- Stahr HM. Analytical Methods in Toxicology. New York, New York: John Wiley & Sons, 1991.
- Poole CF, Evans NJ, Wiberly DG. Determination of selenium in biological samples by gas-liquid chromatography with electron-capture detection. *J Chromatogr* 1977;136:73–83.
- Tracy M, Melton L, Holstege D. Molybdenum quantitation by GFZAA. In: CVDLS Toxicology Laboratory Standard Methods. Davis, California: University of California, 1996.
- Vink R, Cernak I. Regulation of intracellular free magnesium in central nervous system injury. *Front Biosci* 2000;5:D656–D665.
- Goff JP. Macromineral disorders of the transition cow. *Vet Clin NA — Food Animal Practice* 2004;20:471–494.
- Johnson HE, Bleich VC, Krausman PR. Mineral deficiencies in tule elk, Owens Valley, California. *J Wildl Dis* 2007;43:61–74.
- Wong BS, Brown DR, Pan T, et al. Oxidative impairment in scrapie-infected mice is associated with brain metals perturbations and altered antioxidant activities. *J Neurochem* 2001;79:689–698.

Kinetics and role of antibodies against intimin β in colostrum and in serum from goat kids and longitudinal study of attaching and effacing *Escherichia coli* in goat kids

José A. Orden, Ricardo De la Fuente, María Yuste, Susana Martínez-Pulgarín, José A. Ruiz-Santa-Quiteria, Pilar Horcajo, Antonio Contreras, Antonio Sánchez, Juan C. Corrales, Gustavo Domínguez-Bernal

Abstract

The presence of antibodies to the intimin β -binding region (Int280- β) of attaching and effacing *Escherichia coli* (AEEC) in serum from 20 goat kids from 2 herds, as well as in goat colostrum, was investigated by enzyme-linked immunosorbent assay. In addition, the onset and subsequent pattern of shedding of AEEC from the same goat kids over a 6-mo period was investigated. All the colostrum and serum samples tested contained antibodies against Int280- β . The association between the antibody titer and the isolation of AEEC suggests that antibodies to intimin β do not prevent colonization of the intestine by AEEC in goat kids. The AEEC were generally shed only transiently. Most AEEC isolated from the kids belonged to serogroup O26. Three isolates belonged to serogroup O157. These data show that goat kids may be a reservoir of AEEC that are potentially pathogenic for humans.

Résumé

La présence d'anticorps dirigés contre la région d'adhésion β de l'intimine (Int280- β) des *Escherichia coli* attachant et effaçant (AEEC) a été étudiée à partir d'échantillons de sérum de 20 chevreaux provenant de 2 troupeaux, ainsi que dans le colostrum par épreuve immuno-enzymatique. Également, on étudia le début ainsi que le patron d'excrétion des AEEC par les mêmes chevreaux durant une période de 6 mois. Des anticorps dirigés contre Int280- β étaient présents dans tous les échantillons de colostrum et de sérum éprouvés. L'association entre le titre d'anticorps et l'isolement d'AEEC suggère que les anticorps contre l'intimine β n'empêchent pas la colonisation de l'intestin par les AEEC chez les chevreaux. Les AEEC n'étaient généralement excrétés que de manière transitoire. La plupart des AEEC isolées des chevreaux appartenaient au sérotype O26. Trois isolats appartenaient au sérotype O157. Les résultats démontrent que les chevreaux pourraient être un réservoir des AEEC qui sont potentiellement pathogènes pour les humains.

(Traduit par Docteur Serge Messier)

Attaching and effacing *Escherichia coli* (AEEC) have been associated with diarrhea in humans and animals. These bacteria cause attaching and effacing (AE) lesions in the gut mucosa that are characterized by intimate bacterial adhesion to the enterocyte and effacement of brush-border microvilli (1). Enteropathogenic *E. coli* (EPEC) and enterohemorrhagic *E. coli* (EHEC) cause AE lesions in the human intestinal mucosa (1), and ruminants can be reservoirs of these strains (2). In contrast to EPEC, EHEC strains produce verotoxins (VTs) (1). The EPEC strains have been classified as typical (possessing the *bfpA* gene) or atypical (lacking the *bfpA* gene). In contrast to typical EPEC, atypical EPEC strains frequently possess several virulence genes, such as *astA*, *chxA*, and *cnf3* (3,4).

The genes necessary for AE lesion formation are encoded in a pathogenic island called the locus of enterocyte effacement (LEE). The LEE encodes intimin, which mediates intimate bacterial

adhesion to the enterocytes and is encoded by the *eae* gene (1). The overall pattern of the sequences of *eae* genes from different AEEC strains shows high conservation in the N-terminal region and variability in the first 280 amino acids starting from the C terminus of the intimin protein, which are involved in binding to enterocytes (1). On the basis of antigenic variation, polymerase chain reaction (PCR) analysis, and sequencing, several types of intimin have been identified (2).

Human colostrum and milk collected from women living in areas in which AEEC infection is endemic contain antibodies that react with surface antigens, especially intimin, of AEEC strains (5,6). The data suggest that the development of specific immunity to intimin may play a role in protecting against AEEC infection. In goats, in contrast to humans, there is a lack of information regarding the antibody response to intimin.

Departamento de Sanidad Animal, Facultad de Veterinaria, Universidad Complutense, 28040 Madrid, Spain (Orden, De la Fuente, Yuste, Martínez-Pulgarín, Ruiz-Santa-Quiteria, Horcajo, Domínguez-Bernal); Departamento de Sanidad Animal, Facultad de Veterinaria, Universidad de Murcia, 30071 Espinardo, Murcia, Spain (Contreras, Sánchez, Corrales).

Address all correspondence to Dr. José A. Orden; telephone: + 34 91 394 3704; fax: + 34 91 394 3795; e-mail: jaorden@vet.ucm.es

Received October 17, 2008. Accepted January 5, 2009.

Table 1. Herd A: Titers of antibodies to the intimin β -binding region (Int280- β) in serum collected once weekly from goat kids during their first 4 wk of life and characteristics of the attaching and effacing *Escherichia coli* (AEEC) colonies isolated from fecal samples collected once weekly during the first 4 weeks of life and then once monthly for the next 5 months of life

Animal number	Antibody titer ^a				Intimin types and O antigens ^b	
	Week 1	Week 2	Week 3	Week 4	Month 3	Month 4
1	128	64	32	32	eae β (O26)	
2	256	128	64	64		
3	256	128	64	64	eae β (O26)	eae γ 1 (O153)
4	256	128	64	32	eae β (O26)	
5	128	64	32	32	eae β (O26)	eae γ 1 (O162)
6	128	64	32	32	eae β (O26)	eae γ 1 (O162)
7	64	32	32	16	eae β (O26)	
8	512	256	128	64	eae γ 1 (O162)	
9	256	128	64	32	eae β (O26)	

^a Reciprocal of the highest dilution at which a positive reaction was observed by enzyme-linked immunosorbent assay.

^b No AEEC colonies were isolated from the fecal samples in months 2, 5, and 6, although no sample was taken from animal 3 in month 6.

Most of the caprine AEEC isolates previously reported have been EPEC (7,8). Although intimin β has been found to be prevalent among EPEC isolated from healthy and diarrheic goats, EPEC isolates with this intimin type have also been associated with neonatal diarrhea in goat kids (2). Most AEEC isolates from healthy goats have been found in goat kids (7,8), but, to our knowledge, no longitudinal studies in goat kids colonized with this type of *E. coli* have been reported.

This study was designed to determine the presence of antibodies to the intimin β -binding region (Int280- β) of AEEC in serum from goat kids collected during their first 4 wk of life, and in goat colostrum, and to assess the role of such antibodies in preventing intestinal colonization by AEEC in the kids. Other objectives of the study were to investigate the onset and subsequent pattern of shedding of AEEC from goat kids over a 6-mo period and to characterize the AEEC colonies isolated.

The study was conducted on 2 Murciano–Granadina goat herds in the Murcia region of southeastern Spain. The practice of artificial rearing, in which goat kids are withdrawn after parturition and fed pasteurized colostrum and milk replacer, was implemented in 1 of the herds (herd A). In contrast, in the other herd studied (herd B), the goat kids were fed colostrum and milk from their dams. Herd A was studied from June to November 2004, and herd B was studied from November 2004 to April 2005. Serum samples were collected from a total of 20 goat kids (9 from herd A and 11 from herd B) once weekly during the kids' first 4 wk of life. Serum samples were also collected from 2 kids per herd just after birth, before they were fed colostrum. One sample of pasteurized colostrum was collected from herd A. In herd B, serum was collected from female goats approximately 1 wk before parturition, and colostrum was collected at the time of parturition. Additionally, fecal samples were taken from the 20 goat kids once weekly during the first 4 wk of life and then once every month for the next 5 mo of life.

Int280- β , expressed as a His-tagged polypeptide, was prepared as previously described (9), with minor modifications. Briefly, a DNA fragment encoding Int280- β was amplified by PCR from the RDEC-1 strain (a rabbit EPEC strain that possesses intimin β) with use of the following primers and standard PCR amplification conditions: Int280 β F (5'-TCGCGGATCCATTACTGAGATTAAGGCTGA-3') and Int280 β R (5'-GCGAAGCTTGTTTTACACAAAACAGAAAAAG-3'). The PCR product was cloned into *Bam*HI/*Hind*III-digested pET-28a (Novagen; Merck Biosciences, Darmstadt, Germany). The recombinant plasmid was transformed into *E. coli* BL21 cells and His-Int280 expressed under isopropyl- β -D-thiogalactopyranoside induction and affinity-purified with metal resin (Clontech; Clontech-Takara Bio Europe, Saint-Germain-en-Laye, France) with the use of standard protocols.

The enzyme-linked immunosorbent assay (ELISA), used to determine the presence and amount of antibodies to Int280- β in colostrum and serum, was performed as previously described (10), with minor modifications. Briefly, ELISA plates were coated overnight at 4°C with 20 μ g/mL of Int280- β , 50 μ L/well. The plates were incubated with 2-fold serial dilutions of the colostrum and serum samples and the reactions revealed with peroxidase-conjugated rabbit antibodies against goat antigen (Dako Diagnósticos, Barcelona, Spain) and *o*-phenylenediamine as substrate. The serum samples taken from 2 goat kids per herd just after birth, before they were fed colostrum, were used as negative controls.

Immunoblot analysis was used to determine the optical density (OD) cutoff associated with a positive ELISA result. Dilutions of 20 serum samples that had OD values in the ELISA between 0.15 and 0.5, as well as the 4 negative-control samples, were tested with this technique. After Tris–Tricine–polyacrylamide gel electrophoresis, Int280- β (100 μ g/mL) was transferred electrophoretically onto polyvinylidene difluoride membranes. The membranes were incubated with the serum samples and the reactions revealed with

Table II. Herd B: Titers of antibodies to Int280- β in serum from goat kids collected once weekly during their first 4 wk of life and characteristics of the AEEC colonies isolated from fecal samples collected once weekly during the first 4 weeks of life and then once monthly for the next 5 months of life

Animal number	Month ^a and week; antibody titer, along with intimin types and O antigens of the AEEC colonies						
	Week 1	Week 2	Month 1		Month 2	Month 3	Month 6
1	128	64	32/ <i>eae</i> β (026)		32		
2	1024	512	512/ <i>eae</i> β (026)		256		
3	512	256	256/ <i>eae</i> γ 1 ^b (0157)		128		
4	256	128/ <i>eae</i> β (026)	64/ <i>eae</i> β (026)		64		
5	128	64	64		32/ <i>eae</i> γ 1 ^b (0157)		
6	256	256/ <i>eae</i> γ 1 ^b (0157); <i>eae</i> γ 2 (02)		128/ <i>eae</i> γ 2 (02)	128		
7	512	256	256		128	<i>eae</i> γ 2 (02)	<i>eae</i> γ 1 (049)
8	8	4	4		2	<i>eae</i> β (014)	
9	256	128	128/ <i>eae</i> β (026)		64		
10	128	64	32/ <i>eae</i> β (026)		32		
11	256	128	64/ <i>eae</i> β (026)		64/ <i>eae</i> β (026)	<i>eae</i> β (026)	<i>eae</i> β (026)

^a No AEEC colonies were isolated from the fecal samples in months 4 and 5, although no sample was taken from animals 6 and 8 in month 6.

^b AEEC colonies with the *vt2* gene.

Table III. Summary of characteristics of the AEEC colonies isolated from the goat kids

Serogroup	Number of colonies	Intimin type	Gene ^a			
			<i>vt2</i>	<i>astA</i>	<i>ehxA</i>	<i>cnf3</i>
02	3	γ 2/ θ				
014	1	β			+	
026	7	β				+
026	10	β			+	
049	1	γ 1		+	+	
0153	1	γ 1			+	
0157	3	γ 1	+		+	
0162	3	γ 1			+	

^a No colony was positive for the *bfpA* gene.

peroxidase-conjugated rabbit antibodies against goat antigen (Dako) and enhanced chemiluminescence.

For isolation of AEEC, the fecal samples were plated onto MacConkey agar. After overnight incubation, 4 colonies with the typical appearance of *E. coli* were randomly chosen from each sample and identified as *E. coli* by biochemical tests. All *E. coli* isolates were analyzed by PCR for possession of the *eae* gene as described previously (7). All AEEC colonies were tested for the *bfpA*, *astA*, *ehxA*, and *cnf3* genes and the types of *eae* and *vt* genes by PCR as described previously (2,3,4,8). The determination of O antigens for serogrouping was carried out in the Laboratorio de Referencia de *E. coli* (Lugo, Spain).

From the immunoblot studies, the cutoff for a positive ELISA result was considered to be an OD of 0.2 or more above that for the negative controls. All colostrum and serum samples from the adult goats contained antibodies against Int280- β . The titer of these antibodies in the pasteurized colostrum obtained from herd A was 1:2048; the titer in colostrum and serum from adult goats in herd B ranged from 1:128 to 1:2048. Moreover, antibodies to Int280- β

were detected in all the serum samples obtained from goat kids in both herds (Tables I and II). A relationship was observed in herd B between the titer of antibodies in the colostrum from adult goats and the titer in the serum from their respective kids.

Shedding of AEEC by goat kids began in the 2nd week of life in herd B but in the 3rd month in herd A. In all but 1 of the animals studied, AEEC colonies were detected in at least 1 sample, but in most kids in both herds the shedding was transient. When the AEEC colonies from a fecal sample showed the same characteristics (intimin type, possession of the *vt*, *bfpA*, *astA*, *ehxA*, and *cnf3* genes, and serogroup) it was assumed that they were the same isolate. In total, 29 AEEC isolates were identified. The characteristics of the AEEC colonies isolated from the goat kids are shown in Tables I to III. In all but 1 of the kids colonized with AEEC, only 1 isolate per animal was identified in each sample. However, different AEEC colonies were isolated from 4 kids at different times.

In herd B, AEEC colonies were isolated from goat kids during their first 4 wk of life (Table II). In the 7 animals in this herd that shed AEEC possessing intimin β during their first 4 wk of life, the titers

of antibodies to Int280- β measured when the AEEC isolates with this intimin type were found ranged from 1:32 to 1:512. In the 3 kids of herd B that were colonized with AEEC of other intimin types during the same period the titers of antibodies to Int280- β measured when these AEEC colonies were isolated ranged from 1:32 to 1:256.

To our knowledge, this is the first work in which the presence of antibodies to intimin β in colostrum and serum from adult and juvenile goats has been studied. We measured titers of antibodies only to the extracellular C-terminal portion of intimin β that is 280 amino acids long; this portion is involved with binding to enterocytes (1). Our observations are therefore more pertinent to intimin β -positive AEEC than to AEEC that express other intimin variants, and only AEEC that possess intimin β have been associated with diarrhea in goat kids (2).

In both herds, all colostrum and serum samples from adult females contained antibodies against Int280- β . This finding suggests that the dams had been exposed to AEEC that possessed intimin β and may reflect the prevalence of this type of *E. coli* in the environment, the high immunogenicity of intimin, or both (10). Antibodies against Int280- β were also detected in all serum samples from the goat kids. In 1 of the herds studied (herd B) the AEEC colonies were isolated during the kids' first 4 wk of life. Although our data are insufficient for statistical analysis, the association between the titers of antibodies to Int280- β and the isolation of AEEC from the animals in herd B suggests that antibodies to intimin β do not prevent colonization of the intestine of goat kids by AEEC. In agreement with the results of this study, van Diemen et al (9) reported that immunization of calves with the cell-binding domain of intimin type β or γ induced humoral immunity but did not protect against intestinal colonization of EHEC O26:H- (Int280- β) or EHEC O157:H7 (Int280- γ).

The onset of shedding of AEEC was different in the 2 herds that we studied. It is possible that this difference was due to different feeding and management practices. Changes in diet and animal management practices have been shown to affect the shedding of verotoxin-producing *E. coli* (11,12). Although AEEC colonies were detected in at least 1 sample from all the animals studied except 1, AEEC were generally shed transiently by the colonized goat kids.

The present results are consistent with earlier findings that most AEEC isolated from healthy goats possess intimin β and the *ehxA* gene and are negative for the *vt* and *astA* genes and that goats are not a significant reservoir of typical EPEC (none of the EPEC strains found in this study had the *bfpA* gene) (2,3,7,8). In this study, the AEEC colonies isolated belonged to 7 serogroups, but almost 60% belonged to serogroup O26. Seven of the 17 O26 colonies possessed the *cnf3* gene, which encodes a new type of cytotoxic necrotizing factor recently described by our group in atypical EPEC from sheep and goats (4). In addition, 3 isolates belonged to serogroup O157 and carried the *vt2* gene. Since EPEC O26 and EHEC O157 have been implicated as human pathogens (1,13), the results of this study show that goat kids may be a potential source of infection for humans. However, in contrast with the data obtained here, previous studies (2,7,8) have been unable to detect serogroups O26 and O157 among AEEC isolated from healthy goats. The differences between studies in the detection of AEEC serogroups may be at least partially due to the transient nature of the shedding of AEEC by colonized goat kids.

In conclusion, this article describes for the first time the presence of antibodies against intimin β in colostrum and serum

obtained from goat kids. Moreover, the study results suggest that these antibodies do not prevent colonization of the intestine by AEEC in goat kids. The data obtained also show that colonization with AEEC in goat kids is transient and suggest that these animals may be a reservoir of AEEC potentially pathogenic for humans.

Acknowledgments

This study was supported by grants from the Dirección General de Investigación (grant AGL2001-1476), the Universidad Complutense-Comunidad de Madrid (grant CCG07-UCM/AGR-2568), and the Instituto de Salud Carlos III (grants FIS G03-025-COLIREO-O157 and PI051428). We thank Elena Neves and Rocío Sánchez for technical assistance, and Dr. Jorge Blanco (Laboratorio de Referencia de *E. coli*, Facultad de Veterinaria, Universidade de Santiago de Compostela, Lugo, Spain) for serogrouping the attaching and effacing *Escherichia coli* strains.

References

1. Nataro JP, Kaper JB. Diarrheagenic *Escherichia coli*. Clin Microbiol Rev 1998;11:142-201.
2. Orden JA, Yuste M, Cid D, et al. Typing of the *eae* and *espB* genes of attaching and effacing *Escherichia coli* isolates from ruminants. Vet Microbiol 2003;96:203-215.
3. Yuste M, De la Fuente R, Ruiz-Santa-Quiteria JA, Cid D, Orden JA. Detection of the *astA* (EAST1) gene in attaching and effacing *Escherichia coli* from ruminants. J Vet Med B Infect Dis Vet Public Health 2006;53:75-77.
4. Orden JA, Domínguez-Bernal G, Martínez-Pulgarín S, et al. Necrotogenic *Escherichia coli* from sheep and goats produce a new type of cytotoxic necrotizing factor (CNF3) associated with the *eae* and *ehxA* genes. Int Microbiol 2007;10:47-55.
5. Manjarrez-Hernandez HA, Gavilanes-Parra S, Chavez-Berrocal E, Navarro-Ocaña A, Cravioto A. Antigen detection in enteropathogenic *Escherichia coli* using secretory immunoglobulin A antibodies isolated from human breast milk. Infect Immun 2000;68:5030-5036.
6. Parissi-Crivelli A, Parissi-Crivelli JM, Girón JA. Recognition of enteropathogenic *Escherichia coli* virulence determinants by human colostrum and serum antibodies. J Clin Microbiol 2000;38:2696-2700.
7. De la Fuente R, García S, Orden JA, Ruiz-Santa-Quiteria JA, Díez R, Cid D. Prevalence and characteristics of attaching and effacing strains of *Escherichia coli* isolated from diarrheic and healthy sheep and goats. Am J Vet Res 2002;63:262-266.
8. Cortés C, De la Fuente R, Blanco J, et al. Serotypes, virulence genes and intimin types of verotoxin-producing *Escherichia coli* and enteropathogenic *E. coli* isolated from healthy dairy goats in Spain. Vet Microbiol 2005;110:67-76.
9. van Diemen PM, Dziva F, Abu-Median A, et al. Subunit vaccines based on intimin and Efa-1 polypeptides induces humoral immunity in cattle but do not protect against intestinal colonisation by enterohaemorrhagic *Escherichia coli* O157:H7 or O26:H-. Vet Immunol Immunopathol 2007;116:47-58.

10. Adu-Bobie J, Frankel G, Bain C, et al. Detection of intimins α , β , γ , and δ , four intimin derivatives expressed by attaching and effacing microbial pathogens. *J Clin Microbiol* 1998;36:662–668.
11. Kudva IT, Hatfield PG, Hovde CJ. Effect of diet on the shedding of *Escherichia coli* O157:H7 in a sheep model. *Appl Environ Microbiol* 1995;61:1363–1370.
12. Callaway TR, Elder RO, Keen JE, Anderson RC, Nisbet DJ. Forage feeding to reduce preharvest *Escherichia coli* populations in cattle, a review. *J Dairy Sci* 2003;86:852–860.
13. Leomil L, Pestana de Castro AF, Krause G, Schmidt H, Beutin L. Characterization of two major groups of diarrheagenic *Escherichia coli* O26 strains which are globally spread in human patients and domestic animals of different species. *FEMS Microbiol Lett* 2005;249:335–342.

Isolation of *Escherichia coli* from piglets in South Korea with diarrhea and characteristics of the virulence genes

Yeong Ju Kim, Ji Hee Kim, Jin Hur, John Hwa Lee

Abstract

Escherichia coli was isolated from the feces of 122 piglets with diarrhea on 55 farms in Korea. The virulence genes of each isolate were characterized by polymerase chain reaction (PCR). Of the 562 isolates, 191 carried 1 or more of the virulence genes tested for in this study. Of the 191 isolates, 114 (60%) carried 1 or more of the genes for enterotoxigenic *E. coli* (ETEC) fimbriae F4, F5, F6, F18, and F41 and ETEC toxins LT, STa, and STb, 57 (30%) carried 1 or more of the genes for the Shiga-toxin-producing *E. coli* (STEC) toxins Stx1, Stx2, and Stx2e, and 21% and 37% carried the gene for enteropathogenic *E. coli* intimin and for enteroaggregative *E. coli* toxin, respectively. Collectively, our results indicate that other pathotypes of *E. coli* as well as ETEC can be strongly associated with diarrhea in piglets. In addition, detection of the genes for Stx1 and Stx2 indicates that pigs are reservoirs of human pathogenic STEC.

Résumé

Escherichia coli a été isolé des fèces de 122 porcelets avec de la diarrhée provenant de 55 fermes situées en Corée. Les gènes de virulence de chaque isolat ont été caractérisés par réaction d'amplification en chaîne par la polymérase (PCR). Parmi les 562 isolats, 191 étaient porteurs d'au moins un des gènes de virulence testés dans la présente étude. Parmi les 191 isolats, 114 (60 %) étaient porteurs d'un gène ou plus des fimbriae F4, F5, F6, F18 et F41 et des toxines LT, STa et STb associés aux souches entérotoxigéniques de *E. coli* (ETEC), 57 (30 %) étaient porteurs d'au moins un des gènes Stx1, Stx2 et Stx3e des *E. coli* producteurs de Shiga-toxine (STEC), et 21 % et 37 % étaient respectivement porteurs du gène de l'intimine des *E. coli* entéro-pathogènes et de la toxine des *E. coli* entéro-aggrégatifs. Dans son ensemble, les résultats indiquent que les ETEC ainsi que des pathotypes différents peuvent être fortement associés à la diarrhée chez les porcelets. De plus, la détection des gènes codant pour Stx1 et Stx2 indique que les porcs sont des réservoirs pour les STEC pathogènes humains.

(Traduit par Docteur Serge Messier)

Pathogenic *Escherichia coli* is a common agent responsible for a variety of intestinal disorders, such as diarrhea and edema disease syndrome in pigs (1,2). To cause disease, enterotoxigenic *E. coli* (ETEC) must colonize the mucosal surface of the intestine using surface proteins known as fimbriae and produce enterotoxins, whether heat-stable (STa, STb), heat-labile (LT), or both (3,4). The known porcine fimbriae are F4 (K88), F5 (K99), F6 (987P), F18, and F41 (2,3). Different types of fimbriae can be associated with ETEC diarrhea in animals of different ages (3,4). In piglets under 5 d of age, F4-positive strains of *E. coli* cause more severe diarrhea, whereas F5, F6, and F41 strains cause milder diarrhea with a later onset (between 4 and 14 d of age) (3,4). Postweaning diarrhea (PWD) is the most constant disease problem at large-scale farms and particularly among piglets weaned at 3 to 4 wk of age (3). The main adhesive virulence factors of ETEC associated with PWD are F4 (mainly K88ac) and F18 fimbriae (3–5).

The serologically diverse group of Shiga-toxin-producing *E. coli* (STEC), also known as verotoxin-producing *E. coli*, causes disease in humans and animals (6). The common feature of STEC strains is the production of Shiga toxin 1 (Stx1), Shiga toxin 2 (Stx2), a variant

of Stx1 (Stx1c, Stx1d), a variant of Stx2 (Stx2c, Stx2d, Stx2e, Stx2f, Stx2g), or a combination of these toxins (4). The Stx2e variant is produced by the STEC strains that cause edema disease in swine (4). In addition to ETEC and STEC, strains that cause attaching and effacing lesions, similar to those produced by enteropathogenic *E. coli* (EPEC) in humans, have also been associated with diarrhea in pigs (2). These attaching and effacing *E. coli* possess the *eae* gene encoding the outer membrane protein known as intimin, which is involved in attachment of the bacteria to the surface of epithelial cells in the gastrointestinal tract (2). The *eae* gene is a key marker of EPEC infections (7).

The distinctive aggregative pattern of adhesion to cultured human epithelial cells *in vitro* defines enteroaggregative *E. coli*. These strains produce an enterotoxin known as enteroaggregative heat-stable enterotoxin 1 (EAST1) (2,5). The *astA* gene encoding EAST1 has also been detected in *E. coli* of different pathogenic strains, such as ETEC, EPEC, and STEC from humans and animals (2,8).

The present study investigated the distribution of pathotypes of enterovirulent *E. coli* isolated from piglets with diarrhea in Korea and the characteristics of their virulence genes. This kind of work

Veterinary Public Health, College of Veterinary Medicine and Bio-Safety Research Institute, Chonbuk National University, Jeonju 561-756, Republic of Korea.

Address all correspondence to Dr. John Hwa Lee; telephone: +82-63-270-2553; fax: +82-63-270-3780; e-mail: johnhlee@chonbuk.ac.kr

Received October 6, 2008. Accepted February 17, 2009.

Table I. Polymerase chain reaction primers used in this study to detect genes for *Escherichia coli* virulence factors and the product sizes

Virulence factor	Nucleotide sequence	Size ^a	Primer coordinates	Accession number	Reference number
F4	GCTGCATCTGCTGCATCTGGTAGTG CCTACTGAGTGCTGGTAGTTACAGCC	792	31–54 798–822	M29374	2
F5	TATTATCTTAGGTGGTATGG GGTATCCTTTAGCAGCAGTATTTTC	314	21–40 311–334	M35282	9
F6	TCTGCTCTAAAGCTACTGG AACTCCACCGTTTGATCAG	333	193–212 506–525	M35257	2
F18	GTGAAAAGACTAGTGTATTATTC CTTGTAAGTAACCGCGTAAGC	510	160–182 649–669	M61713	10
F41	GCATCAGCGGCAGTATCT GTCCCTAGCTCAGTATTATCACCT	380	34–51 390–413	X14354	9
Intimin	GACCCGGCACAAGCATAAGC CCACCTGCAGCAACAAGAGG	384	27–46 391–410	A3334567	11
LT	ATTTACGGCGTTACTATCCTC TTTTGGTCTCGGTGAGATATG	281	27–47 287–307	S60731	2
STa	GCTAATGTTGGCAATTTTTATTCTGTA AGGATTACAACAAGTTCACAGCAGTAA	190	9–36 171–198	M25607	9
STb	GCCTATGCATCTACACAATC TGAGAAATCGACAATGTCCG	279	515–534 773–793	AY028790	2
EAST1	CCATCAACACAGTATATCCGA GGTCGCGAGTGACGGCTTTGT	111	2–24 94–114	S81691	2
Stx1	ATAAATCGCCATTGCTTGACTAC AGAACGCCCACTGAGATCATC	180	424–446 593–603	EU754740	11
Stx2	GGCACTGTCTGAACTGCTCC TCGCCAGTTATCTGACATTCTG	255	606–626 839–860	EU816442	11
Stx2e	CCACCAGGAAGTTATATTCC TTCACCAGTTGTATATAAAGA	759	223–243 961–981	U72191	10

^a Number of base pairs.

had not been carried out previously in Korea, and the results offer significant epidemiologic information on porcine EPEC.

The strains were isolated from the feces of 122 piglets with diarrhea aged 2 to 72 d on 55 farms in Korea. The fecal samples, obtained per rectum, were inoculated directly onto eosin methylene blue and MacConkey agar (Difco, Sparks, Maryland, USA) and identified by means of the API 32E system (bioMérieux, Marcy l'Etoile, France). Three to eight *E. coli* colonies per sample were collected randomly for study. The reference *E. coli* strains used were O157:H7 (American Type Culture Collection no. 43894; intimin⁺, Stx1⁺, and Stx2⁺), G.C.V. (K88⁺), O9:K35 E-92 (K99⁺ and F41⁺), and O141:K85ab E-127 (987P⁺ and STa⁺), which were kindly supplied by the National Veterinary Research and Quarantine Service, Anyang, Korea. In addition, the *E. coli* strains JOL500 (F18⁺, LT⁺, STa⁺, STb⁺, and Stx2e⁺) and JOL538 (EAST1⁺) isolated in this study were used for reference.

The isolates were cultured on blood agar containing 5% sheep blood for 18 h at 37°C, and the presence of hemolysis was

determined visually. A polymerase chain reaction (PCR) was used to detect the genes for the adhesins F4, F5, F6, F18, F41 and intimin and the toxins LT, STa, STb, Stx1, Stx2, Stx2e, and EAST1 (Table I), as previously described (2,9,10,11). Fisher's exact test was used to analyze the correlation between the presence of adhesin genes and the distribution of adhesin genes within weaning and hemolysis status (12). The results were considered significant when *P*-values were less than 0.05. All statistical analyses were carried out with the SPSS 16.0 program (SPSS, Chicago, Illinois, USA).

Of the 562 isolates tested, 191 carried 1 or more of the virulence-associated genes, and 114 (60%) of the 191 carried 1 or more of the genes for ETEC fimbriae and toxins (Table II). Of the 114 isolates, 38, 34, and 42 possessed 1 or more of the genes for ETEC fimbriae only, ETEC fimbriae and ETEC toxins, and ETEC toxins only, respectively (Figure 1). Among the 72 isolates carrying the genes for fimbriae, the most prevalent fimbrial gene was that for F18, which was identified in 30 isolates (16% of the 191). Among the 76 isolates carrying the

Table II. Distribution of genes for adhesins and toxins among 191 *E. coli* isolates from piglets with diarrhea in Korea

Toxins	Adhesins; no. of isolates carrying the genes															Total	
	F4	F5	F6	F18	F41	Intimin	F4/41	F5/41	F6/18	F18/ intimin	F41/ intimin	F5/6/ 18	F5/18/ 41	F5/41/ intimin	None ^b		
LT																1	1
STa			3	3									1			3	10
STb						1										8	9
Stx1						1	1									2	4
Stx2			1	3	2	4										7	17
Stx2e		1														2	3
EAST1						8										37	45
LT/Stx1																1	1
LT/Stx2																1	1
LT/EAST1	3	1														10	14
STa/STb																4	4
STa/EAST1									1							3	4
Stx1/Stx2			1														1
Stx2/Stx2e			2						2							1	5
Stx2/EAST1						1					1						2
Stx2e/EAST1						1											1
LT/STa/STb																1	1
LT/STa/EAST1	1															1	2
LT/STb/Stx2					1												1
LT/Stx2/Stx2e								1		2		2		1		1	7
LT/Stx2/EAST1																1	1
STa/STb/EAST1				3												2	5
LT/STa/STb/EAST1	1			1													2
LT/STa/Stx2/Stx2e				2		3										1	6
LT/STa/STb/Stx2/ Stx2e										4							4
LT/STa/Stx1/Stx2/ Stx2e				1													1
LT/STa/Stx1/ Stx2e/EAST1				1													1
LT/STa/STb/Stx2/ Stx2e/EAST1				1													1
None ^a	7	4	2	3	8	13											
Total	12	6	9	18	11	32	1	1	3	6	1	2	1	1		87	191

^a No genes carried for LT, STa, STb, Stx1, Stx2, or Stx2e.^b No genes carried for F4, F5, F6, F18, F41, or intimin.

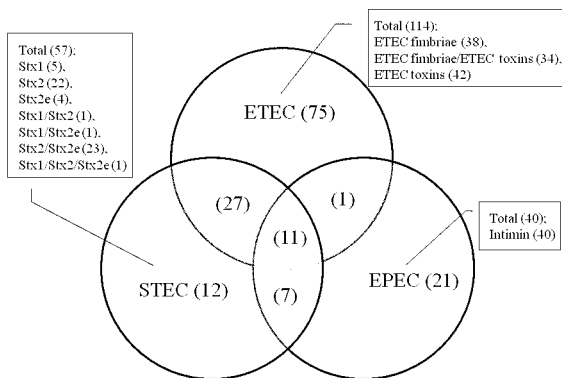


Figure 1. Distribution and relationship of the genes for virulence factors of enterotoxigenic *Escherichia coli* (ETEC), Shiga-toxin-producing *E. coli* (STEC), and enteropathogenic *E. coli* (EPEC) among 191 isolates from piglets with diarrhea in Korea. The numbers in parenthesis are the numbers of isolates carrying the genes.

genes for ETEC toxins, the most prevalent toxin gene was that for LT, which was identified in 44 isolates (23% of the 191). The most common combination of the genes for ETEC fimbriae and ETEC toxins was F18/LT/STa/STb, which was detected in 6 (3%) of the 191 isolates. Among the 57 isolates (30%) carrying 1 or more genes for Shiga toxins, the most prevalent Shiga toxin gene was Stx2, which was detected in 47 isolates (25% of the 191). Of the 191 isolates, 40 (21%) carried the intimin gene, which represents EPEC (Figure 1), and 78 (40.8%) possessed the gene for EAST1 (Table II).

Of the 114 ETEC isolates, the 57 STEC isolates, and the 40 EPEC isolates, 75 (66%), 12 (21%), and 21 (53%) carried the genes for only ETEC, STEC, and EPEC, respectively. Of the 191 isolates, 27 (14%) carried the genes for ETEC/STEC, 1 (0.5%) the genes for ETEC/EPEC, 7 (4%) the genes for STEC/EPEC, and 11 (6%) the genes for ETEC/STEC/EPEC (Figure 1). Of the 71 EAST1-positive isolates, 37 (52%) carried the gene for EAST1 only; 18 (25%), 8 (11%), 5 (7%), 2 (3%), and 1 (1%) carried the genes for ETEC/EAST1, EPEC/EAST1, ETEC/STEC/EAST1, STEC/EPEC/EAST1, and ETEC/STEC/EPEC/EAST1, respectively (Table II). Among these isolates, 5 contained 7 virulence genes, the most complex combinations observed in this study: F18/LT/STa/STb/Stx2/Stx2e/EAST1 (in 1 isolate) and F18/intimin/LT/STa/STb/Stx2/Stx2e (in 4 isolates).

Of the 191 isolates with virulence-associated genes, 86 (45%) and 105 (55%) were isolated from pre- and postweaned piglets, respectively, and 140 (73%) were hemolytic (Table III). The genes for F4, F5, F6, F41, and intimin were isolated from pre- and postweaned piglets ($P > 0.1$), irrespective of hemolytic activity ($P > 0.1$). However, the gene for F18 was detected significantly more often among the isolates from pigs with PWD and the hemolytic isolates ($P < 0.001$).

This study examined the presence of genes for adhesins, enterotoxins, and Shiga toxins representing the virulence factors and their associations in the *E. coli* isolated from piglets with diarrhea. The genes for ETEC, STEC, EPEC, and EAST1 were detected in 114, 57, 40, and 71 of the 562 isolates tested, respectively. Isolates containing the specific genes for ETEC were more common than the other types of *E. coli*. Among ETEC fimbriae, F4 (K88) is the most prevalent contributor to diarrhea in piglets in many countries (2,13). However, in our study the gene for F4 was detected in only 13 (7%) of the

191 isolates with virulence-associated genes. It is believed that the immune pressure elicited by vaccination programs involving mainly F4 antigen may have caused a lower prevalence of F4 fimbriae in ETEC (14,15). Infections with ETEC having the F5, F6, and F41 fimbriae are age-related, occurring primarily in pigs less than 2 wk old (3,4,15). However, this study detected the genes for F4, F5, F6, and F41 fimbriae at similar rates in both pre- and postweaned piglets with diarrhea ($P > 0.1$), which suggests that these fimbriae are not limited to ETEC causing disease in young piglets. A newly identified adhesin, F18, was the most prevalent type of fimbriae in this study. Moreover, the gene for F18 was isolated significantly more often from piglets with PWD ($P < 0.001$). Collectively, our data suggest a need for new vaccination programs to protect pre- and postweaned piglets from PWD. In addition, our results imply that F18 has become the main type of *E. coli* associated with diarrhea and must be considered in vaccination programs.

Among the ETEC toxins, STb is the most frequently isolated from piglets with diarrhea (2,16,17). However, in this study the genes for LT and STa were more widespread than the gene for STb. In addition, this study found the gene combinations for LT/STa, LT/STa/STb, and STa/STb in approximately 5% of isolates each, whereas the gene combination for LT/STb was detected in only 0.5% of the isolates, unlike the rate previously reported (17). Overall, these results suggest that *E. coli* disease in piglets may be associated not with a single toxin and a major gene combination but with more varied and complex toxins as well as their combinations.

The toxins such as Stx1 and Stx2 produced by human, bovine, and ovine STEC are associated with hemorrhagic colitis and hemolytic-uremic syndrome in humans (2,18). Interestingly, in our study the genes for Stx1 and Stx2 were detected in 4% and 25% of isolates, whereas previous studies could not detect these genes in any pig isolates tested (2,19). In addition, positivity for F6, F18, and intimin was significantly more frequent among the isolates producing STEC toxins ($P < 0.05$). Thus, our results indicate that piglets are also reservoirs of STEC pathogenic for humans and that intimin as well as F18 must be considered in vaccination programs for piglets.

The *eae* gene encoding intimin has been recovered from *E. coli* associated with porcine neonatal diarrhea (1) as well as PWD (2,20). Martins et al (1) reported that most *eae*-positive isolates were able to produce STa or Stx2e. Similarly, this study detected *eae* in 20.9% of 191 isolates. On the other hand, the role of EAST1 in swine colibacillosis has not been clearly determined. However, several studies have reported that EAST1 is also distributed among other types of *E. coli*, such as ETEC, and can cause diarrhea in piglets in the presence of other virulence factors, such as enterotoxins (LT, STa, STb), and specific colonization factors, such as F4 (2). We also found a high prevalence (37%) of the EAST1 gene (*astA*), and approximately 50% of the *astA*-positive isolates possessed at least 1 of these virulence factors. These results suggest that EAST1-positive strains are also largely distributed and strongly associated with disease in piglets in this area.

Approximately 37% of the 191 isolates harbored genes for more than 1 pathotype-representative factor. These isolates can be classified into 9 pathotypes according to possession of the virulence genes: ETEC/STEC, ETEC/EPEC, ETEC/EAST1, STEC/EPEC, EPEC/EAST1, ETEC/STEC/EPEC, ETEC/STEC/EAST1, STEC/EPEC/EAST1, and ETEC/STEC/EPEC/EAST1. These types are

Table III. Distribution of adhesin genes according to piglet weaning status and hemolytic activity in the 191 isolates

Weaning status (no. of isolates)	Hemolysis (no. of isolates)	Adhesins; no. of isolates carrying the genes													
		F4	F5	F6	F18	F41	Intimin	F4/F41	F5/F41	F6/F18	F18/ intimin	F41/ intimin	F5/F6/ F18	F5/F18/ F41	F5/F41/ intimin
Preweaned	47	4	2	2	0	1	9	1	1	1	0		0	0	0
-86	– (39)	1	0	6	0	4	6	0	0	0	0		0	0	1
Postweaned	93	6	4	1	18	4	15	0	0	2	6	1	2	1	0
-105	– (12)	1	0	0	0	2	2	0	0	0	0		0	0	0
Total (191)		12	6	9	18	11	32	1	1	3	6	1	2	1	1

more varied and complex than recent studies have indicated (2,16). The observation of these complex pathotypes of *E. coli* may indicate the evolution of pathogenic *E. coli* into forms surviving against the various strategies used for prevention and treatment by acquisition of the necessary virulence genes.

Adhesin genes other than that for F18 fimbriae were not significantly associated with hemolytic activity ($P > 0.1$), in agreement with the report that hemolysis of *E. coli* is not an absolute indication for pathogenicity in pigs (1,4). However, all isolates carrying the F18 fimbrial gene were hemolytic. This indicates that hemolytic isolates contained significantly more F18 ($P < 0.001$), and a test for hemolysis can be a useful indication of the pathogenicity of *E. coli* causing disease in piglets or at least for the presence of the F18 fimbrial gene.

Acknowledgments

This study was supported by grant RTI05-03-02 from the Regional Technology Innovation Program of the Ministry of Commerce, Industry and Energy (MOCIE) and by the Brain Korea 21 Project in the Republic of Korea.

References

- Martins MDF, Martinez-Rossi NM, Ferreira A, et al. Pathogenic characteristics of *Escherichia coli* strains isolated from newborn piglets with diarrhea in Brazil. *Vet Microbiol* 2000;76:51–59.
- Vu-Khac H, Holoda E, Pilipčinec E, et al. Serotypes, virulence genes, intimin types and PFGE profiles of *Escherichia coli* isolated from piglets with diarrhea in Slovakia. *Vet J* 2007;174:176–187.
- Nagy B, Fekete PZ. Enterotoxigenic *E. coli* (ETEC) in farm animals. *Vet Res* 1999;30:259–284.
- Vu-Khac H, Holoda E, Pilipčinec E. Distribution of virulence genes in *Escherichia coli* strains isolated from diarrhoeic piglets in the Slovak Republic. *J Vet Med B Infect Dis Vet Public Health* 2004;51:343–347.
- Smeds A, Pertovaara M, Timonen T, Pohjanvirta T, Pelkonen S, Palva A. Mapping the binding domain of the F18 fimbrial adhesin. *Infect Immun* 2003;71:2163–2172.
- Bettelheim KA. Non-O157 verotoxin-producing *Escherichia coli*: A problem, paradox, and paradigm. *Exp Biol Med* 2003;228:333–344.
- Hornitzky MA, Mercieca K, Bettelheim KA, Djordjevic SP. Bovine feces from animals with gastrointestinal infections are a source of serologically diverse atypical enteropathogenic *Escherichia coli* and Shiga toxin-producing *E. coli* strains that commonly possess intimin. *Appl Environ Microbiol* 2005;71:3405–3412.
- Osek J. Detection of the enteroaggregative *Escherichia coli* heat-stable enterotoxin 1 (EAST1) gene and its relationship with fimbrial and enterotoxin markers in *E. coli* isolates from pigs with diarrhea. *Vet Microbiol* 2003;91:65–72.
- Franck SM, Bosworth BT, Moon HW. Multiplex PCR for enterotoxigenic, attaching and effacing, and Shiga toxin-producing *Escherichia coli* strains from calves. *J Clin Microbiol* 1998;36:1795–1797.
- Imberechts H, De Greve H, Schlicker C, et al. Characterization of F107 fimbriae of *Escherichia coli* 107/86, which causes edema disease in pigs, and nucleotide sequence of the F107 major fimbrial subunit gene, fedA. *Infect Immun* 1992;60:1963–1971.
- Jackson MP, Newland JW, Holmes RK, O'Brien AD. Nucleotide sequence analysis of the structural genes for Shiga-like toxin I encoded by bacteriophage 933J from *Escherichia coli*. *Microb Pathog* 1987;2:147–153.
- Niewerth U, Frey A, Voss T, et al. The AIDA autotransporter system is associated with F18 and Stx2e in *Escherichia coli* isolates from pigs diagnosed with edema disease and postweaning diarrhea. *Clin Diagn Lab Immunol* 2001;8:143–149.
- Alexa P, Stouračova K, Hamrik J, Rychlik I. Gene typing of the colonisation factor K88 (F4) in enterotoxigenic *Escherichia coli* strains isolated from diarrhoeic piglets. *Vet Med-Czech* 2001;46:46–49.
- Chen X, Gao S, Jiao X, Liu XF. Prevalence of serogroups and virulence factors of *Escherichia coli* strains isolated from pigs with postweaning diarrhea in eastern China. *Vet Microbiol* 2004;103:13–20.
- Söderlind O, Thafvelin B, Möllby R. Virulence factors in *Escherichia coli* strains isolated from Swedish piglets with diarrhea. *J Clin Microbiol* 1988;26:879–884.
- Frydendahl K. Prevalence of serogroups and virulence genes in *Escherichia coli* associated with postweaning diarrhea and edema disease in pigs and a comparison of diagnostic approaches. *Vet Microbiol* 2002;85:169–182.
- Osek J, Truszczyński M. Occurrence of fimbriae and enterotoxins in *Escherichia coli* strains isolated from piglets in Poland. *Comp Immunol Microbiol Infect Dis* 1992;15:285–292.
- Coombes BK, Wickham ME, Mascarenhas M, Gruenheid S, Finlay BB, Karmali MA. Molecular analysis as an aid to assess

- the public health risk of non-O157 Shiga toxin-producing strains. *Appl Environ Microbiol* 2008;74:2153–2160.
19. Osek J, Gallien P, Truszczyński M, Protz D. The use of polymerase chain reaction for determination of virulence factors of *Escherichia coli* strains isolated from pigs in Poland. *Comp Immunol Microbiol Infect Dis* 1999;22:163–174.
20. Malik A, Tóth I, Beutin L, et al. Serotypes and intimin types of intestinal and faecal strains of *eae*⁺ *Escherichia coli* from weaned pigs. *Vet Microbiol* 2006;114:82–93.

Pleiotropic effects of polysaccharide capsule loss on selected biological properties of *Streptococcus suis*

Shin-Ichi Tanabe, Laetitia Bonifait, Nahuel Fittipaldi, Louis Grignon,
Marcelo Gottschalk, Daniel Grenier

Abstract

In this study, an unencapsulated *Streptococcus suis* mutant was used to investigate the pleiotropic effects resulting from capsule loss. The capsule deficient mutant of *S. suis* acquired a biofilm-positive phenotype, which was associated with significantly increased cell surface hydrophobicity. Cell-associated fibrinogen-binding and chymotrypsin-like activities were decreased in the unencapsulated mutant. The mutant did not differ significantly from the encapsulated parent strain for minimal inhibitory concentrations to penicillin G, ampicillin, and tetracycline. However, while the encapsulated strain was highly resistant to the bactericidal action of penicillin G and ampicillin, the unencapsulated mutant was approximately 60-fold more sensitive. Compared with the parent strain, the unencapsulated mutant induced a much higher inflammatory response in monocyte-derived macrophages resulting in an increased secretion of tumor necrosis factor (TNF)- α , interleukin (IL)-1 β , IL-6, and IL-8. The capsule appears to hinder important adhesins or hydrophobic molecules that mediate biofilm formation, as well as cell wall components capable of stimulating immune cells.

Résumé

Dans la présente étude, un mutant non-capsulé de *Streptococcus suis* a été utilisé afin d'examiner les effets pléiotropiques résultant de la perte de la capsule. Le mutant déficient de *S. suis* a acquis un phénotype positif pour le biofilm, qui était associé avec une augmentation significative de l'hydrophobicité de surface. La liaison du fibrinogène et l'activité apparentée à celle de la chymotrypsine étaient diminuées chez le mutant non-capsulé. Il n'y avait pas de différence significative entre le mutant et le parent capsulé en ce qui a trait aux concentrations minimales inhibitrices de la pénicilline G, de l'ampicilline et de la tétracycline. Toutefois, alors que la souche capsulée était très résistante à l'action bactéricide de la pénicilline G et de l'ampicilline, le mutant non-capsulé était approximativement 60 fois plus sensible. Comparativement à la souche parentale, le mutant non-capsulé a induit une réponse inflammatoire beaucoup plus marquée sur les macrophages dérivés des monocytes, ce qui a entraîné une sécrétion augmentée du facteur nécrosant des tumeurs (TNF)- α , d'interleukine (IL)-1 β , IL-6 et IL-8. La capsule semble interférer avec des adhésines importantes ou des molécules hydrophobes qui sont impliquées dans la formation de biofilm, ainsi que des composantes de la paroi cellulaire capables de stimuler les cellules du système immunitaire.

(Traduit par Docteur Serge Messier)

Streptococcus suis is an important swine pathogen worldwide that causes meningitis, septicemia, arthritis, and endocarditis (1). This bacterium can also affect humans who have had close contact with sick or carrier pigs or with their derived-products (2). Although 35 serotypes are known, serotype 2 is most commonly associated with infections in swine and humans (1). In recent years, various potential virulence factors produced by *S. suis* have been described, including muramidase-released protein, extracellular protein factor, suilysin, adhesins, and capsule (3). Among the potential virulence determinants identified, the polysaccharide capsule appears to be critical for the pathogenicity of *S. suis*. Indeed, unencapsulated mutants were shown to be avirulent in mice and in 2 different swine models of infection (4,5). Charland et al (6) reported that an unencapsulated mutant of *S. suis* was more susceptible to phagocytosis by macrophages compared with the parent strain. The capsular material

of *S. suis* serotype 2 contains 5 different sugars: rhamnose, galactose, glucose, N-acetylglucosamine, and N-acetyl neuraminic acid (sialic acid), the latter being the 3rd most important in amounts (7). Sialic acid is well known as an antiphagocytic factor for many bacterial species through inhibition of the activation of the alternative complement pathway (8). For a bacterium, the presence of a capsule may provide particular cell surface properties while interfering physically with other cell surface components. The aim of this study was to investigate the pleiotropic effects associated with capsule loss, on selected biological properties of *S. suis*.

Streptococcus suis S735, a reference virulent serotype 2 strain of European phenotype, and the unencapsulated mutant BD101 were routinely grown in Todd Hewitt broth (THB; BBL Microbiology Systems, Cockeysville, Massachusetts, USA) at 37°C under aerobiosis. The mutant BD101 was constructed in a previous study and

Groupe de Recherche en Écologie Buccale, Faculté de Médecine Dentaire, Université Laval, Québec City, Québec (Tanabe, Bonifait, Grignon, Grenier); Groupe de Recherche sur les Maladies Infectieuses du Porc, Faculté de Médecine Vétérinaire, Université de Montréal, Montréal, Québec (Fittipaldi, Gottschalk); and Centre de Recherche en Infectiologie Porcine, Université de Montréal, Montréal, Québec (Gottschalk, Grenier).

Address all correspondence to Dr. Grenier; telephone: (418) 656-7341; fax: (418) 656-2861; e-mail: Daniel.Grenier@greb.ulaval.ca

Received May 19, 2008. Accepted October 1, 2008.

was impaired in capsule production as a result of the deletion of the cognate promoter of the *aro* operon, this in turn resulted in the abolishment of *aroA*, *aroK*, *pheA*, and *orf10* expression (9). Mutant BD101 was devoid of capsular sialic acid, the absence of capsule was confirmed by electron microscopy (9). Although the exact explanation for the absence of capsule in the *aro* deficient mutant is still speculative, it has been proposed that it may be related to abolishment of the expression of *orf10*. This gene is predicted to belong to the LytR-cpsA-psr family of transcriptional regulators; members of this family have been shown to act as positive regulators of capsule expression in other species of streptococci (10).

The culture broth medium used to investigate biofilm formation by *S. suis* S735 and the unencapsulated mutant BD101 contained 0.5% glucose, 2% peptone (Proteose Peptone No. 3; Difco, Detroit, Michigan, USA), 0.3% K_2HPO_4 , 0.2% KH_2PO_4 , 0.01% $MgSO_4 \cdot 7H_2O$, 0.002% $MnSO_4 \cdot 6H_2O$, and 0.5% NaCl. This medium contained sufficient aromatic amino acids required for growth of mutant BD101. Biofilm formation was measured in polystyrene microtiter plates and crystal violet staining, as previously described (11). Assays were run in triplicate and the means \pm standard deviations (*s*) of 2 independent experiments were calculated. The structural architecture of the *S. suis* (S735, mutant BD101) biofilm was examined by scanning electron microscopy. *Streptococcus suis* was inoculated in 35-mm dishes (Nunc, Denmark) containing a 10.5 \times 22 mm plastic coverslip (Thermanox; Nunc). After 24 h of incubation, medium and free-floating bacteria were removed. The biofilms formed on each coverslip were incubated overnight in fixation buffer (4% paraformaldehyde and 2.5% glutaraldehyde in 0.1 M phosphate buffer, pH 7.2), washed with 0.1 M cacodylate buffer (3 \times 20 min), and post-fixed for 90 min at room temperature in 1% osmic acid containing 2 mM potassium ferrocyanide and 6% sucrose in cacodylate buffer. Samples were dehydrated through a graded series of ethanol (50%, 70%, 95%, and 100%), critical point dried, gold sputtered, and examined using a scanning electron microscope (JEOL JSM6360LV; JEOL, Tokyo, Japan) operating at 30 kV.

The relative cell surface hydrophobicity of *S. suis* S735 and the unencapsulated mutant BD101 was determined by measuring their absorption to n-hexadecane according to the procedure described by Rosenberg et al (12). To compare lectin-binding activity, 7 fluorescein isothiocyanate (FITC)-labeled lectins (E-Y Laboratories, San Mateo, California, USA) were used: *Conavalia ensiformis* agglutinin (Con A — specific for mannose and glucose residues), *Dolichos biflorus* agglutinin (DBA — specific for N-acetyl galactosamine residues), *Maclura pomifera* agglutinin (MPA — specific for N-acetyl galactosamine residues), peanut agglutinin (PNA) from *Arachis hypogaea* (specific for galactose residues), soybean agglutinin (SBA) from *Glycine max* (specific for N-acetyl galactosamine and galactose residues), *Ulex europaeus* agglutinin (UEA I — specific for fucose residues), and wheat germ agglutinin (WGA) (*Triticum vulgare*, specific for N-acetyl glucosamine and sialic acid residues). Powdered lectins were dissolved, to a concentration of 1 mg/mL, in phosphate buffered saline (PBS) solution and stored at -20°C until used. Bacterial cells were harvested from THB agar plates, washed in PBS and suspended in diluted lectin solutions (40 μ g/mL) at an optical density (OD) of 0.5 at 660 nm. Following incubation at room temperature under darkness for 60 min, bacteria were washed 3 times in PBS and

suspended in the initial volume. Cell-bound lectins were quantified using a fluorometer with an excitation wavelength of 490 nm and an emission wavelength of 520 nm. These assays were run in triplicate and the means \pm *s* of 2 independent experiments were calculated.

The fibrinogen-binding activity of *S. suis* S735 and the unencapsulated mutant BD101 were quantified using an enzyme-linked immunosorbent assay (ELISA) according to the procedure described by Bonifait et al (13). Cell-associated chymotrypsin-like activity was determined, as previously described, using N-succinyl-Ala-Ala-Pro-Phe-pNa as the substrate (14). Assays for fibrinogen-binding and chymotrypsin-like activities were run in triplicate and the means \pm *s* of 2 independent experiments were calculated.

The minimal inhibitory concentrations (MIC) and minimal bactericidal concentrations (MBC) of planktonic cultures of *S. suis* S735 and the capsule deficient mutant BD101 to penicillin G, ampicillin, and tetracycline were determined using a microdilution procedure. Briefly, 2-fold serial dilutions (5000 ng/mL to 0.6 ng/mL) of antibiotics were prepared in THB. The wells of a microtiter plate, each containing 100 μ L of medium, were inoculated with 100 μ L of an overnight culture of *S. suis* diluted in fresh THB to obtain an OD₆₆₀ of 0.2 (equivalent CFUs for S735 and BD101). The plate was then incubated at 37°C for 24 h. The MICs were the lowest concentrations of antibiotic, for which no significant increase in OD₆₆₀ was noted following inoculation and incubation. To determine the MBCs, 10 μ L of culture was recovered from wells showing no visible growth and spread on THB agar plates. The MBCs were the lowest concentrations of antibiotic at which no colonies grew on THB plates. Three independent experiments were performed.

U937 cells (ATCC CRL-1593.2), a monoblastic leukemia cell line, were cultivated at 37°C in a 5% CO₂ atmosphere in RPMI-1640 medium (HyClone Laboratories, Logan, Utah, USA) supplemented with 10% heat-inactivated fetal bovine serum (FBS) (RPMI-FBS) and 100 μ g/mL of penicillin-streptomycin. Monocytes (2×10^5 cells/mL) were incubated in RPMI-FBS containing 10 ng/mL of phorbol myristic acid (PMA) for 48 h to induce differentiation into adherent macrophage-like cells. Following the PMA treatment, the medium was replaced with fresh medium and the differentiated cells were incubated for an additional 24 h prior to use. Adherent monocyte-derived macrophages were washed and suspended in RPMI with 1% heat-inactivated FBS without antibiotics at a density of 1×10^6 cells/mL and incubated in 6-well plates (2×10^6 cells/well in 2 mL) at 37°C in a 5% CO₂ atmosphere for 2 h prior stimulation. *Streptococcus suis* cells (S735 and mutant BD101) were harvested by centrifugation at 11 000 \times g for 10 min and suspended in RPMI medium to a concentration of 1×10^9 bacteria/mL, as determined using a Petroff-Hausser counting chamber. The bacterial suspensions were added to the monocyte-derived macrophages to obtain a multiplicity of infection (MOI) of 1, 10, 50, and 100. After 24 h of incubation, the culture medium supernatants were collected and stored at -20°C until used. Monocyte-derived macrophages were also stimulated with a cell wall fraction (10, 25, and 50 μ g/mL) of *S. suis*, prepared as previously described (15). Commercial ELISA kits (R&D Systems, Minneapolis, Minnesota, USA) were used to quantify interleukin-1 β (IL-1 β), tumor necrosis factor- α (TNF- α), interleukin-6 (IL-6), and interleukin-8 (IL-8) concentrations in the cell-free culture supernatants according

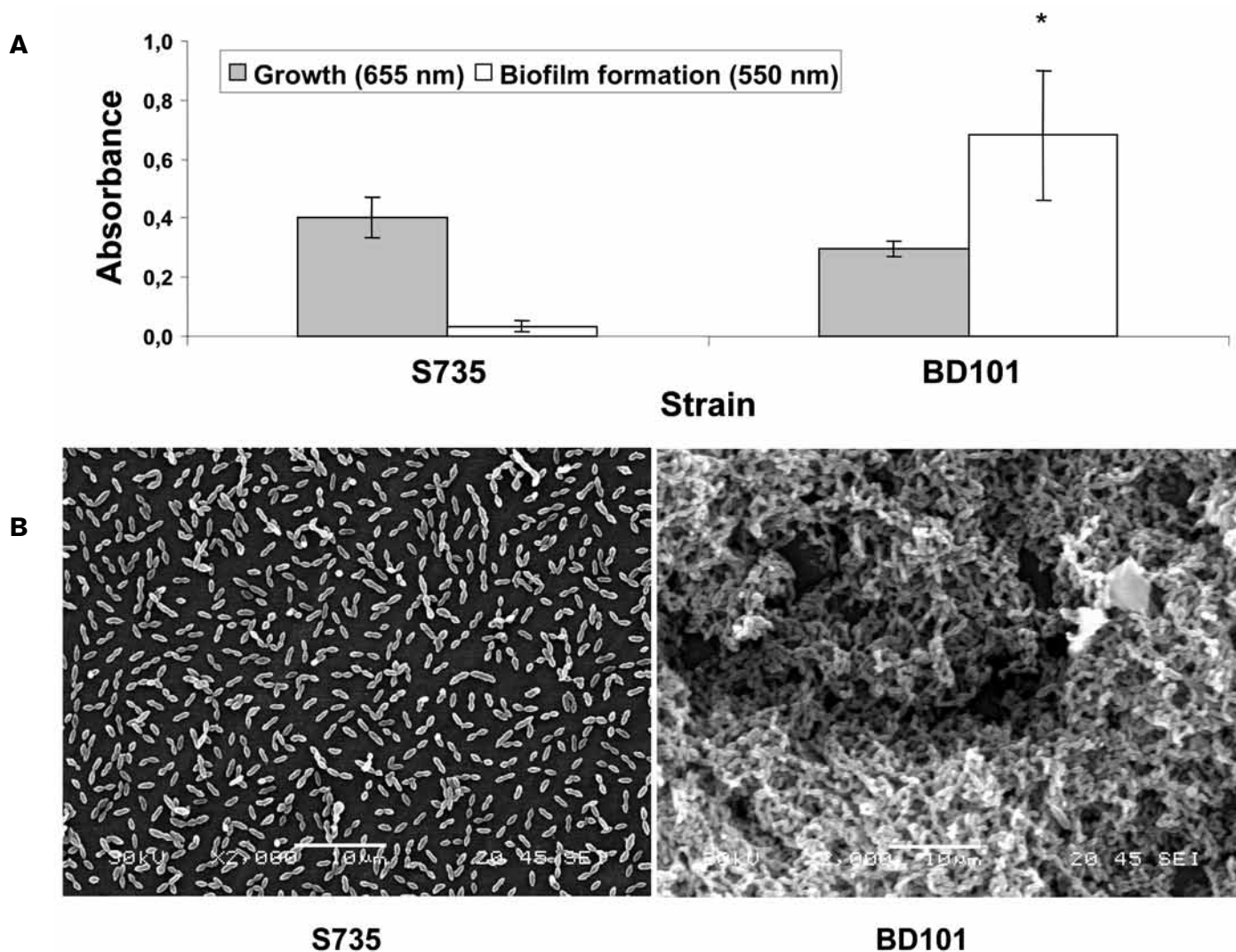


Figure 1. Biofilm formation by *Streptococcus suis* S735 and its unencapsulated mutant BD101. (A) Crystal violet-stained biofilm following growth in polystyrene microplate. (B) Scanning electron micrographs of *S. suis* biofilms formed after 24 h of growth. * indicates a significant difference ($P < 0.01$) with the Student's *t*-test between *S. suis* S735 and its unencapsulated mutant BD101.

to the manufacturer's protocols. The absorbance at 450 nm (A_{450}) was read using a microplate reader with the wavelength correction set at 550 nm. The rated sensitivities of the commercial ELISA kits were 3.9 pg/mL for IL-1 β , 15.6 pg/mL for TNF- α , 9.3 pg/mL for IL-6, and 31.2 pg/mL for IL-8. All stimulation assays were run in triplicate and the means \pm *s* were calculated.

The effect of capsule loss on the capacity of *S. suis* to form biofilms was evaluated using a polystyrene microtiter plate assay. As shown in Figure 1A, the parent strain S735 was unable to form biofilm, whereas the unencapsulated mutant BD101 acquired the capacity to form a thick biofilm that stained with crystal violet. Biofilm formation was not related to a more pronounced growth of the capsule-deficient mutant since the growth of both strains was comparable, as evaluated by measuring the A_{660} . An examination by scanning microscope confirmed the results obtained with the microtiter plate assay (Figure 1B). Individual bacteria and short chains of *S. suis* S735 were observed attached to the polystyrene surface but were rarely bound to each other. On the other hand, aggregates and microcolonies of

the capsule deficient mutant (BD101) almost completely covered the surface of the polystyrene support. The capacity of the unencapsulated mutant BD101 to form a biofilm is in agreement with previous studies reporting that capsule inhibited the adherence of *S. suis* to epithelial (16) and endothelial cells (17). Interestingly, capsules produced by *Neisseria meningitidis* (18) and *Escherichia coli* (19) have also been reported to prevent biofilm formation. The inhibition of bacterial attachment to mammalian cells and of biofilm formation by the capsule of *S. suis* is likely related to the masking of adhesins and other structures, making them non-functional. Infections by such pathogens would thus require modulation of capsule production allowing transitions from highly encapsulated states where bacteria could resist host immune system to lower unencapsulated states where bacteria could form biofilm and adhere to host cells.

The polysaccharide capsule of *S. suis* likely provides particular properties to bacterial cells. First, capsule loss resulted in a significant modification of the cell surface hydrophobicity. The hydrophobicity of the unencapsulated mutant was $90.7\% \pm 1.6$, whereas

Table I. Comparative analyses of *Streptococcus suis* S735 and its unencapsulated mutant BD101 for lectin-binding, fibrinogen-binding, and chymotrypsin-like activities

Activity	<i>S. suis</i>		% change (parent versus mutant)
	S735	BD101	
Lectin-binding activity (RFU)			
WGA	1859 ± 54	431 ± 46	-77 ^a
SBA	743 ± 40	658 ± 45	-11
MPA	613 ± 19	572 ± 23	-7
Fibrinogen-binding activity (ng bound/well)	193 ± 10	136 ± 7	-30 ^a
Chymotrypsin-like activity (A_{405})	1.25 ± 0.07	0.86 ± 0.04	-31 ^a

RFU — Relative fluorescence units; WGA — wheat germ agglutinin from *Triticum vulgare*, specific for N-acetyl glucosamine and sialic acid residues; SBA — soybean agglutinin from *Glycine max*, specific for N-acetyl galactosamine and galactose residues; MPA — *Maclura pomifera* agglutinin, specific for N-acetyl galactosamine residues.

^a Significant difference ($P < 0.01$) with the Student's *t*-test between *S. suis* S735 and its unencapsulated mutant BD101.

Table II. Minimal inhibitory and minimal bactericidal concentrations of *Streptococcus suis* S735 and its unencapsulated mutant BD101 to penicillin G, ampicillin, and tetracycline. Values are representative of 3 independent experiments

Strain	Penicillin G (ng/mL)		Ampicillin (ng/mL)		Tetracycline (ng/mL)	
	MIC	MBC	MIC	MBC	MIC	MBC
<i>S. suis</i> S735	20	1250	20	2500	312	> 5000
<i>S. suis</i> BD101	10	20	20	40	156	1250

MIC — minimal inhibitory concentrations; MBC — minimal bactericidal concentrations.

it was $11.2\% \pm 3.2$ for the parent strain (Table I). This suggests that hydrophilic capsule hinders more-hydrophobic structures or components important for biofilm formation by *S. suis*. The possibility that hydrophobic interactions may be important for biofilm formation by *S. suis* is in agreement with the study by Yi et al (18), who reported a direct correlation between biofilm formation by *Neisseria meningitidis* and cell surface hydrophobicity.

The cell surface of both *S. suis* S735 and the mutant BD101 was further characterized by investigating the binding of fluorescein-labeled lectins. Among the 7 lectins tested, positive binding to *S. suis* S735 cell surface was observed with WGA and to a lesser extent with SBA and MPA (Table I). The unencapsulated mutant showed a significant reduction (77%) in binding of WGA, while it was only slightly affected for SBA and MPA binding. This decreased capacity to bind WGA, a lectin specific for N-acetyl glucosamine and sialic acid residues, is consistent with the fact that sialic acid is a major constituent of the *S. suis* capsule.

The effect of capsule loss on 2 cell-associated properties, namely fibrinogen-binding activity and chymotrypsin-like activity, was then investigated. Using a fibrinogen-binding microplate assay, both the parental strain and the capsule deficient mutant were found to bind human fibrinogen on their surface (Table I). The parent strain possessed significantly higher fibrinogen-binding activity than the mutant BD101. Regarding the cell-associated chymotrypsin-like

activity, the parent strain also showed significantly higher activity compared with the unencapsulated mutant (Table I). This suggests that capsule expression may help stabilize these cell surface activities.

Table II shows the MICs and MBCs for *S. suis* S735 and the mutant BD101 to penicillin G, ampicillin, and tetracycline. Penicillin G and ampicillin were found to be much more effective than tetracycline on *S. suis* S735, as demonstrated by the low MICs. Compared with the parent strain, MICs for the unencapsulated mutant were either not modified (ampicillin) or one dilution lower (penicillin G and tetracycline). The MBCs for the capsule deficient mutant to all 3 antibiotics were found to be markedly decreased. More specifically, MBCs to penicillin G and ampicillin were approximately 60-fold lower for the mutant BD101 compared to the parent strain. This may be related to the fact that the internal concentration of antibiotics required to kill bacteria are more easily reached when the capsule is absent in *S. suis*. It is also possible that the capsule stabilizes the plasma membrane and protecting it from rupture and bacterial death.

The secretion of TNF- α , IL-1 β , IL-6, and IL-8 by monocyte-derived macrophages stimulated with whole cells of either *S. suis* S735 or the mutant BD101 is reported in Figure 2. For all 4 cytokines, stimulation of macrophages with the parental strain induced a dose-dependent increased secretion. In general, MOIs of 50 and 100 were necessary to induce a marked cytokine response. For all cytokines, the response induced by the mutant BD101 was significantly higher ($P < 0.01$) at MOIs of 50 and 100 compared with that induced by *S. suis* S735. More specifically, at an MOI of 100, the secretion of TNF- α , IL-1 β , IL-6, and IL-8 by monocyte-derived macrophages was increased 2-, 4-, 5-, and 2-fold, respectively, compared with the parent strain. A cell wall preparation of *S. suis* was also found to induce dose-dependent TNF- α , IL-1 β , IL-8, and, to a lesser extent, IL-6 responses in monocyte-derived macrophages (Figure 2). The above results suggest that the absence of capsule uncovers the components, namely the cell wall, that triggers the monocyte-derived macrophages. This is in agreement with the results found by Graveline et al (20), who showed that an unencapsulated mutant (B218) derived from a *S. suis* virulent field isolate induced significantly higher levels of TNF- α and IL-1 β in the THP-1 human monocytic cell line. Although the

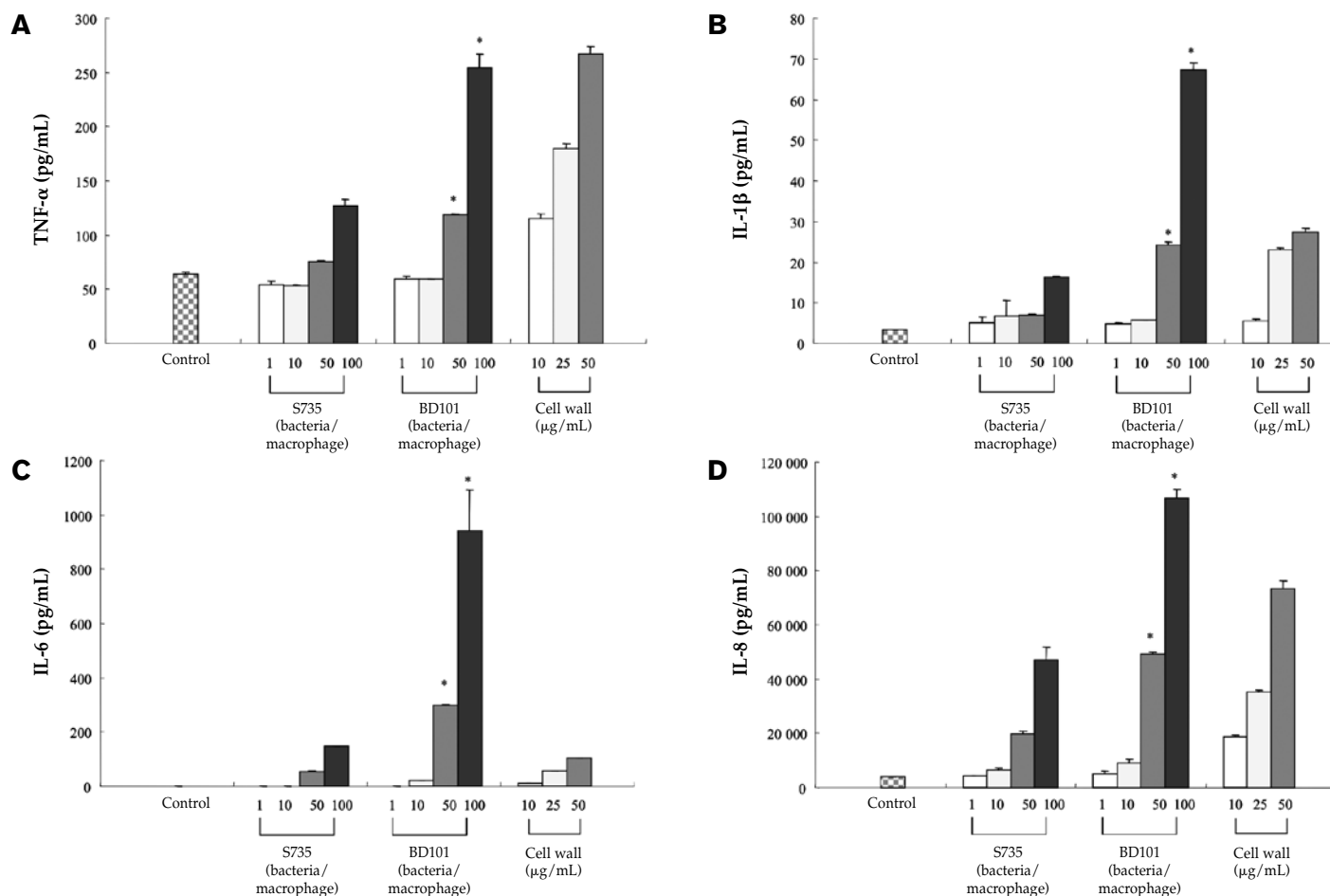


Figure 2. Secretion of tumor necrosis factor (TNF)-α (panel A), interleukin (IL)-1β (panel B), IL-6 (panel C), and IL-8 (panel D) by monocyte-derived macrophages infected with whole cells of *Streptococcus suis* S735 and its capsule deficient mutant BD101 at multiplicities of infection (MOI) of 1, 10, 50, and 100. Monocyte-derived macrophages were also stimulated with a cell wall preparation (10, 25, and 50 μg/mL) of *S. suis*. * indicates a significant difference ($P < 0.01$) with the Student's *t*-test between *S. suis* S735 and its unencapsulated mutant BD101.

biological significance of this observation is unclear, 2 consequences are possible. One, the capsule of *S. suis* may suppress the host's immunological response, a critical step at the early step of infection to prevent the bacteria from growing following by severe septicemia and death. Two, the loss of capsule in *S. suis* may be associated with an exaggerated immunological response induced by cell wall components, leading to uncontrolled inflammatory reactions. This phenomenon can increase the permeability of the blood-brain barrier, of which microvascular endothelial cells are the main constituents. An increased permeability of the blood-brain barrier facilitates the migration of bacteria and leukocytes that may promote the development of an inflammatory exudate and a severe disease outcome.

In conclusion, this study showed that loss of capsule in *S. suis* is associated with several pleiotropic effects. Capsule appears to hinder important adhesins or hydrophobic molecules that mediate biofilm formation, as well as cell wall components capable of stimulating immune cells. These observations suggest that future studies to better understand how the capsule expression is regulated in vivo will also contribute to a better knowledge of the pathogenesis of *S. suis*.

Acknowledgments

The authors thank Marie-Pier Levasseur for her technical assistance. This study was supported by Natural Sciences and Engineering Research Council of Canada (NSERC).

References

- Higgins R, Gottschalk M. Streptococcal Diseases. In: Straw BE, D'Allaire S, Mengeling WL, Taylor DJ, eds. Diseases of Swine, 9th ed. Ames, Iowa: Iowa Univ Pr, 2005:769–783.
- Huang YT, Teng LJ, Ho SW, Hsueh PR. *Streptococcus suis* infection. J Microbiol Immunol Infect 2005;38:306–313.
- Gottschalk M, Segura M. The pathogenesis of the meningitis caused by *Streptococcus suis*: The unresolved questions. Vet Microbiol 2000;76:259–272.
- Charland N, Harel J, Kobisch M, Lacasse S, Gottschalk M. *Streptococcus suis* serotype 2 mutants deficient in capsular expression. Microbiology 1998;144:325–332.

5. Smith HE, Damman M, van der Velde J, et al. Identification and characterization of the *cps* locus of *Streptococcus suis* serotype 2: The capsule protects against phagocytosis and is an important virulence factor. *Infect Immun* 1999;67:1750–1756.
6. Charland N, Kobisch M, Martineau-Doizé B, Jacques M, Gottschalk M. Role of capsular sialic acid in virulence and resistance to phagocytosis of *Streptococcus suis* capsular type 2. *FEMS Immunol Med Microbiol* 1996;14:195–203.
7. Elliot SD, Tai J. The type-specific polysaccharides of *Streptococcus suis*. *J Exp Med* 1978;148:1699–1704.
8. Edwards MS, Kasper DL, Jennings HJ, Baker CJ, Nicholson-Weller A. Capsular sialic acid prevents activation of the alternative complement pathway by type III, group B streptococci. *J Immunol* 1982;128:1278–1283.
9. Fittipaldi N, Harel J, D'amours B, Lacouture S, Kobisch M, Gottschalk M. Potential use of an unencapsulated and aromatic amino acid-auxotrophic *Streptococcus suis* mutant as a live attenuated vaccine in swine. *Vaccine* 2007;25:3524–3535.
10. Cieslewicz MJ, Kasper DL, Wang Y, Wessels MR. Functional analysis in type Ia group B *Streptococcus* of a cluster of genes involved in extracellular polysaccharide production by diverse species of streptococci. *J Biol Chem* 2001;276:139–146.
11. Grenier D, Grignon L, Gottschalk M. Characterisation of biofilm formation by a *Streptococcus suis* meningitis isolate. *Vet J* 2009;179:292–295.
12. Rosenberg M, Gutnick D, Rosenberg E. Adherence of bacteria to hydrocarbons: A simple method for measuring cell-surface hydrophobicity. *FEMS Microbiol Lett* 1980;9:29–33.
13. Bonifait L, Grignon L, Grenier D. Fibrinogen induces biofilm formation by *Streptococcus suis* and enhances its antibiotic resistance. *Appl Environ Microbiol* 2008;74:4969–4972.
14. Jobin MC, Grenier D. Identification and characterization of four proteases produced by *Streptococcus suis*. *FEMS Microbiol Lett* 2003;220:113–119.
15. Segura M, Stankova J, Gottschalk M. Heat-killed *Streptococcus suis* capsular type 2 strains stimulate tumor necrosis alpha and interleukin-6 production by murine macrophages. *Infect Immun* 1999;67:4646–4654.
16. Benga L, Goethe R, Rohde M, Valentin-Weigand P. Non-encapsulated strains reveal novel insights in invasion and survival of *Streptococcus suis* in epithelial cells. *Cell Microbiol* 2004;6:867–881.
17. Vanier G, Segura M, Friedl P, Lacouture S, Gottschalk M. Invasion of porcine brain microvascular endothelial cells by *Streptococcus suis* serotype 2. *Infect Immun* 2004;72:1441–1449.
18. Yi K, Rasmussen AW, Gudlavalleti SK, Stephens DS, Stojiljkovic I. Biofilm formation by *Neisseria meningitidis*. *Infect Immun* 2004;72:6132–6138.
19. Schembri MA, Dalsgaard D, Klemm P. Capsule shields the function of short bacterial adhesins. *J Bacteriol* 2004;186:1249–1257.
20. Graveline R, Segura M, Radzioch D, Gottschalk M. TLR2-dependent recognition of *Streptococcus suis* is modulated by the presence of capsular polysaccharide which modifies macrophage responsiveness. *Int Immunol* 2007;19:375–389.

Rapid serodiagnosis with the use of surface plasmon resonance imaging for the detection of antibodies against major surface protein A of *Mycoplasma synoviae* in chickens

Kiseok Oh, Semi Lee, Jayoung Seo, Dongwoo Lee, Taejung Kim

Abstract

Mycoplasma synoviae, a major worldwide pathogen in poultry, causes respiratory tract infection and arthritis in chickens and turkeys. Two major surface antigens of *M. synoviae* are encoded by a single gene, *vlhA* (variably expressed lipoprotein and hemagglutinin). The gene product is cleaved post-translationally to yield the lipoprotein major surface protein (MSP) B (MSPB) and the hemagglutinin MSPA. The availability of MSPA as an antigen for serodiagnosis was studied by means of a protein chip based on surface plasmon resonance imaging (SPRi). The diagnostic potential of SPRi for measurement of levels of antibody to MSPA was compared with that of a conventional enzyme-linked immunosorbent assay (ELISA) kit. The results from SPRi, a process that took only 1 h, were similar to those from ELISA. Therefore, MSPA can be used as an antigen for serologic studies, and SPRi, a label-free and high-throughput method, may be a valuable tool in avian serodiagnostic studies.

Résumé

Mycoplasma synoviae est un agent pathogène de la volaille mondialement répandu, qui cause des infections du tractus respiratoire et de l'arthrite chez les poulets et les dindons. Deux antigènes de surface majeurs de *M. synoviae* sont codés par un gène unique, *vlhA* (lipoprotéine et hémagglutinine à expression variable). Le produit du gène est clivé post-traduction pour générer la lipoprotéine dénommée protéine majeure de surface (MSP) B (MSPB) et l'hémagglutinine MSPA. La disponibilité de MSPA comme antigène pour le sérodiagnostic a été étudiée grâce à une biopuce protéinique basée sur l'imagerie par résonance de plasmon de surface (SPRi). Le potentiel diagnostique de SPRi pour mesurer les niveaux d'anticorps contre MSPA a été comparé avec celui d'une trousse immuno-enzymatique (ELISA) conventionnelle. Les résultats de SPRi, un processus qui n'a pris que 1 h, étaient similaires à ceux de l'ELISA. Ainsi, MSPA peut être utilisé comme un antigène pour des études sérologiques, et SPRi, une méthode sans marqueur et à haut débit, comme un outil utile dans des études en sérodiagnostic aviaire.

(Traduit par Docteur Serge Messier)

Mycoplasma synoviae is a major worldwide poultry pathogen that causes respiratory tract infection and arthritis in chickens and turkeys. It is an important cause of chronic respiratory disease and synovitis in chickens and causes serious economic losses in the worldwide poultry industry (1). Two of the major surface antigens in *M. synoviae* are encoded by a single gene, *vlhA* (variably expressed lipoprotein and hemagglutinin). The gene product is cleaved post-translationally to yield the lipoprotein major surface protein (MSP) B (MSPB) and the hemagglutinin MSPA (2,3). A previous study revealed that the immunodominant 45- to 50-kDa cluster of membrane proteins in the WVU-1853 strain of *M. synoviae* consists of 2 groups of membrane antigens, MSPA and MSPB, and that MSPB was expressed in all strains tested (3).

Control of *M. synoviae* infection is highly dependent on diagnosis by serologic assays, including rapid slide agglutination tests to detect infections within the flock. However, these assays have limited specificity and sensitivity, primarily because of cross-reactions (4). Several enzyme-linked immunosorbent assays (ELISAs) have been developed to detect antibodies against *M. synoviae* but have generally

been based on poorly defined membrane components (5–9). An ELISA based on recombinant MSPB (rMSPB) has been described (10). Use of an ELISA based on rMSPB from *M. synoviae* strain H improved serologic detection in vaccinated birds relative to the use of an ELISA based on recombinant protein from a heterologous strain (4). However, serodiagnostic studies evaluating MSPA had not been performed until the present work.

Methods using ELISA are quite reliable but also time- and labor-intensive. Most of the currently used protein arrays rely on detection by means of enzymatic or fluorescent tags. In contrast, surface plasmon resonance imaging (SPRi) is a rapid, label-free, surface-sensitive spectroscopic technique used to examine bioaffinity interactions on thin gold films (11). It detects changes in the refractive index within a short distance from the surface of a thin metal film as variations in light intensity reflected from the back of the film and does not require labeling (12–14). This technique has been successfully used to screen various bioaffinity interactions using proteins (15,16). This article describes the use of rMSPA to develop a protein chip based on SPRi to detect antibodies to *M. synoviae* in chicken serum and reports

College of Veterinary Medicine, Chonnam National University, 300 Yongbong-dong, Buk-gu, Gwangju 500-757, Republic of Korea (Oh, S. Lee, Seo, Kim); Merial Korea, Seoul 137-040, Republic of Korea (D. Lee).

The first 2 authors contributed equally to this work.

Address all correspondence to Professor Taejung Kim; telephone: +82-62-530-2858; fax: +82-62-530-2857; e-mail: tjkim@chonnam.ac.kr

Received November 5, 2008. Accepted February 18, 2009.

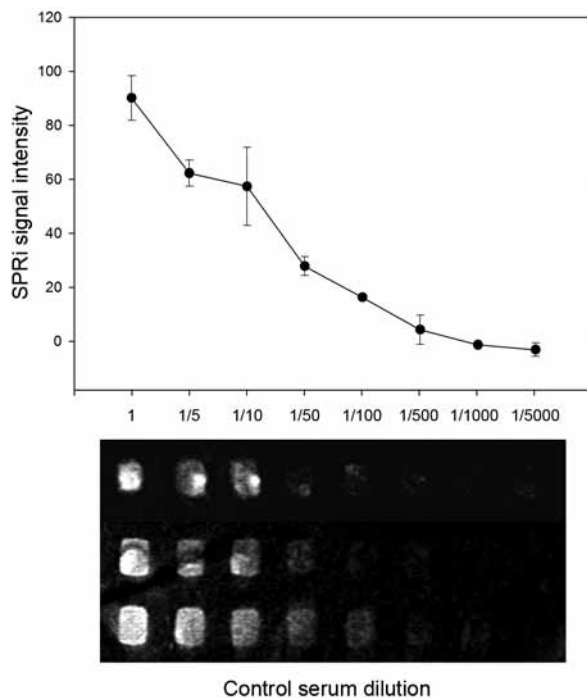


Figure 1. Top: Changes in signal intensity in surface plasmon resonance imaging (SPRI), representing the binding affinity between recombinant major surface protein A (rMSPA), immobilized on a gold chip by ProLinker B, and various dilutions of positive control serum (infected with *Mycoplasma synoviae*). Bottom: Original images of the signal intensity for each dilution.

the diagnostic efficacy of SPRI compared with that of conventional ELISA in detecting *M. synoviae* infections.

The *M. synoviae* strain WVU-1853 (American Type Culture Collection [ATCC] no. 25204) was obtained from the National Veterinary Research and Quarantine Service (NVRQS), Anyang, Korea, and DNA from this strain was used as a template for polymerase chain reaction (PCR) amplification. Recombinant MSPA was prepared with the use of a prokaryotic expression system (pRSET A vector; Invitrogen, Carlsbad, California, USA). Briefly, the MSPA gene (GenBank no. AF035624) was amplified by PCR with 2 primers, MSPA-F (5'-GGCC GGATCC ATG GATGAAGTTAGATTTCTAA-3', from nucleotides 1590 to 1609) and MSPA-R (5'-GGCC AAGCTT TCAACTATTGCTTGCTATTG-3', from nucleotides 2227 to 2246), containing sites (underlined) for 2 restriction enzymes, *Bam*HI and *Hind*III (B + H). The PCR products were cloned into the B + K-digested pRSET A (17), and the recombinant DNA was transformed into BL21(DE3)pLysS (Invitrogen) host cells. The transformants were grown in 25 mL of Luria-Bertani medium with ampicillin and chloramphenicol to an optical density (OD) of 0.5. Protein expression was induced by the addition of isopropyl- β -D-thiogalactopyranoside (final concentration 1 mM). The proteins were purified under denaturing conditions by means of an affinity purification system (Probond, Invitrogen).

A total of 302 field samples (from 14 farms) from chickens that had not been vaccinated against *M. synoviae* were screened by both SPRI and ELISA. Three positive samples from chickens with previously confirmed *M. synoviae* infection and 3 negative samples from specific-pathogen-free (SPF) chickens were used as controls. To rule

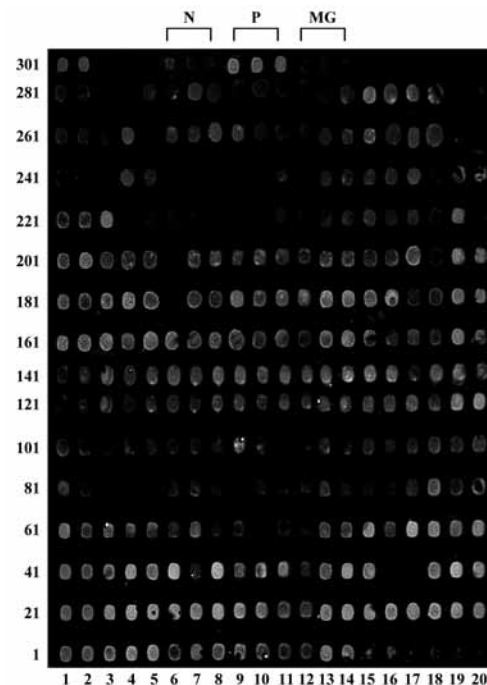


Figure 2. Images from SPRI analysis of the antibodies against MSPA (rMSPA used as the antigen) in 302 field samples of chicken serum. N — negative controls; P — positive controls; MG — species controls (samples infected with *M. gallisepticum*).

out the cross-reactivity caused by antigens in common between *M. synoviae* and *M. gallisepticum*, 3 serum samples from SPF chickens experimentally infected with *M. gallisepticum* S6 (ATCC no. 15302; NVRQS) were used as species controls.

Surface modification of a patterned glass slide chip with a gold film (K-Mac, Daejeon, Korea) for the specific antigen binding was carried out as previously described (18). Briefly, the slides were cleaned with a freshly prepared piranha solution (3:1 mixture of concentrated H_2SO_4 and 30% H_2O_2), coated with ProLinker B (Proteogen, Seoul, Korea), washed in deionized water, and dried under a N_2 stream. The clean chips were soaked in 3 mM ProLinker B solution for 1 h, then rinsed sequentially with chloroform, acetone, ethanol, and deionized water. The chips were dried and the antigens in phosphate-buffered saline (PBS), 100 μ g/mL, spotted onto their surface by means of the ProteoChip (Proteogen), which has miniaturized wells for quantitative antibody assays that contain a minute amount of serum (1 μ L per spot). The chips were then incubated for 20 min in 80% humidity at 37°C, rinsed 3 times with a mixture of PBS-T (PBS + 0.05% Tween-20, pH 7.4), and then rinsed with deionized water. Test samples of antibody or serum in a PBS buffer containing 0.1 mg/mL of bovine serum albumin (BSA), 5 to 10 nL per spot, were mixed with 1% BSA in PBS for 10 min to block the chip surface. The test samples were then applied to the chips for 15 min. The chips were dried and analyzed with the SPRI system (K-Mac).

The minimum detection threshold of the SPRI was determined by testing 8 serially diluted (1 to 1/5000) positive-control serum samples containing chicken polyclonal antibody against *M. synoviae*. The results were compared with those from a commercially available

ELISA kit (FlockChek; IDEXX Laboratories, Westbrook, Maine, USA). The ELISA was performed according to the manufacturer's instructions, and data from 2 separate experiments were compared; the results were expressed as the mean S/P ratio [and standard deviation (*s*)] of the end-point titers. The mean signal intensity (SPRi) and OD (ELISA) values of positive and negative samples were compared by means of Student's *t*-test with the SPSS 14.0 program (SPSS, Chicago, Illinois, USA).

The rMSPA was produced and purified without contamination (data not shown) and used as an antigen for both SPRi and ELISA. The mean S/P ratio (and *s*) by ELISA was 0.044 (0.016) for the negative controls and 4.831 (1.404) for the positive controls; these values were significantly different ($P < 0.005$). The mean S/P ratio for the species controls (infected with *M. gallisepticum*) was 0.054 (0.029) ($P < 0.005$). All the tested field samples but 3 (99%) were positive [mean S/P ratio 2.800 (1.053)], which suggests that *M. synoviae* infection is quite common in Korea and highlights the need for a proper prevention program to protect chickens against *M. synoviae* infection.

Figure 1 shows that the signal intensity in the SPRi increased linearly with increasing antibody concentration; it also presents the original images for each control antibody dilution. The detection limits of the SPRi protein chip corresponded to a 1:500 antibody dilution and a signal intensity of 20. The mean signal intensity (and *s*) was 38.804 (3.177) for the positive controls and 0.714 (2.789) for the negative controls. An OD ≥ 9.080 (corresponding to 3 *s* above the negative-control mean) was considered positive. As a result, 281 of the field samples (93%) were considered positive by SPRi (Figure 2), which suggests that the protein chip based on SPRi diagnostics was as sensitive as the ELISA.

The mean signal intensity (and *s*) for the species controls was 4.518 (3.977) ($P < 0.005$). The antigenic relatedness of the 2 species used in this study makes it difficult to distinguish them with conventional serologic tests (19). In a recent study, *M. synoviae* ELISA kits showed a varying rate of false-positive reactions (due to cross-reactivity), resulting in a specificity ranging from 2% to 96% for serum samples infected with *M. gallisepticum* and from 33% to 100% for uninfected samples (20). In this study, the species controls (infected with *M. gallisepticum*) had a low mean OD and a low mean signal intensity, which indicates that the cross-reactivity between the 2 species of *Mycoplasma* used in this study is not great enough to result in false-positive SPRi results, and there are some antigenic differences among *M. gallisepticum* and *M. synoviae* strains.

The newly developed SPRi was successfully used to detect antibodies against MSPA in chicken serum. This comparative study confirmed that ELISA is reliable but time-consuming. Many serodiagnostic assays using MSPB as an antigen have been performed, and our data suggest that MSPA is a good candidate for development of the serodiagnostic method. Many SPR assays have recently been described for the detection of antibodies against pathogens (12–14). However, the SPR assay can be applied to only 2 to 4 samples simultaneously. Compared with the SPR assay, the newly developed SPRi protein chip with miniaturized wells proved to be rapid tool (assay time 1 h) with high throughput (up to 300 to 400 samples at a time) and value (up to 4 recycles) for the serodiagnosis of *M. synoviae* infection in chickens.

Acknowledgments

The authors acknowledge a graduate fellowship provided by the Korean Ministry of Education and Human Resources Development through the Brain Korea 21 project. The authors also thank Ms. Myeonghwa Kim, College of Veterinary Medicine, Chonnam National University, Gwangju, Korea, for her excellent technical assistance.

References

1. Kleven SH. *Mycoplasma synoviae* infection. In: Saif YM, Barnes HJ, Fadly AM, et al, eds. Diseases of Poultry. Ames, Iowa: Iowa State Univ Pr, 2003:756–766.
2. Noormohammadi AH, Markham PF, Duffy MF, et al. Multigene families encoding the major hemagglutinins in phylogenetically distinct mycoplasmas. *Infect Immun* 1998;66:3470–3475.
3. Noormohammadi AH, Markham PF, Whithear KG, et al. *Mycoplasma synoviae* has two distinct phase-variable major membrane antigens, one of which is a putative hemagglutinin. *Infect Immun* 1997;65:2542–2547.
4. Noormohammadi AH, Browning GF, Jones J, Whithear KG. Improved detection of antibodies to *Mycoplasma synoviae* vaccine MS-H using an autologous recombinant MSPB enzyme-linked immunosorbent assay. *Avian Pathol* 2003;31:611–617.
5. Gurevich VA, Ley DH, Markham JF, et al. Identification of *Mycoplasma synoviae* immunogenic surface proteins and their potential use as antigens in the enzyme-linked immunosorbent assay. *Avian Dis* 1995;39:465–474.
6. Higgins PA, Whithear KG. Detection and differentiation of *Mycoplasma gallisepticum* and *Mycoplasma synoviae* antibodies in chicken serum using enzyme-linked immunosorbent assay. *Avian Dis* 1986;30:160–168.
7. Opitz HM, Cyr MJ. Triton X-100-solubilized *Mycoplasma gallisepticum* and *Mycoplasma synoviae* ELISA antigens. *Avian Dis* 1986;30:213–215.
8. Opitz HM, Duplessis JB, Cyr MJ. Indirect microenzyme-linked immunosorbent assay for the detection of antibodies to *Mycoplasma synoviae* and *Mycoplasma gallisepticum*. *Avian Dis* 1983;27:773–786.
9. Patten BE, Higgins PA, Whithear KG. A urease-ELISA for the detection of *Mycoplasma* infections in poultry. *Aust Vet J* 1984;61:151–155.
10. Noormohammadi AH, Markham PF, Markham JF, et al. *Mycoplasma synoviae* surface protein MSPB as a recombinant antigen in an indirect ELISA. *Microbiology* 1999;145:2087–2094.
11. Steiner G. Surface plasmon resonance imaging. *Anal Bioanal Chem* 2004;379:328–331. Epub 2004 May 5.
12. Cho HS, Kim TJ, Lee JI, Park NY. Serodiagnostic comparison of enzyme-linked immunosorbent assay and surface plasmon resonance for the detection of antibody to *Porcine circovirus type 2*. *Can J Vet Res* 2006;70:263–268.
13. Cho HS, Park NY. Serodiagnostic comparison between two methods, ELISA and surface plasmon resonance, for the detection of antibodies of classical swine fever virus. *J Vet Med Sci* 2006;68:1327–1329.

14. Kim TJ, Cho HS, Park NY, Lee JI. Serodiagnostic comparison between two methods, ELISA and surface plasmon resonance, for the detection of antibody titres of *Mycoplasma hyopneumoniae*. *J Vet Med B Infect Dis Vet Public Health* 2006;53:87–90.
15. Cho HS, Kim TJ. Comparison of surface plasmon resonance imaging and enzyme-linked immunosorbent assay for the detection of antibodies against iridovirus in rock bream (*Oplegnathus fasciatus*). *J Vet Diagn Invest* 2007;19:414–416.
16. Jung JM, Shin YB, Kim MG, et al. A fusion protein expression analysis using surface plasmon resonance imaging. *Anal Biochem* 2004;330:251–256.
17. Studier FW, Moffatt BA. Use of bacteriophage T7 RNA polymerase to direct selective high-level expression of cloned genes. *J Mol Biol* 1986;189:113–130.
18. Lee Y, Lee EK, Cho YW, et al. ProteoChip: A highly sensitive protein microarray prepared by a novel method of protein immobilization for application of protein–protein interaction studies. *Proteomics* 2003;3:2289–2304.
19. Mardassi BB, Mohamed RB, Gueriri I, et al. Duplex PCR to differentiate between *Mycoplasma synoviae* and *Mycoplasma gallisepticum* on the basis of conserved species-specific sequences of their hemagglutinin genes. *J Clin Microbiol* 2005;43:948–958.
20. Feberwee A, Mekkes DR, de Wit JJ, et al. Comparison of culture, PCR, and different serologic tests for detection of *Mycoplasma gallisepticum* and *Mycoplasma synoviae* infections. *Avian Dis* 2005;49:260–268.

Bighorn sheep fetal lung cell line for detection of respiratory viruses

Sudarvili Shanthalingam, Christina Topliff, Clayton L. Kelling, Subramaniam Srikumaran

Abstract

Pneumonia is an important disease of bighorn sheep (BHS) that is primarily responsible for the drastic decline in numbers of these animals in North America. Members of the genus *Mannheimia* and *Pasteurella* have frequently been isolated from the pneumonic lungs of BHS. Antibodies to several respiratory viruses, including bovine parainfluenza virus 3 (BPIV-3), bovine respiratory syncytial virus (BRSV), bovine viral diarrhoea virus (BVDV), and bovine herpesvirus 1 (BoHV-1), have been detected in herds of BHS. The availability of BHS fetal lung cell lines is likely to enhance the chances of isolation of these viruses. Here we report the development of such a cell line. This line is permissive for BPIV-3, BRSV, BVDV, and BoHV-1 infection, as revealed by an enzyme immunoassay of virus-infected cells with antibodies specific for each of these viruses. This cell line should be valuable for detecting these 4, and possibly other, respiratory viruses in BHS.

Résumé

La pneumonie est une maladie importante chez les mouflons et est responsable en grande partie pour le déclin drastique de leur nombre en Amérique du Nord. Les membres du genre *Mannheimia* (anciennement *Pasteurella*) ont fréquemment été isolés de poumons de mouflons avec des lésions de pneumonie. Des anticorps dirigés contre plusieurs virus respiratoires, incluant le virus parainfluenza 3 bovin (BPIV-3), le virus respiratoire syncytial bovin (BRSV), le virus de la diarrhée virale bovine (BVDV) et le herpèsvirus bovin de type 1 (BoHV-1), ont été détectés dans des troupeaux de mouflons. La disponibilité de lignées cellulaires pulmonaires fœtales de mouflon devrait probablement augmenter les chances d'isolement de ces virus. Nous rapportons ici le développement d'une telle lignée cellulaire. Cette lignée est permissive pour une infection par BPIV-3, BRSV, BVDV et BoHV-1, tel que démontré par une épreuve immuno-enzymatique sur des cellules infectées par ces virus avec des anticorps spécifiques pour chaque virus. Cette lignée cellulaire devrait être utile pour détecter ces 4 virus, et probablement d'autres virus respiratoires chez les mouflons.

(Traduit par Docteur Serge Messier)

The North American population of bighorn sheep (BHS), *Ovis canadensis*, has declined from an estimated 2 million at the beginning of the 19th century to fewer than 70 000 today (1). The attributed reasons include loss of habitat, competition with domestic livestock for forage, and disease (1,2), an important type being respiratory disease (1). Several outbreaks of pneumonia during the past decade have reduced the annual population growth by 40% (3). Members of the genus *Mannheimia* and *Pasteurella* have frequently been isolated from the pneumonic lungs of BHS (1). *M. haemolytica* has long been identified as the secondary bacterial pathogen causing severe fibrinonecrotic pneumonia in cattle (4). In cattle, these bacterial infections do not cause pneumonia unless preceded by infection with BoHV-1 (5), BRSV (6), BVDV (6), or BPIV-3 (7). Antibodies to BPIV-3 (8) and BRSV (9), as well as BVDV and BoHV-1 (Mark Drew, Idaho Department of Fish and Game, Caldwell, Idaho: personal communication, 2008), have been detected in several herds of BHS. However, these viruses have not been routinely isolated from pneumonic BHS. The failure to isolate these viruses from the large number of BHS that have died from pneumonia so far could be due to the long delay before arrival of the carcasses or lung tissue at the

diagnostic laboratory. This problem is difficult to circumvent because of the remoteness of the BHS habitats. However, the chances of isolation of these viruses from the pneumonic lungs of BHS are likely to be enhanced by the availability of BHS cell lines, particularly those of lung origin. Here we report the development of a BHS fetal lung cell line and its permissiveness for infection with respiratory viruses.

A 2nd-trimester fetus from a BHS ewe that was euthanized because of a compound fracture of the left femur was used as the source of fetal lung tissue. The tissue, aseptically removed from the fetus, was rinsed in calcium- and magnesium-free phosphate-buffered saline (PBS) (CMF-PBS: NaCl, 8.0 g; Na₂HPO₄ · H₂O, 2.16 g; KCl, 0.2 g; KH₂PO₄, 0.2 g/L; pH 7.2) supplemented with 20 µg/mL of gentamicin (Invitrogen, Carlsbad, California, USA) and placed in a large petri dish containing 300 mL of CMF-PBS. The lung tissue was chopped into small pieces. The tissue suspension was transferred to a beaker and allowed to settle for 10 min. The top 200 mL of PBS was poured off to get rid of debris and erythrocytes. The remaining 100 mL of minced cells and CMF-PBS was placed in a trypsinizing flask to which 200 mL of prewarmed (to 37°C) CMF-PBS and 100 mL of 1% trypsin (Invitrogen) was added. A stirring bar was placed in

Department of Veterinary Microbiology and Pathology, Washington State University, Pullman, Washington 99164-7040, USA (Shanthalingam, Srikumaran); Department of Veterinary and Biomedical Sciences, University of Nebraska, Lincoln, Nebraska 68583-0905, USA (Topliff, Kelling).

The first two authors contributed equally to this work.

Address all correspondence to Dr. Subramaniam Srikumaran; telephone: (509) 335-4572; fax: (509) 335-8529; e-mail: ssrikumaran@vetmed.wsu.edu

Received October 3, 2008. Accepted December 23, 2008.

the flask, which was kept on a stir plate for 30 min in an incubator at 37°C for the trypsinizing process. The flask contents were then strained through sterile gauze over a beaker. The supernatant containing the cells was transferred into 50-mL centrifuge tubes and centrifuged for 10 min at 170 × g. The cell pellets were pooled, resuspended in Dulbecco's modified Eagle's medium (DMEM; Invitrogen), and centrifuged for 10 min at 100 × g. The cells were washed with DMEM until the supernatant was clear. After the last wash, the supernatant was decanted. The cells were counted and then suspended in DMEM containing 10% fetal bovine serum (Atlanta Biologicals, Norcross, Georgia, USA) and 20 µg/mL of gentamicin (complete growth medium) and dispensed into 75-cm² tissue culture flasks. Each flask received approximately 0.5 mL of packed cells suspended in 100 mL of complete growth medium. The flasks were incubated in a humidified incubator at 37°C with 5% CO₂. The growth medium was replenished every 24 h.

The respiratory viruses used for inoculation of the BHS lung cells were BVDV NY-1 (Animal Plant and Health Inspection Service, Center for Veterinary Biologics, Ames, Iowa, USA), BRSV 236-652 (10), BPIV-3, and BoHV-1 (Veterinary Diagnostic Laboratory, University of Nebraska–Lincoln, Lincoln, Nebraska, USA). The enzyme immunoassay was performed as previously described (11). Briefly, BHS lung cells were seeded onto 12-well plates. When 60% confluent, the cells were inoculated with the viruses at a multiplicity of infection (ratio of infectious agents to infection targets) of 0.5. The cells were incubated at 37°C (BVDV, BPIV-3, and BoHV-1) or 33°C (BRSV) in 5% CO₂. Cells inoculated with BPIV-3 or BRSV were incubated for 6 d, BVDV for 4 d, and BoHV-1 for 24 h. The cells were fixed with 20% acetone/PBS for 10 min and allowed to dry overnight at room temperature. The following monoclonal antibodies were used as the primary antibodies in the assay: 348, specific for the E2 glycoprotein of BVDV [Veterinary Medical Research and Development Inc. (VMRD), Pullman, Washington, USA]; 8G12, specific for the F protein of BRSV (12); F2, specific for glycoprotein C of BoHV-1 (VMRD); and 1B6, specific for a 69-kDa protein of BPIV-3 (VMRD). Biotinylated horse immunoglobulin antibodies to mouse antigen (Vector Laboratories, Burlingame, California, USA) were used as the secondary antibody. Streptavidin–horseradish peroxidase complex (Invitrogen) and 3-amino-9-ethyl-carbazole (Sigma Chemical Company, St. Louis, Missouri, USA) were used to complete the immunoperoxidase procedure.

The BHS lung cells were evaluated for mycoplasmal infection with use of the fluorescent dye 4',6-diamidino-2'-phenylindole dihydrochloride (DAPI; Roche Diagnostics Corporation, Indianapolis, Indiana, USA). Briefly, the cells were seeded onto a Teflon-coated spot slide (Thermo Fisher Scientific, Waltham, Massachusetts, USA) and incubated overnight at 37°C in a humidified chamber with 5% CO₂ to allow cell attachment. After incubation the medium was discarded and the cells were washed once with DAPI–methanol (1 µg/mL). The cells were then covered with DAPI–methanol (1 µg/mL) and incubated at 37°C for 15 min. After incubation the DAPI–methanol solution was discarded, the cells were washed once with methanol, and a coverslip was mounted on the slide with the use of glycerol as a mounting medium. The slide was evaluated under a fluorescence microscope with a 340/380 excitation filter and an LP 430-nm barrier filter.

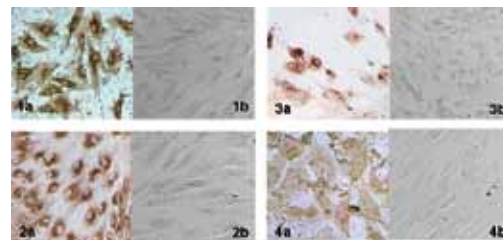


Figure 1. Results of enzyme immunoassay depicting, in the “a” panels, cytoplasmic staining in bighorn sheep (BHS) fetal lung cells infected at a 0.5 multiplicity of infection with the following respiratory viruses: **1,** Bovine respiratory syncytial virus (BRSV); **2,** Bovine viral diarrhea virus (BVDV); **3,** Bovine herpesvirus 1 (BoHV-1); and **4,** Bovine parainfluenza virus 3 (BPIV-3). The results are at 6 d after infection for BPIV-3 and BRSV, 4 d after infection for BVDV, and at 24 h after infection for BoHV-1. The primary antibodies used were 1B6 (specific for a 69-kDa protein of BPIV-3), 8G12 (specific for the F protein of BRSV), 348 (specific for the E2 glycoprotein of BVDV), and F2 (specific for glycoprotein C of BoHV-1), respectively. The “b” panels represent mock-infected BHS lung cells used as negative controls for the respective viruses. Magnification — ×10.

Monolayers of primary cells in the flasks attained more than 70% confluence within 7 d of harvesting and plating. The monolayers were trypsinized and the resultant cells passaged at a 1:4 dilution in 75-cm² flasks. The cells in the flasks attained 100% confluence within 8 d. By the 3rd passage, 100% confluent monolayers were formed in 5 d. The cells from passage no. 8 were used in the enzyme immunoassay for the detection of infection with the respiratory viruses. The assay revealed that the fetal lung cells were permissive for infection with BPIV-3, BRSV, BVDV, and BoHV-1 (Figure 1). The DAPI staining revealed that the cells were free of *Mycoplasma* contamination and hence could be used for routine virus isolation. These cells have undergone 15 passages in our laboratory and thus could be referred to as a cell line (13).

The etiology of pneumonia in BHS has not been resolved completely, but *M. haemolytica*, *Bibersteinia trehalosi*, and *P. multocida* have frequently been isolated from the lungs of BHS that died of pneumonia (1). In bovine respiratory disease complex (BRDC), these organisms are widely accepted as the bacterial pathogens secondary to primary infection with 1 or more of the respiratory viruses, including BPIV-3, BRSV, BVDV, and BoHV-1 (4). Although these bacterial pathogens cause pneumonia in calves when deposited directly into the lungs by intratracheal injection or by means of a bronchoscope, they rarely cause disease if administered intranasally. However, intranasal administration of these bacteria does cause pneumonia if preceded by administration of respiratory viruses such as BoHV-1, BRSV, and BVDV (5–7,14,15). These findings indicate a primary role for these viruses in BRDC. The detection of antibodies specific for these viruses in several herds of BHS (8,9, and Mark Drew, Idaho Department of Fish and Game, Caldwell, Idaho: personal communication, 2008) suggests a role for these viruses in pneumonia in BHS as well. However, these viruses have not been routinely isolated from BHS. There are reports of isolation of BPIV-3 (16) and BRSV (17) from BHS; the cells used were bovine turbinate cells and domestic sheep fetal lung cells, respectively.

Only 3 BHS cell lines have been reported: the kidney and turbinate cell lines were permissive for BPIV-3 and BRSV in BHS (18), and the fetal tongue cell line was permissive for BoHV-1, BVDV, BPIV-3, and BRSV (19). There have been no previous reports of BHS fetal

lung cell lines. The BHS fetal lung cell line developed in this study is easy to grow, is amenable to trypsinization, and easily reverts back to culture from frozen stocks. It is equally sensitive to infection with BPIV-3, BRSV, BVDV, and BoHV-1 and very likely would also be permissive for other respiratory viruses of BHS. This cell line, which is free of contamination with *Mycoplasma* and BVDV, should enhance the chances of isolation of respiratory viruses of BHS and other ruminants. It is freely available to anyone on request.

Acknowledgment

This work was supported by funds from the Foundation for North American Wild Sheep and its Eastern, Idaho, Oregon, and Washington chapters, as well as from the Rocky Mountain Bighorn Sheep Society.

References

1. Miller MW. Pasteurellosis. In: Williams ES, Barker IK, eds. Infectious Diseases of Wild Mammals. Ames, Iowa: Iowa State Univer Pr, 2001:330–339.
2. Callan RJ, Bunch TD, Workman GW, Mock RE. Development of pneumonia in desert bighorn sheep after exposure to a flock of exotic wild and domestic sheep. *J Am Vet Med Assoc* 1991; 198:1052–1056.
3. Cassirer EF, Sinclair ARE. Dynamics of pneumonia in a bighorn sheep metapopulation. *J Wildl Manage* 2007;71:1080–1088.
4. Frank GH: Pasteurellosis of cattle. In: Adlam C, Rutter JM, eds. *Pasteurella* and Pasteurellosis. New York: Academic Pr, 1989: 197–222.
5. Jericho KWF, Langford EV. Pneumonia in calves produced with aerosols of bovine herpesvirus 1 and *Pasteurella haemolytica*. *Can J Comp Med* 1978;42:269–277.
6. Fulton RW, Purdy CW, Confer AW, et al. Bovine viral diarrhea viral infections in feeder calves with respiratory disease: Interactions with *Pasteurella* spp., parainfluenza-3 virus, and bovine respiratory syncytial virus. *Can J Vet Res* 2000;64:151–159.
7. Jericho KWF, Darcel GQ, Langford EV. Respiratory disease in calves produced with aerosol of parainfluenza-3 virus and *Pasteurella haemolytica*. *Can J Comp Med* 1982;46:293–301.
8. Parks JB, Post G, Thorne T, Nash P. Parainfluenza-3 virus infection in Rocky Mountain bighorn sheep. *J Am Vet Med Assoc* 1972;161:669–672.
9. Dunbar MR, Jessup DA, Evermann JF, Foreyt WJ. Seroprevalence of respiratory syncytial virus in free-ranging bighorn sheep. *J Am Vet Med Assoc* 1985;187:1173–1174.
10. Brodersen BW, Kelling CL. Effect of concurrent experimentally induced bovine respiratory syncytial virus and bovine viral diarrhea virus infection on respiratory tract and enteric disease in calves. *Am J Vet Res* 1998;59:1423–1430.
11. Brodersen BW, Kelling CL. Alteration of leukocyte populations in calves concurrently infected with bovine respiratory syncytial virus and bovine viral diarrhea virus. *Viral Immunol* 1999;12:323–334.
12. Klucas CA, Anderson GA. Bovine respiratory syncytial virus-specific monoclonal antibodies. *Vet Immunol Immunopathol* 1988;18:307–315.
13. Freshney RI (ed). *Biology of the cultured cell*. In: *Culture of Animal Cells: A Manual of Basic Technique*. 2nd ed. New York: John Wiley, 1993:7–13.
14. Ganheim C, Johannisson A, Ohagen P, Waller PK. Changes in peripheral blood leukocyte counts and subpopulations after experimental infection with BVDV and/or *Mannheimia haemolytica*. *J Vet Med B Infect Dis Vet Public Health* 2005;52: 380–385.
15. Yates WDG, Babiuk LA, Jericho KWF. Viral-bacterial pneumonia in calves: Duration of the interaction between bovine herpesvirus 1 and *Pasteurella haemolytica*. *Can J Comp Med* 1983;47: 257–264.
16. Rudolph KM, Hunter DL, Rimler RB, et al. Microorganisms associated with a pneumonic epizootic in Rocky Mountain bighorn sheep (*Ovis canadensis canadensis*). *J Zoo Wildl Med* 2007;38:548–558.
17. Spraker TR, Collins JK, Adrian WJ, Olterman JH. Isolation and serologic evidence of a respiratory syncytial virus in bighorn sheep from Colorado. *J Wildl Dis* 1986;22:416–418.
18. DeLong WJ, Hunter DL, Ward AC. Susceptibility of two bighorn sheep cell cultures to selected common ruminant viruses. *J Vet Diagn Invest* 2000;12:261–262.
19. Castro AE, Montague SR, Dotson JF, Jessup DA, DeForge JR. Susceptibility of a fetal tongue cell line derived from bighorn sheep to five serotypes of bluetongue virus and its potential for the isolation of viruses. *J Vet Diagn Invest* 1989;1:247–253.

Influence of parity and litter size on gestation length in beagle dogs

Makoto Seki, Norio Watanabe, Kenyo Ishii, Yoh-ichi Kinoshita, Takehiro Aihara,
Shuji Takeiri, Takeshige Otoi

Abstract

This study was conducted to investigate the effects of parity and litter size on gestation length in beagle bitches. The mean duration of the initial elevation (> 2 ng/mL) in progesterone concentrations after the onset of proestrus was shorter ($P < 0.05$) in bitches without (nulliparous) whelping experience than in bitches with (multiparous) whelping experience (6.9 d versus 8.0 d). When calculated as the interval between the day of initial elevation in progesterone concentrations and the day of whelping, the gestation length in the nulliparous bitches was noted to be similar to that in the multiparous bitches (64.3 d versus 64.2 d). No significant correlation between gestation length and litter size was observed in any of the bitches. Our results indicate that the gestation length in beagle bitches is not affected by parity or litter size.

Résumé

Cette étude a été réalisée afin d'étudier les effets de la parité et de la taille de la portée sur la durée de la gestation chez des chiennes Beagle. La durée moyenne de l'augmentation initiale (> 2 ng/mL) de la concentration de progestérone après le début du proestrus était plus courte ($P < 0,05$) chez les chiennes sans expérience de mise-bas (nullipare) que chez les chiennes avec expérience de mise-bas (multipare) (6,9 j versus 8,0 j). Lorsque calculé comme l'intervalle entre le premier jour de l'élévation des concentrations de progestérone et le jour de la mise-bas, la durée de la gestation chez les chiennes nullipares a été notée comme étant similaire à celui des chiennes multipares (64,3 j versus 64,2 j). Aucune corrélation significative entre la durée de la gestation et la taille de la portée n'a été observée chez aucune des chiennes. Nos résultats indiquent que la durée de la gestation chez les chiennes Beagle n'est pas affectée par la parité ou la taille de la portée.

(Traduit par Docteur Serge Messier)

Predicting the duration of canine gestation aids in managing whelping or in planning cesarean sections. When calculated as the interval between the day of first mating and the day of whelping, the gestation length in bitches ranges widely from 57 to 72 d (1). In contrast, when calculated as the interval between the day of luteinizing hormone (LH) peak and the day of whelping, the gestation length becomes less variable, ranging from 64 to 66 d (1). Some studies have suggested that factors such as breed and litter size affect gestation length (2–4); however, this association has not been consistently reported (5–7). In dogs, the effect of parity on gestation length has not been studied as extensively as that of the above-mentioned factors. It is known that the LH surge in dogs occurs approximately 2 d before ovulation (8). Since the initial elevation in progesterone is strictly associated with the LH surge (8,9), the measurement of progesterone concentrations has been used to determine the optimal time for successful mating. It has been demonstrated that the date of parturition can be accurately predicted based on the day of the initial elevation in progesterone concentrations (7). To investigate the effect of parity on gestation length, we compared the gestation lengths of nulliparous and multiparous bitches. The relationship between gestation length and litter size was also examined.

Beagles in a closed-breeding colony were used in this study. The dogs were housed singly in stainless steel cages, fed a diet of standard commercial dog food once per day, and given water ad libitum. All the animals involved in this study received humane care in compliance with the Guide for the Care and Use of Laboratory Animals prepared by the Institute of Laboratory Animal Resources, National Research Council. All procedures were approved by the Animal Research Committee of the Yamaguchi University. All the dogs were examined daily for the presence of vulval swelling and serosanguineous vaginal discharge; these 2 parameters were used as markers of the onset of proestrus. To assess the effects of parity and litter size on gestation length, which was calculated as the interval between the day of the initial elevation in plasma progesterone concentrations and the day of whelping, blood samples were collected from bitches with (multiparous; $n = 60$, 2 to 4 years of age) and without (nulliparous; $n = 29$, 10 months to < 2 years of age) the whelping experience. Sampling was carried out once a day from Day 1 to Day 13 after the onset of proestrus (Day 0). All bitches were mated twice with male dogs (2 to 5 years of age) on Days 9 and 12 after the onset of proestrus. The whelping dates and litter sizes were recorded at the time of parturition. Gestation lengths

Laboratory of Animal Reproduction, The United Graduate School of Veterinary Sciences, Yamaguchi University, Yamaguchi 753-8515, Japan (Seki, Otoi); Kawasaki Mitaka K. K., Mitaka, Tokyo 181-0013, Japan (Seki, Watanabe, Ishii); Kitayama Iabes Co. Ltd., Kuga, Yamaguchi 740-0601, Japan (Kinoshita, Aikara, Takeiri).

Address all correspondence to Dr. Takeshige Otoi; telephone/fax: +81-83-933-5904; e-mail: otoi@yamaguchi-u.ac.jp

Dr. Otoi's current address is Laboratory of Animal Reproduction, The United Graduate School of Veterinary Sciences, Yamaguchi University, Yamaguchi 753-8515, Japan.

Received August 6, 2008. Accepted December 19, 2008.

Table I. Comparison of duration of the initial elevation in progesterone (P) concentrations, gestation length, and litter size between nulliparous and multiparous bitches

Bitches	Number of bitches examined	Duration of the initial elevation in P levels (day)	Gestation length (day)		Litter size
			Mating	P level	
Nulliparous	29	6.9 ± 2.3 ^a	62.2 ± 2.5	64.3 ± 1.2	5.2 ± 1.6
Multiparous	60	8.0 ± 1.7 ^b	63.2 ± 2.2	64.2 ± 1.9	5.7 ± 1.9

Bitches were mated twice on Days 9 and 12 after the onset of proestrus. Values are expressed as mean ± standard deviation (s).

Duration of the initial elevation in progesterone levels (> 2 ng/mL) after the onset of proestrus. Gestation lengths are expressed as the interval between the day of first mating and the day of whelping (Mating) or that between the day of initial elevation in P levels (> 2 ng/mL) and the day of whelping (P level).

^{a,b} Values with different letters are significantly different ($P < 0.05$).

were calculated as the interval between the day of first mating and the day of whelping or the interval between the day of the initial elevation in plasma progesterone concentrations and the day of whelping. The plasma progesterone concentrations were measured using an enzyme-linked immunosorbent assay (ELISA) kit (enzyme-immunoassay practice P kit; Kawasaki Mitaka K.K., Mitaka, Tokyo, Japan). The intra-assay coefficients of variation for samples with high, medium, and low concentrations of progesterone were 6.5%, 5.9%, and 5.1%, respectively. The interassay coefficients of variation for the same samples were 7.1%, 7.4%, and 6.9%, respectively. The sensitivity of the assay was 0.25 pg/well. The first day at which the plasma progesterone concentrations exceeded 2 ng/mL was recorded as the day of initial elevation in progesterone, which was considered to be the day of the LH peak (10).

Differences between nulliparous and multiparous bitches with regard to the duration of the initial elevation in plasma progesterone concentrations (> 2 ng/mL) after the onset of proestrus and litter size were evaluated using an independent Student's *t*-test. The mean values of gestation length were analyzed by analysis of variance (ANOVA) using the general linear models (GLM) procedure of SAS (SAS for Windows, version 9.1; SAS Institute Japan, Tokyo, Japan). The statistical model included the type of bitches, litter size, and the two-way interactions. Since significant interactions were not observed between the type of bitches and litter sizes, they were excluded from the model. Single linear regression analysis was used to examine the relationship between gestation length and litter size; further, we determined the correlation coefficient of the relationship. The data are expressed as mean ± standard deviation (s). Differences with a probability value (*P*) of ≤ 0.05 were considered significant.

As shown in Table I, the mean duration of the initial elevation in progesterone concentrations after the onset of proestrus was significantly shorter ($P < 0.05$) in the nulliparous bitches than in the multiparous bitches (6.9 d versus 8.0 d). When calculated as the interval between the day of first mating and the day of whelping, the gestation length of the nulliparous bitches tended to be shorter ($P < 0.1$) than that of the multiparous bitches (62.2 d versus 63.2 d). However, no significant difference was observed between the gestation length of nulliparous and multiparous bitches (64.3 d versus 64.2 d) when this parameter was calculated as the interval between

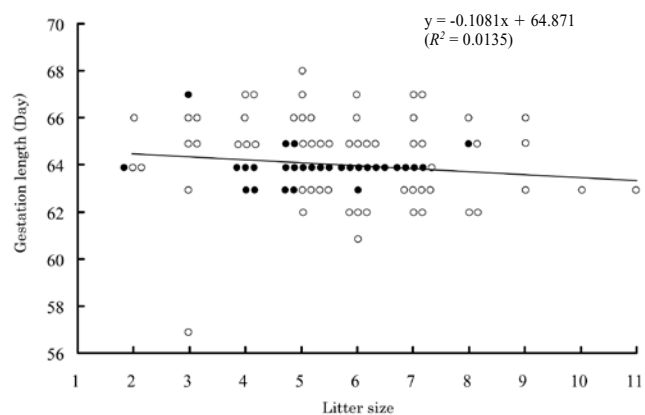


Figure 1. The correlation between gestation length, calculated as the interval between the day of initial elevation in plasma progesterone concentrations and the day of whelping, and litter size. The correlation between gestation length and litter size in all bitches, including the nulliparous (●) and multiparous (○) bitches, was analyzed.

the day of initial elevation in plasma progesterone concentrations and the day of whelping. The mean litter size did not differ between the 2 groups (Table I). Further, no significant correlation ($P > 0.05$) between gestation length and litter size was observed in any of the bitches (Figure 1).

The present study supported the observations of previous studies that parity does not influence gestation length when the latter is calculated as the interval between the day of initial elevation in progesterone concentrations and the day of whelping (2,11). However, we found that, when gestation length was calculated as the interval between the day of first mating and the day of whelping, it tended to be shorter by approximately 1 d in the nulliparous bitches than in the multiparous bitches. It has been reported that the mean duration of proestrus and estrus is significantly shorter in bitches experiencing their first reproductive cycle than in those experiencing their second reproductive cycle (12,13). Moreover, Wildt et al (13) demonstrated that the duration of the LH surge after the onset of proestrus was shorter by approximately 1 d in pubertal bitches than in multiparous bitches. Similarly, in the present study, we found that the duration of the initial elevation in progesterone concentrations after the onset of proestrus was shorter by 1 d in the nulliparous bitches than in the

multiparous bitches. These findings indicate that ovulation after the onset of proestrus may occur earlier in nulliparous bitches than in multiparous ones. Therefore, the shorter gestation length, calculated as the interval between the day of first mating and the day of whelping, in the nulliparous bitches than in the multiparous bitches may result from earlier ovulation after the onset of proestrus.

In the present study, no difference in litter size was noted between the nulliparous and multiparous bitches. Further, no correlation was observed between gestation length and litter size in these bitches. Our results are in agreement with those of previous studies that have indicated that litter size does not influence gestation length (5,7); these studies include one study that used 36 beagle bitches (5) and another that had 63 bitches representing 19 breeds (7). Eilts et al (11) have suggested that small samples with limited statistical power may not be able to detect an association between litter size and gestation length. They used large sample sizes (308 bitches representing 4 breeds) and reported that litter size affects gestation length; further, they showed that litters of 4 or less are more likely to be associated with a long gestation length. Therefore, further studies involving larger sample sizes may be required to determine the influence of litter size on gestation length in the beagle bitches.

In conclusion, our results indicate that gestation length in beagle dogs is not affected by parity or litter size. However, when calculated as the interval between the day of first mating to the day of whelping, gestation length tends to be approximately 1 d shorter in nulliparous bitches than in multiparous ones. This indicates that ovulation in nulliparous bitches may occur earlier than that in multiparous bitches.

References

1. Concannon P, Whaley S, Lein D, Wissler R. Canine gestation length: Variation related to time of mating and fertile life of sperm. *Am J Vet Res* 1983;44:1819–1821.
2. Okkens AC, Hekerman TW, de Vogel JW, van Haaften B. Influence of litter size and breed on variation in length of gestation in the dog. *Vet Q* 1993;15:160–161.
3. Okkens AC, Teunissen JM, Van Osch W, Van Den Brom WE, Dieleman SJ, Kooistra HS. Influence of litter size and breed on the duration of gestation in dogs. *J Reprod Fertil Suppl* 2001; 57:193–197.
4. Holst PA, Phemister RD. Onset of diestrus in the Beagle bitch: Definition and significance. *Am J Vet Res* 1974;35:401–406.
5. Tsutsui T, Hori T, Kirihara N, Kawakami E, Concannon PW. Relation between mating or ovulation and the duration of gestation in dogs. *Theriogenology* 2006;66:1706–1708.
6. Linde-Forsberg C, Forsberg M. Results of 527 controlled artificial inseminations in dogs. *J Reprod Fertil Suppl* 1993;47:313–323.
7. Kutzler MA, Mohammed HO, Lamb SV, Meyers-Wallen VN. Accuracy of canine parturition date prediction from the initial rise in preovulatory progesterone concentration. *Theriogenology* 2003;60:1187–1196.
8. Concannon PW, Hansel W, Visek WJ. The ovarian cycle of the bitch: Plasma estrogen, LH and progesterone. *Biol Reprod* 1975; 13:112–121.
9. Luvoni GC, Beccaglia M. The prediction of parturition date in canine pregnancy. *Reprod Domest Anim* 2006;41:27–32.
10. Nakada K, Adachi Y, Moriyoshi M, Nakao T. Diagnosis of optimal mating time by measurement of gestagen concentration using a bovine plasma progesterone qualitative test EIA Kit in beagle bitches. *J Jpn Vet Med Assoc* 2000;53:747–751.
11. Eilts BE, Davidson AP, Hosgood G, Paccamonti DL, Baker DG. Factors affecting gestation duration in the bitch. *Theriogenology* 2005;64:242–251.
12. Chakraborty PK, Panko WB, Fletcher WS. Serum hormone concentrations and their relationships to sexual behavior at the first and second estrous cycles of the Labrador bitch. *Biol Reprod* 1980;22:227–232.
13. Wildt DE, Seager SW, Chakraborty PK. Behavioral, ovarian and endocrine relationships in the pubertal bitch. *J Anim Sci* 1981; 53:182–191.

Canadian Journal of Veterinary Research

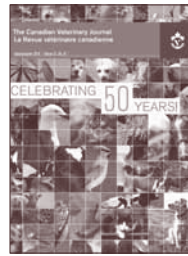
available online now!

Articles are now easily accessible
over the Internet at

PubMed Central
www.pubmedcentral.com

Reaching Canada's Veterinarians

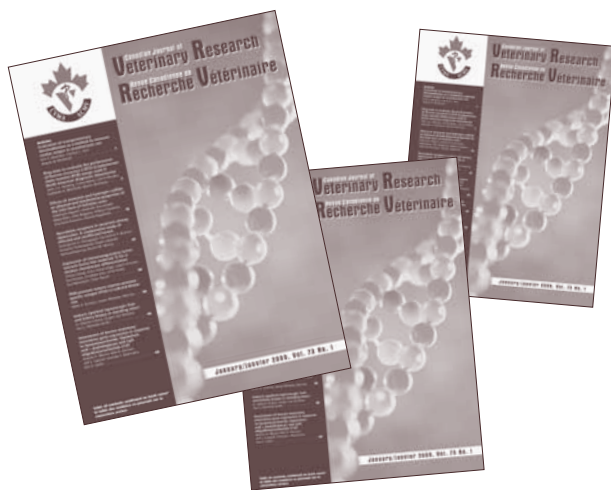
Get your message into



**The Canadian
Veterinary Journal**
For more information contact:
Laima Laffitte
Advertising Manager
Tel.: (613) 673-2659
Fax: (613) 673-2462
e-mail: llaffitte@cvma-acmv.org

RENEW YOUR SUBSCRIPTION
NOW!

RENOUVELEZ VOTRE ABONNEMENT
DÈS MAINTENANT!



Four issues of the
Canadian Journal of Veterinary Research for 2010

Quatre numéros de la
Revue canadienne de recherche vétérinaire pour 2010

\$135 \$ (+\$6.75 \$ GST/TPS)	Canadian/Canadien
\$150 \$ US/É.-U.	Foreign/Étranger
\$25 \$ (+\$1.25 \$ GST/TPS)	Back issues/Anciens numéros
each/chacun	

Contact/Communiquez avec :

Beverley Prieur, Circulation/Tirage
Canadian Journal of Veterinary Research
Revue canadienne de recherche vétérinaire
339 rue Booth Street
Ottawa, Ontario K1R 7K1
Canada

Tel./Tél. : (613) 236-1162
Fax/Télécopieur : (613) 236-9681
E-mail/Courriel : bprieur@cvma-acmv.org

www.canadianveterinarians.net



Tables of contents
Coming events
Article abstracts
Classified advertising
Subscription information
Instructions for authors

Tables des matières
Événements à venir
Résumés d'articles
Annonces classées
Information sur l'abonnement
Directives à l'intention des auteurs

www.veterinairesaucanada.net

Short Communications

Communications brèves

- Pulmonary intravascular macrophages and endotoxin-induced pulmonary pathophysiology in horses**
Karin Aharonson-Raz, Baljit Singh **45**

- Increased risk of chronic wasting disease in Rocky Mountain elk associated with decreased magnesium and increased manganese in brain tissue**
Stephen N. White, Katherine I. O'Rourke, Thomas Gidlewski, Kurt C. VerCauteren, Michelle R. Mousel, Gregory E. Phillips, Terry R. Spraker **50**

- Kinetics and role of antibodies against intimin β in colostrum and in serum from goat kids and longitudinal study of attaching and effacing *Escherichia coli* in goat kids**
José A. Orden, Ricardo De la Fuente, María Yuste, Susana Martínez-Pulgarín, José A. Ruiz-Santa-Quiteria, Pilar Horcajo, Antonio Contreras, Antonio Sánchez, Juan C. Corrales, Gustavo Domínguez-Bernal **54**

- Isolation of *Escherichia coli* from piglets in South Korea with diarrhea and characteristics of their virulence genes**
Yeong Ju Kim, Ji Hee Kim, Jin Hur, John Hwa Lee **59**

- Pleiotropic effects of polysaccharide capsule loss on selected biological properties of *Streptococcus suis***
Shin-Ichi Tanabe, Laetitia Bonifait, Nahuel Fittipaldi, Louis Grignon, Marcelo Gottschalk, Daniel Grenier **65**

- Rapid serodiagnosis with the use of surface plasmon resonance imaging for the detection of antibodies against major surface protein A of *Mycoplasma synoviae* in chicken**
Kiseok Oh, Semi Lee, Jayoung Seo, Dongwoo Lee, Taejung Kim **71**

- Bighorn sheep fetal lung cell line for detection of respiratory viruses**
Sudarvili Shanthalangam, Christina Topliff, Clayton L. Kelling, Subramaniam Srikumaran **75**

- Influence of parity and litter size on gestation length in beagle dogs**
Makoto Seki, Norio Watanabe, Kenyo Ishii, Yoh-ichi Kinoshita, Takehiro Aihara, Shuji Takeiri, Takeshige Otoi **78**